

The Radio and Electronic Engineer

The Journal of the Institution of Electronic and Radio Engineers

Exploitation of the 100–1000 GHz Frequency Range

CONSIDERATION of this part of the frequency spectrum is not new. Classical work by scientists such as Rubens at the beginning of this century using thermal sources, and Gordy and his colleagues in the late 1950s using crystal harmonic generators, demonstrated some of the features and possibilities. In spite of this early work the real exploitation of the shorter millimetric part of the spectrum has remained 'just around the corner' for many years, whilst the submillimetric region has remained relatively unexplored. This lack of attention has been due largely to the extensive development of the flanking regions at microwave and near-infrared wavelengths. These regions have been so highly developed that there are few problems or applications, or potential applications, that cannot be more readily approached using the sophisticated techniques developed in these adjoining parts of the frequency spectrum. Additionally, the basic requirements for system development in the 100–1000 GHz range have proved difficult to satisfy. Low-cost coherent sources at reasonable power levels have not been available, detectors of good sensitivity and rapid response have required cryogenic temperature operation, and a convenient low-cost waveguide system has not yet been developed. The level of activity in the region has increased significantly, however, and three international conferences have been held in recent years.^{1–3} A fourth conference will be held in Miami this December. This special edition has the objective of surveying the present 'state of play', to show some of the distinctive features of this frequency range, to describe some of the basic system elements such as energy sources, receivers and waveguides, and to indicate progress to date in a number of areas of application.

Until recently energy sources have been restricted to:

- (i) Non-coherent thermal generators—usually gas discharge sources—and harmonic generators, both very low energy sources used mainly for spectroscopy.
- (ii) Electron tube sources such as klystrons, and backward wave oscillators. The former are available in the short-millimetric region, whilst the latter have been extended as voltage tunable sources to 1000 GHz but are then too expensive and have too short a life-time for wide-spread applications.
- (iii) Gas discharge and optically pumped lasers. The former are relatively inexpensive to construct but limited to one or two discrete wavelengths whilst the latter give a larger number of available discrete wavelengths, but are expensive and bulky.
- (iv) Solid-state sources. These are the key to large-scale applications and considerable advances have recently been made especially with impatt devices. These are described in the paper by Purcell.
- (v) Relativistic electron-beam sources. A new source—the gyrotron—has recently been described by the Russian originators. It was developed for plasma heating and is capable of producing 1 kW of mean power at 300 GHz, and could well find other applications. (See Ref. 3, p. 385.)

Available detectors include the Golay cell which is very sensitive but slow in response (e.g. <10 Hz), the pyro-electric detector which is cheap and sensitive but also relatively slow (e.g. <5 kHz), and cryogenic photodetectors, such as indium antimonide which combine high sensitivity and fast response, but at the expense of liquid helium temperature operation. Crystal detectors have long been the mainstay for microwave detection, and in recent years they have been developed for operation in the 100–1000 GHz range, including point contact and Schottky barrier devices. The paper by Clifton describes progress in this latter field leading to the development of effective receivers.

Propagation is through the atmosphere for free space applications, or by waveguide where guided propagation is required. The paper by Emery and Zavody discusses the influence of the atmosphere on propagation for both clear air and precipitation. The predominant effect in clear air is attenuation due to water vapour, with several oxygen absorption lines superimposed, although only one at 118 GHz greatly exceeds the normal water vapour absorption. Above 300 GHz the attenuation becomes very

high, with 10 dB per km or more even in the windows. Peak attenuation operation has advantages for secure communications, but applications are likely to lie mainly in the windows at around 95, 140, 220 and 350 GHz, or for very short range applications. The paper by Harris shows the limitations of conventional waveguides such as dominant mode rectangular guide and strip-line, and indicates a number of other possible guides that have potential advantages, although no particular guide type has yet been established for frequencies greater than 300 GHz.

In view of the disadvantages outlined, the 100–1000 GHz range is likely to find applications only where inherent characteristics make it especially favourable. These characteristics include distinctive material and molecular behaviour, including atmospheric absorption effects; a penetration through atmospheric precipitation midway between the low attenuation of microwaves and generally high attenuation of near-infrared and optical wavelengths; a spatial resolution potential between that of microwaves (poor) and optical waves (very good); an ability to penetrate gaseous plasma for which microwaves are opaque; an enormous available bandwidth; and a wave-length dimension that is very short but within careful constructional tolerance capabilities. Antennas with very narrow beam widths but relatively small dimensions can be made. A number of these characteristics have been used for applications to date and are included in the papers of this special edition. Far-infrared astronomy has led to exciting discoveries and uses naturally occurring radiation in this frequency band.

Most of the early experimentation in this frequency range was directed towards the measurement of physical properties of matter. The paper by Stone and his colleagues at NPL includes accounts of spectroscopic studies, the determination of optical constants of materials, the determination of upper atmosphere constituents from the emission spectrum, diagnostic measurement techniques for high density gaseous plasma, and high resolution dimensional measurement. Various possibilities for commercial and industrial applications are outlined by Meinel and Rembold. The accurate measurement of distance, velocity and acceleration can be used for traffic control, including rail and vehicular radar, and for general remote distance measurement, whilst radiometry allows non-contact thermometry with good discrimination to be carried out, and transmission measurements can give constituent information, e.g. for pollution control. The present state of development of radar systems is given by Johnston. A large number of radars have been produced to operate in the 95 GHz window, and a few in the windows at 140 and 220 GHz, with a wide range of applications including police hand-held radars and space object identification. They have the merit of small dimensions and high resolution, but for lower atmosphere operation are restricted to relatively short range. The paper by Cram and Woolcock reports an extended programme on the measurement of practical radar target reflection characteristics using scale models at frequencies up to 890 GHz, with possible extension to still higher frequencies. The application of this frequency range to outer space measurements and technology is discussed in the paper by Clancy. Attention is drawn to the measurement of upper atmosphere constituents by spectral studies, the importance of far-infrared astronomy carried out free of atmospheric effects, and the possible use of the submillimetric wave region for inter-satellite communications. The associated technology is also considered.

It is clear that a great deal of development has taken place, and important applications have been pursued, but there is as yet no breakthrough into large-scale developments. In recent years intensive work on millimetric communication systems using low-loss waveguide promised to extend the well-used frequency range upwards, but this work has recently been mainly concluded in favour of optical communication systems. There is now considerable military activity on short-millimetric homing and guidance systems, and this should result in renewed device and systems activity.

The 100–1000 GHz range has distinctive features that would make it especially appropriate for the solution of a number of particular problems. There have been considerable advances in sources and detectors, but there is still a lack of reasonable-cost components for system applications, and the absence of an urgent problem that requires these frequencies and is of sufficient importance to justify an expensive programme of component and system development has kept work at relatively low key. Progress is being made however, as the papers in this special issue demonstrate, and the basis for more widespread utilization cannot be very far away.

D. J. HARRIS

References

- 1 First International Conference on Submillimeter Waves, Atlanta, USA, June 1974. Conference Digest, IEEE, No. 74 CH 0856–5 MTT, 1974. (*IEEE Trans. MTT-22*, No. 12, pp. 981–1120, 1974.)
- 2 Second International Conference on Submillimeter Waves, San Juan, Puerto Rico, December 1976. Conference Digest, IEEE, No. 76 CH 1152–8 MTT, 1976. (*IEEE Trans.*, MTT-25, No. 6, pp. 455–566, 1977, and QE-13, No. 6, pp. 371–494, 1977.)
- 3 Third International Conference on Submillimeter Waves, Guildford, UK, March 1978. Conference Digest, Institute of Physics, 1978. (*Infrared Physics*, 18, No. 5/6, pp. 375–927, 1978.)

Announcements

Annual General Meeting

The Annual General Meeting of the Institution will be held at the London School of Hygiene and Tropical Medicine, Keppel Street, Gower Street, London WC1 on Thursday 25th October 1979. The Agenda for the Annual General Meeting which will start at 6 p.m. is printed on page 328.

Immediately following the conclusion of the Annual General Meeting (at about 6.45), Professor William Gosling will give his Presidential Address which he has entitled 'Electronics—A Profession in its Golden Age'.

Only Corporate and Non-Corporate Members of the Institution may attend the Annual General Meeting; attendance of non-members will however be welcomed at the Presidential Address and tickets of invitation may be obtained on application to the Institution.

Technology—Employment—Education International Conference

'Technology—Employment—Education' is the title of an international conference at Southampton University, which is being organized by the Southern Science and Technology Forum and the University from 10th to 12th September 1979.

The theme of the conference will be the new technology in industry, its effects on job structures and skills required and how these factors may lead to changes in the educational curriculum for future generations.

The conference will provide an opportunity for those in industry and education to get together on common problems and to generate ideas for action so that real work on solutions may begin. 'Education' includes secondary and higher education.

Personalities from both the public and private sectors of industry, academia, and the trades unions in the UK and overseas have accepted invitations to participate in this conference. The keynote address will be given by Sir James Redmond, President IEE, whose Institution is presently involved in the requirements of industry for highly trained engineers, who will be able to tackle effectively the challenging problems of industry today and in the future.

Fees will be £40 for 'non-residential' and £75 for residential in college, both inclusive of all meals and refreshments. For further information and registration form contact: Southern Science & Technology Forum, Building 25, University of Southampton, SO9 5NH (Tel.: Southampton (0703) 559122, Ext. 2430 or 2434).

Communications in Microprocessor Industrial Instrumentation

A two-day seminar on 'Communications in Microprocessor Industrial Instrumentation', jointly organized by Sira Institute Ltd and Warren Spring Laboratory in association with The City University, will be held on 12th–13th September 1979, at The City University, London EC1.

The use of microprocessors in process instrumentation is opening up new opportunities for more cost-effective communication methods. Claimed advantages include reduced cabling costs and increased communication system flexibility. Several instrument manufacturers, and electronics and computer companies, have introduced new communication systems, but no standard appears to be emerging and there is inevitably a body of opinion opposed to any particular system.

This seminar aims to examine the differences in the several approaches to communications and to compare these approaches with practical user requirements.

The programme will consist of three sessions and a forum:

Session 1—Tutorial

Keynote paper presented by Dr. D. J. Holding (Queen Mary College, London) and G. Wood (Foxboro-Yoxall)

'Communications and distributed systems'

G. Bryan and Dr P. J. King (Warren Spring Laboratory)

Session 2—Approaches adopted by suppliers of process control systems

'A distributed architecture communication system for process control'

R. E. Daniel (Taylor Instrument Co)

'Kent communication systems for instrument supervision and distributed control'

Dr A. R. Farmer (Kent Instruments)

'High-speed multi-master communications in a distributed process management and control system'

G. L. Fraser (Foxboro-Yoxall)

'The Honeywell TDC 2000 data highway for distributed process control'

B. Reynolds (Honeywell)

'Communication within the MPC 80 distributed system'

P. Middleton (Negretti & Zambra)

'A microprocessor distributed plant controller'

P. G. Harrison (Hawker Siddeley Dynamics Engineering)

Session 3—Approaches desired by users

Several papers, including:

'Pilkington experience and intentions in the use of Hytron optical fibres and system components within the company's industrial systems'

K. J. Butler (Pilkington Bros)

'Instrumentation systems for chemical plants with flammable hazards: present problems and future solutions'

R. C. Moore (ICI Plastics Division)

'Communications requirements for distributed computer control and instrumentation systems on CEGB plant'

Dr W. S. Jones (Central Electricity Research Laboratory)

The seminar will conclude with a Forum for general discussion, led by a panel of speakers.

Further information may be obtained from Mrs R. G. Keiller, Sira Institute Ltd, South Hill, Chislehurst, Kent BR7 5EH.

Electronic Engineering Teaching for the 80's

Organized by the University of Hull in association with the Institution of Electrical Engineers and the Institution of Electronic and Radio Engineers, a conference to be held at the University of Hull from 1st–3rd April 1980 will be the third in the series with the theme 'The Teaching of Electronic Engineering in Degree Courses'. The two previous very successful conferences were held in 1973 and 1976.

It is hoped that the conference will provide a lively forum for delegates to exchange and debate their ideas.

To aid the selection of material for the conference, the Organizing Committee has designated the following topics for inclusion in the programme.

Enhanced/enriched Degree Courses

- Course structure and content
- Industrial involvement
- Professional recognition
- Type 'A and B' courses
- Accreditation
- Funding
- Student selection

Engineering Research

- Funding—an ERC or ECRD?
- Postgraduate education
- Industrial collaboration

Microprocessors

Microprocessor education at undergraduate and postgraduate level

The Role of Industry

- Project schemes
- Teaching companies
- Postgraduate co-operation
- Graduate requirements
- Employment prospects
- Teaching from industry
- Management courses

Professional Requirements

- Chartered Engineer status
- Technician Engineer
- Role of 'The British Engineering Council'
- Professional engineering practice
- Registration

International Comparisons

EEC and North American degree courses

Undergraduate Degree Courses

- University and Polytechnic course structure
- Admissions techniques
- The teaching of design
- Project schemes

Educational Technology

- Programmed learning
- Use of the computer
- Audio-visual aids
- New developments

Continuing Education

Retraining and up-dating courses

Assessment

In courses
Examinations, and Laboratory classes.

Further information and the conference programme and registration forms may be obtained from Conference Secretariat, Department of Electronic Engineering, The University of Hull, Hull HU6 7RX.

Inter-University Institute of Engineering Control—Short Courses

A series of two- or three-day courses in Control and related topics is now being organized at the three Universities within the I.U.I.E.C.: University College, Bangor and the Universities of Sussex and Warwick. It is thought that they will be particularly useful as refresher courses for those with some experience in industry and for those who wish to learn of, or keep pace with, new developments. It is hoped that there may be some follow-up work with industry and that the courses themselves may in the future be modules for an industry-based M.Sc. degree.

Courses currently planned include:

Introduction to Digital Signal Processing
(12th–13th September, University of Sussex)

Introduction to Microcomputers
(24th–26th September, University of Sussex)

Information can be obtained from Sandra Jones, School of Engineering and Applied Sciences, University of Sussex, Brighton (Tel. Brighton (0273) 606755, Ext. 78 or 73).

'Smaller Project Management Directory'

The Smaller Project Management Directory, published by the British Overseas Trade Board, is intended to help British firms win more contracts to carry out smaller overseas turnkey projects—those below £10 million.

The Directory gives details of some project management companies and consultants who are experienced in negotiating contracts with overseas clients and in co-ordinating the activities of sub-contractors and who are willing to manage smaller projects. The Directory will enable British sub-contractors, nursing information about smaller projects on offer overseas in which they wish to participate, to approach a potential project manager and interest him in leading a bid.

British companies have sometimes been frustrated in supplying their equipment or services for projects because they do not have the capacity to take the lead with the overseas buyer—and they are unaware of companies and other organizations which will assume this responsibility. The Directory provides a solution to this problem. Free copies of the Directory are available to companies from Mr J. Hopkins, BOTB, Room G16, Export House, 50 Ludgate Hill, London EC4M 7HU or from the nearest BOTB regional office.

Institution Premiums for 1978

The Council of the Institution announces that authors of the following papers are to receive Premiums for outstanding papers published in the Journal during 1978.

MAIN PREMIUMS

CLERK MAXWELL PREMIUM *Value £75*

For the most outstanding paper on any subject published in the Institution's Journal during the year.

Professor J. G. Simmons and A. A. El-Badry (University of Toronto)
'Switching phenomena in metal-insulator-n/p structures: theory, experiment and applications'
(May 1978 issue of the Journal)

HEINRICH HERTZ PREMIUM *Value £50*

Physical or mathematical aspects of electronics or radio

G. Kompa (Endress & Hauser)
'Design of stepped microstrip components'
(January/February)

MARCONI PREMIUM *Value £50*

Engineering

F. T. Sakane and R. Steele (University of Technology, Loughborough)
'Two-bit instantaneously adaptive delta modulation for p.c.m. encoding'
(April)

SPECIALIZED TECHNICAL PREMIUMS

LORD BRABAZON PREMIUM *Value £25*

Aerospace, maritime and military systems

Professor D. E. N. Davies and Mrs M. S. A. Rizk (University College London)
'A broadband experimental null-steering antenna system for mobile communications'
(October)

REDIFFUSION TELEVISION PREMIUM *Value £50*

Communications

N. M. Maslin (Royal Aircraft Establishment, Farnborough)
'Assessing the circuit reliability of an h.f. sky-wave air ground link'
(October)

DR NORMAN PARTRIDGE PREMIUM *Value £25*

Audio Frequency Engineering

V. Schiffer (Wandel & Goltermann) and W. A. Evans (University College of Swansea)
'Approximants in sinewave generation and synthesis'
(March)

J. LANGHAM THOMPSON PREMIUM *Value £50*

Systems and Control Engineering

Cdr. M. J. Ashworth, RN (RNEC) and Professor D. R. Towill (UWIST)
'Computer-aided design tracking systems'
(October)

ARTHUR GAY PREMIUM *Value £25*

Production Techniques

W. Goedbloed (ELCOMA, Eindhoven), H. Hieber (Philips, Hamburg) and A. G. van Nie (Philips Research Laboratories, Eindhoven)
'Ageing tests on microwave integrated circuits'
(January/February)

GENERAL PREMIUMS

LESLIE McMICHAEL PREMIUM *Value £25*

Management Techniques

E. E. Barnard, Chartered Patent Agent
'Patent law reform'
(May)

SIR J. C. BOSE PREMIUM *Value £25*

Paper by Indian Scientist or Engineer

T. S. Lamba and Professor M. N. Faruqui (Indian Institute of Technology)
'Intelligible voice communication through adaptive delta modulation at bit-rates lower than 10 kbit/s'
(April)

Papers of sufficiently high standard were not published within the terms of the following Premiums and they are withheld:

Charles Babbage Premium (Computers)

A. F. Bulgin Premium (Components or circuits)

Lord Rutherford Premium (Nuclear physics or engineering)

P. Perring Thoms Premium (Radio or television reception)

Sir Charles Wheatstone Premium (Instrumentation or measurement)

Dr V. K. Zworykin Premium (Medical and biological electronics)

Admiral Sir Henry Jackson Premium (History of radio or electronics)

Eric Zepler Premium (Education)

Hugh Brennan Premium (North Eastern Section Paper)

Local Sections Premium

INSTITUTION OF ELECTRONIC AND RADIO ENGINEERS

Notice of Annual General Meeting

NOTICE IS HEREBY GIVEN that the EIGHTEENTH ANNUAL GENERAL MEETING of the Institution since incorporation by Royal Charter will be held on THURSDAY 25th OCTOBER 1979 at 6.00 p.m. in the Large Theatre at the London School of Hygiene and Tropical Medicine, Keppel Street, Gower Street, London W.C.1.

AGENDA

1. To receive the Minutes of the Seventeenth Annual General Meeting of the Institution since Incorporation by Royal Charter held on 5th October 1978.
(Reported on pages 631–635 of the December 1978 issue of *The Radio and Electronic Engineer*.)
2. To receive the Annual Report of the Council for the year ended 31st March 1979.
(To be published in the September 1979 issue of *The Radio and Electronic Engineer*.)
3. To receive the Auditors' report, Accounts and Balance Sheet for the year ended 31st March 1979.
(To be published in the September 1979 issue of *The Radio and Electronic Engineer*.)
4. To confirm the election of the Council for 1979–80.

In accordance with Bye-Law 49 the Council's nominations were sent to Corporate Members by a Notice dated 15th May 1979 in the May 1979 issue of *The Radio and Electronic Engineer*. As no other nominations have been received under Bye-Law 50 for the following offices, a ballot will not be necessary and the following members will be elected:

President

Professor W. Gosling, A.R.C.S., B.Sc.

Vice-Presidents

Under Bye-law 46, all Vice-Presidents retire each year but may be re-elected provided they do not serve thereby for more than three years in succession.

For Re-election: H. E. Drew, C.B.; Brigadier R. W. A. Lonsdale, B.Sc.; S. J. H. Stevens, B.Sc.(Eng.)

For Election: Professor J. R. James, Ph.D.; P. K. Patwardhan, M.Sc., Ph.D.; J. Powell, B.Sc., M.Sc.

Honorary Treasurer

For Re-election: S. R. Wilkins

Ordinary Members of Council

Under Bye-law 48, Ordinary Members of Council are elected for three years and may not hold that office for more than three years in succession.

Fellows

The following must retire: L. A. Bonvini; L. F. Mathews, O.B.E.

For Election: Colonel W. Barker; R. Larry

Members

The following must retire: N. G. V. Anslow; K. Copeland; Group Captain J. M. Walker, R.A.F.

For Election: Instructor Commander D. J. Kenner, B.Sc., M.Sc., R.N. (Ret.); B. Mann, M.Sc.; K. R. Thrower

Associate Member

The following must retire: Lieutenant-Commander J. Domican, R.N.

For Election: P. J. Hulse

Associate

The following must retire: T. D. Ibbotson

For Election: M. W. Wright

The remaining members of Council will continue to serve in accordance with the period of office laid down in Bye-law 48.

5. To appoint Auditors and to determine their remuneration.
(Council recommends the re-appointment of Gladstone, Jenkins and Co., 50 Bloomsbury Street, London W.C.1.)
6. To appoint Solicitors
(Council recommends the re-appointment of Braund and Hill, 6 Gray's Inn Square, London W.C.1.)
7. Awards to Premium Winners
8. Any other business.
(Notice of any other business must have reached the Secretary not less than forty-two days prior to the meeting.)

By Order of the Council
S. M. DAVIDSON, Secretary

Members' Appointments

BIRTHDAY HONOURS

The Council has sent its congratulations to the following members whose names appeared in Her Majesty's Birthday Honours List:

MOST EXCELLENT ORDER OF THE BRITISH EMPIRE

To be an Ordinary Officer of the Civil Division (O.B.E.)

Robert Brennand (Member 1955) who has recently been promoted to Superintending Engineer in the Science and Technology branch of the Department of Health and Social Security. Mr Brennand has been associated with the Institution's Medical and Biological Electronics Group since its formation in 1959 and he served for several years as Chairman.

To be Ordinary Members of the Civil Division (M.B.E.)

Frederick George Jacobs (Graduate 1949) is Deputy Chief Engineer of Ultra Electronic Communications.

Angus Arthur McKenzie (Fellow 1975, Member 1972) is Principal of the audio and sound recording consultancy, Angus McKenzie Facilities Limited, and he receives the award 'for service to audio research for the blind and disabled'.

To be an Ordinary Member of the Military Division (M.B.E.)

Squadron Leader Raymond Charles Ryan Johnston, RAF (Member 1972, Graduate 1969), recently stationed at RAF Gatow.

CORPORATE MEMBERS

H. W. Akester, M.B.E. (Fellow 1970, Member 1947) who has been working as Consultant on electrical and electronic engineering to the timber industry in South Africa, is shortly

returning to the United Kingdom. Since the war he has held senior appointments with the broadcasting organizations in Ghana, South Africa and Liberia.

F. K. El-Jadiry, M.Sc. (Fellow 1974, Member 1960) has joined the Emirates Telecommunications Corporation as Contracts Manager. Earlier this year he successfully completed a postgraduate course at Trinity College, University of Dublin in the System Development Programme.

P. M. Elliott (Member 1962) who has been a Technical Officer on the Institution's staff dealing principally with conference organization since 1972, has joined Walmore Electronics where he will be concerned with quality assurance aspects of the company's military contracts. Following commissioned service with the Royal Air Force, part of it at the then Telecommunications Research Establishment, Malvern, Mr Elliott joined Ferranti to work on radar and computers and he subsequently operated a private consultancy for computer personnel. While in Edinburgh, he was a member and later Chairman of the Scottish Section Committee and he helped organize conferences on computers and medical electronics. He also served on the Computer Group Committee prior to 1972.

P. J. Burleigh, B.Sc. (Member 1978, Graduate 1976) has recently left to take up an appointment as a Project Engineer in Oman where he will be responsible for installing and commissioning a large microwave system on behalf of Cable and Wireless with whom he has been since 1965.

R. S. Davidson (Member 1973, Graduate 1965) who has been with British Gas since 1966 has been appointed Chief Systems Planning Engineer in the Communications and Instrumentation Department at its Headquarters in London. He was previously an Operations and Maintenance Engineer with the Eastern Region.

S. A. Jinadu (Member 1964, Graduate 1959) until recently Deputy Chief Engineer with the Nigerian Broadcasting Corporation has joined BBC Brown Boveri (Nigeria) as Project Coordinator for Ikorodu External Transmitter Installation. This project involves the installation and commissioning of 500 kW high frequency transmitters for the Voice of Nigeria External Service of the Federal Radio Corporation of Nigeria.

Sqn Ldr V. J. Ludlow, M.Sc., R.A.F. (Ret.) (Member 1976) who was to have taken up an appointment in Iran for British Aerospace is now concerned with the management support for a major weapons system at Bristol.

NON-CORPORATE MEMBERS

P. A. Lam (Graduate 1976) who has been Senior Supervisory Engineer with Commercial Television (Hong Kong) since 1975 has joined Electronic Industry, Hong Kong, as Manager, Instrumentation.

Lee Kam Biu (Graduate 1978) has been appointed Assistant Training Officer with Cable and Wireless in Hong Kong. He has been with the company since 1966 and latterly was Technical Supervisor/Instructor at the Technical College in Hong Kong.

M. A. Renman, B.Sc., M.Sc. (Graduate 1979) who joined Standard Telephone and Cables as a Senior Engineer working on circuit design last year, is moving to Standard Telecommunication Laboratories as a Senior Research Engineer I in the Microelectronics Division.

D. A. Wintle (Graduate 1978) has moved from Rediffusion (SW) where he was Test Engineer in Bristol to Redifon Computers, Crawley as a Customer Engineer.

Sqn Ldr D. M. McKeown, M.B.E., R.A.F. (Associate Member 1975) has been posted to R.A.F. Brize Norton as Officer Commanding No. 81 Signals Unit. In the past year he was on the Electrical Engineering Staff at the Headquarters Strike Command R.A.F.

G. J. Reece (Associate Member 1976) has been appointed Product Manager (Industrial Lasers) with Walmore Electronics, London For the past two years he was with Seer TV Surveys as an Electronics Engineer.

Members are invited to notify the Institution of changes in their appointments for inclusion under the above heading. Details may be sent in using the 'Members' Records' form which is printed occasionally at the back of the Journal, or in a letter.

Applicants for Election and Transfer

THE MEMBERSHIP COMMITTEE at its meeting on 5th June 1979 recommended to the Council the election and transfer of the following candidates. In accordance with Bye-law 23, the Council has directed that the names of the following candidates shall be published under the grade of membership to which election or transfer is proposed by the Council. Any communication from Corporate Members concerning the proposed elections must be addressed by letter to the Secretary within twenty-eight days after publication of these details.

June Meeting (Membership Approval List No. 260)

GREAT BRITAIN AND IRELAND

CORPORATE MEMBERS

Transfer from Member to Fellow

ANSLOW, Nigel George Victor. *East Molesey, Surrey.*
TEED, Cyril Frederick H. *Little Baddow, Essex.*

Direct Election to Fellow

DORÉ, John Raymond. *Wilmslow, Cheshire.*

Transfer from Graduate to Member

AGGARWAL, Om Prakash. *Manchester.*
CROASDALE, James Walter. *Preston, Lancashire.*
DILLIEN, Paul. *Colchester, Essex.*
IMPEY, Alan Adrian. *Romsey, Hants.*
MASON, David Frank. *Chalfont St. Giles, Buckinghamshire.*
TAYLOR, Dhansukh Maganlal. *Cambridge.*

Direct Election to Member

BRICE, William Sidney James. *Tiverton, Devon.*
ELSHEIKH, Khalafalla Elhag. *Canterbury, Kent.*
KINSEY, Michael. *Willington, Derby.*
MSUTTA, Gurbux Singh. *Wickford, Essex.*
REYMOND, John Francis. *Rochester, Kent.*
WHARTON, Colin. *Stourport-on-Severn, Worcestershire.*

NON-CORPORATE MEMBERS

Transfer from Student to Graduate

LEWIS, David Kenneth. *Cheltenham, Glos.*
WILLESLEY-COLE, Oliva Ayodele Lois. *Basildon, Essex.*

Direct Election to Graduate

TAILOR, Mahendra. *London.*

Transfer from Student to Associate Member

METAXAS, Sotos. *London.*

Direct Election to Associate Member

BECKLEY, Anthony. *London.*
HULL, David John. *Wincanton, Somerset.*
LARKINS, Michael John William. *Thatcham, Berkshire.*

Direct Election to Associate

WILSON, Anthony George. *Bracknell, Berkshire.*

Direct Election to Student

CHOW, Yew Meng. *Strathclyde, Glasgow.*
DESIMONE, Robert Vincenzo. *Bath, Avon.*

OVERSEAS

CORPORATE MEMBERS

Transfer from Graduate to Member

MONDAL, Kalyan. *Goleta, California, USA.*

Direct Election to Member

NAVARATNAM, Ratnakumar. *Damman, Saudi Arabia.*
TAN, Seng. *Petaling Jaya, Selangor, Malaysia.*
YU, Luk Kai. *Kowloon, Hong Kong.*

NON-CORPORATE MEMBERS

Direct Election to Companion

A'ABAD, A. M. M. *Dacca, Bangladesh.*

Transfer from Student to Graduate

LO, King Chuen. *Kowloon, Hong Kong.*

Direct Election to Graduate

MARECHERA, Gervase Tony. *Christchurch, New Zealand.*
NAZEMI-MOGHADAM, Moosarza. *Mashad, Iran.*

Transfer from Student to Associate Member

HO, Ser Poon. *Singapore.*
YU, Kwok Chu Peter. *Kowloon, Hong Kong.*

Direct Election to Associate Member

IGWE, Levi Orjika. *Owerri, Imo State, Nigeria.*
LAI, Kam Chan. *Kowloon, Hong Kong.*
LEONG, Choon Luen. *Singapore.*
LEWIS, Nelson. *Lae, Papua New Guinea.*
NG, Hoy Kee. *New Territories, Hong Kong.*
N'JIE, Bakary Kebba. *Banjul, The Gambia.*
YEUNG, Wing Chuen. *Kowloon, Hong Kong.*

Direct Election to Student

AU, Kui Hing. *Wah Fu Estate, Hong Kong.*
CHAN, Cheuk To. *Tze Wan Shan, Hong Kong.*
CHAN, Ka Yeu. *Kowloon, Hong Kong.*
CHAN, Kwan Chak. *Hung Hom, Hong Kong.*
CHAN, Kwok Yin. *New Territories, Hong Kong.*
CHAN, Wai Lung. *Aberdeen, Hong Kong.*
CHENG, Chun Wing. *Kowloon, Hong Kong.*
CHIANG, Yuk Lun. *Aberdeen, Hong Kong.*
CHOW, Chi Ming Tommy. *Ching Yi Island, Hong Kong.*
CHU, Hong Kit. *Kowloon, Hong Kong.*
CHUEN, Tai Hoo. *North Point, Hong Kong.*
CHUNG, Chi Ming Tony. *Kennedy Town, Hong Kong.*
HO, Chi Tim Timothy. *Kowloon, Hong Kong.*
HO Kwong Pui. *Hong Kong.*
HUNG, Yeung Ming. *Hong Kong.*
KAM, Chi Sing. *Kowloon, Hong Kong.*
LEUNG, Chi Wing. *Hong Kong.*
LEUNG, Hon Wai. *Kowloon, Hong Kong.*
LI, Yin Fai. *Kowloon, Hong Kong.*
MAK, Chun Wah. *Kowloon, Hong Kong.*
MAN, Kam To. *Kowloon, Hong Kong.*
SHEK, Chung Ming. *Kowloon, Hong Kong.*
TANG, Man Shan. *Kowloon, Hong Kong.*
TEO, Buan Choo Willy. *Singapore.*
TO, Check Ming. *Chai Wan, Hong Kong.*
TONG, Kok Ping. *Kowloon, Hong Kong.*
TSUN, Ka Yin. *Kowloon, Hong Kong.*
WONG, Kwong Hung. *Hong Kong.*
WONG, Pak Kui. *Kowloon, Hong Kong.*
WU, Sing Wai. *Kowloon, Hong Kong.*
YIP, King Hoi. *Hong Kong.*
YUEN, Hoi Leung. *Kowloon, Hong Kong.*
YUEN, Man Fai. *Kowloon, Hong Kong.*

Advance Information on London Meetings

October 9th

100 Years of Piezoelectricity

Professor M. Redwood
At the London School of Hygiene and
Tropical Medicine

Evening Meeting (6 p.m.)

October 16th

Design of Control Systems for Advanced Aircraft

At the Royal Institution

Full-day Colloquium (10 a.m.)

October 23rd

Storage Devices for Medical and Biological Signal Analysis and Recording

Royal Institution

Half-day Colloquium (2 p.m.)

October 25th

A.G.M. and Presidential Address (see page 325)

November 6th

Analogue Filters

At the Royal Institution

Full-day Colloquium (10 a.m.)

November 20th

Maintenance in an Age of Micro-processors

At the Royal Institution

Full-day Colloquium (10 a.m.)

December 4th

Vibration

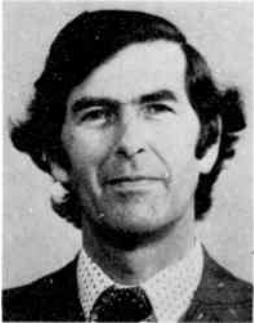
At the Royal Institution

Full-day Colloquium (10 a.m.)

This list is based upon information available at the time of going to press.

For any further information contact the Meetings Secretariat, IERE, 99 Gower Street, London WC1E 6AZ (Tel. 01-388 3075).

Contributors to this issue



Douglas Harris (Fellow 1975) graduated in electrical engineering and obtained his Ph.D. from Queen Mary College, University of London. Subsequent research and lecturing appointments were held at the Admiralty Laboratory, Baldock, Stanford University, California, Sheffield University and Portsmouth Polytechnic. He was professor and head of electrical engineering at Ahmadu Bello University, Nigeria, for seven

years, and a visiting professor at University College London. Since 1975 he has been professor and head of the Department of Physics, Electronics and Electrical Engineering at the University of Wales Institute of Science and Technology, Cardiff. Research interests have included high voltage and microwave discharges, microwave electron tubes, m.h.d. generation and atmospheric electricity, but present research centres around millimetre and submillimetre waves.



Roger Emery obtained a B.Sc. physics degree in 1964 and a Ph.D. in 1968 from Queen Mary College, University of London, for work on microwave spectroscopy. He then worked as a National Science Foundation Research Associate at the Electronics Research Center, Boston, in 1969 and at the Goddard Institute for Space Studies, New York, from 1970 to 1972, being involved with a programme of infra-red astronomy

using a stabilized balloon platform. In 1973 Dr. Emery joined the Appleton Laboratory, Slough (then known as the Radio and Space Research Station) and has worked on atmospheric propagation at near millimetre wavelengths and in the infra-red.



Jeffrey Purcell received the B.Sc.(Hons) degree in physics in 1962 and the M.Sc. and Ph.D. degrees in 1963 and 1968 respectively from the University of London. From 1967 to 1968 he was a Research Associate at Surrey University and from 1968 to 1969 a Research Associate at the University of Michigan, Ann Arbor, USA. For the past 9½ years he has worked at the Allen Clark Research Centre of the Plessey

Company, Towcester, where he has been a group leader of avalanche devices, and is now a research associate.



Albin Zavody obtained an honours degree in electrical engineering from the University of Sheffield in 1960. After working with microwave generated plasma discharges at the University, in 1964 he joined the Appleton Laboratory, Slough (then known as the Radio Research Station). His interests lie in studying the effect of the atmosphere on radio links at millimetre and sub-millimetre wavelengths and also in the infra-red.



Leonard Cram graduated in 1949 in physics from the University of Bristol. He then worked for the Services Electronics Research Laboratory on klystron development and later for the Imperial Tobacco Company before joining EMI Electronics at Wells in 1955 to do systems research on miniature radars. He now holds the position of Senior Staff Scientist. In 1958 Mr Cram initiated research which has, under his supervision, developed into a National Facility for Radio

Modelling. He has, since 1965, been supervising work between 100 GHz and 1 THz for many purposes including holographic imaging, communication and radar modelling. Mr Cram was the Director of AGARD lecture series No. 59 on Determination and Use of Radar Scattering Characteristics and has published and presented papers on topics in radar scale modelling, radio holography and radar systems assessment.



Sydney Woolcock graduated from Exeter University in 1951 and, following a period in the Royal Air Force as an Education Officer at No. 1 Radio School, joined EMI at the end of 1954 as a Development Engineer to work on missile telemetry. In 1958 he transferred to the Research Department at EMI Electronics, Wells, where he was engaged in experimental and theoretical studies related to target radar

scattering. From 1961 to the present he has led an ever-growing team concerned with the evolution of the Radio Modelling facility and with the study of radar/target scattering interaction. At present, in addition to being Head of Radio Modelling, Mr Woolcock occupies the position of Deputy Research Manager at Wells. He has published several papers relating to scale modelling and target scattering. In addition, he has given post-graduate lectures at the University of Birmingham on the Bosworth course and has also been engaged in international co-operative radar scattering studies.



Stephen Johnston gained the B.E.E. degree with Honors in 1948 and the M.S.E.E. degree in 1949 from the Georgia Institute of Technology. He continued at Georgia Tech. until 1950 as a research assistant in the Engineering Experiment Station, and then entered the Federal Civil Service in 1950 at the Joint Long Range Proving Ground, Patrick AFB, Florida. He has been employed by the US Army Missile

Command at Redstone Arsenal, Alabama since 1951, and is now in the Advanced Systems Concepts Office, US Army Missile Research and Development Command.

Mr Johnston has published and presented over fifty papers at numerous international technical symposia, both professional and government, including the Tri-Service Radar Symposia, Joint EW Conferences and AOC EW Symposium and he holds several patents. His areas of interest include electronic warfare, weapon system simulation, penetration aids for ballistic missiles, radar analysis, target signature characteristics, ballistic missile trajectory and guidance analysis, counter-mortar radars, magnetic bubbles, and millimetre/sub-millimetre wave radar.

A member of the Radar Systems Panel of the IEEE Aerospace and Electronic Systems Society and Chairman of the Radar ECCM Committee of that panel, Mr Johnston created the term 'ECCM Improvement Factor' which was recently incorporated into the IEEE Standard Radar Definitions. He is Editor in Chief of the International Radar Directory which is currently under preparation, and of the forthcoming reprint volume: 'Radar Electronic Counter-Countermeasures'.



Paul Clancy was educated at University College, Dublin, where he received the B.Sc. degree in physics, mathematics and chemistry in 1969. Subsequently at Newcastle upon Tyne Polytechnic he received the M.Sc. degree in semiconductor physics in 1970 and the Ph.D. degree in 1974 for a thesis entitled 'Gaseous impurity effects in high frequency discharge plasma'.

In 1973 Dr. Clancy joined Marconi Space and Defence Systems in Stanmore, England, where he worked on the elimination of multipactor and other discharge problems in space communications hardware. Since 1975 he has been employed by ESA at the European Space Research and Technology Centre, Noordwijk, working on research and development activities in the fields of microwave technology and microwave amplifier and filter development. For the past year he has co-ordinated and managed development contracts for material science instrumentation and for submillimetre and far infra-red spacecraft payload hardware.



Brian Clifton received the B.Sc. degree with Honours in electrical engineering and the Ph.D. degree from the University College of North Wales, Bangor, in 1961 and 1964 respectively. From 1964 to 1966 he was a Visiting Assistant Professor in the Department of Electrical Engineering at the Massachusetts Institute of Technology. In 1966 he joined the M.I.T. Lincoln Laboratory, Space

Communications Division, where he engaged in research into the microwave behaviour of semiconductor devices and circuits and the development of low-noise GaAs Schottky barrier diodes for the LES-8/9 millimetre-wave communications systems. He also worked on low-noise parametric amplifiers and mixers for use at millimetre-wave frequencies. In January 1976 Dr Clifton joined the Solid State Division for the specific purpose of developing Schottky barrier diodes for submillimetre applications. His current work continues in this area with the development of quasi-optical receiver systems and monolithic integrated circuits for the millimetre and submillimetre region.



Bernhard Rembold received the Dipl.-Ing. and Dr.-Ing. degrees in electrical engineering from the Technical University of Darmstadt in 1968 and 1974 respectively. From 1968 to 1975 he was at the Technical University of Darmstadt, first as an assistant and from 1972 as a lecturer, working in areas of line and field theory and antennas. Since joining AEG Telefunken, four years ago, he has been engaged in the

development of the mm-wave group.



Holger Meinel received his Diplom Ingenieur's degree in 1973 from the Rheinisch-Westfälische Technische Hochschule of Aachen, Germany. Since then he has been with AEG-Telefunken, Ulm, involved with research and development in the mm-wave range. In 1977 he became laboratory leader and he is now working in the field of mm-wave integration and sub-assembly.

See also page 418.

The Radio and Electronic Engineer, Vol. 49, No. 7/8

Schottky diode receivers for operation in the 100-1000 GHz region

BRIAN J. CLIFTON, B.Sc., Ph.D., M.I.E.E.E.*

SUMMARY

Increased interest in the millimetre and submillimetre wavelength regions during the past decade has stimulated the development of sensitive heterodyne receivers for a wide range of applications. The GaAs Schottky-barrier diode has received the most attention as a mixer in this wavelength range as a result of its sensitivity, reliability, mechanical stability and wide bandwidth and its ability to operate at room temperature. The concepts of receiver design and the particular problems associated with this region of the frequency spectrum are discussed. The optimization of material parameters and the device topology for low-noise operation are considered. The extension of fundamental waveguide mixers into the submillimetre region and the development of various types of quasi-optical receivers are reviewed. The development of integrated monolithic receivers in which antenna, coupling structure, mixer diode and intermediate-frequency filter network are fabricated on the GaAs surface offers the possibility of increased reliability, repeatable and improved performance, and the potential economy associated with integrated circuit technology. In addition, the possibility of monolithic receiver arrays provides the systems designer with a capability that was not previously attainable using discrete diode receivers. This newly emerging technology is reviewed and the potential impact on the 100-1000 GHz region is discussed.

* Lincoln Laboratory, Massachusetts Institute of Technology, Lexington, Massachusetts 02173.

1 Introduction

The past decade has seen an increased interest in the millimetre and submillimetre regions of the spectrum and in the related receiver technology. Until the early 1970s, submillimetre wave receivers were used mainly for metrology in a laboratory environment. They lacked sensitivity and tended to be mechanically unreliable. The development of heterodyne receivers with improved sensitivity has resulted in a wide range of applications in radio astronomy, plasma physics, frequency standards and spectroscopy, radar, aeronomy and in satellite-based radiometry. A brief review of a few selected applications will illustrate the diversity, and also the need for continuing development of heterodyne receiver technology in the millimetre and submillimetre wave regions.

Present day receivers with improved sensitivity and reliability have provided radio astronomers with access to a spectral region with many interesting molecular resonance lines. However, ground-based millimetre and submillimetre radio astronomy is limited to observation in the so-called 'atmospheric windows' and to observation from high-and-dry locations. The possibility of extended above-atmosphere observation in the decades ahead will remove the constraints imposed by atmospheric absorption and will allow full use to be made of the millimetre and submillimetre regions; however, this will also require the development of receivers with improved reliability. Atmospheric spectroscopy, in which atmospheric constituents, in particular pollutants, are measured from the ground or from a satellite, is becoming increasingly important to the future well-being of mankind. Both this and satellite-based radiometry for earth resources evaluation need reliable low-noise radiometric receivers.

A potentially powerful diagnostic tool has become available to nuclear physicists who, by examining the Doppler-shifted submillimetre laser radiation scattered by the plasma in a tokamak fusion reactor, will be able to determine plasma temperature and density, both critical parameters in the quest for controlled thermonuclear fusion. Improved receiver performance will be very welcome in this area.

The problems caused by atmospheric absorption and the success of optical-fibre technology have considerably limited the application of the millimetre and submillimetre spectral regions to terrestrial communications. However, the extremely large bandwidths available in the millimetre and submillimetre regions, and the larger antenna beamwidths compared to the optical region, offer the potential for useful space communication systems, in particular for satellite-to-satellite communications.

Although there are a number of interesting devices based upon different physical phenomena which are used as detectors and as heterodyne receivers in the 100 to 1000 GHz region of the spectrum, this paper will limit consideration to Schottky-barrier diode receivers and to coherent or heterodyne detection. A general review of

the different types of submillimetre mixer was presented by McColl¹ in 1977 including an extensive bibliography. Also in 1977, Kimmitt² reviewed the developments in both coherent and incoherent detectors for the wavelength range below 1 mm. More recently, Wrixon and Kelly³ have provided a comprehensive review of Schottky-barrier diode mixers for wavelengths below 1 mm.

The 100 to 1000 GHz frequency range draws on two related but different technologies. On the one hand is the long-wavelength regime of the microwave in which waveguide structures play a dominant role and in which the dimensions of circuit elements are comparable to the wavelengths involved. On the other hand is the optical regime in which optical beams propagate freely between optical surfaces, mirrors or lenses, whose transverse dimensions are typically many orders of magnitude larger than the wavelengths involved. The overlap of these two technologies in the millimetre and submillimetre regions has resulted in the so-called quasi-optical techniques in which circuit functions which would be performed by waveguide components in the microwave region are accomplished using the techniques of classical optics, but with beam diameters that are not many orders of magnitude greater than the wavelength. As Martin and Lesurf⁴ have pointed out, a submillimetre wave optical system designed with the aid of geometrical optics may perform in unexpected ways as a result of signal loss due to, for example, diffraction, poor collimation, poor focusing and imperfect coupling to the detector.

In the following Sections receiver design concepts are discussed with emphasis on the particular problems of applying them to the millimetre and submillimetre spectral regions. The Schottky-barrier diode is considered in terms of device topology and device optimization for the wavelengths of interest. The several different receiver

design approaches that have and are being used to cover the 100 to 1000 GHz region are described and compared. Diplexers and local oscillator sources are crucial components in any receiver, and they both present particular problems in this wavelength region. These problems and their possible solutions are discussed.

2 Receiver Design Concepts

The purpose of a heterodyne receiver is to convert a high-frequency signal to a lower-frequency signal, preserving the phase information of the high-frequency signal and adding a minimum of noise or degradation to the signal in the conversion processes. A block diagram of a typical millimetre or submillimetre-wave heterodyne receiver is shown in Fig. 1. The heart of any heterodyne receiver is the non-linear mixing element that combines a low-level radio-frequency input signal with a local oscillator signal to produce a signal at the difference or intermediate frequency. The receiver elements after the i.f. amplifier are essentially independent of the frequency of the input signal. They depend mainly on the signal processing performed on the information in the i.f. signal and are not dealt with here.

The l.o. signal is usually many orders of magnitude larger than the r.f. input signal and gives rise to the non-linearity of the mixer by driving or switching the mixer element over some portion of its non-linear range. This large signal switching by the l.o. gives rise to harmonics of the l.o. frequency which appear as harmonic voltages across the mixer element and as harmonic currents through the mixer. This fact is made use of in harmonic mixers, where the l.o. frequency is much lower than the signal frequency and mixing is between the signal and one of the harmonics of the l.o. generated internally by the mixer. A typical millimetre or submillimetre mixer requires 1 to 10 mW of l.o. power, which is close to the maximum output power of typical present-

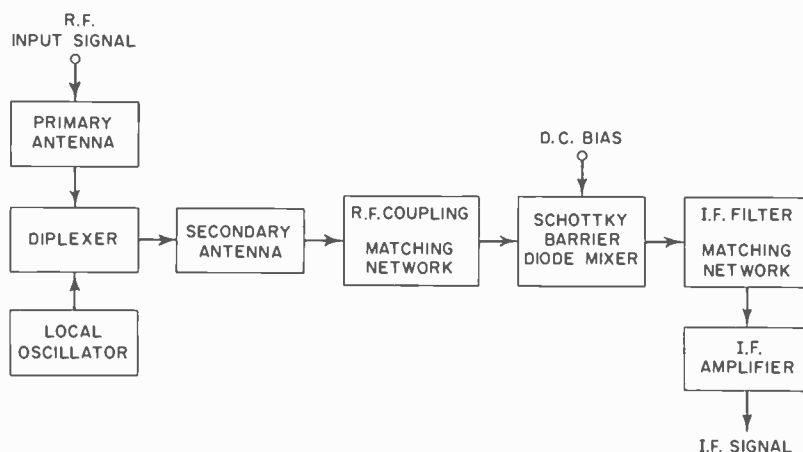


Fig. 1. Block diagram of a typical millimetre or submillimetre-wave heterodyne receiver.

day l.o. sources in the submillimetre region. Thus, in contrast to the microwave frequency range where there is abundant l.o. power available, the 100–1000 GHz frequency range requires that nearly all the available l.o. power be delivered to the mixer element.

The function of the diplexer is to combine the l.o. signal with the r.f. input signal and to send both signals to the mixer with a minimum of loss. In the microwave or low-millimetre wave range, the diplexer could be a hybrid, magic T or even a directional coupler with, in all cases, the signal and l.o. energy propagating as guided waves confined within the component. At higher frequencies, where quasi-optical techniques are more appropriate, the diplexer will be a quasi-optical component and the signal and l.o. wave energy will propagate in free-space beam modes within the diplexer.

The primary antenna receives the input signal as a free-space plane wave and focuses the energy into a beam of appropriate diameter to send to the diplexer with minimum reflection and loss. The signal and l.o. energy exiting from the diplexer in overlapping beams must be appropriately coupled to the secondary antenna whose purpose is to convert the free-space energy propagating in beam modes into guided or confined wave energy that can be coupled to the Schottky-barrier junction where it appears as current through and voltages across the junction. Martin and Lesurf⁴ provide a comprehensive discussion of the problems of applying classical geometrical optics to the design of submillimetre-wave optics and indicate how beam-mode concepts can be applied. The antenna and mixing theorems^{5,6,7} must also be taken into consideration in the design of quasi-optical coupling structures located between the primary antenna and the diode junction.

The function of all the elements preceding the mixer is to collect, focus and convert the energy of the signal and l.o. waves, which are propagating as free-space electromagnetic waves, into electrical current flowing in the non-linear mixing element. In the case of a Schottky-barrier device, the actual diode has a diameter of the order of a few micrometres whereas the signal and l.o. free-space waves can have beam diameters of the order of centimetres. This implies a power-density concentration of the order of 10^8 in coupling the free-space energy to the diode junction. Losses and reflections should be minimized between the antenna and diode junction, and the diplexer must have very low loss in both signal and l.o. paths.

The Schottky-barrier diode presents impedances at the signal, l.o., all of their harmonics and at the i.f., which are dependent on diode parameters, l.o. wave-form, and d.c. bias. To obtain optimum performance, these impedances must be appropriately matched (signal, l.o. and i.f.) or terminated (harmonics) by the mixer embedding circuit. The diode also introduces loss and generates noise. The converted signal at the i.f. is amplified by an i.f. amplifier before further signal processing.

At microwave frequencies the signal and l.o. waves are guided and coupled to the diode by coaxial, waveguide, stripline, microstrip or other transmission-line media. Since the dimensions of the guiding media must be of the order of a wavelength to prevent energy propagation in undesirable modes, an upper-frequency limit is imposed by problems in fabricating the guiding structures, by difficulties in mounting signal processing components within the guide structures, and by guide attenuation that increases rapidly as dimensions are reduced and frequency is increased. Overmoded guiding structures have much lower loss and component integration is easier but problems of multimoding make it difficult to couple energy efficiently into the mixing element.

The frequency range under consideration corresponds to wavelengths in air of 3 to 0.3 mm. For most practical purposes, mechanical fabrication is limited to components with dimensions greater than about 0.1 mm, although tolerances and surface finish can be held to much smaller dimensions. Typical matching and coupling structures in the microwave region have dimensions from a quarter to one-tenth wavelength. Thus, if similar structures are to be scaled to operate in the millimetre and submillimetre regions, present-day mechanical fabrication techniques will restrict fabrication of critical coupling and matching components to frequencies lower than about 400 GHz. However, photolithographic techniques used in semiconductor device fabrication allow dimension control down to about one micrometre, and X-ray or electron beam lithography can extend dimension control down to below 0.1 μm . Clearly, it is attractive to consider using these techniques to build coupling and matching elements for the frequency range above 400 GHz where mechanical fabrication techniques are extremely difficult, if not impossible, to apply. Thus, there is considerable interest in the fabrication of monolithic integrated circuits in which the elements in Fig. 1, from the secondary antenna up to and possibly including the i.f. amplifier, are fabricated on a single piece of GaAs. Critical circuit elements can be located close to the diode junction with the possibility of much lower coupling loss.

3 Schottky-barrier Diodes

The structure of a typical Schottky-barrier diode is shown in Fig. 2(a) and is similar to that described by Young and Irvin.⁸ The n on n⁺ GaAs chip is typically 0.25 mm square by 75 μm thick. The surface of the epitaxial layer is covered with a protective layer of silicon dioxide approximately 4500 Å thick and an alloyed ohmic contact is made onto the lapped and polished surface of the n⁺ substrate material. Holes are opened through the silicon dioxide layer and Schottky-barrier junctions are formed on the exposed GaAs surface by electroplating, sputtering or evaporation. A chip will typically have upwards of 1000 individual Schottky-barrier diodes, but only one is contacted by an etched metal wire or whisker. Whiskers are made of various

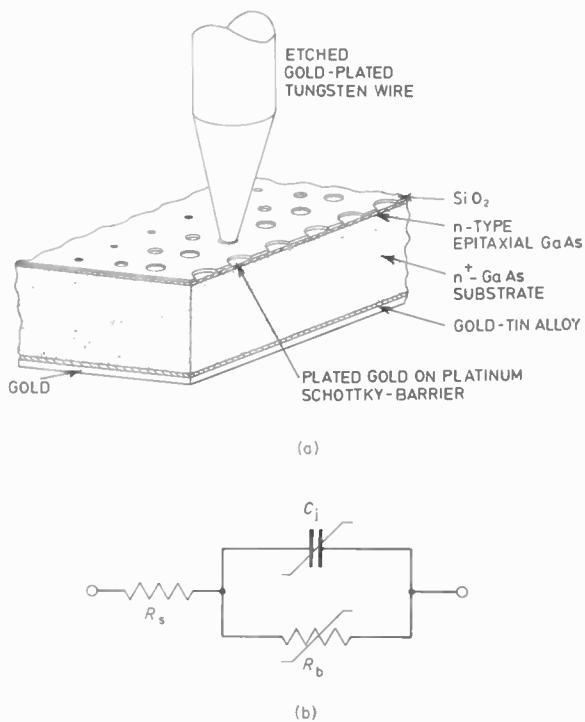


Fig. 2. A typical point-contact Schottky-barrier diode.
 (a) Structure.
 (b) Simple equivalent circuit.

metals and metal alloys and range from 12.5 to 50 μm in diameter. The function of the whisker is to provide a reliable low-loss electrical contact to the Schottky-barrier metallization. In the submillimetre region the whisker also serves as secondary antenna, coupling and matching structure and is therefore a critical element in the determination of receiver performance.

In the equivalent circuit for a Schottky-barrier diode (Fig. 2(b)) the non-linear barrier resistance, R_b , is in parallel with the non-linear depletion layer capacitance, C_j . The series resistance, R_s , arises from the undepleted epitaxial layer, spreading resistance in the substrate, chip-edge resistance and ohmic contact resistance.⁹ At high frequencies, the depletion-layer capacitance will tend to short out the barrier resistance, R_b , resulting in degraded performance.

Extensive investigations into the theory of resistive mixers have been published.¹⁰⁻¹³ The so-called diode parasitics, R_s and C_j , degrade the diode performance as a mixer by introducing loss at both the signal and intermediate frequencies. Saleh¹² has shown that in the submillimetre region the only mixer circuit that is realizable is the so-called Y mixer in which all the out-of-band frequencies (all frequencies except the l.o., signal, image and i.f.) are short circuited by C_j . Held and Kerr¹³ have shown that the 'anomalous' noise observed in millimetre-wave mixers can be accounted for by correlation of down-converted components of the time-varying shot noise.

Several authors^{3,9,14-16} have considered the influence of material and circuit parameters on the performance of Schottky-barrier diodes as heterodyne detectors in the millimetre and submillimetre region. Epitaxial layer carrier concentration should be in the low 10^{17} cm^{-3} range and the epitaxial layer should have a thickness of 0.1-0.2 μm to minimize the contribution of the undepleted epitaxial layer to series resistance. Diode diameters in the 1 to 2 μm range are suitable for the 100-1000 GHz frequency region. Champlin and Eisenstein¹⁷ have proposed a high-frequency model for Schottky-barrier diodes on heavily doped bulk material which includes the influence of skin effect, carrier inertia and displacement current. The high-frequency model indicates that operation near the plasma frequency is impractical, but that above the plasma frequency a broad frequency range is available where operation should be feasible. Kelly and Wrixon,^{16,3} in extending the high-frequency model of Champlin and Eisenstein to diodes on epitaxial material with epitaxial layer carrier concentration in the low 10^{17} cm^{-3} range, have shown that optimum diode diameters on GaAs range from 2 μm at 100 GHz to 1.2 μm at 1000 GHz. They also show that below 1000 GHz, GaAs exhibits lower conversion loss than silicon for the same epitaxial layer thickness. Careful control of material parameters and close control of diode dimensions will be required for efficient operation in the region around 1000 GHz. X-ray and electron beam lithography will probably help in this regard.

As diode diameter is reduced, diode series resistance increases very rapidly and severe current crowding can occur at the diode periphery. Increasing the diode perimeter for a given area will reduce the spreading resistance. Diodes of rectangular or stripe geometry have greater perimeter-to-area ratio than circular diodes of the same area. Wrixon¹⁸ used electron beam lithography to fabricate diodes in the form of crossed stripes and reported a 30% reduction in spreading resistance over circular diodes of approximately the same area. McColl *et al.*¹⁹ have proposed a contact-array diode in which a large number of submicron-size diode contacts fabricated by electron-beam techniques are connected in parallel. Schneider *et al.*²⁰ have fabricated diodes with a bathtub-like shape (1.6 \times 6.8 μm) to minimize spreading resistance. These diodes, which also had very thin epitaxial layers grown by molecular beam epitaxy, are reported to have given the lowest noise temperature ever reported for a resistive mixer.

4 Waveguide Mixers

The fundamental waveguide mixer, used extensively throughout the microwave region, has been extended into the millimetre region with considerable success (Fig. 3). The waveguide-equivalent circuit is well understood²¹ and mixer theories^{12,13} are easily applied to the structure. A horn antenna is usually used to couple the r.f. input

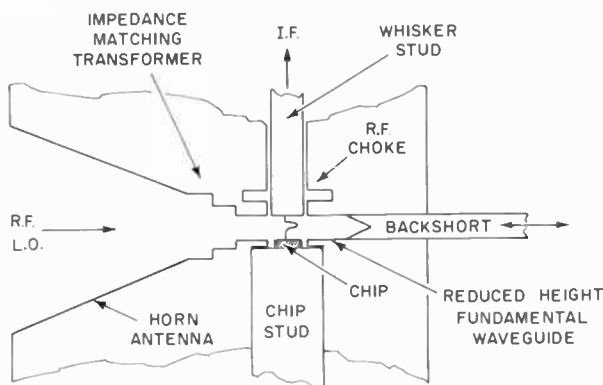


Fig. 3. Cross-sectional details of a typical millimetre-wave fundamental waveguide mixer.

and l.o. signals into the mixer. If the diode is mounted in reduced-height waveguide in order to provide the optimum impedance environment to the diode, then an impedance transformer is required to match the free-space impedance of the input antenna horn to the reduced height mixer mount. At the higher millimetre-wave frequencies, the additional fabrication complexity and loss introduced by the transformer and reduced-height waveguide usually favour mounting the diode in full-height guide. A movable or fixed backshort located approximately a quarter wave behind the diode presents a high impedance at the whisker-diode location and provides reactive tuning of the whisker and chip parasitics so that the diode junction will see a real impedance at the signal frequency. The r.f. choke in the i.f. output port can be located on either the whisker or chip stud. At the higher frequencies, the coaxial structure dimensions that are necessary to prevent waveguide-mode propagation in the i.f. output port present a considerable challenge to the millimetre-wave circuit designer and to the machinist. Suspended stripline with photolithographically formed filters¹⁸ provides better control over the critical i.f. port filter dimensions. The backshort is a source of loss and both contacting and non-contacting shorts have been used. Non-contacting shorts give more repeatable results but are difficult to make at the higher frequencies and have slightly more loss than the best contacting shorts. At lower millimetre frequencies, the diode is frequently mounted in a Sharpless-wafer mount²² which permits easy diode replacement.

In 1974, Wrixon¹⁸ reported results on fundamental waveguide mixers at 140, 175 and 230 GHz. For mixers operating at 140 and 175 GHz, the diodes were mounted in conventional Sharpless wafers. At 230 GHz, a quartz stripline mixer mount was used in which the contact whisker was bonded onto a stripline metallization photoetched on a 50- μm -thick silica substrate. At 140 GHz, a minimum double sideband (d.s.b.) noise figure of 3.8 dB was obtained with a 2- μm -diameter diode; this corres-

ponds to a mixer noise temperature of 400 K. At 175 GHz, a minimum d.s.b. conversion loss of 8.1 dB (noise temperature 1570 K) was obtained using a $0.4 \times 4 \mu\text{m}$ electron-beam-fabricated crossed-stripe diode. At 230 GHz, the stripline mixer with a 2- μm circular diode gave a minimum d.s.b. noise figure of 12.6 dB (noise temperature approximately 5000 K). It was reported that at 175 and 230 GHz there was insufficient l.o. power available to achieve minimum conversion loss.

In 1975, Kerr²³ reported on two mixers designed to operate in the 80–120 GHz range for use on the National Radio Astronomy Observatory's 36-ft. radio telescope at Kitt Peak, Arizona. One mixer for room-temperature operation used a contact whisker mounted on a four-section coaxial choke supported in stycast dielectric. This mixer was unstable when cooled due to relative motion between the whisker and diode. The other mixer, for cryogenic operation, was a modification of the room-temperature mixer with the whisker-chip contact replaced by a quartz diode-mounting structure. Two quartz strips with metallized r.f. choke structures were supported by and glued to a third unmetallized quartz strip. A diode chip was soldered to a gold bracket on one of the metallized quartz strips and a contact whisker was bonded to the other metallized strip. The whisker was brought into contact with the diode before the metallized quartz strips were glued to the unmetallized quartz strip. Typical values of the single sideband (s.s.b.) conversion loss and s.s.b. mixer noise temperature measured at 115 GHz were reported to be 5.5 dB and 500 K, respectively, for the room-temperature mixers with a 1.49-GHz i.f.; and 5.8 dB and 300 K, respectively, for the cryogenic mixer at 77 K, or 18 K with a 4.75-GHz i.f. Both mixers used 2.5- μm -diameter GaAs diodes in 4:1 reduced-height fundamental waveguide.

In 1977, Kerr, Mattauch and Grange²⁴ reported a new mixer design for the 140–220 GHz range. This fundamental waveguide mixer uses 4:1 reduced height waveguide with a four-step, electroformed-copper, waveguide transformer. The r.f. choke in the i.f. port is fabricated photolithographically on a 127- μm -thick fused-quartz substrate and the diode chip with 2.5- μm -diameter diodes is soldered to the end section of the r.f. choke filter so that it is flush with the waveguide wall. The waveguide height in the vicinity of the diode is only 0.16 mm, which is comparable to the thickness of the diode chip so that little space is available for the contact whisker unless the chip is recessed into the waveguide wall. At 170 GHz, s.s.b. mixer noise temperatures of 1100–1300 K with s.s.b. conversion loss of 6.2–7.2 dB were reported. The authors believe the asymmetrical split-block configuration used for the mixer should be usable up to 300 GHz.

In 1978, Erickson²⁵ reported a fundamental-mode waveguide mixer for the 318–348 GHz range that uses a 2- μm -diameter Schottky-barrier diode on GaAs. A 4×6 mm waveguide horn produces a $f/3.2$ beam and tapers down to 0.2×0.65 mm at the plane of the diode.

The i.f. port contains a filter consisting of a quarter-wave, low-impedance, coaxial section followed by a radial line choke. A 0.25-mm-diameter hole in the top of the waveguide above the diode chip stud permits insertion of a 0.37-mm-diameter electrosharpened phosphor bronze whisker, which is soldered to the centre conductor of the i.f. port. A Michelson interferometer diplexer and ellipsoidal mirrors provide very low-loss coupling for the l.o. and signal beams into the horn antenna. At 318 GHz, a conversion loss of 9.3 dB (s.s.b.) and a mixer noise temperature of 3100 K were measured to give a s.s.b. system noise temperature of 4000 K.

More recently, Vizard *et al.*²⁶ have reported measurements using a mixer similar to that described by Kerr *et al.*,²⁴ but with a 1- μ m-diameter platinum Schottky-barrier diode that was fabricated on GaAs with an abrupt transition between the epitaxial layer and the substrate. The epitaxial layer was prepared by organometallic cracking at low pressure as reported by Lacombe *et al.*²⁷ One of the most interesting aspects of this work was the extremely low l.o. power requirements. At 170 GHz, using a 4-GHz i.f. the best noise performance was obtained with only 125 μ W of pump power and for l.o. input powers between 50 and 250 μ W the s.s.b. noise temperature was reported to be less than 1200 K. Similar results were obtained with 2.2- μ m-diameter Schottky diodes made on molecular-beam epitaxial material. Measurements made at 111 GHz at a temperature of 295 K gave a minimum s.s.b. mixer noise temperature of under 650 K with a l.o. input power of 300 μ W. Cooling to a temperature of 16 K reduced the l.o. requirement for minimum noise by a factor of 3 to 4. At 16 K the mixer required only 100 μ W of l.o. power to give a minimum s.s.b. noise temperature of 265 K and for l.o. input powers between 10 and 200 μ W the mixer s.s.b. noise temperature remained below 350 K.

As a result of the difficulty in making l.o. sources above 100 GHz and the low efficiency of frequency multipliers, there is considerable interest in harmonic mixers, and, in particular, in second-harmonic mixers. The theoretical work of Meredith and Warner²⁸ indicates that the frequency conversion efficiency of a second-harmonic mixer is not greatly inferior to that of a fundamental mixer. Since frequencies differing by a factor of two must be coupled into the diode, the usual configuration adopted is a crossed-waveguide mount with the diode chip mounted in the smaller cross-section signal waveguide. The contact whisker traverses both the l.o. guide and signal guide passing through a small coupling hole between the waveguides.

Kawasaki and Akaike²⁹ have reported a broadband second-harmonic mixer covering 76–106 GHz. The mixer uses a 3- μ m-diameter GaAs Schottky-barrier diode and operates with a 1.7-GHz i.f. The measured mixer conversion loss was close to 15 dB over the 76–106 GHz frequency range. Goldsmith and Plambeck⁶⁷ reported a 230-GHz second-harmonic mixer of crossed-waveguide construction with a GaAs Schottky-barrier diode located

in the smaller signal waveguide. A d.s.b. system noise temperature of 6000 K (noise figure of 13 dB) was measured at 230 GHz with a 1.4 GHz i.f., which is comparable to the system performance reported previously for a fundamental mixer.¹⁸ Higher-order harmonic mixers, although useful, have, in general, a performance considerably inferior to both second harmonic and fundamental mixers.

One of the more interesting mixer developments of the past few years is the subharmonically pumped down-converter^{30,31} that uses an antiparallel diode-pair. A pair of diodes connected in parallel, with the anode of one connected to the cathode of the other, have a combined current-voltage characteristic which is symmetrical about the origin. No direct current flows through the diode-pair and the diode-pair current contains only odd-order harmonics. Thus it is possible to use half-frequency pumping or even quarter-frequency pumping if the half-frequency current can be suppressed.

Henry *et al.*³² have shown that the l.o. noise spectrum is reduced substantially at the i.f. output port of a subharmonically pumped, antiparallel, diode-pair mixer relative to that from a conventional single-ended mixer using the same local oscillator. McMaster *et al.*³¹ constructed a subharmonic mixer at 100 GHz using a Schottky-barrier diode-pair mounted on a quartz suspended-stripline circuit. Waveguide-to-stripline transitions were used to couple the subharmonic l.o. and signal into the stripline mixer circuit. A conversion loss of 6.0 dB and a s.s.b. receiver noise figure of 11.0 dB were measured at 100 GHz.

At the higher frequencies, the dimensions of fundamental waveguide become extremely small, waveguide losses become extremely high,³³ and surface finish and dimensional tolerances are difficult to control. Low-loss single-mode waveguides have been investigated for use in the millimetre and submillimetre region, in particular, H guide³⁴ and groove guide.^{35,36} Although it should be possible to construct various components using these new guiding structures, there are no reports to date of Schottky-barrier diodes embedded in groove guide or in H-guide mixer mounts.

5 Quasi-optical Mixers

For frequencies above 300–400 GHz it becomes exceedingly difficult to fabricate a guided-wave mixer circuit around a non-linear mixing element. As a result, mixers have been built in a quasi-optical free-space environment. Early experimental work by Fetterman *et al.*³⁷ and Mizuno *et al.*³⁸ located a Schottky-barrier diode at the focus of a spherical mirror using the whisker contact as a simple wire antenna. However, the distribution of energy in the various modes is not easily determined, and it is difficult to calculate the coupling of the wave energy to the diode junction and thus to evaluate mixer performance. The crossed circular-guide mixer

described by Fetterman *et al.*³⁹ and the overmoded waveguide mixer of Clifton¹⁵ are properly classified as quasi-optical mixers since the propagating energy was not constrained to a single mode.

In 1970, Matarrese and Evenson⁴⁰ applied long-wire antenna theory to the whisker contacts of point-contact diodes, which they previously had observed were many wavelengths long in workable harmonic mixers. They demonstrated that the whiskers, in fact, behaved as long-wire antennas. They showed that the effective length of the antenna is limited to the straight portion of the whisker between the semiconductor contact and any bend, kink, or right-angled bend occurring at some point along the length of the whisker. The whisker behaves electrically as if the whisker structure after the bend did not exist at all. They speculate that, since simple antenna theory has worked so well with the whisker contact wire, perhaps other types of antenna can be used to couple to the diode, in particular, the biconical antenna, which is many wavelengths transversely, the crossed-wire antenna and the V-antenna.

Electrical measurements in the millimetre and sub-millimetre region are much more difficult to perform than at the lower microwave frequencies. Fortunately mixer structures can be scale modelled at microwave frequencies where impedance and power measurements can be made easily and accurately. This fact has been used to good advantage in the development of several quasi-optical mixer structures reported to date.

A quasi-optical mixer mount developed by Gustincic^{41–43} (Fig. 4) consists of a biconical antenna with the diode chip mounted on a machined flat at the

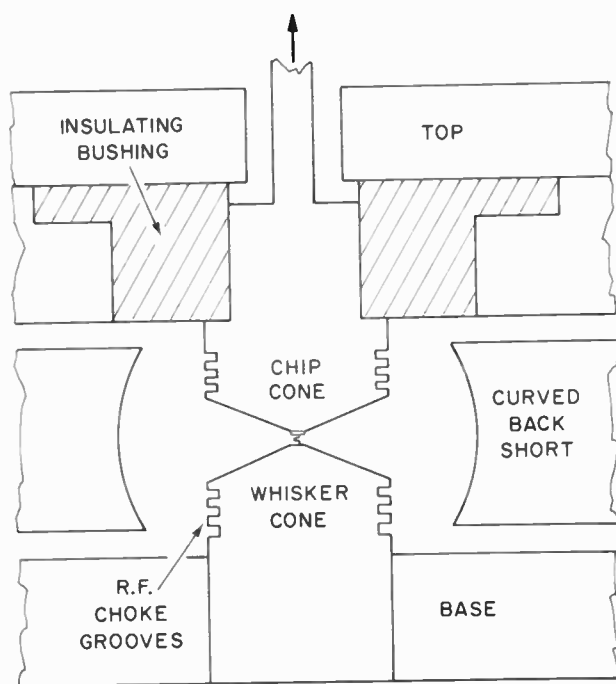


Fig. 4. Quasi-optical biconical mixer mount of Gustincic.⁴³

apex of one of the cone-shaped pieces forming the biconical antenna. The other cone has the whisker contact wire attached to a machined flat at its apex. The biconical transmission line has a full flare 40° angle giving a characteristic impedance of about 50Ω . The separation of the two flats at the apex is 0.25 mm . A series of choke grooves, equally spaced by one-half wavelength at the design frequency and one-quarter wavelength deep, are machined into the cylindrical extension of the cone body to prevent r.f. currents flowing on the cylindrical body sections. The open end of the biconical antenna forms a radiating aperture approximately four wavelengths high. The circular symmetry of the bicone results in a radiation pattern that is uniform around the axis of the cone. To provide a directed beam suitable for illumination by a collimating lens, a curved back-short was placed around the bicone with a small circular aperture about 3.5 wavelengths in diameter located at the front of the mount. A movable section, four wavelengths in diameter, at the back of the mount serves to tune the mixer mount. GaAs Schottky-barrier diodes $2.5 \mu\text{m}$ in diameter were used in several versions of this mixer at frequencies up to 671 GHz .⁴⁴

Kraus⁴⁵ has indicated that the radiation between the cones in a biconical antenna propagates in a TEM mode with a spherical wavefront that is easily coupled to a radiating free space wave. Perhaps the most interesting feature of the biconical antenna is that the characteristic impedance is essentially independent of frequency and is determined by the cone angle. Thus optimum r.f. matching to the diode should be possible simply by selecting the appropriate cone angle.

Results have been reported⁴⁴ for three mixers covering the 186 to 671 GHz frequency range using an i.f. of 1.42 GHz . One mixer which was operated at both 186 and 244 GHz gave a d.s.b. mixer noise temperature of about 2000 K . A second mixer at 361 GHz gave a d.s.b. mixer noise temperature of about 4000 K , while a third mixer at 671 GHz gave a d.s.b. mixer noise temperature of about 15000 K .

Kräutle *et al.*⁴⁶ have used the diode whisker as a long-wire antenna, and by placing a corner reflector behind the wire, were able to produce a narrow high-gain beam of approximately circular cross section. They obtained an increase in gain of 12 dB relative to the antenna wire alone.

Fetterman *et al.*⁴⁷ adopted this approach in a number of mixer mounts covering the $120 \mu\text{m}$ to 1 mm wavelength range. The corner-reflector diode mount (Fig. 5) uses a 4-wavelength-long antenna wire located 1.2 wavelengths from the corner of a 90° corner reflector. The corner reflector is made in two pieces using split block construction, and the reflecting surfaces are highly polished. The highly polished ground plane is made from a separate piece of copper. The diode chip is mounted on a copper stud that is inserted through a hole in the ground plane so that the surface of the semiconductor chip is

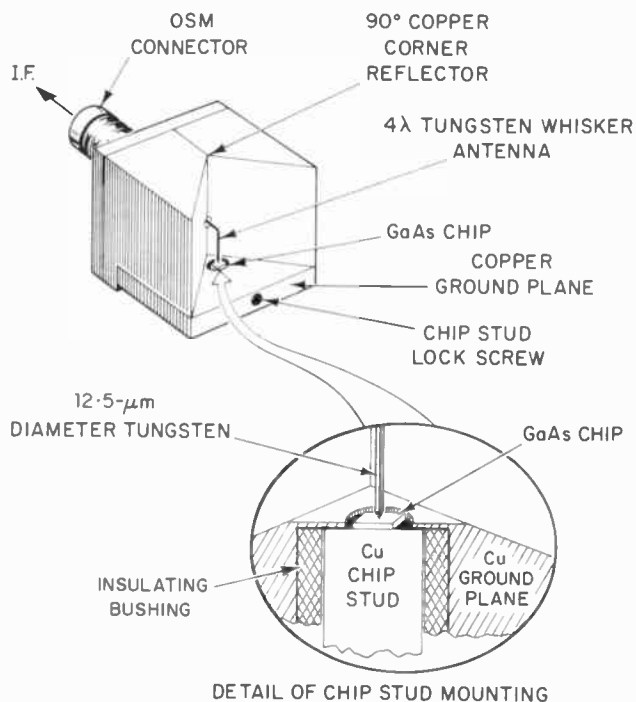


Fig. 5. Quasi-optical corner-reflector diode mount.

flush with the surface of the ground plane. Diodes having diameters in the range $1\ \mu\text{m}$ to $2\ \mu\text{m}$ are contacted by lowering the whisker into contact with the diode, while observing the contacting operation through a high power optical microscope. Measurements on scaled models of the antenna at X-band frequencies were used to optimize

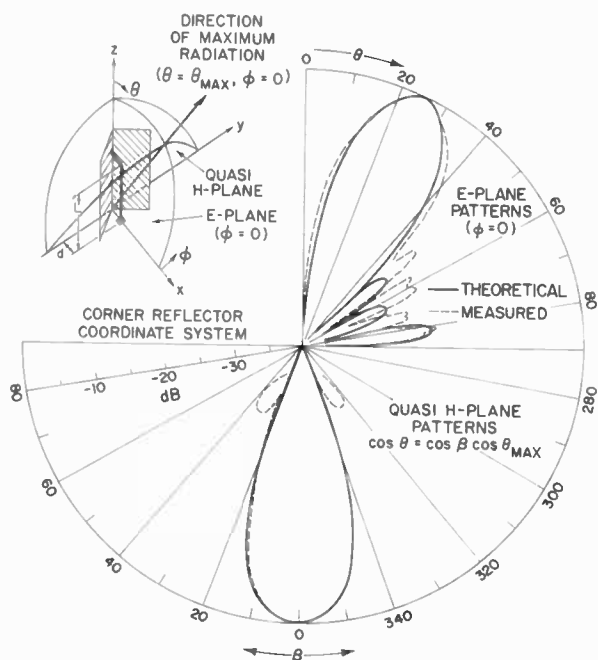


Fig. 6. Antenna characteristics of a long wire antenna in a 90° corner reflector ($L=4\lambda$, $d=1.2\lambda$) obtained by scale modelling at 7 GHz.

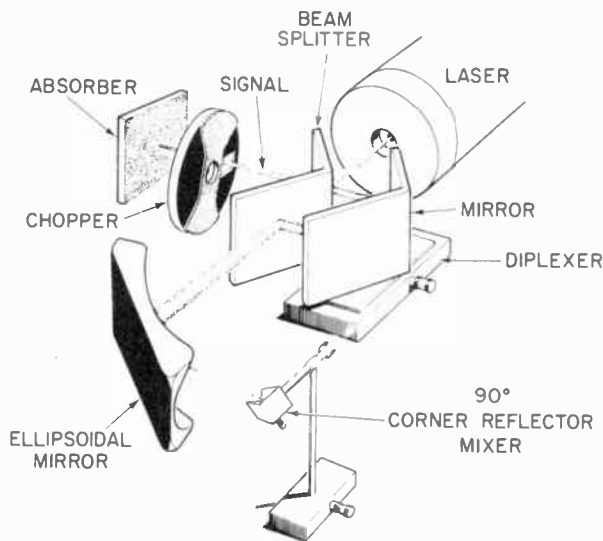


Fig. 7. Quasi-optical radiometer operating between $170\ \mu\text{m}$ and $1\ \text{mm}$.

the mixer mount design. Theoretical and measured antenna patterns were obtained at 10 GHz on a scale model of the corner reflector mixer with a 4-wavelength-long wire antenna located 1.2 wavelengths from the corner (Fig. 6). The beam has an almost circular cross-section with a 14° beamwidth at the 3-dB points. Antenna patterns measured on a submillimetre wave corner-reflector mount at $394\ \mu\text{m}$ gave a slightly narrower beam with a beamwidth of 10° in the H-plane and 9° in the E-plane, both measurements being made at the 3-dB points. The apparent difference between Fig. 6 here and Fig. 8 in Wrixon and Kelly³ is in the choice of H-plane. The latter choice gave the illusion of an elliptical beam, whereas the quasi-H-plane (Fig. 6) gives the correct circular cross-section for the beam. The corner-reflector mixer mounts were evaluated in a Dicke-type radiometer (Fig. 7). The diplexer consists of a folded interferometer similar in principle to that of Erickson.⁴⁸ The results of blackbody radiometric measurements using a standard Y-method⁴⁹ interpretation of the data are shown in Table 1.

Kerr *et al.*⁵⁰ have described a simple quasi-optical mixer for 100–120 GHz (Fig. 8) that should be usable into the submillimetre-wavelength region with appropriate frequency scaling. A two-slot antenna radiator is used with the slots driven in phase. The two-slot antenna over-

Table 1

$\lambda/\mu\text{m}$	Frequency GHz	Total Systems Noise Temp. (dsb)/K	Mixer Temp./K	Conversion Loss/dB
887.0	338.2	7 400	3 600	9.2
447.1	670.5	9 680	5 860	11.9
432.6	692.9	13 000	7 860	13.2
419.6	716.2	14 000	8 460	13.5
393.6	761.6	14 440	8 470	13.6

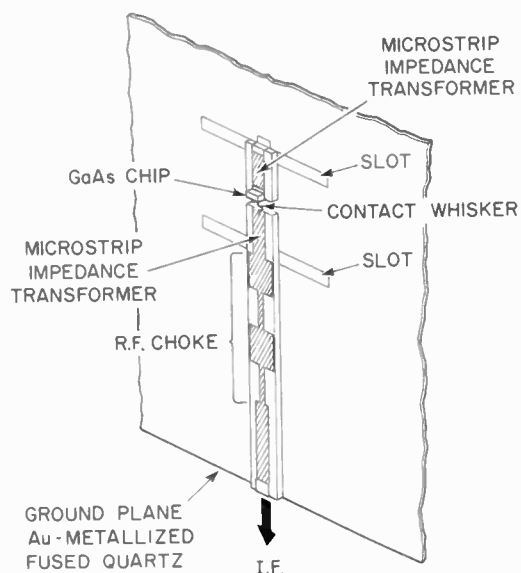


Fig. 8. Quasi-optical mixer of Kerr *et al.*⁵⁰

comes the principal problem of a single slot in a ground plane, namely, that the E- and H-plane radiation patterns are widely different, making it impossible to illuminate a circular aperture efficiently. With two slots, the E- and H-patterns can be well matched over approximately 15% bandwidth by choice of slot length and slot spacing. For slot spacings close to a half wavelength, ground-plane currents away from the immediate vicinity of the slots are small so that the ground-plane size has little effect on the radiation pattern. Radiation from the rear of the ground plane is prevented by a tuned cavity. Coupling between the slots and mixer diode is achieved using microstrip lines. Impedance matching between the slots and diode can be controlled by the slot width, back-cavity tuning, and characteristic impedance of the microstrip quarter-wavelength impedance transformers between the slots and the diode. The ground plane is gold on 0.18-mm-thick fused quartz into which the slots are etched photolithographically. The microstrip lines are formed on 76- μm -thick fused quartz that are later glued onto the ground plane. The diode chip is soldered to the end of one microstrip line and a whisker contact is attached to the end of the other microstrip line. The whisker is brought into contact with the diode by advancing the whisker microstrip line until a diode I - V characteristic is obtained; the whisker is advanced a further 2 μm to provide spring pressure, and then the microstrip line is glued in place. GaAs Schottky-barrier diodes 2.5 μm in diameter were used in the mixer. Radiometric measurements at 112 GHz indicated a s.s.b. mixer noise temperature of 1000 K and a diode conversion loss of 8.6 dB, which is about 3 dB worse than the best reported waveguide mixers in this frequency range. This quasi-optical mixer structure uses a planar antenna, and with minor modification, such as replacing

the microstrip lines with coplanar transmission line, would be quite applicable to monolithic circuit integration.

Averin and Popov⁵¹ describe a quasi-optical mixer using two orthogonal cones for signal and l.o. that taper to 1.5 mm diameter. The whisker contact to a 2- μm -diameter Schottky-barrier diode is mounted at the intersection of the two cones. Dielectric matching lenses are used on the input aperture of the two cones. This structure appears to be very similar to the crossed circular-guide mixer of Fetterman *et al.*³⁹ with similar sensitivity. A room temperature limiting sensitivity of 10^{-16} W/Hz at 280 GHz was obtained.

Tien-lai Hwang *et al.*⁵² have recently demonstrated a planar sandwich V-antenna that could be of considerable interest to designers of quasi-optical Schottky-barrier diode receivers. The antenna, combined with a thin-film bolometric detector, is sandwiched between substrates of 1-mm-thick crystal quartz, the arms of the V being ten wavelengths long in the dielectric. The antenna possesses a single lobe along the symmetry axis of the V and has a gain of 8 dB at a wave-length of 119 μm .

Kräutle *et al.*⁵³ have recently reported an extensive study of long-wire antennas in combination with various adjustable reflectors. The influence of different parameters such as antenna length, spacing, corner angle of corner reflectors, and radius of curvature of cylindrical reflectors on the antenna pattern and gain were investigated in detail. The authors conclude that the highest efficiency is obtained with the smallest cylindrical reflector with a 2.4-wavelength radius of curvature, but that the 90° corner reflector with an antenna length of 4–6 wavelengths has only slightly lower efficiency and will be easier to manufacture.

6 Surface-oriented Diodes and Monolithic Integrated Mixers

Although excellent results have been obtained with whisker-contacted diodes in waveguide and quasi-optical mixer mounts, it is considerably more difficult to make contact to the smaller-diameter diodes used at the higher frequencies and the reliability of the resulting diodes is inferior to that obtained at lower frequencies. The assembly of whisker-contacted diodes in mixer mounts is very labour-intensive, time consuming, and expensive. Thus, there has been considerable interest in replacing the whisker contact to the Schottky barrier with a photolithographically-fabricated contact on the surface of the diode. In the microwave region of the spectrum this has been achieved in the beam-lead diode that has been integrated in hybrid fashion with microstrip, stripline or dielectric-guide circuit elements. Similar hybrid techniques using quartz suspended-stripline and discrete diodes have been applied in the millimetre-wave region with some success.

A typical planar beam-lead diode has considerable parasitic capacitance associated with the beam leads that pass over and are separated from the conducting substrate

by only a thin insulating oxide layer. This parasitic capacitance has been a problem in extending the use of conventional beam-lead devices to higher frequencies. A number of groups have developed surface-oriented diode structures for use in the millimetre- and submillimetre range by limiting the region of conducting GaAs to only that necessary to support proper device operation. Small pockets of conducting GaAs are created in a high resistivity GaAs wafer with the Schottky-barrier contact made close to the edge of the conducting region. The several different approaches used in making these devices and the technical difficulties involved have been reviewed by Murphy and Clifton.⁵⁴

Bellamy and Cho⁵⁵ used molecular beam epitaxy to create pockets of conducting GaAs in windows in a layer of silicon dioxide deposited on a high-resistivity GaAs substrate. These devices, measured in a double-balanced, thin-film, downconverter circuit had a conversion loss of 8.5 dB at 103 GHz. Murphy *et al.*^{56, 59} have used proton bombardment to define conducting pockets in n on n⁺ epitaxial GaAs producing planar surface-oriented devices (Fig. 9). Two layers of GaAs are grown epitaxially on semi-insulating substrates. The first layer (n⁺) is 3 μm thick and has an n-type carrier concentration of 1 × 10¹⁸ cm⁻³. The top n-layer is 0.5 μm thick and has an n-type carrier concentration of 1 × 10¹⁷ cm⁻³. Selective Se⁺ ion implantation is used to decrease the specific resistance of the Au-Ge alloyed ohmic contact. The diode and ohmic contact areas are shielded by gold and the wafer is proton bombarded to convert the n and n⁺ layers in the unshielded regions to high-resistivity material. After removal of the bombardment shield a 2-μm-diameter Schottky barrier is defined by sputter deposition of platinum or titanium. A stripline overlay metallization contacts the Schottky barrier and ohmic contact of each device. A single device thermocompression bonded to

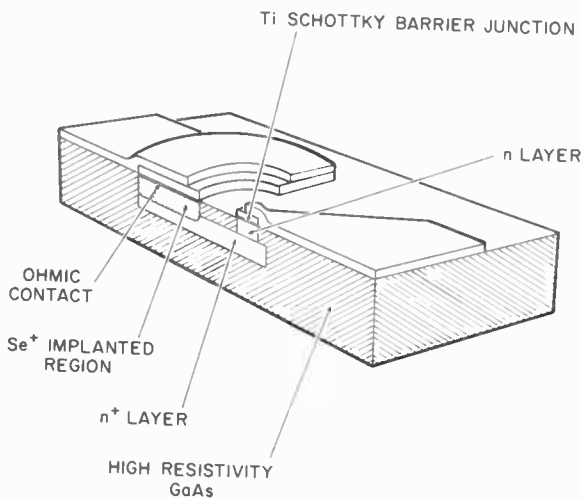


Fig. 9. Surface oriented Schottky-barrier diode.

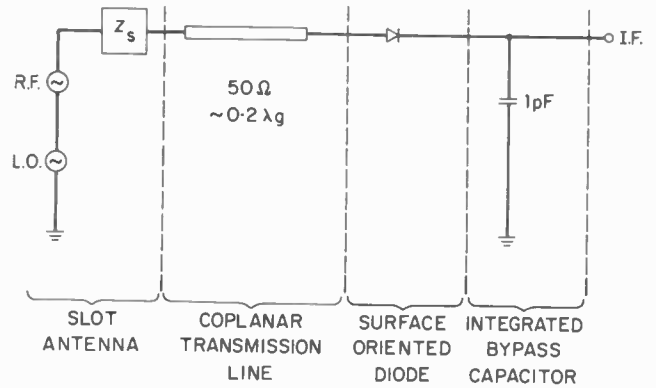


Fig. 10. Circuit diagram of an integrated mixer module designed for quasi-optical operation at 350 GHz.

microstripline on an alumina substrate was used to demonstrate video detection at frequencies up to 891 GHz and harmonic mixing up to 668 GHz. Recently, Cardiasmenos^{57, 58} has reported surface-oriented beam-lead devices usable from 20 to 300 GHz with Schottky-barrier contacts of 2, 3 and 4 μm diameter. Low-parasitic capacitance has been obtained by deposition of a 2 to 3 μm thick passivating glass layer on top of the epitaxial layer and by etching away all the GaAs not in the immediate vicinity of the active device. The passivation layer thus acts as the main structural member supporting the two beam leads in position. The diodes mounted in a suspended-stripline mixer are reported to have given typical s.s.b. conversion loss of about 6.5 dB and a typical overall s.s.b. system noise figure of 8.5 dB at 94 GHz. Single sideband noise figures as low as 7.0 dB are reported to have been measured on selected mixers.

The finite size of the beam-lead diode chip, which has dimensions comparable to a wavelength in the submillimetre region, makes it difficult to extend hybrid integration to submillimetre wavelengths. Clearly, monolithic integration of diode and circuit on the same piece of material is very desirable, if not essential, for optimum receiver performance in the millimetre and submillimetre region. Murphy *et al.*⁵⁴ have described the fabrication of an integrated mixer module (Fig. 10) for use at 350 GHz. The radiation is received by a slot antenna and is coupled to the diode by an appropriate section of coplanar transmission line. The integrated bypass capacitor completes the mixer circuit providing a short circuit to radio frequencies and an open circuit to the i.f. The design of the planar antenna is complicated by the presence of the high resistivity GaAs. The phase velocity of propagation of radiation in the GaAs dielectric is lower than the phase velocity of waves propagating on the metallization on the GaAs surface. Thus radiation tends to be into the dielectric, and the radiation pattern of the slot antenna exhibits about 8 dB front-to-back ratio for radiation received through the dielectric. The 350 GHz monolithic mixer module (Fig. 11(a)) and its measured radiation

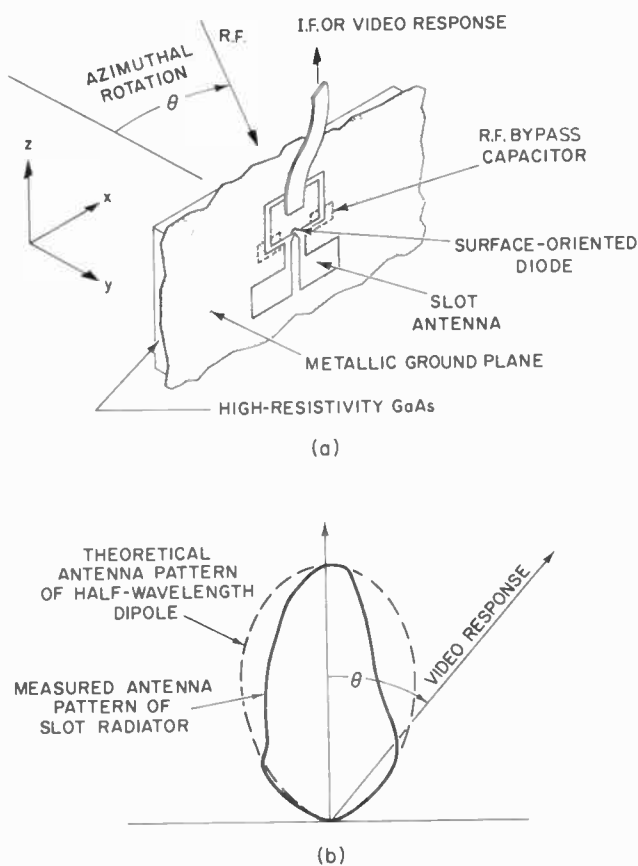


Fig. 11. 350-GHz integrated mixer module.
 (a) Configuration of the surface oriented diode and circuit elements. Radiation is coupled through the GaAs as shown.
 (b) Measured radiation pattern at 350 GHz.

pattern at 350 GHz (Fig. 11(b)) is essentially the same pattern as was predicted from measurements on a frequency-scaled model at 4 GHz. The patterns in both cases were obtained by monitoring the video response of the surface-oriented diode as the direction of the incident radiation was changed. The theoretically expected radiation pattern for a half-wavelength dipole is also shown in Fig. 11(b) for comparison. Measurements on a frequency-scaled model of the module indicate that a conversion loss of about 7 dB should be obtained. This has yet to be demonstrated at 350 GHz.

Mizuno *et al.*⁶⁰ have investigated printed half-wave dipole antennas on dielectric substrates. Scaled antenna models were measured at 10 GHz to obtain design data for monolithic antenna structures for use at millimetre and submillimetre wavelengths. Recently Daiku *et al.*⁶¹ have extended the scale modelling at 10 GHz to investigate printed Yagi-Uda type dipoles on dielectric substrates in which a parasitic element is located in front of the half-wave main dipole element. The length of the dielectric substrate extending in front of the parasitic element can be adjusted to obtain maximum detector response, however, the optimum length of dielectric also depends on the

dielectric constant and on the thickness of the dielectric substrate. The authors have shown that the optimum length can be calculated according to the Hansen-Woodyard condition⁶² assuming a TE₀ surface-wave mode on the dielectric plate. Calculated design dimensions are given for antennas on GaAs and quartz for use at 337 μm .

Rutledge *et al.*,⁶³ in an extensive study of infrared and submillimetre antennas, have also considered printed dipole antennas on dielectric substrates. In simulation studies at 10 GHz on substrates of dielectric constant 12 they have shown that current will not propagate on the metallization unless the conductor pattern is narrower than $\lambda/30$. Even when the conductor pattern is narrow enough to support propagation, the antenna gain cannot be increased by increasing the length of the conductor since the velocity of propagation is so slowed by the dielectric that the antenna has little gain. The authors conclude that a better approach would be to add another dielectric layer to form a top sandwich and suggest the V-antenna as a 'good sandwich' antenna. The planar sandwich antenna described by Tien-lai Hwang *et al.*⁵² should, in principle, be applicable to monolithic integrated mixers on GaAs. However, the necessity to embed the diode in the centre of a dielectric sandwich adds an additional complication to the structure that is not present with slot or dipole antennas. The double-slot quasi-optical mixer of Kerr *et al.*,⁵⁰ mentioned previously, would appear to be very suitable for monolithic integration on GaAs.

7 Diplexers and Local Oscillator Sources

The diplexer is a common element in all receiver designs whose purpose is to couple the signal and l.o. into the mixer with a minimum of loss. In addition, it is desirable that the diplexer have very high rejection of the noise sidebands of the local oscillator which occur in the signal passband. Wrixon and Kelly³ have presented a comprehensive review of submillimetre diplexers using quasi-optical versions of conventional Fabry-Perot, Michelson and Mach-Zehnder optical interferometers. Figure 12 shows two submillimetre diplexers based on the Mach-Zehnder interferometer as used by Fetterman *et al.*⁴⁷ and by Erickson.^{25,48} In both cases, the signal and l.o. beams are split and recombined by mylar beamsplitters. The difference in path length for the two beam paths is adjusted to be a half wavelength at the i.f. Wrixon and Kelly³ have pointed out that wire grids can be used in place of the mylar beamsplitters in these diplexers with a consequent increase in operating frequency range.

Local oscillator sources are essential to the development of low-noise receivers in the millimetre and submillimetre regions. Martin and Mizuno⁶⁴ have presented a comprehensive review of the situation in the submillimetre range and very little has changed in the meantime.

In the 100–400 GHz region carcinotrons are available with output powers of tens of milliwatts and with 20%

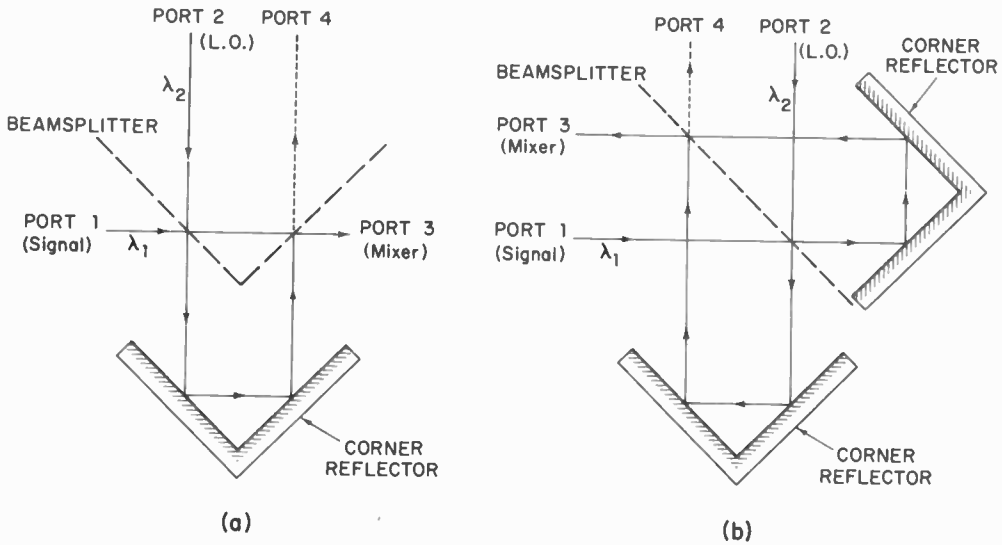


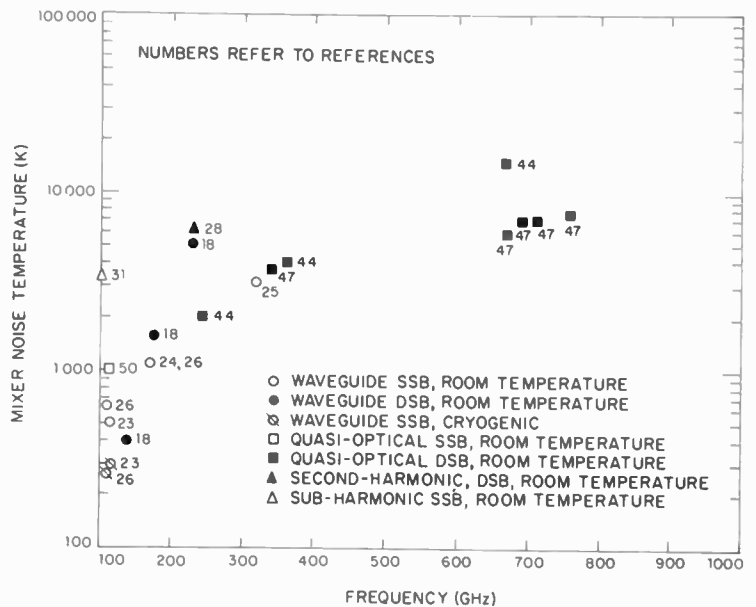
Fig. 12. Submillimetre duplexers based on the Mach-Zehnder interferometer.
 (a) As developed by Fetterman *et al.*⁴⁷
 (b) As developed by Erickson.⁴⁸

tuning range that are more than adequate as mixer local oscillators. Optically pumped gas lasers can operate as efficient sources of l.o. power from 150 to 1000 GHz with several hundred laser lines available. In general, they are non-tunable, but possibilities do exist for pressure- or Stark-tuning over a limited range. Solid-state silicon impatt oscillators have recently been reported⁶⁵ with output powers of a few milliwatts in the 300–400 GHz frequency range. Shur and Eastman⁶⁶ have indicated that surface-oriented, transferred-electron devices (t.e.d.) should have an extended range of frequency operation compared to regular t.e.d.s and that operation into the

100 GHz region should be possible.

Perhaps the most significant development is the low l.o. power requirements of mixers reported by Vizard *et al.*²⁶ If these low power requirements hold for the higher-frequency region, it is possible that solid-state devices now under development could conceivably generate sufficient power to cover the 100–1000 GHz range. The subharmonically-pumped down-converter, if extended to the higher frequency region with both half-frequency and quarter-frequency pumping, might also allow solid state l.o. sources to be used over the complete 100–1000 GHz frequency range.

Fig. 13. State-of-the-art in low-noise receiver technology in the 100–1000 GHz range.



8 Conclusions

The state-of-the-art in low noise receiver technology in the 100–1000 GHz frequency range is summarized in Fig. 13. The best performance in the 100–400 GHz range is obtained from fundamental waveguide mixers. Quasi-optical mixers have made significant improvements in performance in the 400–1000 GHz range, although they have not as yet given better performance than waveguide mixers in the 100–400 GHz region. The most recently developed monolithic receivers have still to demonstrate their capabilities, although scale-model measurements indicate that very competitive performance should be achieved. The use of electron-beam fabrication could lead to improved Schottky-barrier diodes which will benefit all types of mixers. Development of improved tunable l.o. sources and mixers requiring very low l.o. drive power will have a significant impact in several areas, in particular, space-borne radio astronomy and spectroscopy.

9 Acknowledgments

Lincoln Laboratory is supported in part by the Department of the Air Force, the US Army Research Office, the Department of Energy and the National Science Foundation.

The views and conclusions contained in this paper are those of the contractor and should not be interpreted as necessarily representing the official policies, either expressed or implied of the United States Government.

10 References

- 1 McColl, M., 'Review of submillimetre wave mixers', *Proc. Soc. Photo-Opt. Instrum. Engrs*, **105**, pp. 24–34, 1977. (59 references.)
- 2 Kimmitt, M. F., 'Recent development of infrared detectors', *Infrared Physics*, **17**, pp. 459–66, 1977. (24 references.)
- 3 Wrixon, G. T. and Kelly, W. M., 'Low noise Schottky barrier diode mixers for wavelengths <1 mm', *Infrared Physics*, **18**, no. 5/6, pp. 413–28, December 1978. (32 references.)
- 4 Martin, D. H. and Lesurf, J., 'Submillimetre wave optics', *Infrared Physics*, **18**, no. 5/6, pp. 405–12, December 1978.
- 5 Siegman, A. E., 'The antenna properties of optical heterodyne receivers', *Proc. IEEE*, **54**, no. 10, pp. 1350–6, October 1966.
- 6 Kingston, R. H., 'Detection of Optical and Infrared Radiation' (Springer-Verlag, New York, 1978).
- 7 Mandel, L. and Wolf, E., 'Optimum conditions for the heterodyne detection of light', *J. Opt. Soc. Am.*, **65**, no. 4, pp. 413–20, April 1975.
- 8 Young, D. T. and Irvin, J. C., 'Millimeter frequency conversion using Au-n-type GaAs Schottky barrier epitaxial diodes with a novel contacting technique', *Proc. IEEE*, **53**, no. 12, pp. 2130–1, December 1965 (Corresp.).
- 9 Clifton, B. J., Lindley, W. T., Chick, R. W. and Cohen, R. A., 'Materials and processing techniques for the fabrication of high quality millimeter wave diodes', Proc. of Third Biennial Cornell Eng. Conf. (Ithaca, N.Y.), pp. 463–75, 1971.
- 10 Torrey, H. C. and Whitmer, C. A., 'Crystal Rectifiers', MIT Rad. Lab. Ser., **15** (McGraw-Hill, New York, 1948).
- 11 Barber, M. R., 'Noise figure and conversion loss of the Schottky barrier mixer diode', *IEEE Trans. on Microwave Theory and Techniques*, **MTT-15**, no. 11, pp. 629–35, November 1963.
- 12 Saleh, A. A. M., 'Theory of Resistive Mixers', Research Monograph, no. 64 (MIT Press, Cambridge, Mass., 1971).
- 13 Held, D. N. and Kerr, A. R., 'Conversion loss and noise of microwave and millimeter-wave mixers: Parts I and II', *IEEE Trans.*, **MTT-26**, no. 2, pp. 49–61, February 1978.
- 14 McColl, M., 'Conversion loss limitations on Schottky-barrier mixers', *IEEE Trans.*, **MTT-25**, no. 1, pp. 54–9, January 1977.
- 15 Clifton, B. J., 'Schottky-barrier diodes for submillimeter heterodyne detection', *IEEE Trans.*, **MTT-25**, no. 6, pp. 457–63, June 1977.
- 16 Kelly, W. M. and Wrixon, G. T., 'Schottky-barrier diodes for low noise mixing in the far infrared', *Appl. Phys. Lett.*, **32**, no. 9, pp. 525–7, May 1978.
- 17 Champlin, K. S. and Eisenstein, G., 'Cutoff frequency of submillimeter Schottky-barrier diodes', *IEEE Trans.*, **MTT-26**, no. 1, pp. 31–34, January 1978.
- 18 Wrixon, G. T., 'Low noise diodes and mixers for the 1–2 mm wavelength region', *IEEE Trans.*, **MTT-22**, no. 12, pp. 1159–65, December 1974.
- 19 McColl, M., Hodges, D. T. and Garber, W. A., 'Submillimeter wave detection with submicron size Schottky barrier diodes', *IEEE Trans.*, **MTT-25**, no. 6, pp. 463–7, June 1977.
- 20 Schneider, M. V., Linke, R. A. and Cho, A. Y., 'Low noise millimeter-wave mixer diodes prepared by molecular beam epitaxy (MBE)', *Appl. Phys. Lett.*, **31**, no. 3, pp. 219–21, August 1977.
- 21 Eisenhart, R. L. and Khan, P. J., 'Theoretical and experimental analysis of a waveguide mounting structure', *IEEE Trans.*, **MTT-19**, no. 8, pp. 706–19, August 1971.
- 22 Sharpless, W. M., 'Wafer-type millimeter wave rectifiers', *Bell. Syst. Tech. J.*, **35**, pp. 1385–1402, November 1956.
- 23 Kerr, A. R., 'Low-noise room-temperature and cryogenic mixers for 80–120 GHz', *IEEE Trans.*, **MTT-23**, no. 10, p. 787, October 1975.
- 24 Kerr, A. R., Mattauich, R. J. and Grange, J. A., 'A new mixer design for 140–220 GHz', *IEEE Trans.*, **MTT-25**, no. 5, pp. 399–401, May 1977.
- 25 Erickson, N. R., 'A 0.9 mm heterodyne receiver for astronomical observations', IEEE 1978 International Microwave Symposium Digest MTT-S, pp. 438–9, Ottawa, June 1978.
- 26 Vizard, D. R., Keen, N. J., Kelly, W. M. and Wrixon, G. T., 'New Schottky barrier diodes at 111 and 170 GHz with low local oscillator power requirements', to be published.
- 27 Lacombe, J., Duchemin, J. P., Bonnet, M. and Huyghe, D., 'Schottky mixer diode made by a new method', *Electronics Letters*, **13**, no. 16, pp. 472–3, 4th August 1977.
- 28 Meredith, R. and Warner, F. L., 'Superheterodyne radiometers for use at 70 GHz and 140 GHz', *IEEE Trans.*, **MTT-11**, no. 9, pp. 397–411, September 1963.
- 29 Kawasaki, R. and Akaike, M., 'A broad-band second-harmonic mixer covering 76–106 GHz', *IEEE Trans.*, **MTT-26**, no. 6, pp. 425–7, June 1978.
- 30 Cohn, M., Degenford, J. E. and Newman, B. A., 'Harmonic mixing with an antiparallel diode pair', *IEEE Trans.*, **MTT-23**, no. 8, pp. 667–73, August 1975.
- 31 McMaster, T. F., Schneider, M. V. and Snell, Jr., W. W., 'Millimeter wave receivers with subharmonic pump', *IEEE Trans.*, **MTT-24**, no. 12, pp. 948–52, December 1976.
- 32 Henry, P. S., Glance, B. S. and Schneider, M. Y., 'Local-oscillator noise cancellation in the subharmonically pumped down-converter', *IEEE Trans.*, **MTT-24**, no. 5, pp. 254–7, May 1976.
- 33 Tischer, F. J., 'Excess conduction losses at millimeter wavelengths', *IEEE Trans.*, **MTT-24**, no. 11, pp. 853–8, November 1976.
- 34 Doswell, A. and Harris, D. J., 'Modified H guide for millimeter and submillimeter wavelengths', *IEEE Trans.*, **MTT-21**, no. 9, pp. 587–9, September 1973.
- 35 Harris, D. J., Lee, K. W. and Batt, R. J., 'Low-loss single mode waveguides for submillimetre and millimetre wave-

- lengths', *Infrared Physics*, 18, no. 5/6, pp. 741-7, December 1978.
- 36 Harris, D. J., 'Groove- and H-waveguide design and characteristics at short millimeter wavelengths', *IEEE Trans., MTT-26*, no. 12, pp. 998-1001, December 1978.
- 37 Fetterman, H. R., Clifton, B. J., Tannenwald, P. E. and Parker, C. D., 'Submillimeter detection and mixing using Schottky diodes', *Appl. Phys. Lett.*, 24, no. 2, pp. 70-2, January 1974.
- 38 Mizuno, K., Kuwahara, R. and Ono, S., 'Submillimeter detection using a Schottky diode with a long-wire antenna', *Appl. Phys. Lett.*, 26, no. 11, pp. 605-7, June 1975.
- 39 Fetterman, H. R., Clifton, B. J., Tannenwald, P. E., Parker, C. D. and Penfield, H., 'Submillimeter heterodyne detection and harmonic mixing using Schottky diodes', *IEEE Trans., MTT-22*, no. 12, pp. 1013-15, December 1974.
- 40 Matarrese, L. M. and Evenson, K. M., 'Improved coupling to infrared whisker diodes by use of antenna theory', *Appl. Phys. Lett.*, 17, no. 1, pp. 8-10, July 1970.
- 41 Gustincic, J. J., 'A quasi-optical radiometer', Second International Conference and Winter School on Submillimeter Waves and their Application, IEEE Cat. No. 76CH 1152-8 MTT, pp. 106-7, 1976.
- 42 Gustincic, J. J., 'Receiver design principles', *Proc. Soc. Phot-Opt. Instrum. Engrs*, 105, pp. 40-3, April 1977.
- 43 Gustincic, J. J., 'A quasi-optical receiver design', 1977 IEEE MTT-S International Microwave Symposium Digest, IEEE Cat. No. 77CH 1219-5 MTT, pp. 99-101, June 1977.
- 44 Gustincic, J. J., deGrauw, Th., Hodges, D. T. and Luhmann, Jr., N. C., 'Extension of Schottky Diode Receivers into the Submillimeter Region', Unpublished report 1977.
- 45 Kraus, J. D., 'Antennas', pp. 217-29 (McGraw-Hill, New York, 1950).
- 46 Kräutle, H., Sauter, E. and Schultz, G. V., 'Antenna characteristics of whisker diodes used as submillimeter receivers', *Infrared Physics*, 17, pp. 477-83, 1977.
- 47 Fetterman, H. R., Tannenwald, P. E., Clifton, B. J., Parker, C. D., Fitzgerald, W. D. and Erickson, N. R., 'Far-ir heterodyne radiometric measurements with quasioptical Schottky diode mixers', *Appl. Phys. Lett.*, 33, no. 2, pp. 151-4, July 1978.
- 48 Erickson, N. R., 'A directional filter diplexer using optical techniques for millimeter to submillimeter wavelengths', *IEEE Trans., MTT-25*, no. 10, pp. 865-6, October 1977.
- 49 Mumford, W. W. and Scheibe, E. H., 'Noise Performance Factors in Communications Systems' (Horizon House-Microwave, Dedham, Mass., 1968).
- 50 Kerr, A. R., Siegel, P. H. and Mattauch, R. J., 'A simple quasioptical mixer for 100-120 GHz', 1977 IEEE MTT-S International Microwave Symposium Digest, IEEE Cat. No. 77CH 1219-5 MTT, pp. 96-8, June 1977.
- 51 Averin, S. V. and Popov, V. A., 'A mixer employing a Schottky C barrier diode for the short-wavelength portion of the millimeter and submillimeter wavelength bands', *Radiotekhnika i Elektronika*, 22, no. 8, pp. 1722-4, August 1977 [English translation, *Radio Engng Electron. Phys.*, 22, no. 8, pp. 126-8, 1977].
- 52 Tien-lai Hwang, Rutledge, D. B. and Schwarz, S. E., 'Planar sandwich antennas for submillimeter applications', *Appl. Phys. Lett.*, 34, no. 1, pp. 9-11, January 1979.
- 53 Kräutle, H., Sauter, E. and Schultz, G. V., 'Properties of a submillimetre mixer in an open structure configuration', *Infrared Physics*, 18, no. 5/6, pp. 705-12, December 1978.
- 54 Murphy, R. A. and Clifton, B. J., 'Surface-oriented Schottky-barrier diodes for millimeter and submillimeter wave applications', 1978 International Electron Devices Meeting Digest, IEEE Cat. No. 78 CH1324-3ED, pp. 124-7, December 1978.
- 55 Bellamy, W. C. and Cho, A. Y., 'Planar isolated GaAs devices produced by molecular beam epitaxy', *IEEE Trans. on Electron Devices*, ED-23, no. 4, pp. 481-4, April 1976.
- 56 Murphy, R. A., Bozler, C. O., Parker, C. D., Fetterman, H. R., Tannenwald, P. E., Clifton, B. J., Donnelly, J. P. and Lindley, W. T., 'Submillimeter heterodyne detection with planar GaAs Schottky barrier diodes', *IEEE Trans.*, MTT-25, no. 6, pp. 494-5, June 1977.
- 57 Cardiasmenos, A. G., 'Low noise thin-film down converters for millimeter systems applications', 1978 IEEE MTT-S International Microwave Symposium Digest, IEEE Cat. No. 78CH1355-7 MTT, pp. 399-401, Ottawa, June 1978.
- 58 Cardiasmenos, A. G., 'New diodes cut the cost of millimeter wave mixers', *Microwaves*, 17, no. 9, pp. 78-88, September 1978.
- 59 Murphy, R. A., Alley, G. D., Bozler, C. O., Fetterman, H. R., Tannenwald, P. E. and Clifton, B. J., 'Submillimeter wavelength surface-oriented diode mixers', 1978 IEEE-MTT-S International Microwave Symposium Digest, IEEE Cat. No. 78CH1355-7 MTT, pp. 430-2, Ottawa, June 1978.
- 60 Mizuno, K., Daiku, Y. and Ono, S., 'Design of printed resonant antennas for monolithic-diode detectors', *IEEE Trans., MTT-25*, no. 6, pp. 470-2, June 1977.
- 61 Daiku, Y., Mizuno, K. and Ono, S., 'Dielectric plate antenna for monolithic Schottky-diode detectors', *Infrared Physics*, 18, no. 5/6, pp. 679-82, December 1978.
- 62 Hansen, W. W. and Woodyard, J. R., 'A new principle in directional antenna design', *Proc. IRE*, 26, no. 3, pp. 333-45, March 1938.
- 63 Rutledge, D. B., Schwarz, S. E. and Adams, A. T., 'Infrared and submillimetre antennas', *Infrared Physics*, 18, no. 5/6, pp. 713-29, December 1978.
- 64 Martin, D. H. and Mizuno, K., 'Generation of coherent submillimeter waves', *Advances in Physics*, 25, no. 3, pp. 211-46, May 1976.
- 65 Ishibashi, T., Ino, M., Makimura, T. and Ohmori, M., 'Liquid-nitrogen-cooled submillimetre-wave silicon impatt-diodes', *Electronics Letters*, 13, no. 10, pp. 299-300, 12th May 1977.
- 66 Shur, M. S. and Eastman, L. F., 'Surface-oriented transferred-electron devices', *IEEE Trans.*, MTT-26, no. 12, pp. 1023-8, December 1978.
- 67 Goldsmith, P. F. and Plambeck, R. L., 'A 230-GHz radiometer system employing a second-harmonic mixer', *IEEE Trans.*, MTT-24, no. 11, pp. 859-61, November 1976.

Manuscript received by the Institution on 24th April 1979.
(Paper No. 1886/CC 305)

Millimetre wavelength impatt sources

J. J. PURCELL,
B.Sc., Ph.D., C.Eng., M.I.E.E.*

SUMMARY

The paper presents a review of the present capabilities of solid-state 'avalanche-diodes' at frequencies between 90 and 400 GHz.

Applications of solid-state sources are given with information on the relationship of reliability and performance.

The diode design and fabrication details are described briefly, and present-day laboratory capabilities are outlined and compared with those of commercially available sources.

* Plessey Research (Caswell) Limited, Allen Clark Research Centre, Towcester, Northants NN12 8EQ.

1 Introduction

The rapid technological development of solid-state millimetre-wave components has resulted in a significant increase in interest in the exploitation of the frequency spectrum above 90 GHz. There are two mechanisms which are currently exploited to produce solid-state oscillators at frequencies as high as 100 GHz; the Gunn-effect and the Avalanche Transit Time effect. The Gunn effect describes the N-shaped current-voltage characteristic exhibited by Group III-V semiconductors such as GaAs or InP. The negative differential resistance decreases, however, with increasing modulation frequency owing to energy relation effects, and imposes a practical upper-frequency limit of about 100 GHz. The present 'state-of-the-art' of about 100 mW at 94 GHz from both InP and GaAs devices is probably within 3 dB of the Gunn diode's potential performance. The avalanche diode, on the other hand, has produced power at fundamental frequencies as high as 400 GHz, and exhibits an almost constant conversion efficiency from 40 to 100 GHz.

The advent of reliable, small sized, impatt sources producing continuous power levels of hundreds of milliwatts and pulsed powers of watts at frequencies around 100 GHz has allowed the atmospheric 'windows' at 94 to 140 GHz to be used in system applications such as:

Radar,
Communications,
Missile guidance,
Imaging,

whilst in the laboratory, the availability of relatively low-cost and reliable sources has extended the spectroscopists' field of interest into the 'microwave' spectrum of 90 to 300 GHz.¹

Military applications are predominantly concentrated upon guidance and imaging, where the high resolution conferred by the millimetre wavelengths, and the relative immunity to smoke and fog can offer an all-weather capability superior to both microwave and far-infra-red frequencies.

2 Microwave Generation by Impatts

The IMPact ionization Avalanche Transit Time diode (or avalanche diode) was first proposed as a solid-state microwave source by W. T. Read in 1958.² Read proposed that an antiphase voltage/current relationship could be sustained at microwave frequencies by the combined delay of avalanche multiplication in a reverse-biased diode, coupled with the drift of generated carriers through the depletion layer of the junction. In 1965,³ Johnston, De Loach and Cohen at Bell Laboratories demonstrated the concept with a commonplace silicon computer diode embedded in a C-band (4-8 GHz) waveguide circuit.

In the relatively short period of 14 years, the silicon impatt has matured, to become a commercially available solid-state alternative to thermionic devices such as klystrons and carcinotrons over the spectrum from 8 to 300 GHz. Manufacturers' estimates of life-times are of the order of tens of thousands of hours for continuous operation with junction temperatures of about 200°C. Recent developments have been in the fields of high power operation (1–10 watts) over short pulse lengths for imaging and guidance applications, mainly in the United States,⁴ and in extending the upper frequency limit as high as 400 GHz through operation in harmonic modes, in both England¹ and Japan.⁵

3 Diode Design and Fabrication

In theory, almost any semiconductor which could be doped to appropriate levels could be used as a p–n junction avalanche diode oscillator. However, the available power from a particular material is determined simply by a figure of merit, F , where

$$F = V_s E_g$$

and V_s and E_g are the saturated drift velocity of carriers and the semiconductor bandgap.

Maximizing F and confining the choice to practical materials with well-developed growth and processing technologies at present restricts the designer to either GaAs or Si. Comparison of the values of F ($E_g = 1.44$ eV, $V_s = 0.6 \times 10^7$ cm s⁻¹ for GaAs, $E_g = 1.1$ eV and $V_s = 1.0 \times 10^7$ cm s⁻¹ for Si) would appear to offer comparable power performance. However, a more detailed examination of the avalanche mechanism indicates an upper frequency limit of about 60 GHz for GaAs, beyond which Si diodes offer an increasingly marked advantage.

Millimetre-wave impatts are produced from a single-crystal layer which is deposited by vapour phase epitaxy onto a high conductivity substrate. Small quantities (a few parts in 10⁶) of impurities are included within the lattice to produce either acceptor or donor-type semiconductor material of a prescribed carrier-density level. The diode structure is commonly of one of three forms:

$p^+ - n - n^+$	'n-type'	single drift
$p^+ - p - n^+$, or $n^+ - p - p^+$	'p-type'	single drift
$p^+ - p - n - n^+$		double drift

labelled in the direction of surface to substrate.

The double-drift diode is, in effect, two back-to-back single-drift diodes, and has advantages of higher power and higher impedance when compared with a single drift diode at the same frequency. However, technological limitations tend to confine use of this structure to frequencies below 100 GHz at the present time.

Theoretical analysis of the alternative 'n' and 'p'-type single-drift diodes suggests that higher output powers

and higher frequency limits could be realized through use of the 'complementary' hole-drift device, though in practice, most laboratories favour the production of 'n'-type diodes owing to the practical difficulty of achieving low parasitic losses with p-type material. Power dissipation is predominantly confined to the undepleted epitaxy, where the current is conducted by carriers under the influence of low electric fields. It is important, therefore, that the low-field mobility of the semiconductor should be high, maximizing the conductivity ($Nq\mu$), otherwise power dissipation will counteract the power generation of the avalanche process. The relative mobilities, at room temperature, at impurity levels of 10¹⁷ cm⁻³ are about 250 cm² V⁻¹ s⁻¹ for holes, and 650 cm² V⁻¹ s⁻¹ for electrons.

The impatt is a 'transit-time' device and hence, assuming a constant conversion efficiency, follows the customary $PZF^2 = \text{const.}$ power decrease with increasing frequency, where P is the available power and Z is the minimum circuit impedance which can be realized. This expression is a direct result of the output power being proportional to the chip volume, the cross-sectional area and length being each inversely proportional to frequency. Peak power is generated at a frequency determined by the mean depletion layer width, and this width in turn is determined by the layer doping level. A typical 100 GHz single-drift diode might have an optimum space-charge layer width of only 0.6 μm and a breakdown voltage of about 12 V. Diodes designed for operation at frequencies as high as 300 GHz require layer widths as narrow as 0.2 μm, which is probably close to the technological limit of current fabrication techniques.

A 100 GHz impatt has a cross-sectional area of about 10⁻⁵ cm² and an active-layer width of 6 × 10⁻⁵ cm. The dissipation of 2 watts of input power therefore represents a remarkably high power density of 3 × 10⁹ W cm⁻³! Clearly the diode must be in contact with a heat sink presenting a sufficiently low thermal

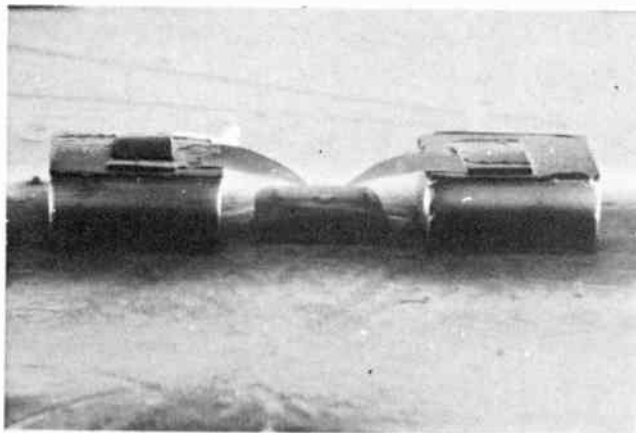


Fig. 1. Typical millimetre-wave impatt device, showing quartz 'stand-offs', bond tape and plated heat sink.

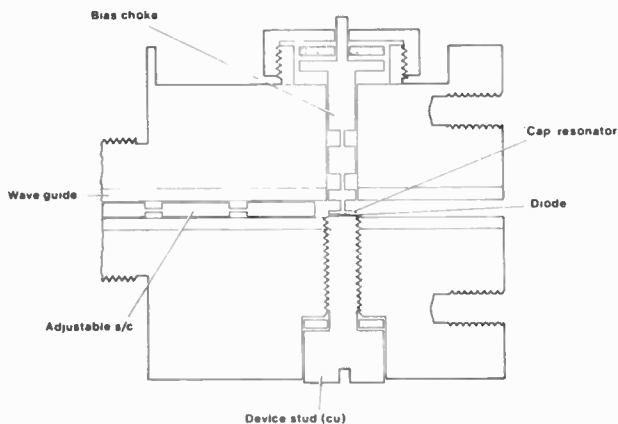
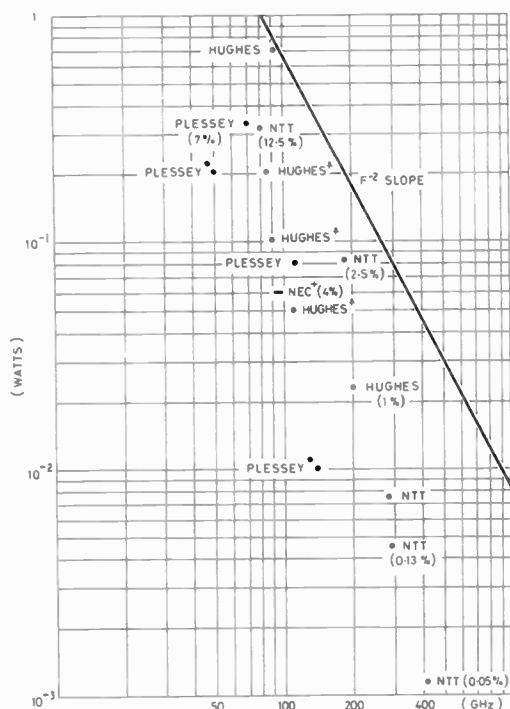


Fig. 2. Schematic diagram of typical 100 GHz impatt oscillator.

impedance (deg C/W) to restrict the temperature rise to within safe limits. In practice, manufacturers either electroplate a high conductivity integral heat sink of gold, copper or silver onto the junction contact, or for highest powers, bond the diode directly to a diamond heat sink. (Type IIA diamonds have a thermal conductivity, at room temperatures, of 2 to 5 times that of copper.)

A typical millimetre wave silicon impatt with a gold heat sink is shown in Fig. 1. The device would be mounted on a post by either wafer-bonding (solder) or ultrasonic-bonding.



- COMMERCIALY AVAILABLE ATO 244, ATO 283, PLESSEY
- + COMMERCIALY AVAILABLE 47175 H, 47-75 H, 47176 H HUGHES
- + COMMERCIALY AVAILABLE NO 869E W-IT, NEC

Fig. 3. 'State-of-the-art (1978)' impatt performance (c.w.).

At millimetre wavelengths, it is necessary to minimize the parasitic reactances associated with the diode encapsulation and commercially available device packages are usually unsuitable. Most manufacturers use a stand-off or quartz-ring 'encapsulation' of their own design.

The diode is embedded in a microwave circuit tuned to resonate at the appropriate frequency. The resonator is usually either of the 'radial cap' or 'coupled post' designs. Manufacturers pay particular attention to the cavity surface finish and mechanical stability in order to produce sources with low noise and stable output.

Figure 2 is a cross-sectional schematic drawing of a 100 GHz impatt oscillator of the radial cap design.

4 Present Status

In Figs. 3 and 4 are shown the present performance of millimetre-wave impatts from laboratories in the US, UK and Japan. Most activity is centred around the low atmospheric attenuation windows of 94, 140 and 225 GHz. At 94 GHz, c.w. impatt sources can produce output powers as high as 850 mW (Hughes) whilst powers of 50 to 100mW are available commercially. High-powered, short pulse length operation enables the diode to be operated at current densities limited purely by space-charge effects. With pulse lengths of only 300 ns, output powers as high as 5 to 10 watts have been reported at 94 GHz (Hughes).⁴

The upper frequency for operation in a fundamental mode is about 400 GHz, determined by physical limitations which include diffusion, the rate of change of ionization coefficients with electric field, energy relaxation and the onset of tunnelling at high electric fields. However, microwave power is available, at low levels, at frequencies as high as 600 GHz by harmonic selection.¹

As far as their suitability for systems' usage is concerned, the output power level of impatt sources is primarily determined by the device lifetime required. Impatts generally either fail in a very short time known as the 'infant mortality', which can be encompassed within the manufacturers' burn-in period, or at a constant rate following a log-normal temperature dependence. The life expectancy follows the classical 'bath-tub' pattern in which mortality rates are high during infancy and senility and at a low constant level between the two. At a junction temperature of 250°C, for example, an m.t.t.f. of greater than 10⁶ hours would normally be expected. The activation energy is such that a change in junction temperature of 10°C has the effect of changing the m.t.t.f. by a factor of about 2 times. A typical plot of diode reliability with junction temperature is shown in Fig. 5. Clearly in a practical situation, the user gains dramatically increased reliability at the expense of either relatively modest reductions in output power, or the use of a cooled environment.

Analysis of failure modes indicates that the diode's

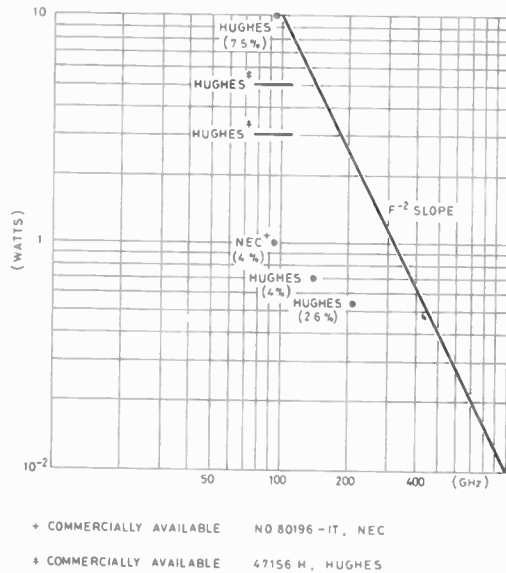


Fig. 4. 'State-of-the-art (1978)' peak impatt power.

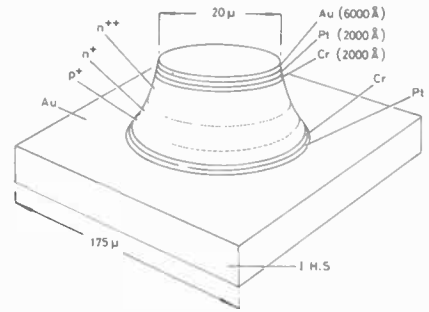


Fig. 6. Schematic diagram showing the construction of a '100 GHz' single drift N-type impatt.

applications using short (50–300 ns) pulse operation tend to require output powers as high as 10 watts. State-of-the-art laboratory results⁴ have shown that 10 watts is achievable from double-drift silicon impatts at 94 GHz. The frequency 'chirp' is high (1 GHz/100 ns) owing to the large temperature excursion over the pulse length; however, Hughes workers successfully controlled the frequency variation by shaping the applied bias pulse. No information is currently available on the effects on reliability of pulsing diodes at these power levels but it is likely that diode or circuit combining techniques will be necessary in order to achieve such operation with useful reliabilities.

As far as higher frequencies are concerned, theoretical work has indicated that tunnelling injection rather than avalanching may extend operation as high as 1000 GHz.⁶ To date, however, Tunnel injection Transit Time (tunnett) diodes have produce only small amounts of power (1 mW) at frequencies up to 278 GHz.

7 Acknowledgment

This paper has been published with the kind permission of the Directors of Plessey Research (Caswell) Limited.

6 References

- 1 Llewellyn-Jones, D., 'Spectroscopy at frequencies near 180 GHz utilising the harmonic content of a millimetre-wave impatt oscillator', Proc. 4th European Microwave Conference, Montreux, 1974, pp. 86.
- 2 Read, W. T., 'A proposed high frequency negative resistance diode', *Bell Syst. Tech. J.*, 37, pp. 401–46, March 1958.
- 3 Johnston, R. L., De Loach, B. C. and Cohen, G. B., 'A silicon diode microwave oscillator', *Bell Syst. Tech. J.*, 44, pp. 369–72, February 1965.
- 4 Kramer, N. B., 'Solid state technology for millimetre waves', *Microwave J.*, August 1978, pp. 57–61.
- 5 Ino, M., Ishibashi, T. and Ohmori, M., 'Submillimetre wave Si p⁺-n⁺ IMPATT diodes', *Jap. J. Appl. Phys.*, 16, pp. 89–92, 1966.
- 6 Nishizawa, J., Motoya, K. and Okuno, Y., 'Tunnel injection oscillator over 200 GHz', Proc. 8th European Microwave Conference, Paris (1978), pp. 780–4.

Manuscript received by the Institution on 24th June 1979
(Paper No. 1887/CC306)

demise is associated with an incursion of the contact metallization into the bulk of the semiconductor. High reliability figures have been achieved through the use of intermediate refractory layers such as Pt or W between the surface metallization of Cr or Ti and the Au wire bond. A schematic diagram showing a typical metallization pattern is shown in Fig. 6.

5 Future Prospects

Industrial activity in solid-state millimetre-wave source development is a direct reflection of the level of interest of mainly military applications in the atmospheric windows at 94 to 140 GHz. These frequencies are being utilized for tracking, guidance, radiometry and communications systems. Source requirements tend to fall into two distinct categories: either low-power, stable, c.w. outputs for local oscillators, parametric amplifier pumps and sources for Doppler radars, radiometers and transponders, or high-power pulsed oscillators for such applications as missile seekers, terminal homing and imaging. The low-power requirement is within the capabilities of established sources. However, those

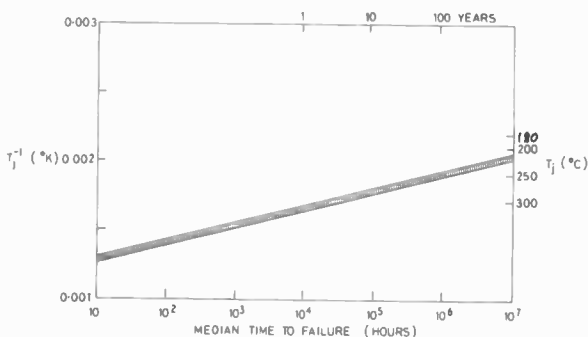


Fig. 5. Typical impatt reliability plot.

Commercial and scientific applications of millimetric and sub-millimetric waves

H. MEINEL, Dipl.-Ing.*

and

B. REMBOLD, Dr.-Ing.*

SUMMARY

Until recently, the application of microwave systems has been hampered by the relatively large and expensive equipment, particularly in the millimetre and submillimetre-wave range. The development of more reliable and efficient solid-state sources up to the submillimetre-wave range has now stimulated new interest in commercial applications. Three different approaches can be distinguished, radar, radiometry and transmission measurement applications.

The widest spread applications are found in radar systems for traffic control and industrial and scientific use. High resolution, high antenna gain and easy acquisition, even of non-metallic objects, in conjunction with contact-free or remote sensing, makes the millimetre-wave approach best suited for measurement purposes. Applications are the contactless measurement of velocity, distance and acceleration on rail vehicles, and radiometry in medicine and industry, e.g. for cancer diagnostics and atmospheric remote sensing.

The behaviour of materials and gases can be examined, using the transmission measurement approach. Atmospheric pollution control and the non-destructive evaluation of solid materials are realizations of this technique.

Employing millimetre- and submillimetre-wave frequencies for these applications gives inherent improvement of the measurement accuracy and due to the high transmission loss for this frequency range the risk of interference between different measurement systems is effectively reduced.

1 Introduction

The technical and scientific applications of microwaves have a long history. Microwave communication systems and radar, as well as microwave radio astronomy and remote sensing, are well known today. Based on these traditional applications, a new branch has grown up rapidly in recent years in industrial process control.¹⁻⁵ This is the measurement of non-electrical variables such as quantity of materials, flow rates, geometrical dimensions, physical properties, etc. Until recently, industrial application was hampered by the relatively bulky and expensive equipment necessary, particularly in the millimetre and submillimetre-wave range. The development of more reliable and efficient solid-state sources up to the submillimetre-wave range requiring only relatively simple low-voltage power supplies now gives millimetre- and submillimetre-wave instrumentation an all solid-state status and has stimulated new interest in commercial applications, such as traffic control or measurement purposes in industry, science and sports.

Three different types of measurement can be distinguished, concerning the application of millimetre- and submillimetre-waves: radar, radiometry, and transmission measurement.

The widest spread applications are found in radar systems. The contactless measurement of velocity, distance and acceleration of railbound vehicles or the stock level measurement in blast furnaces are applications of this type.

Radiometry, i.e. the receiving and evaluation of thermal microwave noise, is utilized in medicine and industry. Examples are cancer diagnostics and microwave thermometers, and contact-free measurement through thermally insulating, but microwave transparent, materials.

Transmission measurement systems are used to examine the behaviour of materials or gases inserted between a given transmitter and receiver; the entire field of radiospectrometry belongs to this class. Pollution control, in the atmosphere as well as in industrial production processes, can be carried out using this technique. The non-destructive evaluation of solid materials like ceramic, is another interesting application.

This survey shows the wide variety of microwave applications. The principles underlying these basic types of measurements are explained and various specific applications are discussed.

2 Radar Applications

Radar systems in the industrial and scientific field have to meet special demands, which differ widely from normal radar requirements. The important differences are set out in Table 1.

* AEG-Telefunken, Geschäftsbereich Hochfrequenztechnik,
Postfach 1730, D-7900 Ulm, Germany.

For various applications these requirements can be met by employing millimetre- or submillimetre-wave radar sets. This equipment has specific benefits for a number of measuring tasks:

- contact free and remote sensing
- insensitive against dirty and hot environments, like dust or material pollution
- insensitive against electromagnetic interference
- transmission through otherwise opaque media, like fog or chemical gas clouds.

Additional advantages, like high resolution, high antenna gain and easy acquisition of non-metallic objects are rendered possible by the short wavelength.

Radar sensors at millimetre- and submillimetre-wavelengths allow fast and continuous measurements; no alteration of the material under test is necessary; the measurement response is an electrical signal; no transducers are required, thus giving the possibility of on-line signal processing, an important feature in the case of process control.

However, there are also some difficulties and problems in conjunction with the installation of millimetre- and submillimetre-wave measuring systems. Traditional equipment is large and expensive, caused mainly by the employment of transmitter tubes like b.w.o.s or klystrons. The subsequent use of state-of-the-art technology in the millimetre- and submillimetre-wave range now gives an opportunity to overcome this problem. Today we can use semiconductor devices as transmitters up to the submillimetre-wave region. Much work has been carried out concerning millimetre-wave integration techniques and can be used here, thus resulting in small size and lightweight components.

Three different kinds of radar-sets can be distinguished for the various applications in the discussed field:

- Doppler or continuous wave (c.w.) radar
- frequency modulated continuous wave (f.m.c.w.) radar, and
- pulse radar.

They are all used for different purposes, as shown in Table 2.

The simplest type of radar is the c.w. or Doppler radar (Fig. 1). It consists of a solid-state transmitter, in

Table 1

Comparison between standard and industrial radar applications. (From W. Schilz.¹)

	Standard radar	Industrial radar
Range	100 km	10 m
Resolution	10 m	1 mm
Power	kW	mW
Volume	m ³	cm ³
Direction	any	one

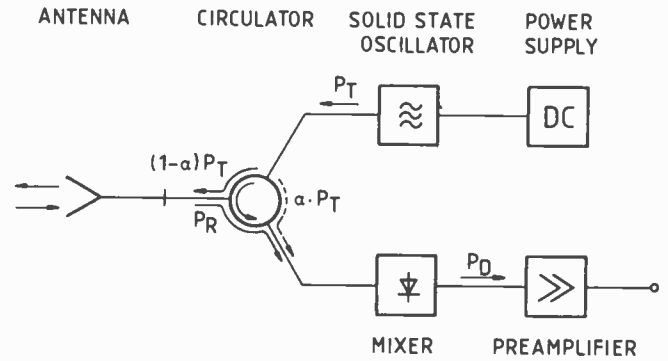


Fig. 1. Basic block diagram of a solid-state c.w. radar.

most cases a Gunn or impatt oscillator, producing the signal, which is fed to the antenna via the diplexer, a circulator, for example. This signal is reflected by a moving object back to the antenna; the reflected signal reaches the mixer via the diplexer. A certain fraction of the oscillator power is fed to the mixer as well, by means of a reflection screw between diplexer and antenna for example, thus generating the Doppler frequency f_d at the output of the mixer:

$$f_d = \frac{2f_s v}{c} \cos \alpha \quad (1)$$

where f_s is the transmitter frequency, v is the speed of the moving object, c is the velocity of e.m. waves, and α is the angle between radar beam and direction of movement.

This Doppler signal is amplified and can be processed subsequently.

The design described is rather simple, there are only three r.f. components, oscillator, diplexer and mixer, and the resultant performance is not high. For most purposes the temperature drift and long-term stability of the oscillator can be neglected. The directivity of the diplexer should be low ($\alpha \cdot P_T$ path to the mixer) and the mixer conversion loss can be greater than 10 dB, because of the short measurement range of not more than 10 m. This gives low production costs, which is of inherent importance from the industrial point of view.

Table 2

Comparison between different radar principles

Radar type	Application	Cost
C.w. radar	Velocity measurement (distance, acceleration), vibration detection	Low
F.m. c.w. radar	Distance meter for measurement systems with only one dominating target	Medium
Pulse radar	Distance measurement under more sophisticated conditions, like several targets, received echoes from other transmitters, etc.	Medium

2.1 Traffic and Traffic Control

A 35 GHz Doppler radar, the vsb-RADAR, being developed at AEG-Telefunken for contactless velocity, distance and acceleration measurements on railborne vehicles⁶ is an example of this approach. The r.f. unit is designed as shown in Fig. 1. Operation under railway conditions demanded a specific antenna design, especially because of modulation caused by sleepers. For mounting purposes, the antenna should be flat and easily adjustable. These problems can be solved employing a waveguide slot antenna. Because of the nearly constant power density in the irradiated area, this antenna generates a smaller Doppler spectrum than a comparable horn antenna under the conditions described; the machined antenna is only 24 mm high and can be mounted horizontally. Figure 2 shows a vsb-RADAR unit mounted on a locomotive bogie.

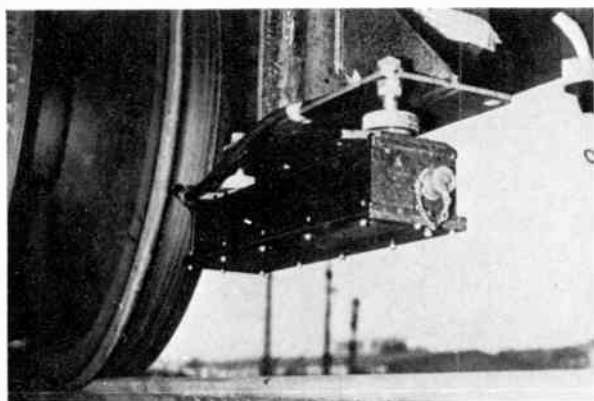


Fig. 2. AEG-Telefunken vsb-RADAR mounted on a locomotive bogie.

Since 1976 several tests have been carried out, showing that this radar can be used to measure distances with an accuracy of better than 4% standard deviation which is adequate for most applications in industry and traffic control. Modern railborne traffic, however, and especially the partly automatized railway technique of tomorrow, requires a more accurate measurement. A signal processor has therefore been developed at AEG-Telefunken with which distance measurements having an accuracy of 0.1% standard deviation have been made; velocity and acceleration are then measured with an accuracy of 1%. These figures hold for the velocity range from 20 to 250 km/h.

The application of the vsb-RADAR for non-railborne vehicles is also possible. In general the swinging of the body of the vehicle has an influence on the measurement accuracy. Nevertheless the vsb-RADAR has shown good results under test, a 5% accuracy having been achieved for distance measurements on a delivery van.

The collision avoidance radar for automobiles,^{7,8} developed by AEG-Telefunken in conjunction with



Fig. 3. AEG-Telefunken 35 GHz collision avoidance radar for automobiles.

Bosch (Fig. 3), is an example of a more complex design approach, in order to satisfy the requirements of road traffic. Insensitivity to countertraffic, no interference with other anticollision radars, and a good performance even on a gradual curve, were the main problems that had to be solved.

For this purpose, a non-coherent 35 GHz pulse radar has been developed. The propagation time Δt of the transmitted and reflected pulse signals is taken to determine the distance of the reflecting target R :

$$R = \frac{c\Delta t}{2} \quad (2)$$

The all-solid-state radar consists of separate transmitting and receiving sections, as in Fig. 4. Easy decoupling of receiver and transmitter can be achieved, without the need for expensive and less reliable diplexer components like circulators and pin-attenuators, using this two-antenna design. The horizontal and vertical beam-width of the antennas was chosen in such a way that an area 4.5 m wide by 6 m high at a distance of 100 m is

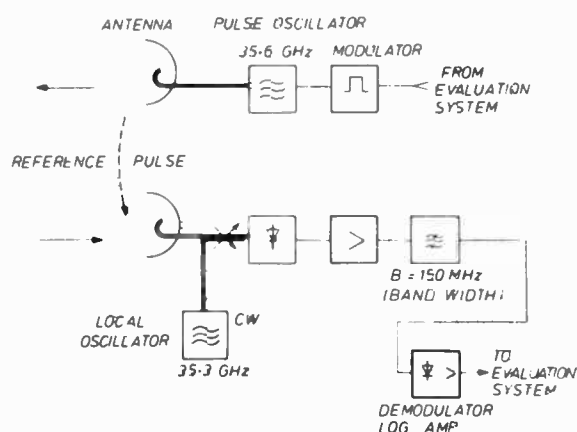


Fig. 4. Simplified block diagram of the collision avoidance radar.

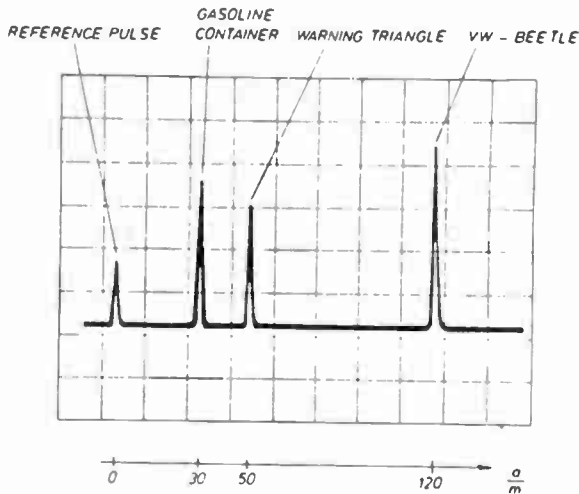


Fig. 5. Echo pulse oscillogram of various objects.

irradiated. The evaluated detection range of the radar is a function of the actual speed of the vehicle in which it is installed. The maximum evaluated detection range is 120 m, while the maximum achievable detection range is greater than 600 m. Figure 5 shows a radar echo oscillogram with different objects on the road. The left-hand pulse is the reference or cross-talk pulse. A gasoline container at 30 m, a warning triangle at 50 m and a VW-Beetle at 120 m generate the subsequent pulses. Measurements have shown that even under heavy rain conditions the radar will work quite well up to a distance of 100 m. Due to the pulse-sampling technique employed, no interference with other anticollision radars has been observed.

Since 1977 a number of different types of cars and buses have been equipped with the collision avoidance system. The usefulness of the system has been proved over several hundred thousand kilometres. At present an experimental programme is under way with the aim of clarifying the effects of the traffic situation in connection with the best physiological alarm presentation.

This principle of radar distance measurement by means of a pulse radar can be used in many other areas too. Examples are protective systems for construction sites, distance warning for heavy cranes, and fully automatic marshalling operations on railway goods yards.

Further applications may be mentioned. It is useful, for instance, to measure the height of trucks approaching bridge building sites so that if necessary they can be stopped. Shipping also offers a wide range of applications. Distance measurement between ship and quay is an important manoeuvring aid for large-capacity tankers. The loading and unloading of supply vessels can be performed more safely, even in heavy seas, by measuring the distance between ship and drilling rig. Radar at millimetre wavelengths can also be useful on inland waterways. Measurement of the length and

position of ships close to locks allows full exploitation of the lock lifting capacity.

Due to the measurement situation being dominated by one target only, the latter applications are well suited for the use of an f.m. c.w. radar system. A description of this type of radar will be given in the next Section.

2.2 Industrial Applications

In industry millimetre- and submillimetre-wave radar can be employed in any situation where length and height have to be measured in a contact-free manner.⁹⁻¹¹ Measurement of length of rolled steel sections for subsequent cutting is one example, the monitoring of the continuous refilling of furnaces for coal-gasification is another. In steel industries, the measurement of the stock level in blast furnaces also needs a contact-free distance meter.

All the applications mentioned have the following in common: the reflection is dominated by one target, scatter from other objects can be neglected, and the measurement range is rather short, e.g. 2 to 20 m. For these purposes a millimetre- or submillimetre-wave f.m. c.w. radar is best suited. The basic block diagram of this type of radar is the same as shown in Fig. 1, except that the frequency of the oscillator is no longer constant, but swept linearly in a sawtooth manner, as in Fig. 6, thus resulting in an output frequency f_{if} of:

$$f_{if} = \frac{2\Delta f l}{Tc} \quad (3)$$

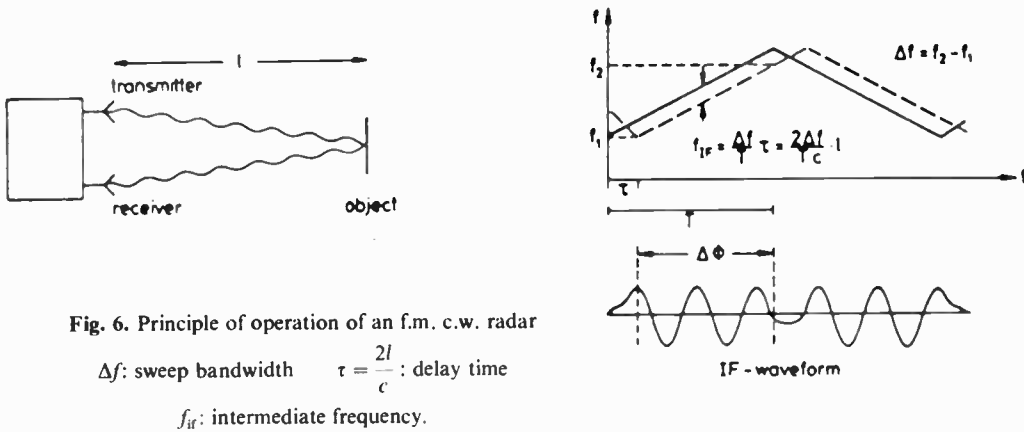
where Δf is the sweep bandwidth, T is the sweep time and l is the distance to be measured.

The calibration of the system mainly depends on the accuracy of the frequency variation Δf , while the resolution depends only on the magnitude of Δf , thus making the millimetre- or submillimetre-wave approach the best choice. A high transmitter frequency enables a large value for Δf , resulting in a high resolution, i.e. a high measurement accuracy.

Stock level measurements in blast furnaces have been carried out using transmitter frequencies of 10, 35 and 86 GHz. The achieved results show the advantage of the mm-wave approach. Due to the smaller wavelengths the antenna beamwidth for a given aperture size can be reduced, resulting in fewer false measurements caused by reflections of the furnace walls for example. Further details of this measurement system, which is under development now, will be published later.

The non-contact measurement of the filling level in tanks is likewise an important application in chemical and petrochemical industries. For this purpose a special 90 GHz Doppler radar has been developed. The large-scale production of synthetic paints in chemical processes, for example, requires the mixing of various liquids in proper quantities.

Distances are usually measured with pulse or f.m. c.w.



radars, as described above. Distance is determined by the pulse propagation time or the frequency variation respectively. (Measurement of the phase difference between the emitted and the reflected wave of a Doppler radar is a third possibility; however, this method is only valid for a distance less than half a wavelength.) Taking into account the measurement environment, with distance set to zero at time t_0 , the movement of the liquid height at a time $t > t_0$ can be determined by counting the phase difference zeros in the time range $t - t_0$, thus resulting in a relative distance measurement method. Due to the distance increment a_i being a function of the transmitter frequency f_s ,

$$a_i = \lambda/4 = \frac{c}{4f_s} \quad (4)$$

The resolution depends directly on the frequency chosen. The application of this technique to the measurement of liquids has one particular requirement. In order to overcome the problem of splashing during the measurement, the Doppler radar must be able to distinguish

between forward and backward movements. Figure 7 shows the block diagram in principle. A 90 GHz impatt-oscillator with an isolator-matched output feeds the antenna via two feed-through mixers. The distance between these mixers is adjusted to obtain a 90° phase difference between the two Doppler signals. Used as feed-through devices the conversion loss of these mixers is rather high, about 20 dB, but as the measurement range is below 5 m this value is of minor importance. After amplification, both Doppler signals are passed to a processing unit. Again the design is simple, giving a low production cost, which can be reduced even more by the subsequent employment of circuit integration techniques.

2.3 Scientific Applications

Scientific research and investigation is the third field of application for millimetre and submillimetre-wave radar techniques. Behaviour research on bats, carried out by using a 35 GHz f.m. c.w. radar, is one example. Remote supervision of heart beat and respiration rate of patients

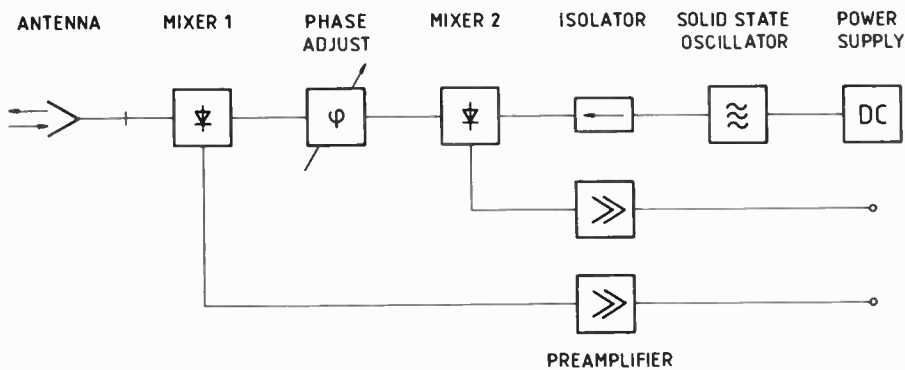


Fig. 7. Block diagram of a 90 GHz Doppler direction sense radar.

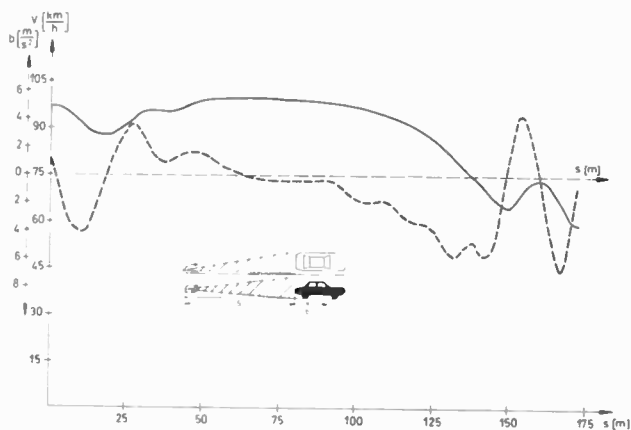


Fig. 8. Velocity and acceleration of a car approaching the traffic lights of a road/railway crossing as a function of distance. (From P. Wimber.¹²)

under intensive care unit conditions is another. A 86 GHz c.w. radar is used to determine the particle speed in a micro-meteoroid simulation chamber. This high frequency is necessary to detect the very small glass beads, less than 0.5 mm diameter, used as projectiles in the research launcher.

In order to optimize the operation of warning lights at railway–street crossings, investigations on the behaviour of car drivers in front of these crossings have been carried out.¹² By means of a 35 GHz c.w. radar, velocity and acceleration of cars approaching the lights are recorded and evaluated as a function of distance, as shown in Fig. 8. Using this arrangement, the effect of changes in the switching of the lights is studied under psychological supervision. Thus the most suitable sequence of switching can be found.

2.4 Sports

A very recent field for millimetre- and submillimetre-wave radar applications is in the area of sport. The vsb-RADAR has been used, for example, to monitor the speed of bob-sleds in an ice-channel, in order to improve training possibilities. A 35 GHz c.w. radar is now used to measure the speed and acceleration of bob-sleds in the initial start-phase.

Perhaps the next Olympic Winter Games will introduce another novel millimetre-wave system, with 35 GHz Doppler radars being used to establish a direct measurement system for ski-jumping competitions, as in Fig. 9.^{13–15}

3 Radiometry Applications

In radio astronomy the thermal radiation of extra-terrestrial matter is used to obtain information about the universe. The Earth’s surface and atmosphere is also investigated with remote sensing techniques, again using



Fig. 9. Sketch of the measurement arrangements at a ski-jumping site. (From U. Pramann.¹⁵)

their thermal radiation behaviour. Integrated wideband and low noise receivers today make it possible also to apply this technique for industrial purposes.^{19, 20}

From Planck’s law, the radiated energy of matter is proportional to temperature for millimetre- and submillimetre-waves over a wide temperature range, thus allowing simple calibration of microwave thermometers. Thermometers of this type can be applied successfully in any case where the object to be measured is hidden behind a solid wall which is transparent to millimetre-waves, e.g. ceramics, mineral or other thermal insulating materials. Being able to look through hot gases, microwave radiometers are used to determine the temperature distribution in the core of nuclear reactors.

There is increasing interest in millimetre-wave thermographs for medical diagnostics, in order to detect and locate subcutaneous tumours, such as in breast cancer or in the human spine. Remote, non-invasive temperature sensing of the human body can be carried out with penetration depths from 0.1 mm to 1 cm, using this technique.^{16, 17} Figure 10 shows a millimetre-wave thermograph equipment being used for clinical tests. Some results, achieved with thermographic scans at 45 GHz, are given in Fig. 11.

Atmospheric remote sensing is not only used for scientific investigations, but for weather observation purposes too. A microwave atmospheric sounding radiometer (m.a.s.r.) was developed¹⁸ to obtain three-

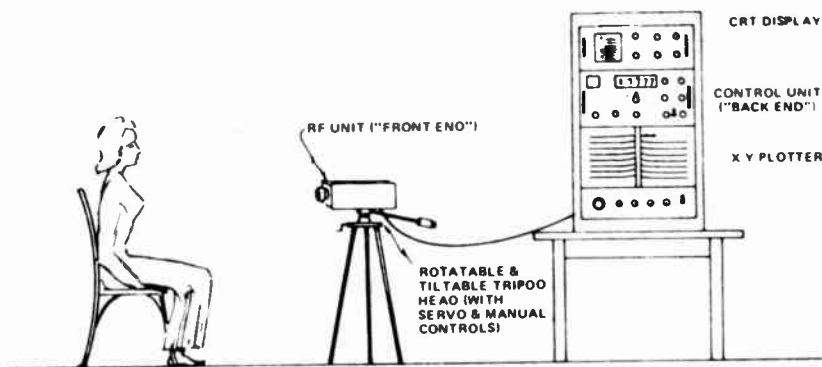


Fig. 10. Millimetre-wave thermography set up for automatic breast scans. (From J. Edrich.¹⁶)

dimensional temperature and humidity fields from geosynchronous orbit. The observation and prediction of severe storms and other weather phenomena should be facilitated by the use of a four-band millimetre-wave radiometer, with channel frequencies of 104, 118, 140 and 183 GHz, as shown in Fig. 12.

4 Transmission Measurement Systems

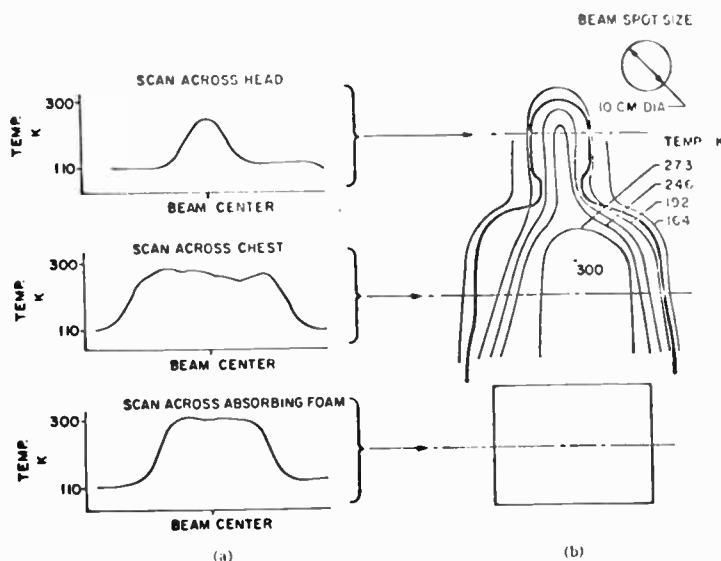
A microwave signal propagating through any kind of passive media is subjected to dispersion and absorption. This can directly be utilized for the non-destructive evaluation of materials, such as ceramics for example. In many cases the interaction of microwaves with a given material is also frequency selective, thus giving the opportunity to analyse composite materials, such as gas mixtures.

The ability of millimetre waves to penetrate some kinds of ceramic materials at frequencies of 100 GHz and above makes the microwave technique a useful tool for the non-destructive evaluation of such materials. Experimental results²¹ demonstrate the basic feasibility of using this technique to detect and locate various types of inclusions or even voids in silicon nitride, Si_3N_4 . A

block diagram of the experimental arrangement is shown in Fig. 13. Physically, the transmitter and receiver antenna apertures were placed directly opposite one another, with the ceramic sample placed in between. Swept frequency scattering measurements from 75 to 110 GHz were made to determine the best operating frequency for each type of inclusion. Figure 14 shows a so-called 'C scan' image of hot pressed Si_3N_4 with four types of inclusions. Inclusions as small as 125 μm in diameter have been detected.

Many gases exhibit an electric dipole moment, which can interact with r.f. radiation. Transitions between different rotational states of a molecule are induced by the r.f. radiation, resulting in selective absorption of the transmitted signal. This phenomenon can be used to build up a spectrometer.^{22,23} Figure 15 shows the basic block diagram of such a gas spectrometer operating in the frequency range from 18 to 26 GHz. A balanced arrangement, and 'Stark modulation', is applied here in order to improve the sensitivity of the system. The measurement set-up is all-solid-state and may operate automatically. The determination of the components of a gas mixture is carried out continuously and quanti-

Fig. 11. (a) Typical thermographic scans at 45 GHz. (b) Thermogram of a human subject produced from experimental scan data. (From J. Edrich.¹⁶)



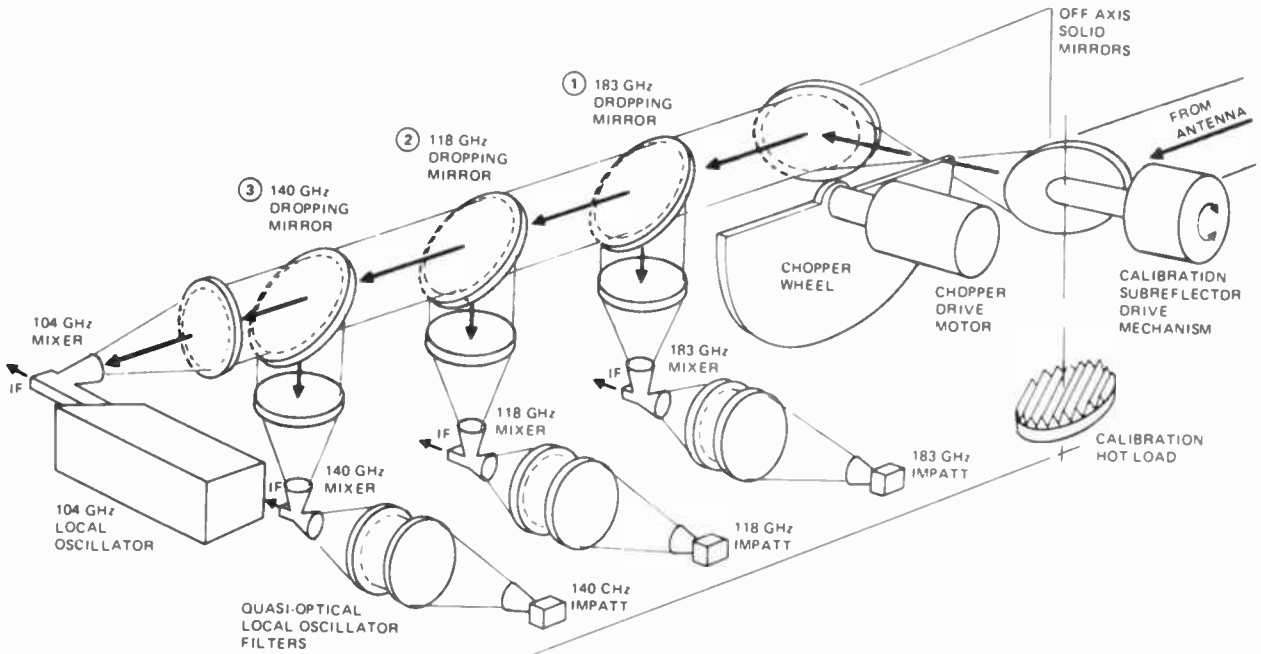


Fig. 12. Isometric view of a microwave atmospheric sounding radiometer. (From F. E. Goodwin *et al.*⁸)

tatively. Several gases and gas mixtures have been investigated, using this measurement system, the detection limit achieved being 1–50 parts in 10⁶.

5 Conclusions and Prospects

Millimetre-wave technology is now being used for a wide variety of applications in traffic control, industry and science. However, it is only in recent years that this technology has spread. The new impetus evident today is based on two assumptions, the availability of solid-state devices up to the submillimetre-wave range and increasing activities on millimetre-wave circuit design and integration techniques.

Due to the rapid development in semiconductor technology solid-state devices can now be used for power generation, signal detection and frequency conversion, even in the millimetre- and submillimetre-wave range. Details of sources and receivers are given in papers by Purcell²⁴ and Clifton²⁵ in this issue.

The problems of waveguides are also considered in this issue in the paper by Harris.²⁶ Industrial installations of millimetre- and submillimetre-wave systems demands waveguide and components that are of good quality and high reliability, but are also inexpensive.

One alternative that we have investigated to overcome this problem is the employment of quasi-planar structures, like fin-line, combining the waveguide with microstrip-, slot- or related-line configurations.^{27,28} With these lines high mechanical precision is no longer

the key to the development of millimetre-wave circuitry. Nearly all microwave components can be realized using this technique, unless high *Q*-factors are required. At the present time quasi-planar integrated millimetre-wave components are available in the frequency range from 20 to 110 GHz; and an extension up to 200 GHz and perhaps more should be possible. Another alternative to waveguide is the employment of quasi-optical devices, as shown in Fig. 12. This approach is suited for frequencies above 100 GHz.²⁹

Nearly all applications described have been carried out so far at frequencies below 100 GHz. This is due mainly to availability and costs of the components being used and the situation will change on the development of low cost components of satisfactory quality for higher frequencies. The attenuation level for earthbound transmission is discussed in the paper by Emery and

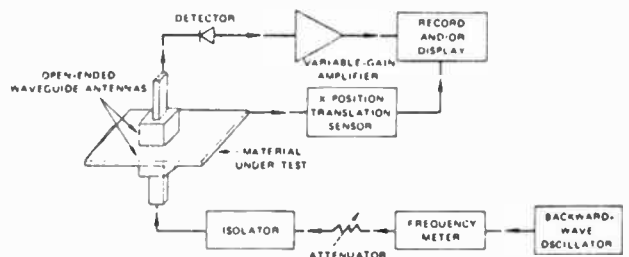


Fig. 13. Experimental arrangement for cross-polarized transmission measurements. (From A. J. Bahr.²¹)

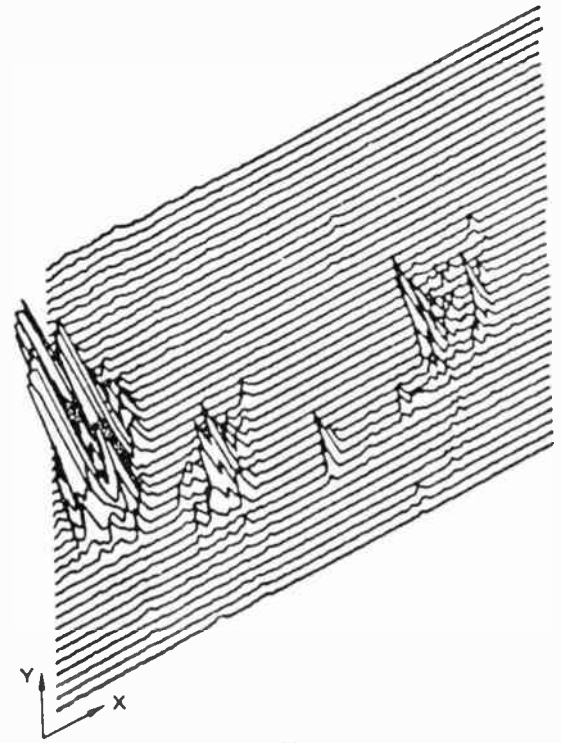
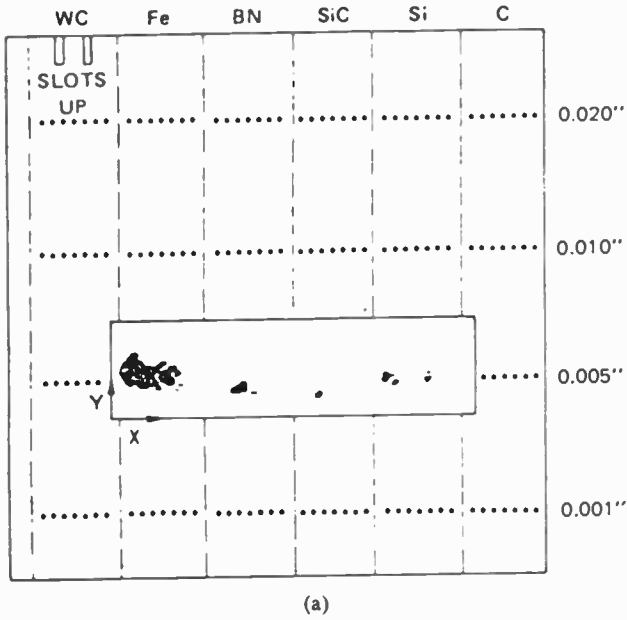


Fig. 14. 'C scan' image of four types of inclusions in Si_3N_4 measured at 91 GHz. (a) Excess signal versus position. (b) Amplitude versus position. (From A. J. Bahr.²¹)

Zavody³⁰ in this issue, and will affect frequency choice. For outdoor medium range applications, e.g. the collision avoidance system, the frequency range around 60 GHz will be useful, while frequencies around 120 or 180 GHz may be used for indoor, short range, measurements. The low attenuation windows of the atmosphere, at 90, 140 and 230 GHz, should be kept free for those particular applications requiring low transmission loss, such as 'long' range millimetre-wave radar or radiometer systems.

The main advantage of the employment of higher frequencies lies in the inherent improvement of measurement accuracy. Regarding equation (3), the resolution of an f.m. c.w. radar distance meter is proportional to the sweep bandwidth Δf . The value of Δf can be increased easily if the transmitter frequency f_s is increased. The accuracy of the Doppler direction sense radar is directly proportional to the transmitter frequency f_s (see eqn. (4)). An important factor is also the reduced risk of interference between different millimetre-

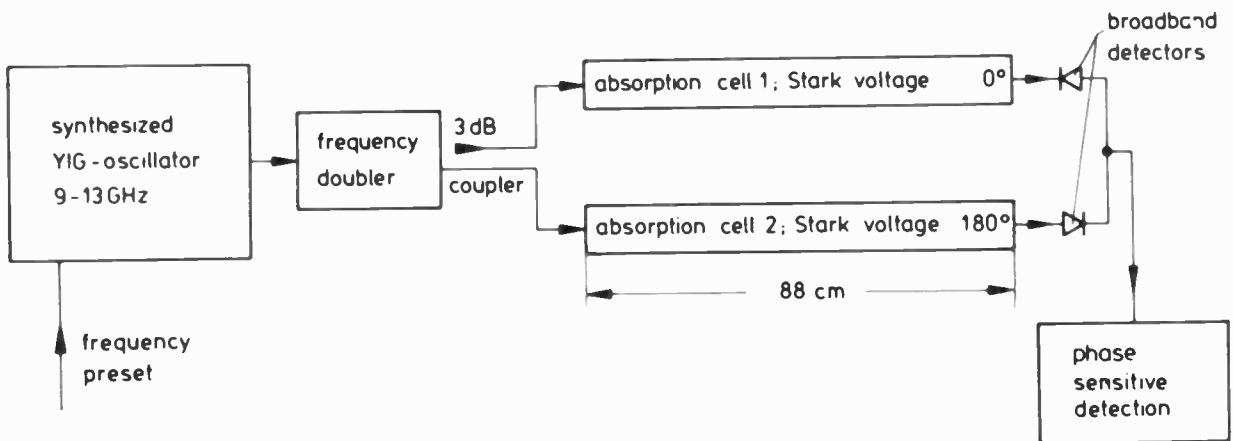


Fig. 15. Balanced measuring system of a microwave spectrometer for industrial gas analysis. (From B. Schiek *et al.*²³)

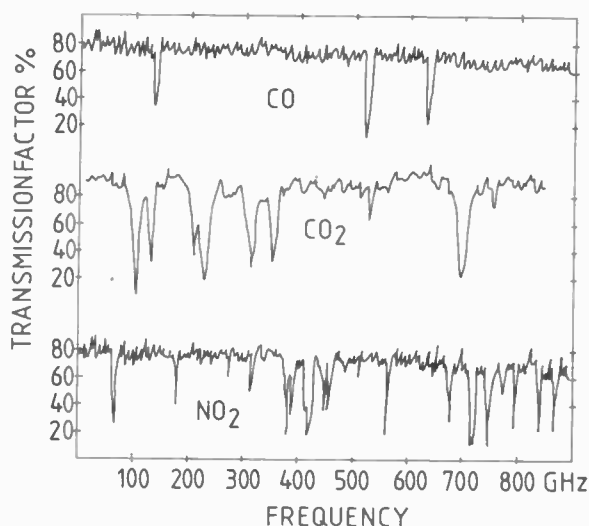


Fig. 16. Resonance absorption of different gases versus frequency.³⁴

wave measurement systems, due to the high transmission loss for the frequencies being proposed.

Considering industrial spectrometry and pollution control, the frequency range of interest also extends far into the submillimetre-wave region. Figure 16 displays resonance absorption spectra³¹ of CO, CO₂ and NO₂ between 100 and 800 GHz. Such characteristic properties enable constituents to be identified.

6 References

- Schilz, W., 'Novel microwave technique for industrial measurements', Symposium Digest 8th European Microwave Conference, 1978, Paris, pp. 166-75.
- Griffin, D. W., 'Development in microwave instrumentation for industrial process control', Electronic Instrumentation Conference, Hobart, Australia, 17th-19th May 1972, pp. 180-5.
- Ramachandriah, M., 'A survey of the application of microwaves in non-communication areas', Vol. II, chap. 15.1. Symp. Dig. 3rd EuMC, 1973, Brussels.
- Whetton, C. P., 'Industrial and scientific applications of Doppler radar', *Microwave J.*, pp. 39-42, November 1975.
- Howe, H., 'Microwaves for the masses', *Microwave System News*, pp. 81-94, August 1977.
- Keller, B., Meinel, H. and Rembold, B., 'vsb-RADAR, a 35 GHz Doppler radar for velocity, distance and acceleration measurements on railbound vehicles', Symp. Dig. 8th EuMC 1978, Paris, pp. 598-602.
- Lindner, K. and Wiesbeck, W., '35 GHz-Impulsradarsensor zur Verwendung in Abstandswarngeräten für Kraftfahrzeuge', *NachrTech. Z.*, 29, no. 9, pp. 667-72, 1976.
- Dull, E. H. and Peters, H. J., 'Collision avoidance system for automobiles', SAE Conf., Detroit 1978, Paper no. 780, p. 263.
- Meinel, H., 'Millimetre-wave f.m. radar for length and distance measurements', AEG-Telefunken Progress, pp. 67-8, 1977.
- Jacobson, R., Schiek, B. and Schilz, W., 'Microwave distance meter with ± 2.5 mm resolution', Symp. Dig. 5th EuMC, 1975, Hamburg, pp. 203-7.
- 'Industrieanwendungen von Mikrowellen', *Valvo Brief*, 26th August 1975.
- Wimber, P., 'Ein Verfahren zur Messung des Fahrverhaltens des Fahrers vor Bahnübergängen', *Straßenverkehrstechnik*, 1978, no. 5.
- Meinel, H., 'Millimetre-Wellen Doppler-Radar', AEG-Telefunken Press Information, Hannover Fair, April 1976.
- Kreiselmeier, K., Bolkart, M. and Schmall, K. H., 'Elektronische Sprungweitenmessung' (W. Steinbrück Verlag, Baden-Baden, 1976).
- Pramann, U., 'Skispringen, Sender in der Sohle', *Stern*, no. 7, p. 110, 1977.
- Edrich, J., 'A millimetre-wave thermograph for human breast and spine scans', Symp. Dig. 6th EuMC, Rome, 1976, pp. 137-40.
- Edrich, J. and Smith, C. J., 'Millimetre-wave thermograph as subcutaneous indicator of joint inflammation', Symp. Dig. 7th EuMC, Copenhagen, 1977, pp. 713-17.
- Goodwin, F. E., Hersman, M. S. and Shiue, J. C., 'A four band millimetre-wave radiometer design for atmospheric remote sensing', IEEE Symp. Digest MTT-S, Ottawa, 1978, pp. 245-7.
- Skou, N., 'A multifrequency radiometer system', Symp. Dig. 7th EuMC, Copenhagen, 1977, pp. 419-23.
- Lüdeke, K. M., Schiek, B. and Köhler, J., 'Radiation balance microwave thermograph for industrial and medical applications', *Electronics Letters*, 14, no. 6, pp. 194-6, 1978.
- Bahr, A. J., 'Nondestructive microwave evaluation of ceramics', *IEEE Trans. on Microwave Theory and Techniques*, MTT-26, no. 9, pp. 676-83, 1978.
- Leskovar, B., Hopkins, D. B. and Kolbe, W. F., 'Optimal design criteria for millimetre-wave spectrometers', Symp. Dig. 5th EuMC, Hamburg, 1975, pp. 228-32.
- Schiek, B., Paukner, T. and Schilz, W., 'A microwave spectrometer suitable for gas analysis in industrial applications', Symp. Dig. 7th EuMC, Copenhagen, 1977, pp. 251-5.
- Purcell, J. J., 'Millimetre wavelength impatt sources', *The Radio and Electronics Engineer*, 49, no. 7/8, pp. 347-50, July/August 1979.
- Clifton, B. J., 'Schottky diode receivers for operation in the 100-1000 GHz range', *The Radio and Electronic Engineer*, 49, no. 7/8, pp. 333-46, July/August 1979.
- Harris, D. J., 'Waveguides for the 100-1000 GHz frequency range', *The Radio and Electronic Engineer*, 49, no. 7/8, pp. 389-94, July/August 1979.
- Hofmann, H., Meinel, H. and Adelseck, B., 'New integrated millimetre-wave components using fin-lines', Symp. Dig. IEEE MTT-S, Ottawa, 1978, pp. 2-23.
- Meinel, H. and Rembold, B., 'New millimetre-wave fin-line attenuators and switches', Symp. Dig. IEEE MTT-S, Orlando, 1979, pp. 249-52.
- Kerr, A. R., Siegel, R. M. and Mattauch, R. J., 'A simple quasi-optical mixer for 100-1000 GHz', Symp. Dig. IEEE MTT-S, 1977, San Diego, pp. 96-8.
- Emery, R. J. and Zavody, A. M., 'Atmospheric propagation in the frequency range 100-1000 GHz', *The Radio and Electronic Engineer*, 49, no. 7/8, pp. 370-80, July/August 1979.
- Elektrospezial GmbH, Hamburg, 'Experimentalstudie über die Eignung und Realisierung eines Mikrowellenradiometers zur Analyse von Fremdgasen in der Atmosphäre, pp. 26-7.

Manuscript received by the Institution on 6th April 1979
(Paper No. 1888/AMMS 95)

Radar systems for operation at short millimetric wavelengths

STEPHEN L. JOHNSTON,
B.E.E., M.S.E.E., Sen. M.I.E.E.E.*

SUMMARY

A number of radar systems are now being developed for operation in the 100–1000 GHz frequency range. A few special-purpose radars are already in limited use in this region. This paper is a survey of radars at short millimetric wavelengths. The new IEEE Standard definition of radar and IEEE Standard letter designations for radar bands are presented with a note on the transitional nature of this frequency region. Possible radar applications and principal advantages of short millimetric wavelength radar are given. Technical characteristics of a number of representative civilian and military radars are given. It is shown that the characteristics of some of these radars are similar, but characteristics of other radars vary considerably. A discussion of future trends and issues concludes this survey paper.

* Editor-in-Chief, *International Radar Directory*, Huntsville, Alabama 35802, U.S.A.

1 Introduction

Although practical radar is now almost half a century old and therefore presumably has reached a plateau of technology, recent developments now give radar a new look, both literally and figuratively. This paper will consider two developments in radar—certain new applications, and employment of a new frequency region (short millimetric waves). The latter development has necessitated some new radar technology which in turn has resulted in this new look. The term *radar* is now being used for apparatus which bears almost no physical resemblance to our well-known microwave radar.

In recognition of this new look, the Radar Systems Panel of the Institute of Electrical and Electronics Engineers has changed the definition of radar from Radio Detection And Ranging to: 'An electromagnetic device for detecting the presence and location of objects. The presence of objects and their distance (range) are determined by the transmission and return of electromagnetic energy; direction is usually obtained also, through use of a movable or rotating directive antenna pattern. Original name derived from radio detection ranging': IEEE Standard.¹ This definition now encompasses 'laser radars', 'lidars', and 'laser range finders'. It also includes some missile guidance systems, e.g. 'seekers'. A semi-active missile seeker is actually a bistatic radar! For this paper we will exclude 'pseudo-radars' which are used solely for attenuation or propagation measurements.

The main objective of this paper is to consider the other radar development—employment of a new frequency region, namely short millimetric waves (s.m.w.). Radar originally operated in the high frequency region, e.g. 20 MHz, then progressed to higher frequencies as technology permitted. Most radars currently operate in the 'microwave' region, especially 1–10 GHz. Operational radars have also been developed at 35 GHz. The new IEEE Standard radar letter bands designations with corresponding ITU frequencies are shown in Table 1.^{2,3} The frequency range 40–300 GHz was designated as 'millimetre' since there is no currently established ITU radar (radio-location) band in this region. Figure 1 (after Altshuler) shows the IEEE radar letter bands, ITU radio-location bands and the atmospheric attenuation over the region of 10 to 300 GHz.⁴

The region above 300 GHz (variously to 3000 GHz) is generally known as the 'submillimetre' region. Accordingly, the region of this paper—100 to 1000 GHz—therefore embraces part of the IEEE mm radar band and part of the 'submillimetre' band. This region has also been referred to by some as 'near millimetre'. Since Fig. 1 shows that there is an atmospheric 'window' with minimum attenuation at about 95 GHz, this paper will also include 95 GHz. As will be seen later, there is

Table 1 Comparison of radar-frequency letter band nomenclature with ITU nomenclature

Radar nomenclature		International Telecommunications Union nomenclature			
Radar letter designation	Frequency range	Frequency range	Band no.	Adjectival band designation	Corresponding metric designation
HF	3-30 MHz	3-30 MHz	7	High Frequency (HF)	Decametric Waves
VHF	30-300 MHz	30-300 MHz	8	Very High Frequency (VHF)	Metric Waves
UHF	300-1000 MHz	0.3-3.0 GHz	9	Ultra High Frequency (UHF)	Decimetric Waves
L	1.0-2.0 GHz				
S	2.0-4.0 GHz				
C	4.0-8.0 GHz	3.0-30 GHz	10	Super High Frequency (SHF)	Centimetric Waves
X	8.0-12.0 GHz				
Ku(J†)	12.0-18.0 GHz				
K	18.0-27.0 GHz				
Ka(Q†)	27.0-40 GHz	30-300 GHz	11	Extremely High Frequency (EHF)	Millimetric Waves
mm	40-300 GHz				

† These are the more usual British designations. Another system, combining letters and numerals, is being introduced by NATO.—*Editor.*

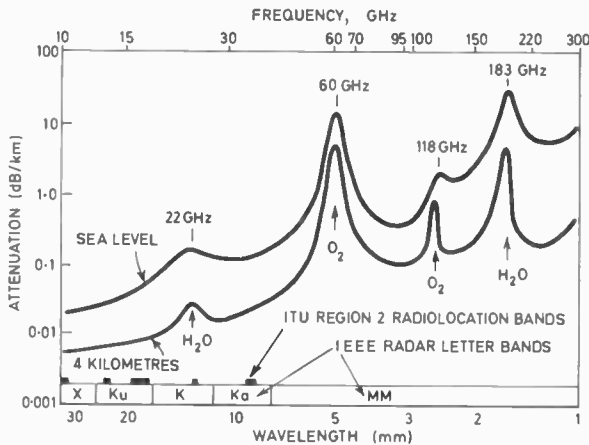


Fig. 1. Atmospheric attenuation at millimetre wavelengths with IEEE radar letter bands and ITU radiolocation bands for Region 2. (After Altshuler *et al.*⁴)

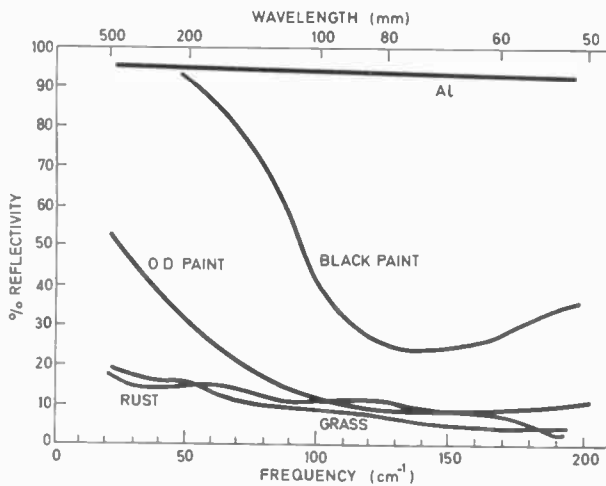


Fig. 2. Normal reflectivity in percent for common materials. Included are a normally oxidized aluminium surface (AL), aluminium sprayed flat-black paint (BLACK PAINT), olive-drab paint on brass (OD PAINT), a freshly cut blade of grass (GRASS), and a rusty iron surface (RUST). (From Blue and Perkowitz.⁶)

currently considerable radar activity at 95 GHz with lesser activity at 140, 220 and 890 GHz.

As Senitzky and Oliner⁵ observed, this is indeed a region of transition. This transitional nature is extremely important in the case of radar, e.g. in r.f. sources (from electron devices to lasers), in antennas (from parabolic reflectors to optical lenses and mirrors), in r.f. 'transmission lines' (from waveguides to mirrors) and, possibly of principal importance, in the nature of scattering from the target itself. Figure 2 from Blue⁶ illustrates the change of scattering from several materials over part of this frequency region—600 to 6000 GHz.

Skolnik^{7,8} enumerated several possible applications of 'submillimetre' radar as listed in Table 2. These will be treated more fully subsequently.

The principal advantages of short millimetric waves over microwaves (not necessarily in order of importance) are as follows:

- Smaller antenna diameter required for same antenna gain/beamwidth.

- Increased angular resolution for the same antenna diameter.

- Increased bandwidth (a bandwidth of 1% at 300 GHz is equal to all frequencies below S-band centre frequency (3 GHz)).

- Increased immunity to friendly interference (Electromagnetic Compatibility (EMC)) by virtue of smaller beamwidth and relatively low present employment density.

- Increased immunity to unwanted detection by hostile forces.

- Increased sensitivity to Doppler velocity effects.

- Less attenuation due to fog, smoke and dust than electro-optical or optical systems operating in infra-red regions.^{27,30}

These applications have differing importance in various radar applications.

Table 2 Suggested radar applications

Low-angle tracking†	Remote sensing of the environment
'Secure' military radar†	Surveillance
Interference-free radar†	Target acquisition
Cloud sensing radar†	Missile guidance
High resolution radar†	Navigation
Imaging radar	Obstacle detection
Ground mapping	Clutter suppression
Map matching	Fuzes
Space object identification	Harbour surveillance radar
Lunar radar astronomy	Airport surface detection radar
Target characteristics	Landing aids
Weather radar	Air traffic control beacons
Clear-air turbulence sensor	Jet engine exhaust and cannon blast

† Applications in which Skolnik believed⁷ that sub-millimetre waves offer more advantage than microwave frequencies.

2 Past/Present S.M.W. Radar Applications

Tables 3–5 adapted from Johnston⁴ list representative civilian millimetre band radar applications, representative 95 GHz millimetre band radars and 140 GHz–1 THz s.m.w. radar applications respectively. Figures 3–8 from Johnston⁴ show a number of the 95 GHz radars of Tables 3 and 4. A novel millimetre-band radar of the U.S. Army Ballistic Missile Research Laboratories (not illustrated)^{35, 36} has a special antenna. The r.f. heads of this conical scan tracking radar may be changed in ten minutes to permit operation at 95, 140 or 220 GHz as desired. Figure 9 shows the 140 GHz scale model radar cross-section measurement radar developed at EMI.^{37–40} The applications of the unique 140 and 890 GHz radars are discussed more fully elsewhere in this issue.³⁹ Technical characteristics of a number of these radars are contained in Tables 6 and 7. Table 8 contains further characteristics of the EMI radars.

The data of Tables 6 and 7 are very instructive. There is indeed a wide variety of application represented here—from police radar to space object identification. With one notable exception—space object identification—detection/tracking ranges are very small as compared to microwave radars—usually a maximum of 3 km. Average r.f. power outputs are about one watt (30 dBm) or less. R.f. sources used include thermionic and solid

state devices and lasers. Thermionic devices similarly include a wide variety—magnetrons (both US and UK), travelling wave tubes, EIO, carcinotron, klystron and gyrotron. The impatt diode is a very popular solid-state r.f. source. Both gas-pumped lasers and 'straight' lasers are to be used. The EMI 280 GHz radar of Table 8 is noteworthy in that it employs pulsed operation of the carcinotron in contrast to usual carcinotron c.w. or f.m. operation as in the first BRL 140 GHz radar of Tables 5 and 7.³⁴ Pulsed carcinotron operation was not mentioned by Convert and Yeou,⁴³ although discussed by Favre⁴⁴ a decade earlier.

Antenna diameters are usually less than one metre and guided missile antennas are generally less than 25 cm. Most of the systems listed in these two tables operate around 95 GHz but the two highest frequency systems of Table 7 are essentially electro-optical rather than microwave, the battlefield surveillance radar of Table 7 actually operating in the next atmospheric window to the 280 GHz r.c.s. radar. This surveillance radar, which is now under construction, is an example of the proclivity, cited by Senitzky and Oliner,⁵ to employ techniques which are most familiar to the designer. Thermionic devices (carcinotrons and b.w.o.s) which operate at frequencies as high as 600 GHz have been built.

Antenna types used in the radars of these two tables include both 'conventional' microwave types and optical types (lens and mirror). The Cassegrain r.f. type is very popular due to its shorter waveguide length and its resulting lower waveguide loss.

Receiver types employed have a similar wide variety from the conventional microwave types through optical. The superheterodyne or a variant of it is almost universally used in all systems because of its increased sensitivity (30 dB or more) over the 'crystal-video' receiver. One application utilizes a homodyne (zero frequency or 'video frequency' i.f.) with one r.f. source which serves a dual function of transmitter and local oscillator in a Doppler radar.

3 Future Trends and Issues

The past/present s.m.w. radar applications reported above are indeed interesting. It must be noted, however, that most of these systems are very recent and none of them are yet 'operational', i.e. are not now in commercial or military use and have not been produced

Table 3 Representative civilian millimetre band radar applications

Application	Identification	Country/Source	Year	Frequency	References
Ground temperature	Airborne radiometer	West Germany/IFFM	1973	90 GHz	9
Harbour speed monitoring		USA/Coast Guard	1977	95 GHz	10, 11
Police radar		USA/Hughes Aircraft	1977	95 GHz	10
Unknown	Unknown	West Germany/Telefunken	1979	90 GHz	12

Table 4 Representative military 95 GHz band radar applications

Application	Identification	Country/Source	Year	References
Land	Monopulse tracker	USA/NADC	1969	13
Land	Space object identification	USA/Aerospace	1969	14, 15
Land	Instrumentation, backscatter GT-M	USA/Georgia Tech.	1966	16-18
Land	Arctic terrain avoidance	USA/APL	1973	19-21
Helicopter	Wire detection (Noter)	USA/APL	1975	22, 23
Land	Imaging	USA/Hughes	1975	24
Airborne	Mapping	USA/Goodyear	1974	25
Land	C.w. Doppler radar	USA/Hughes	1975	10
Land	Noise modulated radar	USA/BRL	1976	
Missile	Seeker	USA/Hughes	1977	26
Land	Antitank radar (<i>Startle</i>)	USA/Martin/Rockwell	1977	27
RPV	Battlefield surveillance (<i>Aquila</i>)	USA/Norden	1977	28-30
Air	Solid state radiometer	USA/Sperry	1977	31, 32
Missile	Seeker	USA/USAMIRADCOM	1977	33
Land	Tracking, r.c.s. measurement	USA/BRL	1966	34
Missile	Radiometer	USA/Minn. Honeywell	1978	
Land	Re-entry instrumentation	USA/BMDATC	1980	

Table 5 Representative military 140 GHz-1 THz radar applications

Application	Identification	Country/Source	Year	Frequency	References
Land	Tracking, r.c.s. measurement	USA/BRL	1966	140 GHz	34
Land	Tracking, r.c.s. measurement	USA/BRL	1979	140 GHz	35
Land	Scale model, r.c.s. measurement	UK/EMI	1977	140 GHz	37-39
Land	Tracking, r.c.s. measurement	USA/BRL	1979	220 GHz	36
Land	Scale model, r.c.s. measurement	UK/EMI	1979	280 GHz	37-39
Land	Battlefield surveillance	USA/MIRADCOM	1979	530 GHz	40
Land	Scale model, r.c.s. measurement	UK/EMI	1979	890 GHz	37-39

Table 6 Selected characteristics of representative 95 GHz band radars

Identification	Average power output dBm	R.f. source	P.r.f. kHz	Antenna	Antenna dia. cm	Receiver type
Police radar } Harbour radar }	20	Impatt	c.w.	Cassegrain	15 61	Homodyne
Monopulse tracker	28	Magnetron	1.5	Cassegrain	61	Superhet
Space object identification	50	TWT				Superhet
Instrumentation	73	Gyrotron	NS	Paraboloid	460	Paramp
	30	Extended interaction oscillator	0.4	Cassegrain	30	Log superhet
SEV arctic radar	25	Magnetron	2	Parabolic cylinder Pill box line feed	150 250	Superhet
Wire detection	25	Magnetron	2	Parabolic	45	Superhet
Imaging	28	Magnetron	3	Cassegrain	61	Superhet
<i>Startle</i>	27	Impatt	NS	NS	35	Superhet
<i>Aquila</i> r.p.v.	26	Magnetron	4	Shaped reflector	63	Superhet
Missile seeker	30 (peak)	Impatt	NS	Cassegrain Conical scan	25	Log superhet

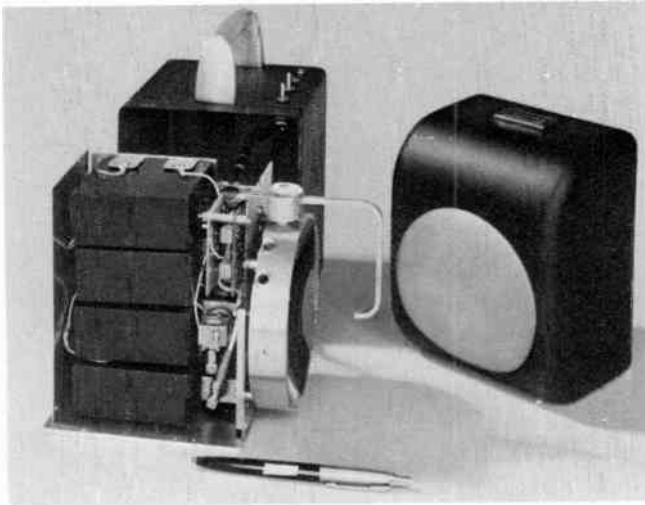


Fig. 3. Hand-held 95 GHz police radar. (Courtesy Hughes Aircraft.)



Fig. 5. 95 GHz missile seeker. (Courtesy Hughes Aircraft.)

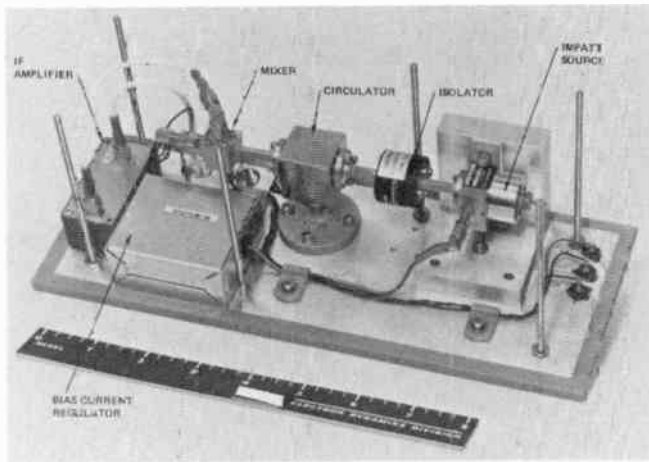


Fig. 4. R.f. assembly for police radar. (Courtesy Hughes Aircraft.)

Detector type	Target types	Max. range km	Purpose	I.f. MHz	Pulse width ns	Local oscillator	Ref.
Silicon Schottky	Autos Ships	NS 3	Auto speed Ship speed	0.02 (video) 400	c.w.	Homodyne	10 10, 11
Cooled Schottky NS	Various Space Objects Various	8000 NS	Space object identification Various	NS 160	NS 20	NS NS	13 14, 15 16-18
NS	Ground obstacles	5	Obstacle detection	NS	NS	Klystron	19-21
NS	Wire, rope	2	Wire detection	NS	100	Klystron	22, 23
NS	Ground	10	Ground mapping	335	28	Klystron	25
NS	Ground vehicles	3	Target location, tracking	NS	NS	NS	27
NS	Ground objects		Ground mapping, target location	160	20/50	NS	28-30
Schottky	Ground targets	3	Air-to-surface missile	NS	NS	NS	31-32

NS = not stated

Table 7 Selected characteristics of representative 140 GHz–1 THz radars

Identification	Frequency GHz	Average power output dBm	R.f. source	P.r.f. kHz	Antenna	Antenna dia. cm	Receiver type
Ground tracker	140	20/27	Klystron/ Carcinotron	1	Fresnel zone plate/Cassegrain	43/91	Double conversion superhet
Ground tracker	140	10	Impatt	20	Conical scan	NS	Superhet
Scale r.c.s. measurement	140	29	Extended interaction oscillator	500	NS	1–5	Superhet
Ground tracker	220	7	Impatt	20	NS	NS	Superhet
Scale r.c.s. measurement	280	14	Carcinotron	NS	NS	0.5–3	Superhet
Battlefield surveillance	530	0	Gas-pumped laser	NS	Mirror	100	Superhet
Scale r.c.s. measurement	890	15	HCN laser	c.w.	Lens	5	Homodyne

in quantities yet. While the developers are naturally optimistic, it is too early confidently to predict the future of s.m.w. radar. It is interesting to note that neither Barton⁴¹ nor Walsh⁴² in their recent radar forecast papers gave any consideration to millimetre or s.m.w. radar. While it is possible that these wavelength radars could reach significant levels of use, it is unlikely that this

will be anything approaching microwave radar. Barring radical changes, it is not anticipated that s.m.w. radar will challenge microwave radar in its principal role of aircraft and ship detection and tracking at long ranges.

In its principal application of very short range detection and tracking there are several issues affecting utilization of s.m.w. radars: component capability/

Table 8 Parameters of 0.1 to 1 THz modelling radars made and being used by EMI Electronics Ltd.

Precision short range measurement radars as specified below are in use at EMI Electronics Ltd., Wells, for accurate determination of radar echoing area properties by scale model methods.

Frequency GHz	Transmitter			Antennae (Note 1)	
	Type	Peak power	Mean power	Beamwidth (3 dB two-way) (Note 2)	Sidelobes (max. one-way)
140 GHz	Extended interaction oscillator (Varian VKT 2419C1)	30 W	750 mW	3° to 15° say 10°	– 30 dB
280 GHz	Carcinotron (CSF CO-10 Pulse)	1.0 W	25 mW	3° to 15° say 5°	– 30 dB
890 GHz	HCN laser (made in-house)	30 mW	30 mW	0.5° to 5° say 1½°	– 23 dB

RADAR SYSTEMS FOR OPERATION AT SHORT MILLIMETRIC WAVELENGTHS

Detector type	Target types	Max. range km	Purpose	I.f. MHz	Pulse width ms	Local oscillator	Ref.
Point contact diode	Various	0.3	R.c.s. measurement, target tracking	750 and 30	Sawtooth	2nd harmonic klystron	34
Schottky	Various	3	R.c.s. measurement, target tracking	NS	100	Klystron	35
Schottky diode	Aircraft	0.02	R.c.s. measurement	4000	50	Klystron	37-39
Quasi-optical mixer	Various	2	R.c.s. measurement, target tracking	NS	100	Impatt	36
Schottky diode	Aircraft	0.02	R.c.s. measurement	4000	NS	Carcinotron	37-39
NS	Ground vehicles	1	Battlefield surveillance	NS	NS	NS	40
InSb He cooled	Aircraft, ships	0.02	R.c.s. measurement	500 Hz	c.w.	Homodyne	37-39

NS = not stated

availability, radar performance, system integration, design trade-offs, investigation of novel guidance schemes, comparison with other approaches, and present lack of available s.m.w. radar frequency allocations. All of these are important and have been discussed previously⁴—and in the interest of brevity will not be treated here.

It should be noted that the present WARC-79 could well provide much needed relief for this last issue. Indeed, as Tables 6 and 7 show, technology is now available to permit at least limited employment of s.m.w. radars.

4 Acknowledgments

The author gratefully acknowledges many helpful discussions with his colleagues both in government and industry.

Contributions by Mr L. A. Cram, EMI Electronics Ltd., Wells, Somerset, England, of Table 8 and Fig. 9 are greatly appreciated.

Views expressed herein are those of the author and not necessarily those of the Department of the Army or Department of Defense.

Polarization available (Note 3)	Receiver			
	L.o. type	Intermediate frequency	Final bandwidth	Echoing area to give 30 dB S/N
All combinations for Rx and Tx	Klystron (Varian VRT 2123B)	3.9 GHz	1, 10 or 500 Hz	10^{-4} m ² at 22.5 m
All combinations for Rx and Tx	Carcinotron (CSF CO 1 CW)	3.9 GHz	1 or 10 Hz	10^{-4} m ² at 22.5 m
All combinations for Rx and Tx	Homodyne	(500 Hz)	1 or 10 Hz	10^{-4} m ² at 15 m

Note 1: Separate antennae are used for transmitter and receiver.

Note 2: A wide choice of aeriels is available over a range of beamwidths.

Note 3: With separate transmitter and receiver antennae multiple polarization switching has been arranged to permit any of the following combinations to be chosen: VV, HH, VH, RR, LL, RL, LR.

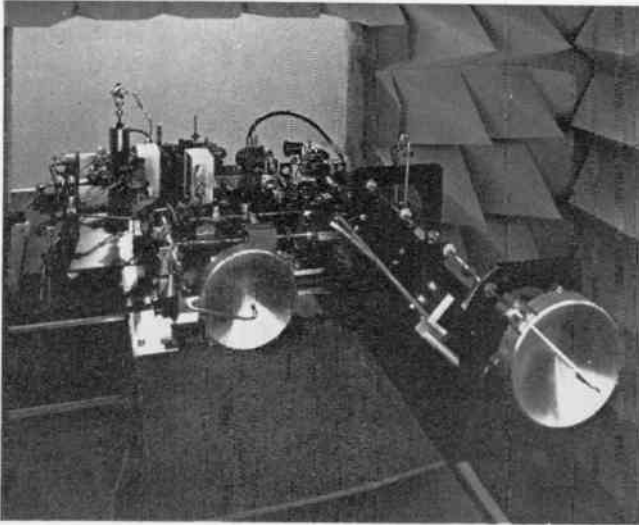


Fig. 6. 94 GHz radar for measuring radar cross-sections. (Courtesy Aerospace Corporation.)

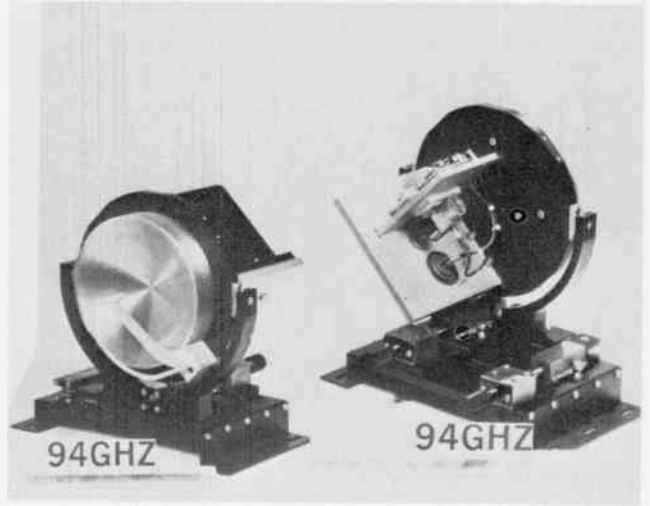


Fig. 7. 94 GHz ground intrusion radar. (Courtesy US Naval Avionics Facility.)

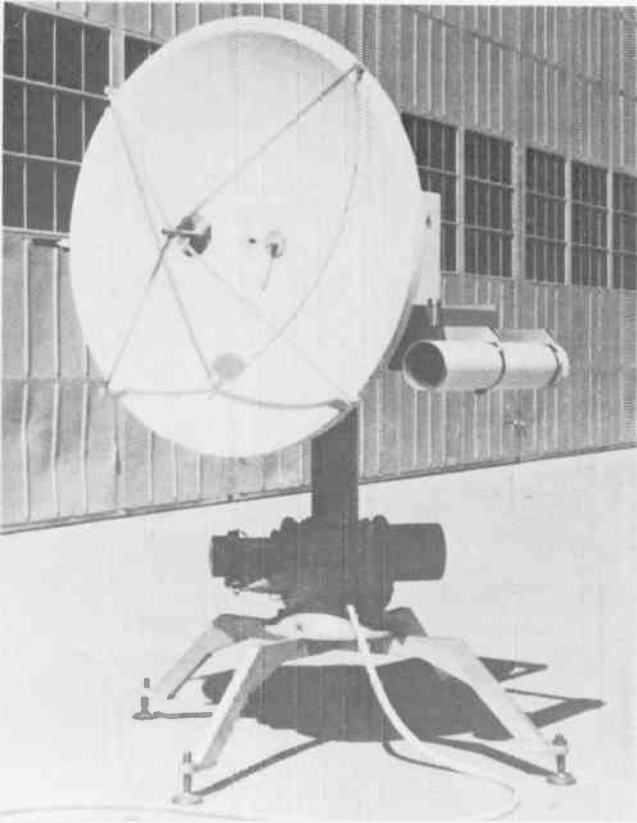


Fig. 8. 95 GHz ground-based radar imagery antenna mount. (Courtesy Goodyear Aero-space.)

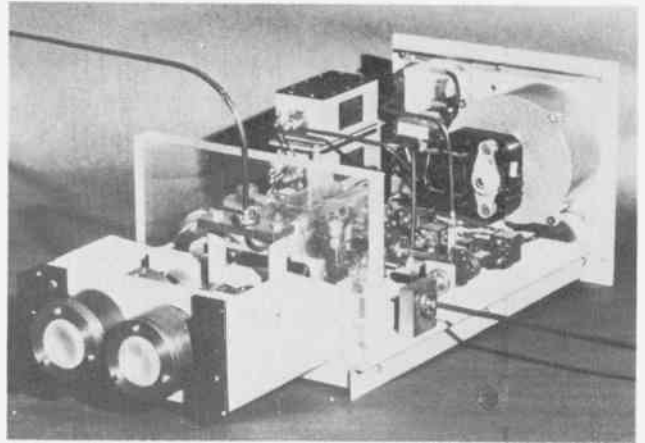


Fig. 9. 140 GHz measurement radar: r.f. unit and antennae. (Courtesy EMI Electronics.)

5 References

- 1 'IEEE Standard Radar Definitions' IEEE Standard 686 1977, November 1977.
- 2 'IEEE Standard Letter Designations for Radar Bands', IEEE Standard 521 1976, November 1976.

- 3 'IEEE Radar-Frequency Designations', *Microwave J.*, **20**, no. 6, p. 68, June 1977.
- 4 Johnston, S. L., 'Some aspects of millimeter radar', Proc. Int. Conf. on Radar, Paris, pp. 148-59, 4th-8th December, 1978.
- 5 Senitzky, B. and Oliner, A. I., 'Introduction: submillimeter waves—a transition region', Proc. Symp. on Submillimeter Waves, Polytechnic Press of the Polytechnic Institute of Brooklyn, pp. xxv-xxvii ff, 1970.
- 6 Blue, M. S. and Perkowitz, S., 'Reflectivity of common materials in the submillimeter region', *IEEE Trans. on Microwave Theory and Techniques*, MTT-25, no. 6, pp. 491-3, June 1977.
- 7 Skolnik, M. I., 'Millimeter and submillimeter wave applications', Proc. Symp. on Submillimeter Waves, Polytechnic Press of the Polytechnic Inst. of Brooklyn, New York, pp. 9-26, 1970.
- 8 Skolnik, M. I., 'Millimeter and Submillimeter Wave Applications', NRL Memorandum Report 2159, 12th August 1970, AD 712055.
- 9 Aumiller, B., 'An Airborne 90 GHz Radiometry Receiver', November 1973, DFVLR, DLR MTT 74 05, in German (Translation, NASA N76 11410, FSROTT-163).
- 10 Bernues, F. J. *et al.*, 'A solid state 94 GHz Doppler radar', 1975 IEEE MTT-S International Microwave Symposium Proc., pp. 258-60.

- 11 'Field Test of an Experimental 94 GHz Doppler Radar', US Coast Guard Research and Development Center Report, October 1975.
- 12 Barth, H. and Bischoff, M., 'A 90 GHz fm-cw radar transmitter', paper F-3, IEEE/MTT-S International Microwave Symposium and Workshops, Orlando, 30th April 4th May, 1979.
- 13 Foral, M. J., 'Millimeter wave radar investigations', 1969 IEEE GMTT International Microwave Symposium, Dallas, Texas, 5th-7th May, 1969, pp. 489-92.
- 14 Hoffman, L. A. *et al.*, 'A 94 GHz radar for space object identification', *IEEE Trans.*, MTT-17, pp. 1145-9, December 1969.
- 15 Dybdal, R. B., 'Millimeter radar application to space object identification', EASCON-77 Rec., pp. 16/4 A-1.
- 16 Dyer, F. B. *et al.*, 'Review of Millimeter Wave Radar Development at Georgia Tech.', Radar and Instrumentation Laboratory, Engineering Experiment Station Georgia Institute of Technology, Internal Technical Report 77-01, May 1977.
- 17 Scheer, J. A., Eaves, J. L. and Currie, N. C., 'Modern millimeter instrumentation radar development and research methodology', EASCON-77 Proc., pp. 16/6 A-H.
- 18 Currie, N. C., Scheer, J. A. and Holm, W. A., 'Millimeter wave instrumentation radar systems', *Microwave J.*, 21, no. 8, pp. 35ff, August 1978.
- 19 Kilgus, C. C., 'High resolution antenna system', pp. 132-3 in 'Developments in Science and Technology', APL/JHU,† Rpt DST-1, FY 73.
- 20 Gooding, O. E. and Schneider, J. D., 'Experimental obstacle detection system for an arctic surface effect vehicle', pp. 84-6 in 'Developments in Science and Technology', APL/JHU,† Rpt DST-2, FY 74.
- 21 Warnke, L. L., 'High speed color television display system', pp. 86-8, *loc. cit.*
- 22 Schenkel, F. W. and Finkel, A., 'NOTER (Nap of the Earth), 95 GHz Radar Wire Avoidance System', APL/JHU,† Report S3-R-029, QM 75-081, July 1975.
- 23 Schenkel, F., 'Note-R (Nap-of-the-Earth Radar), Helicopter Wire Detection System', Report of the ARPA/Tri-Service Millimeter Wave Workshop, APL/JHU,† QM-75-009, January 1975, pp. 149-62.
- 24 Heney, J. F., 'A 94-GHz imaging radar', p. 147, *loc. cit.*
- 25 Wilcox, F. P., 'Development and test of a 95 GHz terrain imaging radar', 1974 Millimeter Waves Techniques Conference, Naval Electronics Laboratory Center.
- 26 'Guidance seeker for missiles developed', *Aviation Week and Space Technology*, p. 63, 5th December 1977.
- 27 Balcerak, R., Ealy, W., Martino, J. and Hall, J., 'Advanced IR sensors and target acquisition', *Proc. Soc. Photo Opt. Instrum. Engrs*, 128, pp. 172-84, 27th-29th September 1977 (Effective Utilization of Radar).
- 28 Le Boss, B., 'Experimental millimeter radar system' (News update) *Electronics*, 50, no. 18, p. 8, 1st September 1977.
- 29 Kosowsky, L. H. *et al.*, 'A millimeter wave radar for RPV's', Army Aviation Electronics Symposium, April 1976.
- 30 Kosowsky, L. *et al.*, 'A millimeter wave radar for the mini-RPV', Proc. AIAA/DARPA Conf. on Smart Sensors, Hampton, Va., pp. 27/1-18, 14th-16th November 1978.
- 31 Adair, J. E., 'Millimeter wave radiometry', *Microwave J.*, 20, no. 11, pp. 32ff, November 1977.
- 32 Davis, Richard, 'Millimeter waves, a solution that's finally found a problem', *Microwave System News*, 7, no. 9, pp. 63-7, September 1977.
- 33 Green, Jr., A. H., 'Applications of millimeter wave technology to army missile systems', EASCON-77 Record.
- 34 Kammer, J. E. and Richer, K. A., '140 GHz millimeter bistatic wave measurements radar', BRL Memo Report 1730, January 1966, AD 484693.
- 35 McGee, R. A. and Loomis, J. M., 'Radar tracking of an M-48 tank at 94 and 140 GHz', DARPA-Tri Service Millimeter Workshop, November 1977.
- 36 McGee, R. A., private communication.
- 37 Cram, L. A. and Staveley, J. R., 'Recent developments in scale modeling of radar reflections by radar and sonar methods', 'Radar-77', 25th-28th October 1977, pp. 473-7, IEE Conference Publications No. 155.
- 38 Cram, L. A. and Woolcock, S. C., 'Review of two decades of experience between 30 GHz and 900 GHz in the development of model radar systems', AGARD Conf. Proc., pp. 1-6-1 to 12, Munich, 4th-8th September 1978.
- 39 Cram, L. A. and Woolcock, S. C., 'Development of model radar systems between 30 and 900 GHz', *The Radio and Electronic Engineer*, 49, no. 7/8, pp. 381-8, July/August 1979.
- 40 Hartman, R. L. and Kruse, P. W., 'Submillimeter system for imaging through inclement weather', Conf. Digest, Second Int. Conf. and Winter School on Submillimeter Waves and their Applications, IEEE Cat. no. 76 CH 1152-8 MTT, San Juan, December 1976, pp. 229-30.
- 41 Barton, D. K., 'Radar technology for the 1980's', *Microwave J.*, 21, no. 11, pp. 81ff, November 1978.
- 42 Walsh, T. E., 'Military radar systems: history, current position and future forecast', *Microwave J.*, 21, no. 11, pp. 87ff, November 1978.
- 43 Convert, G. and Yeou, T., 'Backward wave oscillators', Chap. 4 in: Benson, F. A. (ed.), 'Millimetre and Submillimetre Waves' (Iliffe, London, 1969).
- 44 Favre, M., 'Results obtained on cross field carcinotrons under pulsed operations', *Proc. Instn Elect. Engrs*, 105, pt 5, sup. 10, pp. 533-7 and 542-3, 1958 (Proc. Int. Conf. on Microwave Valves, May 1958).

*Manuscript received by the Institution on 6th April 1979
(Paper No. 1889/AMMS 96)*

† APL/JHU = Applied Physics Laboratory, Johns Hopkins University.

Atmospheric propagation in the frequency range 100–1000 GHz

R. J. EMERY, B.Sc., Ph.D.*

and

A. M. ZÁVODY, B.Eng.*

SUMMARY

The influence of the atmosphere on propagation in the frequency range 100–1000 GHz is discussed in terms of molecular absorption, effects due to particles or droplets, and refractive effects. Compared with propagation at lower frequencies, molecular absorption shows a substantial increase in effect, mainly due to absorption by water vapour molecules and this aspect is given particular attention. Molecular absorption may be modelled using published line parameters, but attention must also be given to significant absorption caused by double molecules of water vapour (dimers), which at present are not included in the line tabulations. The total predicted absorption accounts for the main aspects of molecular absorption observed in the field, but at frequencies with minimum attenuation, away from the strong resonance absorption regions, field measurements have shown significant differences which are not understood. Refractive effects and the influence of particles, involving both absorption and scattering, can be modelled, but prediction is limited by the need for appropriate meteorological data which has a particular relevance to propagation in this frequency range. Comparison with prediction is made both for horizontal transmission paths and slant paths through the atmosphere.

* Science Research Council, Appleton Laboratory, Ditton Park, Slough, Berks. SL39JX, U.K.

1 Introduction

Studies of atmospheric propagation in the frequency range 100–1000 GHz relate to a number of research areas. Apart from the development of communications, both civil and military, basic research in this field is important in atmospheric physics and meteorology, as well as in astronomy where there is a need to characterize the atmosphere through which observations are made. This paper will first cover the main factors influencing atmospheric propagation at these frequencies, and then outline how they may be treated for modelling purposes. This will be used to discuss propagation over a horizontal path in the lower atmosphere, and then extended to the problem of a slant transmission path through the atmosphere.

Many aspects of system performance, such as antenna gain and usable bandwidth, etc., are improved by increasing the operating frequency. However, with propagation systems which are required to have good performance in low visibility conditions, an upper limit to the frequency will be encountered in the range 100–1000 GHz, due to atmospheric effects. The influence of the atmosphere on propagation in this frequency range, often termed near-millimetre waves, differs from more conventional experience with microwave systems in two main respects. First there is a moderate increase in the effect of particles, derived mainly from small water drops in mist and fog, and secondly there is a substantial increase in the effect of molecular absorption. These aspects receive particular attention in the present discussion.

2 Basic Characteristics of Attenuation

The influence of the atmosphere on electromagnetic propagation may be separated into three main categories—molecular absorption, refractive effects, and extinction due to particles or droplets involving both scattering and absorption, as shown in Table 1. Molecular absorption is present in all atmospheric conditions, whereas refractive effects are dependent on the spatial structure of the atmosphere and the geometry of the system. The wide range in the number density of particles in the atmosphere makes their effect very variable. These categories will be treated separately, although in the atmosphere they combine to produce the total attenuation.

2.1 Molecular Absorption

Atmospheric molecules with an electric or magnetic moment may absorb energy from an incident electromagnetic wave by making a transition to a higher energy state. Resonance absorption occurs when the frequency ν of the incident wave matches the difference between the two energy states, so that

$$E_{\text{higher}} - E_{\text{lower}} = h\nu$$

Table 1
Main atmospheric effects on propagation in the frequency range 100–1000 GHz

Atmospheric visibility	Clear air		Low visibility
Atmospheric influence	Molecular absorption	Refractive effects	Absorption and scattering
Physical mechanism	Rotation and vibration spectra mainly of H ₂ O (and complexes), CO ₂ , O ₃ , N ₂ O, CO, O ₂ , and CH ₄	Variations in refractivity structure	Water as rain, cloud, mist, fog, snow and hail. Aerosols (solutions in water). Solids as dust, smoke, etc.
Attenuation	×		×
Amplitude scintillation	×	×	×
Phase scintillation		×	
Depolarization			×
Backscatter			×

where h is Planck's constant. For the frequency range 100–1000 GHz these transitions mostly involve changes in the rotational energy of the molecules, with vibrational transitions becoming more significant at higher frequencies. For transmission paths in the lower atmosphere, molecular absorption in the near millimetre wavelength range is mainly dominated by the complicated spectrum of monomeric water. Atmospheric molecules which may need to be considered for transmission calculations are shown in Fig. 1, with their variation in number density with altitude. Collisions between molecules broaden the resonance absorption to cover a range of frequencies, giving a characteristic spectral line shape. A basic treatment of this 'collision broadening' is given by Townes and Schawlow¹ and Goody,² for example. The variation of temperature and pressure with altitude may be obtained from the US Standard Atmosphere,⁷ and is summarized by Goody² and McClatchey.⁸

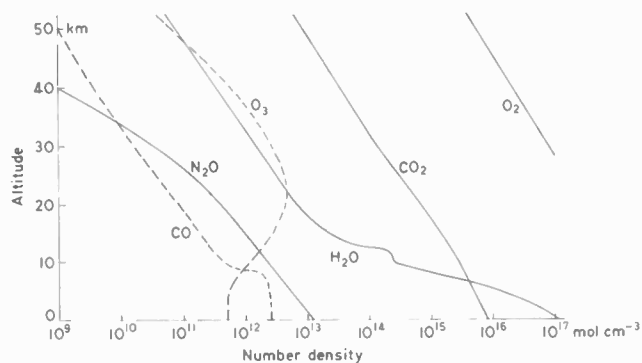


Fig. 1. The variation of density with altitude for atmospheric molecules, with tabulated line parameters,¹¹ which can give significant absorption in the atmosphere. The data are derived from the following references: H₂O (Ref. 3), O₃ (Ref. 4), N₂O (Refs 4, 5), CO (Ref. 6), and for CO₂ and O₂ a constant volume mixing ratio has been assumed^{7,8} with temperate summer conditions.

2.1.1 The absorption equation

When molecular absorption occurs in the atmosphere at altitudes less than about 50 km, the lifetime of the excited molecule is longer than the mean time between collisions, and so local thermal equilibrium applies. In this case a general formula for the absorption coefficients $\gamma(\nu)$ at the frequency ν in Hz may be written as follows:⁹

$$\gamma(\nu) = [10^6 \log_{10} e] \frac{8\pi^2 N}{3hcg} \sum_{ij} |\mu_{ij}|^2 v_{ij} \nu^2 \times \exp(-E_i/k\theta) - \exp(-E_j/k\theta) \times \frac{4\Delta v_{ij}}{[(v_{ij})^2 - \nu^2]^2 + 4(\Delta v_{ij})^2 \nu^2} \text{ dB/km} \quad (1)$$

where $[10^6 \log_{10} e]$ is the conversion factor to give units of dB/km

g = partition function(s), for values see Elsasser¹⁰ or McClatchey¹¹

v_{ij} = frequency of line (Hz)

Δv_{ij} = linewidth parameter (Hz atm⁻¹)

E_i = energy of initial state i derived from $h\nu_i$, and subscript j denoting the final state (erg)

h = Planck's constant (6.625×10^{-27} erg s)

k = Boltzmann's constant (1.3804×10^{-16} erg K⁻¹)

θ = temperature in kelvins

c = velocity of light (2.998×10^{10} cm s⁻¹)

N = number density of molecules (cm⁻³)

$|\mu_{ij}|^2$ = square of the dipole moment matrix element,^{1,9} involving the permanent dipole moment of the molecule.

$$\frac{\nu^2}{\pi} \left[\frac{4\Delta v_{ij}}{(v_{ij}^2 - \nu^2)^2 + 4\nu^2(\Delta v_{ij})^2} \right] = \text{line shape equation (discussed in Sect. 2.1.2)} \quad (2)$$

Equation (1) is evaluated for a range of frequencies and summed for each transition frequency v_{ij} to give an

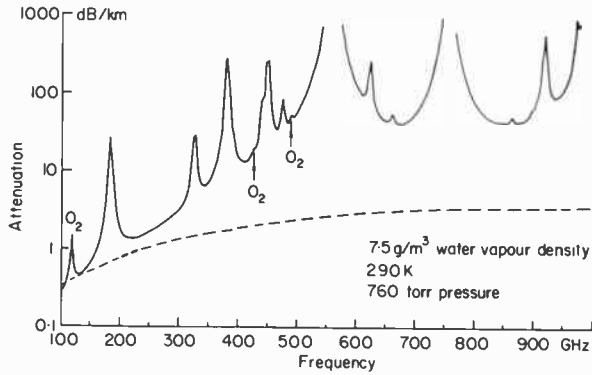


Fig. 2. The solid line shows a predicted absorption spectrum using the AFGL tabulation of atmospheric lines,¹¹ for a horizontal path with the conditions shown. It is dominated by absorption due to water vapour monomers, and some significant absorption due to O₂ is labelled. The dashed line shows a predicted water dimer spectrum,¹⁴ for the same conditions.

absorption spectrum, shown as the solid line in Fig. 2. The spectrum relates to a horizontal transmission path, for the conditions indicated, and shows the regions of minimum attenuation which may be considered for propagation. Most of the attenuation peaks are caused by the resonance absorption of water vapour molecules, and any significant absorption by other atmospheric molecules is indicated. The contribution to absorption from the wings of strong lines outside the specific frequency range of interest must also be included. Persistent errors have occurred with calculated spectra in the literature due to a misprint in the line shape equation of reference 9, as noted by Falcone¹² and Emery.¹³

For calculations of atmospheric absorption, a listing of line parameters has been compiled by AFGL (previously known as AFCRL).¹¹ This contains details of the molecules shown in Fig. 1 and their isotopes, based on direct measurement and calculation. These values are periodically updated as new or revised data become available.¹⁵ The parameters given for each line are:

ν_{ij} = resonant frequency of the line (cm⁻¹)
 S = line intensity per absorbing molecule (cm⁻¹ mol⁻¹ cm²) where

$$S = \frac{8\pi^2}{3hg} |\mu_{ij}|^2 [\exp(-E_i/k\theta) - \exp(-E_j/k\theta)]$$

$\Delta\nu'_{ij}$ = line width parameter (cm⁻¹ atm⁻¹)
 E'_i = energy of the lower state (cm⁻¹)
 ν_{ij} from equation (1) is given by $c\nu'_{ij}$.

The line intensity S is temperature dependent through the Boltzmann factor and the partition function g . The temperature variation of the line width parameters may be taken from specific tabulated values, for example, for water monomer see Benedict,¹⁶ or by using the approximations suggested in the handbook.¹¹

2.1.2 The line shape equation

The line shape equation specifies the variation of absorption with frequency over the line and with broadening pressure. The line shape shown as equation (2) is due to Gross¹⁷ and was first used by Zhevakin and Naumov,⁹ and appears to be a good general form for use in the frequency range 100–1000 GHz. There has been considerable discussion in the literature about the form of line shape which should be used in equation (1) for near-millimetre wavelength propagation in the lower atmosphere, where collision effects are dominant. Equations have been developed using various models of the collision process, but there is no fundamental reason to prefer any one particular form. Attempts have also been made to manipulate the line shape so that the measured absorption, particularly in the regions between the strong water monomer lines, may be accounted for entirely by the wing absorption of those lines. This approach, however, is of limited value and likely to obscure identification of the processes involved. For molecular absorption at altitudes of about 50 km and greater, the line widths are governed by Doppler broadening with a characteristic line shape as discussed by Goody² and McClatchey.¹¹

2.1.3 Absorption by water dimers

Water molecules in the gaseous state are known to form loosely bound complexes with each other through the action of hydrogen bonding, i.e. dimers (H₂O)₂ and trimers (H₂O)₃, etc. These complexes have their own characteristic absorption spectra, which will be combined with the rotational and vibrational absorption of the water monomers present. Although the strength of the hydrogen bond is weak in comparison to the bonds that hold the constituent water molecules together, significant numbers of water dimers are predicted to exist in normal atmospheric conditions. Viktorova¹⁸ and Viktorova and Zhevakin¹⁹ first suggested that water dimers could cause significant absorption in the atmospheric window regions in the near-millimetre wavelength range. This suggestion was investigated by a number of people, and involved spectroscopic measurements in the laboratory^{20,21} and measurements with submillimetre maser sources.²² Absorption by water dimers at infrared wavelengths was also considered.²³

A translinear structure for the dimer was predicted by Curtiss and Pople,²⁴ Dill *et al.*²⁵ and others, and this form has been confirmed by the molecular beam experiments of Dyke and Muentner.²⁶ Although many aspects of the water dimer are still not known, the strength of the hydrogen bond B , which determines the variation in its number density with temperature, has been calculated to have a value of 0.12 eV molecule⁻¹. The dimer absorption coefficient $\gamma^d(\theta, \rho)$ can be given in the following form:

$$\gamma^d(\theta, \rho) = A\rho^2 \exp(B/k\theta) \quad (3)$$

where

- A = constant of proportionality involving the appropriate absorption cross-section
- ρ = water vapour density
- k = Boltzmann's constant (8.62×10^{-5} eV K^{-1})
- θ = temperature (K).

The temperature dependence is a fundamental property of the water dimer and values of B , derived from laboratory and field measurements, can be compared with the predicted value. The dependence on the square of the water vapour density, in equation (3), arises from the probability of dimer formation by the collision of two monomers. Figure 2 includes a dimer absorption spectrum for the stated conditions, derived from laboratory measurements at low spectral resolution and from theory by Bohlander.¹⁴ In the window regions between the absorption line centres, it is seen to be significant in comparison to water monomer absorption. Present understanding of the water dimer, however, does not allow it to be included in the AFGL tabulation in the same form as the other atmospheric molecules. Dimer absorption may be estimated from a spectrum, such as included in Fig. 2, by scaling to the required temperature and water vapour density using equation (3). The absorption is expected to be complicated by internal modes, producing closely spaced lines which in lower atmosphere conditions will overlap to give a smooth spectrum. A discussion of these aspects is given by Bohlander.¹⁴

2.2 Attenuation due to Particles

The effect of solid and liquid phase particles can dominate near-millimetre wavelength propagation. Energy removed from the transmitted beam is partly scattered and partly absorbed. Scattering occurs when the refractive index of the particle is different from that of the surrounding medium, and absorption occurs when there is a finite imaginary part to its refractive index; the absorbed power is turned into heat.

Scattering and extinction coefficients can be derived by solving Maxwell's equations and satisfying the boundary conditions on the surface of the particle and at infinity. Formulae for a spherical particle were first obtained by Mie²⁷ and the attenuation coefficient α due to N particles per unit volume and of radius a is given by:

$$\alpha = 4.34 \times 10^5 \frac{Nc^2}{2\pi v^2} \text{Real} \sum_{n=1}^{\infty} (2n+1) \times (a_n + b_n) \text{ dB km}^{-1} \quad (4)$$

- where c = velocity of light (2.998×10^{10} cm s^{-1})
- v = frequency of the incident radiation (Hz)
- N = particle density (cm^{-3})

a_n and b_n = coefficients of the n th magnetic and electric multipole excited in the particle which depend on the size and refractive index of the particle and the frequency, and may be calculated using the details given by Stratton.²⁸

Particle attenuation in the atmosphere is usually dominated by water in liquid form, i.e. by rain and fog. The refractive index of water in this frequency range has been measured by Afsar *et al.*²⁹ and values for frequencies up to about 200 GHz can be calculated using the Debye formula.³⁰ Ice has only a small imaginary part to its refractive index³¹ and so the attenuation due to hail and snow, for the same mass density as liquid water, is less than 10% of the water value, and so of little practical importance.

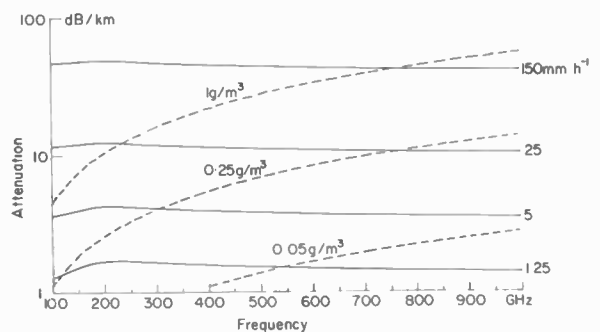


Fig. 3. Calculated extinction due to rain (—) for the precipitation rates shown, and due to fog (---) for the densities indicated, all for a temperature of 293 K. The rain extinction assumes a Laws and Parsons drop size distribution,³² and the fog densities shown correspond to visibilities in the range 17 to 350 metres.

Attenuation values computed for rain, fog and mist are shown in Fig. 3. The attenuation due to rain was calculated using the Laws and Parsons drop-size distribution.³² Measurements at the lower end of the frequency range^{33–35} around 100 GHz, and in the infrared^{36,37} indicate that it gives reasonable agreement between the mean observed and predicted values. Drops less than 1 mm diameter have a strong influence on attenuation in the frequency range 200–1000 GHz. Since these drops only make a small contribution to the rainfall rate and their number density in rain shows large fluctuations, only mean attenuation values can be predicted for a given uniform rainfall rate. Field measurements in this frequency range are urgently needed.

Fog, cloud and mist particles are usually much smaller than the wavelength in the near-millimetre wavelength region so the attenuation becomes almost independent of the drop-size distribution (Rayleigh region). The effect of a dense fog of 1 g/m³ water density, giving a visible range of about 20 m, is shown in Fig. 3, and the attenuation

can be seen to reach very high values at the higher frequencies. At these frequencies, however, it is still much less than in the visible (~800 dB km⁻¹) or in the infra-red (~600 dB km⁻¹). The frequency dependence of attenuation in mist is similar to that of fog, and was calculated for a liquid water density of 0.05 g/m³. The visible range in this case is about 500 m, with the attenuation at 0.63 μm wavelength being about 50 dB km⁻¹ and at 10.6 μm wavelength about 30 dB km⁻¹.

2.3 Refractive Effects

Changes of refractive index in the propagation path can introduce two kinds of non-dissipative loss. If there is a layer type structure in the refractive index over areas very much larger than the wavelength, reflection or refraction can occur and give rise to interference between the direct and indirect beams. The resulting signal variations, called multipath fading, can be a severe limitation on microwave links longer than about 30 km. This effect is unlikely to be of importance in the frequency range 100 to 1000 GHz, since path lengths will be limited to less than 30 km by molecular absorption.

Random changes in refractive index with scale sizes in the range of a few millimetres to tens of metres can cause fluctuations in the signal, known as scintillation. In most conditions, refractive index fluctuations may be characterized by the 'two-thirds' law³⁸ so that the variance of the log amplitude fluctuations may be given by³⁸

$$\overline{(\log_e [A(t)/A_0])^2} = 0.31 C_n^2 \left(\frac{2\pi}{\lambda}\right)^{\frac{2}{3}} L^{\frac{1}{3}} \quad (5)$$

where

- A(t) = signal power (W)
- A₀ = mean signal power (W)
- C_n² = refractive index structure parameter (m⁻³), being a measure of the magnitude of the refractive index fluctuations
- L = path length (m)
- λ = wavelength (m)

It follows from equation (5) that the standard deviation of the signal fluctuations in dB is given by 7.06[C_n²L^{1/3}λ^{-2/3}]^{1/2}. Equation (5) is valid for path lengths where the dominant contribution to the fluctuations comes from inhomogeneities with sizes within the range that satisfies the two-thirds law. For near-millimetre wavelengths this condition holds for links up to tens of kilometres pathlength. The value of C_n² varies with the meteorological conditions. For a link near ground level, the value can be expected to range typically from a low of 6 × 10⁻¹⁷ m⁻³ in cool and calm conditions, to 3 × 10⁻¹¹ m⁻³ as an upper value observed in a city environment.³⁹ At 200 GHz with a link 1 km long, the latter value would give rise to signal fluctuations of ±1 dB.

3 Transmission Measurements in the Lower Atmosphere

Applications for 100–1000 GHz transmission in the lower atmosphere range from ground-based communications, with a short horizontal transmission path within a few metres of the ground, to long path ground/aircraft communications. The extent to which predictions, involving direct application of the modelling outlined in Section 2, match field measurements will now be examined. There are two main categories of field measurement, one involving the effects of droplets in the form of rain, mostly at the low frequency end of the range where these effects can predominate, and the other involving molecular absorption at the middle and higher frequencies. Only a few measurements have been made of refractive effects. There has been little experimental overlap, so it is convenient to continue to consider these separately.

3.1 Molecular Absorption Measurements

Lower atmosphere molecular absorption in the frequency range 100–1000 GHz is dominated by water vapour. For most applications, interest lies in using frequencies in the so-called 'window' regions, away from the centres of strong atmospheric absorption lines. The three windows occurring in the frequency range 100–400 GHz may be seen in Fig. 4. Confidence in the prediction of absorption in the window regions is lower than at the line centres because the validity of the line shape equation is uncertain for frequencies far from the line centre. Here, the absorption depends on details of the closest approach between the colliding molecules and this cannot be given satisfactorily at present.

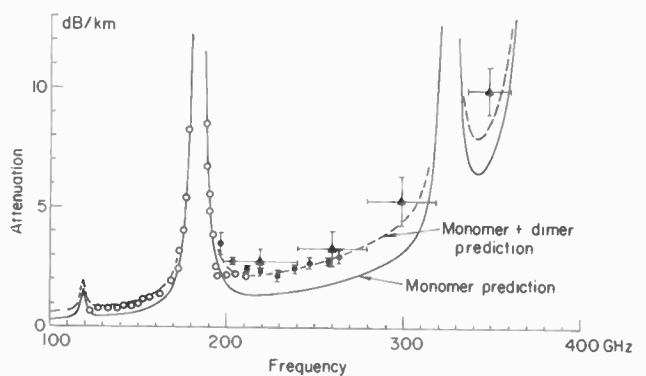


Fig. 4. A predicted absorption spectrum, covering the frequency range 100–400 GHz, using the AFGL line tabulation¹¹ is shown as the solid line for a water vapour density of 7.5 g/m³, a temperature of 293 K and one atmosphere pressure. The dashed line shows the total predicted attenuation when dimer absorption is included,¹⁴ for the same conditions. The experimental points are from Dryagin *et al.*⁴³ shown as open circles, Kugin *et al.*⁴⁶ shown as dots and Emery *et al.*⁴⁹ shown as triangles. Vertical bars show the standard deviations of the measurements, and horizontal bars show the frequency range over which the value is averaged for the broadband measurements.

Measurements of absorption in the window regions require long path lengths. This is often a practical limitation to laboratory measurements, whereas in the field, long path lengths are relatively easily achieved. However, it is difficult to assign an absolute absorption scale to field measurements, since a reference spectrum, equivalent to a vacuum background spectrum in the laboratory, cannot be obtained. Calibration for field measurements involving extinction by particles at the lower frequencies is obtained by assuming negligible signal attenuation in clear conditions. For measurements of molecular absorption, the calibration must be obtained with ancillary equipment, or by modelling the results using assumptions which may not be accurately valid. Particular attention must also be given to the measurement technique, when considering fluctuations, either at one frequency or with transmission spectra which may be varying with time.

Field measurements have generally shown more attenuation in the window regions than can be accounted for by the predicted absorption of water monomers. The early measurements by Straiton and Tolbert⁴⁰ using microwave techniques at frequencies up to 150 GHz, followed by other measurements at higher frequencies,⁴¹ showed excess attenuation and led to the suggestion^{18,19} that this could be due to absorption by hydrogen-bonded dimers of water. Laboratory studies have now determined some aspects of dimer absorption in the near-millimetre wavelength range and in particular its dependence on temperature⁴² and water vapour density.^{14,20,42}

Extensive field measurements have been made by Dryagin *et al.*,⁴³ Ryadov and Furashov^{44,45} and Kukin⁴⁶ using microwave sources at frequencies up to 420 GHz, as shown in Fig. 4. Kukin modelled the variation of absorption with water vapour density to discriminate between monomer and dimer absorption in the atmosphere. Calibration was obtained by adjusting the absorption scale so that a best fit curve to points on an absorption plot for various water densities passed through the origin. Absorption in excess of monomer prediction was found, but the analysis attributed only a portion of this to dimers, the remainder being assigned as excess monomer. This result is not satisfactorily explained, so must bring into question the strict use of density dependence for assigning monomer and dimer absorption in the open atmosphere.

Atmospheric transmission measurements have also been made using spectroscopic techniques with thermal sources,^{47,48} mainly for frequencies higher than 200 GHz. In common with the microwave results, these have shown absorption significantly in excess of water monomer prediction. However, the analysis of these results has concentrated on the temperature dependence of the excess absorption, and this is found generally to be higher than prediction for a water dimer. These results

are supported by recent spectroscopic measurements of the atmosphere,⁴⁹ included in Fig. 4, which were obtained with an absorption scale derived from instrumental calibration, and therefore not relying on assumptions about the absorption. The possibility of spectral features which may be attributed to water dimers has been discussed.^{46,50} At present this aspect is still open to question, since the structure observed is very variable, and not necessarily repeatable with different measurements. However, since the dimer spectrum is expected to be smooth, the appearance of spectral structure in atmospheric measurements may indicate the presence of a molecular species other than the predicted dimer.

This leads to the conclusion, based on both the microwave and the spectroscopic results, that the absorption measured in the atmosphere may not always be entirely accounted for by water monomer and dimer prediction as outlined in Section 2. The range of absorption values reported from field measurements is outside the uncertainties given for the individual measurements for similar conditions. This range may be due, in part, to atmospheric differences which at present are not included in the prediction model. In particular, the presence of an evaporating surface close to the transmission path, such as wet ground, or a water surface, may substantially influence the equilibrium description of water monomers and dimers assumed in the modelling.

For practical purposes, the measured absorption may be taken as representative for conditions not far different from those of the measurement. The level of uncertainty, although of fundamental interest, should normally be within the performance range of a system. Variability due to molecular absorption, however, in addition to that arising from refractive and particle effects, may further limit system performance, but the extent of this effect is not known.

3.2 Measurements involving Particles

Rain is usually the most important cause of scattering in the frequency range 100–1000 GHz, and field measurements have been aimed mainly at finding the relationship between rainfall rate and attenuation. In general, measurements are required not only to test the Mie theory for non-spherical drops, but also to check the rain drop-size distribution and the spatial homogeneity of the rain. This allows extrapolations to be made to other locations and other possible frequencies. Practical rain profiles have now been established⁵¹ but, as indicated in Section 2.2, the drop-size distribution relevant at these frequencies is a more difficult problem.

Measurements at 36 and 110 GHz³⁴ have shown that the drop-size distribution can change from one rain event

to another and during individual events, hence statistical distributions of drop-sizes are needed. For south-east England, the Laws and Parsons³² distribution was found to be satisfactory for predicting mean values of attenuation.^{33,34} Measurements in Holland at 94 GHz⁵² also showed a large spread for similar rainfall rates, but indicated worse attenuation statistics than predicted from rainfall data using the Laws and Parsons distribution. The use of drop-size distributions shifted towards smaller drop diameters, as derived by Joss *et al.*⁵³ or Marshall and Palmer,⁵⁴ were considered more appropriate. In heavy rain, measurements of attenuation at 52, 91 and 150 GHz³⁵ were found to differ by only about 20%. The 150 GHz results also suggest that the Laws and Parsons drop-size distribution underestimates the number of small drops which make a contribution at that frequency. There are only a few measurements of rain attenuation at frequencies between 200 and 1000 GHz. Limited results at 313 GHz⁵⁵ and at 890 GHz⁵⁶ showed attenuation values in broad agreement with prediction, with mean attenuation values at 890 GHz about 25% higher than those measured at 110 GHz. In snow, the highest attenuation at 313 GHz was measured⁵⁷ to be 6 dB km⁻¹ when the rate of snow fall had an equivalent water precipitation of 2 mm/h.

3.3 Measurements of Refractive Effects

Equation (5) in Section 2.3 shows that amplitude fluctuations increase almost linearly with frequency. There are no measurements available for frequencies greater than 110 GHz, but the limited data published by Ho *et al.*⁵⁸ obtained at 36 and 110 GHz shows good agreement with theoretical prediction for the frequency dependence. Ho *et al.*⁵⁹ also obtained good agreement between values of refractive index structure parameter C_n^2 measured by a refractometer, and values deduced from the log amplitude variances of amplitude fluctuations measured at 36 GHz. The refractive index fluctuations were found to be consistent with models of a homogeneous turbulent atmosphere and under these conditions the transverse wind speed across the propagation path could be determined to $\pm 20\%$ of the value measured at one point.⁶⁰ In practice, at frequencies greater than 100 GHz, scintillations are likely to be of importance in humid conditions when the propagation path is near the ground.

4 Slant Path Measurements

Modelling procedures, in addition to those given in Section 2, are required for the prediction of slant path propagation in the frequency range 100–1000 GHz. Interest in slant paths is associated with Earth/space communications, and also with astronomical observations so that absolute flux levels of astronomical sources

may be given. Both atmospheric absorption, normally using the Sun as a source, and atmospheric emission have been used to make the measurements. Molecular absorption spectra over a slant path involve more computation than those for horizontal paths because the density of the absorbing molecules, and the atmospheric temperature and pressure, vary along the path. This is modelled by considering the atmosphere as being made up of stratified layers, each of uniform composition. The number of layers required to give an accurate representation varies from one, characterized by a scale height value, to many tens of layers, depending primarily on the frequency and spectral resolution required. The final spectrum is taken as a sum of the absorption coefficients of the individual strata. Detailed descriptions of these calculations and the geometry have been given by Goody² and Marten *et al.*⁶¹ for example, and will not be considered further here. Generally, more molecular species need to be considered for slant paths than with lower atmosphere calculations, particularly at high spectral resolution. Figure 1 gives the main molecules which may need to be included, with parameters which can be obtained from the AFGL compilation.¹¹ A general treatment of the molecular spectroscopy is given by Goody² and specific references may be obtained from McClatchey.¹¹ Spectra showing calculated vertical attenuation through the atmosphere from sites at three altitudes are shown in Fig. 5.

Slant path attenuation of the atmosphere has been determined from measurements of the Sun and of the sky brightness temperature using microwave radiometers. Measurements at 231 and 345 GHz by Goldsmith *et al.*⁶² for a range of elevation angles enabled the zenith attenuation to be found. A correlation has been observed^{63,64} between the atmospheric attenuation A in dB, at near millimetre wavelengths, and the ground level water vapour density ρ in g/m³. The measurements of

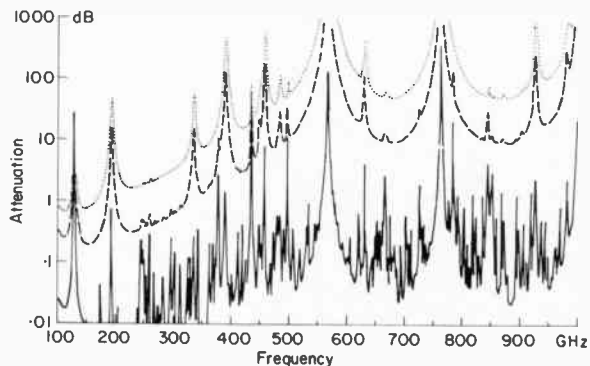


Fig. 5. Predicted attenuation for a vertical path through the atmosphere using the AFGL data¹¹ for sites at three heights above sea level. The curves are computed for temperate winter conditions^{7,8} with altitudes of 0 km (···), 3 km (---) and 12 km (—).

Plambeck⁶³ at 225 GHz for clear sky conditions gave $A = 0.5\rho$, the numerical factor being dependent on the elevation of the observation site. This form is discussed by Waters,⁶⁵ and in particular the empirical correction term proportional to (frequency)² introduced by Gaut and Reifstein,⁶⁶ which was found necessary to give agreement between observation and prediction based on absorption by water monomers. This is similar to the situation found with lower atmosphere measurements, and absorption by water dimers must be considered as a possible cause. Applying values for water dimer absorption obtained from laboratory measurements¹⁴ to model atmospheres for mid-latitude summer and winter conditions⁸ gives the total predicted zenith attenuation values shown in Fig. 6 for the frequencies 130, 225 and 342 GHz. Attenuation values for a range of surface water vapour density were obtained by scaling the model water values by the same factor over the range of altitudes. The plotted points indicate the relationship used by Plambeck,⁶³ and these are seen to be in good agreement with the prediction for 225 GHz relating to winter conditions.

Broadband detectors have also been used for observations in the frequency range 100–1000 GHz. Ulaby and Straiton⁶⁷ made measurements of total zenith attenuation for a range of frequencies between 183 and 325 GHz using wire mesh band-pass filters. Their results showed fair agreement with the empirical Schulze-Tolbert line shape,⁶⁸ but analysis based on the procedure outlined in Section 2 for absorption by water monomers and dimers, also gives fair agreement. Measurements

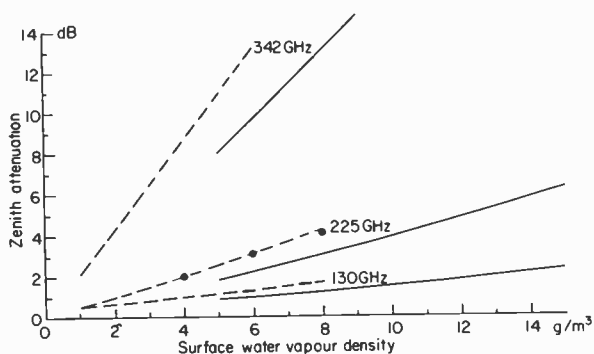


Fig. 6. Predicted attenuation at three 'window' frequencies for a vertical path through the atmosphere using the AFGL data¹¹ together with prediction for water dimers described in Section 2.1.3, for different water vapour densities at ground level. A standard atmosphere^{7,8} is assumed, with the solid curves relating to temperate summer conditions and the dashed curves relating to temperate winter conditions. The water vapour density profile was scaled by the same factor at all altitudes to give the various densities at sea level. The three points are taken from the data of Plambeck⁶³ for a frequency of 225 GHz.

using interferometric spectroscopy have been made, both of sky emission and absorption using the Sun as a source. Measurements calibrated instrumentally⁶⁹ have been found at times to be inconsistent with calibration based on the zenith angle dependence, suggesting that the assumption of a horizontally stratified atmosphere may not always be valid. Solar spectra recorded from a sea-level site⁷⁰ covering the frequency range 60–360 GHz, and from a mountain site⁷¹ have included a tentative assignment of spectral features around 240 GHz to water dimers. More recent measurements^{72,73} have included detailed instrumental calibration so that an absolute scale could be assigned to the emission and absorption values. These have shown the importance of including absorption by water dimers in the prediction, but have not resolved the question of the existence of spectral features in the excess absorption. Measurements of sky emission from balloons^{74–76} and from aircraft,^{77–79} mainly at higher frequencies, have enabled many upper atmosphere constituents to be studied quantitatively. This includes their variation in concentration with altitude and also some details of their global distribution. Measurements at high resolution⁷⁸ have allowed useful comparison to be made with the AFGL tabulation,¹¹ particularly with the isotopic species. Some isolated lines and broad spectral features remain unassigned.

In conditions involving scattering, when the particles are not perfectly spherical, the transmitted signal of a communications link can become depolarized. This can arise from rain drops being distorted into spheroids by air drag and wind shear, or the presence of high altitude ice particles which are predominantly needle or plate shaped.⁸⁰ Theoretical calculations for frequencies in the range 100–1000 GHz indicate that depolarization due to rain will be lower, and hence the crosspolar discrimination will be higher than that observed at 30 GHz. Predictions for the depolarization effect of ice particles have not been made and there are no measurements for frequencies above 30 GHz. The size and spatial distribution of the ice particles is not known, but indications are that ice depolarization is likely to be more severe at frequencies in the 100–1000 GHz range due to the increasingly important effect of the smaller ice particle.

When the propagation path passes through rain or fog, the attenuation can be calculated as outlined in Section 2.2. With slant paths, the effect of clouds will also have to be considered, and these can be obtained from the fog results by scaling to the appropriate liquid water density since Rayleigh scattering is involved in both cases. The liquid water density in clouds is in the range 0.1–4 g/m³ and the thickness in the range 300 m–6 km.⁸⁰ The highest values of attenuation at 94 GHz have been measured in cumulo-nimbus, being up to 10 dB in the vertical direction.⁸¹

5 Conclusions

In clear conditions, atmospheric propagation in the frequency range 100–1000 GHz is dominated by molecular absorption, mainly due to water vapour. For propagation purposes, interest lies in the window regions with relatively low absorption which occur between the strong resonance absorption lines. Field measurements of absorption in the lower atmosphere give higher values in these regions than predicted by calculations, and part of this excess is now generally accepted to be due to absorption by water dimers. This identification is based on laboratory measurements which show a dependence for the excess absorption on temperature and water vapour density in agreement with calculations for the water dimer. However, values of absorption measured in the field are still not accurately accounted for by using a model based on absorption by water monomers and dimers. The field values are often higher and can show wide variability, and these differences are not understood at present. Simple prediction can be obtained from laboratory values scaled to the appropriate conditions or by using field values measured in conditions which are close to those required.

Water particles either from rain or fog can have a dominant influence on propagation in the frequency range 100–1000 GHz. In fact, peak extinction values due to rain occur in this range. However, only mean extinction values can be predicted, due to the relatively strong effect of smaller particles, which can have wide variations in number density for the same overall rainfall rate. Field measurements at frequencies around 150 GHz indicate that the drop-size distributions commonly used for predictions at lower frequencies underestimate the number of these small drops. In low visibility conditions, the attenuation due to fog increases almost linearly with frequency and, at frequencies above about 400 GHz, can exceed that due to heavy rain.

Depolarization due to rain, at frequencies in the range 100–1000 GHz, will be less than at microwave frequencies, but with slant paths through the atmosphere, depolarization may be enhanced by the presence of small high altitude ice crystals. Clouds will have a variable and, at times, substantial effect on slant path propagation.

6 Acknowledgments

The authors wish to acknowledge the helpful comments of their colleagues and in particular Dr J. A. Lane for his interest and encouragement in the preparation of this paper.

7 References

- 1 Townes, C. H. and Schawlow, A. L., 'Microwave Spectroscopy' (McGraw-Hill, New York, 1955).
- 2 Goody, R. M. 'Atmospheric Radiation. I. Theoretical Basis' (Clarendon Press, Oxford, 1964).
- 3 Harries, J. E., 'The distribution of water vapour in the stratosphere', *Rev. Geophys. Space Phys.*, **14**, pp. 565–75, 1976.
- 4 Shimazaki, T. and Whitten, R. C., 'A comparison of one-dimensional theoretical models of stratospheric minor constituents', *Rev. Geophys. Space Phys.*, **14**, pp. 1–12, 1976.
- 5 Elhalt, D. H., 'In situ measurements of stratospheric trace constituents', *Rev. Geophys. Space Phys.*, **16**, pp. 217–24, 1978.
- 6 Seiler, W. and Warneck, P., 'Decrease of the carbon monoxide mixing ratio at the tropopause', *J. Geophys. Res.*, **77**, pp. 3204–14, 1972.
- 7 US Standard Atmosphere Supplement, US Government Printing Office, 1966.
- 8 McClatchey, R. A., Fenn, R. W., Selby, J. E. A., Volz, F. E. and Garing, J. S., 'Optical properties of the atmosphere', 3rd edn, Air Force Cambridge Research Labs., AFCRL-72-0497, 1972.
- 9 Zhevakin, S. A. and Naumov, A. P., 'Absorption coefficient of water vapour for electromagnetic waves in the wavelength range 10 μ to 2 cm', *Izv. V.U.Z Radiofizika (USSR)*, **6**, pp. 674–94, 1963, and **10**, pp. 1213–43, 1967.
- 10 Elsasser, W. M., 'Far infrared absorption of atmospheric water vapour', *Astrophys. J.*, **87**, pp. 497–507, 1938.
- 11 McClatchey, R. A., Benedict, W. S., Clough, S. A., Burch, D. E., Calfee, R. F., Fox, K., Rothman, L. S. and Garing, J. S., 'AFCL Atmospheric absorption line parameters compilation', Air Force Cambridge Research Laboratories, AFCRL-TR-73-0096, 1973.
- 12 Falcone, V. J., 'Comments on attenuation of millimeter wavelength radiation by gaseous water vapour', *Applied Optics*, **6**, pp. 2005–6, 1967.
- 13 Emery, R. J. 'Further comments on attenuation of millimetre wavelength radiation by atmospheric water vapour', *Applied Optics*, **7**, p. 1247, 1968.
- 14 Bohlander, R. A., 'Spectroscopy of Water Vapour', Ph.D. Thesis, University of London, 1979.
- 15 Rothman, L. S., 'Update of the AFGL atmospheric absorption line parameters compilation', *Applied Optics*, **17**, pp. 3517–8, 1978.
- 16 Benedict, W. S. and Kaplan, L. D., 'Calculation of line widths in H₂O–H₂O and H₂O–O₂ collisions', *J. Quant. Spectrosc. Radiat. Transfer*, **4**, pp. 453–69, 1964.
- 17 Gross, E. P., 'Shape of collision-broadened spectral lines', *Phys. Rev.*, **97**, pp. 395–403, 1955.
- 18 Viktorova, A. A., 'The rotational spectrum and the absorption rate of dimers of water vapour in the atmosphere', *Izv. V. U. Z. Radiofizika (USSR)*, **7**, pp. 415–23, and 424–31, 1964.
- 19 Viktorova, A. A. and Zhevakin, S. A., 'The water-vapour dimer and its spectrum', *Soviet Physics-Doklady*, **11**, pp. 1059–61 and 1065–7, 1967, and **15**, pp. 836–9 and 852–5, 1971. (English translations.)
- 20 Harries, J. E., Burroughs, W. J. and Gebbie, H. A., 'Millimetre wavelength spectroscopic observations of the water dimer in the vapour phase', *J. Quant. Spectrosc. Radiat. Transfer*, **9**, pp. 799–807, 1969.
- 21 Burch, D. E., 'Absorption of infrared radiant energy by CO₂ and H₂O, III Absorption by H₂O between 0.5 and 36 cm⁻¹', *J. Opt. Soc. Am.*, **58**, pp. 1383–94, 1968.
- 22 Birch, J. R., Burroughs, W. J. and Emery, R. J., 'Observation of atmospheric absorption using submillimetre maser sources', *Infrared Phys.*, **9**, pp. 75–83, 1969.
- 23 Bignell, K. J., 'The water-vapour infrared continuum', *Quart. J. R. Met. Soc.*, **96**, pp. 390–403, 1970.
- 24 Curtiss, L. A. and Pople, J. A., 'Ab initio calculation of the vibrational force field of the water dimer', *J. Mol. Spectrosc.*, **55**, pp. 1–14, 1975.
- 25 Dill, J. D., Allen, L. C., Topp, W. C. and Pople, J. A., 'A systematic study of the nine hydrogen-bonded dimers involving NH₃, H₂O and HF', *J. Am. Chem. Soc.*, **97**, pp. 7220–6, 1975.
- 26 Dyke, T. R. and Muenter, J. S., 'Microwave spectrum and structure of hydrogen bonded water dimer', *J. Chem. Phys.*, **60**, pp. 2929–30, 1974.
- 27 Mie, G. 'Beiträge zur Optik trüber Medien, speziell kolloidaler Metallösungen', *Ann. Phys. (Germany)*, **25**, pp. 377–445, 1908.
- 28 Stratton, J. A., 'Electromagnetic Theory' (McGraw-Hill, New York, 1941).

- 29 Afsar, M. N. and Hasted, J. B., 'Submillimetre wave measurements of optical constants of water at various temperatures', *Infrared Phys.*, **18**, pp. 835–41, 1978.
- 30 Saxton, J. A., 'Dielectric dispersion in pure liquids at very high radio frequencies', *Proc. Roy. Soc. A.*, **213**, pp. 473–91, 1952.
- 31 Ray, P. S., 'Broadband complex refractive indices of ice and water', *Applied Optics*, **11**, pp. 1836–44, 1972.
- 32 Laws, J. O. and Parsons, D. A., 'The relation of raindrop-size to intensity', *Trans. Am. Geophys. Union*, **24**, pp. 423–60, 1943.
- 33 Harden, B. N., Llewellyn-Jones, D. T. and Zavody, A. M., 'Investigations of attenuation by rainfall at 110 GHz in south-east England', *Proc. Instn Elect. Engrs*, **122**, pp. 600–4, 1975.
- 34 Zavody, A. M. and Harden, B. N., 'Attenuation/rain rate relationships at 36 and 110 GHz', *Electronics Letters*, **12**, pp. 422–4, 1976.
- 35 Sander, J., 'Rain attenuation of millimetre waves at $\lambda = 5.77$, 3.3 and 2 mm', *Trans. IEEE, AP-23*, pp. 213–20, 1975.
- 36 Chu, T. S. and Hogg, D. C., 'Effect of precipitation on propagation at 0.63, 3.5 and 10.6 microns', *Bell Syst. Tech. J.*, **47**, pp. 723–59, 1968.
- 37 Rensch, D. B. and Long, R. J., 'Comparative studies of extinction and backscattering by aerosols, fog and rain at 10.6 μ and 0.63 μ ', *Applied Optics*, **9**, pp. 1563–73, 1970.
- 38 Tatarski, V. I., 'Wave Propagation in a Turbulent Medium' (Dover, New York, 1959).
- 39 Vilar, E. and Matthews, P. A., 'Summary of scintillation observations in a 36 GHz link across London', Conference on Antennas and Propagation, pp. 36–40 (IEE Conf. Pub. no. 169, 1978).
- 40 Straiton, A. W. and Tolbert, C. W., 'Anomalies in the absorption of radiowaves by atmospheric gases', *Proc. IRE*, **48**, pp. 898–903, 1960.
- 41 Ryadov, V. Ya. and Sharonov, G. A., 'Experimental investigation of the transparency of earth's atmosphere at submillimetre wavelengths', *Radio Engng and Electronic Phys.*, **11**, pp. 902–9 (1966).
- 42 Llewellyn-Jones, D. T., Knight, R. J. and Gebbie, H. A., 'Absorption by water vapour at 7.1 cm^{-1} and its temperature dependence', *Nature*, **274**, pp. 876–8, 1978.
- 43 Dryagin, Yu. A., Kislyakov, A. G., Kukin, L. M., Naumov, A. L. and Fedoseyev, L. I., 'Measurement of atmospheric radio wave absorption in 1.36–3.0 mm range', *Izv. V.U.Z. Radiofizika (USSR)*, **9**, pp. 1078–84, 1966.
- 44 Ryadov, V. Ya. and Furashov, N. I., 'Investigations of the spectrum of radio wave absorption by water vapour in the 1.15–1.5 mm band', *Izv. V.U.Z. Radiofizika (USSR)*, **15**, pp. 1469–74, 1972.
- 45 Ryadov, V. Ya. and Furashov, N. I., 'Investigations of radio wave absorption in the atmospheric window $\lambda = 0.73$ mm', *Izv. V.U.Z. Radiofizika (USSR)*, **15**, pp. 1475–85, 1972.
- 46 Kukin, L. M., Nozdrin, Yu. N., Ryadov, V. Ya., Fedoseyev, L. I. and Furashov, N. I., 'Determination of the contribution of water vapour monomers and dimers to atmospheric absorption from measurement data in the $\lambda = 1.15$ –1.55 mm band', *Radio Engng and Electromag. Phys.*, **20**, no. 10, pp. 7–13, 1975 (English translation).
- 47 Emery, R. J., Moffat, P., Bohlander, R. A. and Gebbie, H. A., 'Measurements of anomalous atmospheric absorption in the wavenumber range 4 cm^{-1} –15 cm^{-1} ', *J. Atmos. Terrest. Phys.*, **37**, pp. 587–94, 1975.
- 48 Gimmestad, G. G. and Gebbie, H. A., 'Atmospheric absorption in the range 12 cm^{-1} to 32 cm^{-1} measured in a horizontal path', *J. Atmos. Terrest. Phys.*, **38**, pp. 325–8, 1976.
- 49 Emery, R. J., Zavody, A. M. and Gebbie, H. A., 'Measurements of atmospheric absorption in the range 4 cm^{-1} –17 cm^{-1} and its temperature dependence', *J. Atmos. Terrest. Phys.* (to be published).
- 50 Harries, J. E. and Ade, P. A. R., 'The high resolution millimetre wavelength spectrum of the atmosphere', *Infrared Phys.*, **12**, pp. 81–94, 1972.
- 51 Harden, B. N., Norbury, J. R. and White, W. J. K., 'Attenuation/rain-rate relationships on terrestrial microwave links into the frequency range 10–40 GHz', *Electronics Letters*, **14**, pp. 154–5, 1978, and **10**, pp. 483–4, 1974.
- 52 Keizer, W. P. M. N., Snieder, J. and de Haan, C. D., 'Propagation measurements at 94 GHz and comparison of experimental rain attenuation with theoretical results derived from actually measured raindrop size distribution', Conference on Antennas and Propagation, pp. 72–6 (IEE Conference Pub. no. 169, 1978).
- 53 Joss, J., Thams, J. C. and Waldvogel, A., 'The variation of raindrop size distribution at Lucarno', Proc. Int. Conf. on Cloud Physics, Toronto, Canada, pp. 369–73, 1968.
- 54 Marshall, J. S. and Palmer, W. McK., 'The distribution of rain with size', *J. Meteorol.*, **5**, pp. 165–6, 1948.
- 55 Babkin, Yu. S. *et al.*, 'Measurement of attenuation in rain over 1 km path at a wavelength of 0.96 mm', *Radio Engng Electronic Phys.*, **15**, pp. 2164–6, 1970.
- 56 Llewellyn-Jones, D. T. and Zavody, A. M., 'Rainfall attenuation at 110 and 890 GHz', *Electronics Letters*, **7**, pp. 321–2 (1971).
- 57 Babkin, Yu. S., Iskhakov, I. A., Sokolov, A. U., Stroganov, L. I. and Sukhonin, Ye. V., 'Attenuation of radiation at a wavelength of 0.96 mm in snow', *Radio Engng Electronic Phys.*, **15**, pp. 2171–4, 1970.
- 58 Ho, K. L., Mavroukoukoulakis, N. D. and Cole, R. S., 'Wavelength dependence of scintillation fading at 110 and 36 GHz', *Electronics Letters*, **13**, pp. 181–3, 1977.
- 59 Ho, K. L., Mavroukoukoulakis, N. D. and Cole, R. S., 'Determination of the atmospheric refractive index structure parameter from refractivity measurements and amplitude scintillation measurements of 36 GHz', *J. Atmos. Terrest. Phys.*, **40**, pp. 745–7, 1978.
- 60 Ho, K. L., Cole, R. S. and Mavroukoukoulakis, N. D., 'The effect of wind velocity on the amplitude scintillation of millimetre radio waves', *J. Atmos. Terrest. Phys.*, **40**, pp. 443–8, 1978.
- 61 Marten, A., Balutean, J. P. and Bussoletti, E., 'High resolution infrared spectra of the earth's atmosphere—I. Numerical simulation of atmospheric spectra', *Infrared Phys.*, **17**, pp. 197–209, 1977.
- 62 Goldsmith, P. F., Plambeck, R. L. and Chiao, R. Y., 'Measurement of atmospheric attenuation at 1.3 and 0.87 mm with an harmonic mixing radiometer', *IEEE Trans. Microwave Theory and Techniques*, **MTT-22**, pp. 1115–6, 1974.
- 63 Plambeck, R. L., 'Measurements of atmospheric attenuation near 225 GHz: correlation with surface water vapour density', *IEEE Trans. Antennas and Propagation*, **AP-26**, pp. 737–8, 1978.
- 64 Robson, E. I. and Rowan-Robinson, M., 'Measurements of atmospheric attenuation by water vapour', *Infrared Phys.*, **19**, pp. 115–20, 1979.
- 65 Waters, J. W., 'Absorption and emission by atmospheric gases', chap. 2.3, 'Methods of Experimental Physics', vol. 12, part B (Academic Press, New York, 1976).
- 66 Gaut, N. E. and Reifstein, E. C., 'Interaction Model of Microwave Energy and Atmospheric Variables', Environmental Res. and Tech. Rep. no. 13, Lexington, Mass. (1971).
- 67 Ulaby, F. T. and Straiton, A. W., 'Atmospheric attenuation studies in the 183–325 GHz region', *IEEE Trans. Antennas and Propagation*, **AP-17**, pp. 337–42, 1969.
- 68 Schulze, A. E. and Tolbert, C. W., 'Shape, intensity and pressure broadening of the 2.53 mm wavelength oxygen absorption line', *Nature*, **200**, pp. 747–50, 1963.
- 69 Moffat, P. H., Bohlander, R. A., Macrae, W. R. and Gebbie, H. A., 'Atmospheric absorption between 4 and 30 cm^{-1} measured above Mauna Kea', *Nature*, **269**, pp. 676–7, 1977.
- 70 Harries, J. E. and Burroughs, W. J., 'Observations of millimetre wavelength solar radiation at sea level', *Infrared Phys.*, **10**, pp. 165–72, 1970.
- 71 Nolt, I. G., Martin, T. Z., Wood, C. W. and Sinton, W. M., 'Far infrared absorption of the atmosphere above 4.2 km', *J. Atmos. Sci.*, **28**, pp. 238–41, 1971.
- 72 Hills, R. E., Webster, A. S., Alston, D. A., Morse, P. L. R., Zaramit, C. C., Martin, D. H., Price, D. P. and Rolson, E. I., 'Absolute measurements of atmospheric emission and absorption in the range 100–1000 GHz', *Infrared Phys.*, **18**, pp. 819–25, 1978.
- 73 Saunders, R., 'The Absolute Transmission of the Atmosphere at Millimetre Wavelengths', Ph.D. Thesis, University of London, 1979.
- 74 Harries, J. E., Swann, N. R. W., Carruthers, G. P. and Robinson, G. A., 'Measurements of the submillimetre stratosphere emission spectrum from a balloon platform', *Infrared Phys.*, **13**, pp. 149–55, 1973.

- 75 Clark, T. A. and Kendall, D. J. W., 'Far infrared emission spectrum of the stratosphere from balloon altitudes', *Nature*, **260**, pp. 31-32, 1976.
- 76 Rebours, B. and Rabache, P., 'Quantitative analysis of H₂O and O₃ concentration in the lower stratosphere using far-infrared spectroscopy', *Infrared Phys.* **19**, pp. 107-13, 1979.
- 77 Harries, J. E. and Burroughs, W. J., 'Measurements of submillimetre wavelength radiation emitted by the stratosphere', *Quart. J. Roy. Met. Soc.*, **97**, pp. 519-36, 1971.
- 78 Baluteau, J. P., Marten, A., Busoletti, E., Anderegg, M., Beckman, J. E., Moorwood, A. F. M. and Coron, N., 'High resolution infrared spectra of the earth's atmosphere. III—Airborne observations in the 100-140 cm⁻¹ range', *Infrared Phys.*, **17**, pp. 283-91, 1977.
- 79 Harries, J. E., 'Measurements of some hydrogen-oxygen-nitrogen compounds in the stratosphere from Concorde 002', *Nature*, **241**, pp. 515-18, 1973.
- 80 Mason, B. J., 'The Physics of Clouds' (Oxford University Press, 1971).
- 81 Lo, Lai-lun., Fannin, B. M. and Straiton, A. W., 'Attenuation of 8.6 and 3.2 mm radiowaves by clouds', *Trans. IEEE on Antennas and Propagation*, **AP-23**, pp. 782-6, 1975.

Manuscript received by the Institution on 24th April 1979
(Paper No. 1890/Comm. 184)

Development of model radar systems between 30 and 900 GHz

L. A. CRAM, B.Sc.*

and

S. C. WOOLCOCK, B.Sc., C.Eng., M.I.E.E.*

This paper, in a slightly fuller form and entitled 'Review of two decades of experience between 30 GHz and 900 GHz in the development of model radar systems', was presented at the 25th Meeting of the Electromagnetic Wave Propagation Panel of AGARD held in Munich on 4th-8th September 1978.

SUMMARY

Practical use has been made of frequencies above 30 GHz for the last 20 years in the UK National Radar Modelling Facility to investigate the characteristics of radar reflections from typical radar targets. This paper discusses the purposes, principles and methods of radar scale modelling. It also describes the several different types of measuring radar which are being used at frequencies up to 890 GHz to investigate various aspects of radar scattering. Some comments are made on methods of data reduction to simplify their use in the investigation of real radar problems. Possible future trends towards operation at frequencies up to 2 THz are indicated.

* EMI Electronics Limited, Wells, Somerset, BA5 1AA.

1 Introduction

A National Radio Modelling Facility, developed and used by EMI Electronics Limited for the Ministry of Defence (Procurement Executive) and the Royal Signals and Radar Establishment^{1,2} has been in operation for the last two decades to obtain detailed data on the scattering characteristics of radar targets. Continuous development is necessary to increase the scope of measurements and to extend the range of radio frequencies available. This development provides, as it has for 20 years, a stimulus for the advancement of technology at frequencies above 30 GHz up to 2 THz.

The initial interest of EMI Electronics Limited arose from a need to design, test and assess its own novel operational radar systems and it quickly became evident that the target reflection characteristics, required for such assessments, could only be obtained in sufficient detail by modelling methods. In order to perform modelling at scaled wavelengths, special purpose mm and sub-mm radars were designed and developed for use as reliable measuring instruments. Many of the components needed for such radars were not available so that the development of passive components, and also of some of the sources and mixers, was necessary. The aim has always been the practical one of obtaining, in the most economical way, the target scattering information needed to assess the behaviour of a full-scale radar in operational conditions. To this end, considerable emphasis has been given, first, to stability and reliability in the measuring equipment and, second, to rapid and economical processing of the data.

Initial measurements were made in 1958 with a non-coherent pulsed radar at 35 GHz. The facility now covers three decades of frequency from 800 MHz to 890 GHz and comprises more than 30 different specialized radars. At any one time, seven of these radars may operate without mutual interference. Models of many different types of target have now been made using a wide range of scaling factors.

2 Radar Target Reflection Characteristics

Any target which reflects radar power imparts several characteristics to the received signal which may be of considerable significance to the operation of the radar. Signal strength is an obvious feature since, if this is inadequate over the radar integration period, the radar will fail to detect the target. The target aspect may not be constant over that period, however, and, as shown in Fig. 1, the signal strength from a typical aircraft target varies rapidly with aspect angle and may change by 30-40 dB for very small angular changes. Furthermore, even if the signal is detected, the modulation of signal strength as the aspect of the target varies may have an

important effect on the operation of the radar, and the modulation frequency and depth would then be significant.

The target will also impart Doppler frequency and radar polarization characteristics to the signal and some radars may be sensitive not only to these but also to their modulations with respect to time. The directional data derived by a radar can be in error because of the glinting characteristics of the target, and the radar signal can even appear to come from a point outside the envelope of the target. To assess the performance of a given radar properly, a quantitative knowledge of all such target reflection characteristics is essential.

Most man-made targets are made of conductive metals or of substantially lossless dielectrics and these will be represented in the model by lossless metal or by dielectric materials of the same dielectric constant. However, if the target does contain lossy materials in its outer structure, i.e. either resistive conductors or dielectrics with loss, then these have to be represented in the model by more highly conducting materials. This is because the dimensions of electrical resistance require that it be scaled down by the same scaling factor S .

All the scattering effects, including interference effects, polarization effects and travelling-wave phenomena are correctly represented by such scale modelling.

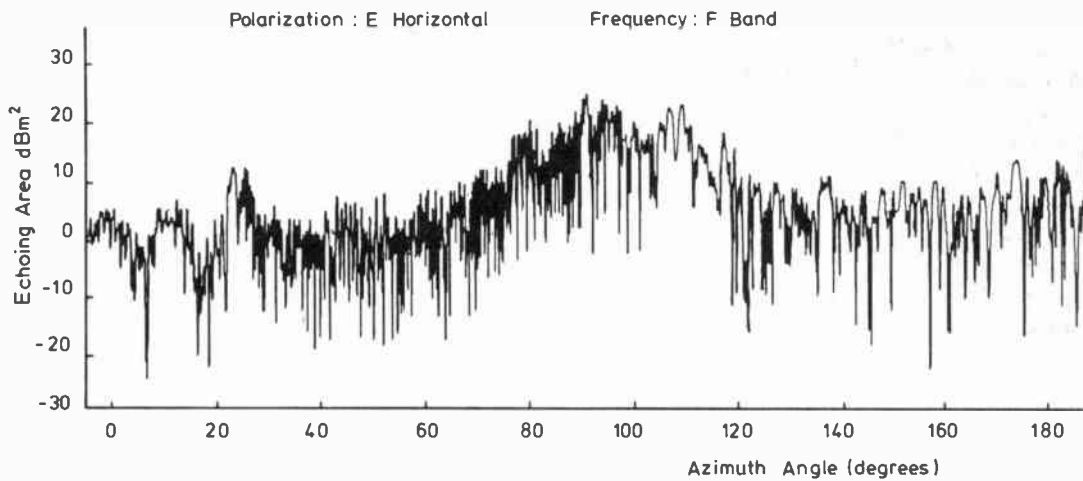


Fig. 1. Typical echoing area of HS125.

The determination and use of radar scattering characteristics was the subject of an AGARD lecture series.³ This series considered three methods of determining the data: full-scale trials, calculation, and scale modelling. Results from some full-scale trials have been used to validate the scale modelling technique. Scale modelling is the only method which provides sufficient data efficiently and economically to permit an adequate assessment of modern radar.

3 Methods of Radar Scale Modelling

The properties of electromagnetic waves are such that, if all the linear dimensions are scaled down in the same proportion, S , then the fields will be of the same form. The echoing area of a target, in the modelled system, will be reduced by the square of S . Radar modelling makes use of these scaling properties; an accurate scale model of the target is made and viewed by a radar whose wavelength and modulation parameters have been appropriately scaled by the same factor as the target.

3.1 Model Targets and Their Support

Experience has shown the need for attention to detail in the model target. Any orifices and the cavities behind them are particularly important, as are those internal corners which cause multiple reflections. As an example, the internal parts of a jet engine may be more important than the external parts of the aircraft which it propels. Likewise any airscops, landing lights, flaps, etc., are also significant. Signals 40 dB, or even 50 dB, down on peak reflections may still appreciably affect the performance and design of a radar. Also, the important detail of the backscatter signal is usually dependent more on the multiple small features than on the gross features of the shape.

For convenience and economy, the maximum dimension of a model target is usually in the range from 0.5 m to 5 m. This is large enough to permit correct modelling of the important small detail and yet is still convenient for handling. As a consequence, the scaling factor used for aircraft targets will usually be in the range from 1 : 4 to 1 : 20, while for ship targets a scale of 1 : 100

or even 1:200 may be used. The models must be supported in a manner to permit precise control of their attitude with respect to the model radar and to minimize the radar backscatter from the supporting system. This may be achieved either by the use of a tapered column to support the target or by suspending it on dielectric strings. Stability of the target requires isolation from wind and weather, achieved by operating indoors.

3.2 Elimination of Background Clutter

Interference between the backscatter from the building and that from the model target is avoided by using sharply-defined aerial beams on the radars and by pulse range-gating whenever possible. This is more effective than the use of radar absorbent materials and permits the operation of several radars in the one building without any mutual interference so long as p.r.f. interleaving is employed. The model radar pulse usually corresponds to at least three times the model target length, thereby ensuring a period when returns from all parts of the target coexist. As a result, the central part of the received signal is equivalent to that from a radar of longer pulse length (or even c.w.) and this central portion is extracted by gating in the receiver. If the full-scale radar uses a pulse which is shorter than three times the target length, then this pulse length is correctly scaled in the model radar.

3.3 Frequencies Used for Radar Modelling

Full-scale radars are in use from 0.4 GHz to 94 GHz and possibly beyond this range, but the greatest use is made of frequencies between 3 GHz and 10 GHz. Consequently, with scaling factors from 1:200 to 1:4 in the model targets (and even 1:1 sometimes), model radars from 0.8 GHz to 890 GHz have been required and built with a predominant interest in the upper region of this band, 30 GHz to 890 GHz.

Precise and stable radars for measurement purposes are now available throughout the band. The chart in Fig. 2 indicates how the model radar frequency and the scale factor of the model target may be chosen to simulate any given full-scale application.

4 Radar Modelling Facility

The first measurements with the facility were made in 1958 and 1959 using 30 ns pulsed radars at 35 GHz and 70 GHz respectively. Scale model targets at scales 1:100 and 1:4 were used and sensitivities were adequate to measure 10^{-6} m² echoing area anywhere in a 5 m cube. This initial work was aimed at plotting the radar echoing area amplitude as a function of target aspect. For this type of measurement, the target is hung from dielectric strings and is then rotated about a vertical axis as radar measurements are being made. The radar

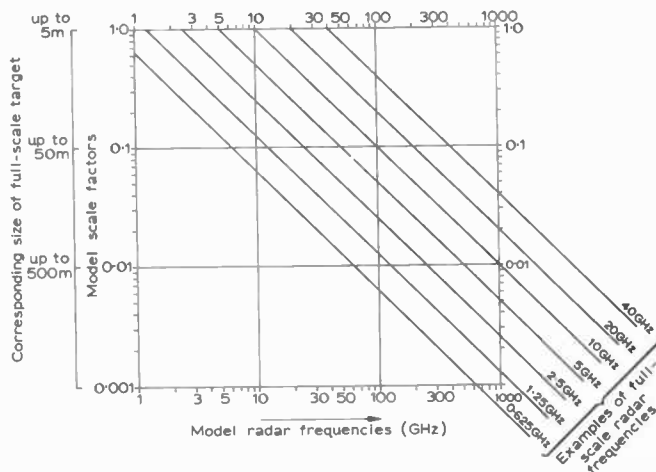


Fig. 2. Choice of model radar frequency and scale factor.

sightline is slightly elevated so as to avoid any orthogonal reflection from the suspension strings and the radar is calibrated by measuring the reflection from an accurately made metal sphere which can be substituted for the target. The facility has been expanded in terms of frequency coverage, as was indicated in Fig. 2, and also of the type of measurement which can be made.

4.1 Non-coherent Radars

Many full-scale radars have non-coherent receiver systems so it is still necessary to make scale model measurements appropriate to these by using non-coherent model radars.

4.2 Coherent Radars

Operational radars using coherent reception are also common. Most of our model radars include coherent receivers and, typically, may be used to measure either the monostatic or the bistatic reflection characteristics of a model target as it is rotated in front of the radar.

4.3 Directional Glint Measurement Radars

The directional indication of a radar is subject to variations, i.e. to angular glint of the apparent target direction, caused by interference between reflections from different parts of the target. Model radar systems have been designed to measure these effects. One method uses a coherent radar which measures r.f. phase as well as amplitude and such systems are being used from 35 GHz to 890 GHz. The information from these radars may be used to construct mathematical representations of the target as described in Section 6.1.

4.4 Polarization Measurement Radars

During the last decade there has been a growing appreciation of the importance of polarization of the reflected signal and many measurement radars now incorporate facilities for transmitting and receiving any type of linear or circular polarization. Recently, a model radar system has been developed for measuring the relative phase and amplitude of orthogonally polarized signals received from a target which is illuminated by plane polarized radiation.

4.5 Doppler Measurement

Model radars have been made which are specialized for measuring the Doppler signal variations. These may be caused either by gross movement of the target itself or by the relative movement of elements within the target.

4.6 Overall Facility

With so many different types of data required, it has been necessary to establish a number of different, separate facilities within one building. These are indicated in Fig. 3. There are nine independent radar facilities which share seven different target support equipments. In some of these systems, the radar is stationary while the target is either rotated or moved in range with respect to the radar. In other systems, the target is stationary during measurement and it is the radar which moves, either linearly past, or on arc around, the target. Bistatic radars can be modelled, if desired, with the bistatic angle as an experimental variable. One system is specialized for measurements in which a water surface, subject to a controlled amount of disturbance, is at least a part of the target scene.

5 Model Radars

A diagrammatic representation of the radio modelling measurement system is given in Fig. 4. For pulse range gating, the transmitter has a pulse length of about 10 ns to 50 ns so as to envelop the model target completely. These pulses have sharp rise and fall times of order 1–3 ns and, consequently, a wide bandwidth intermediate frequency receiver is required. The i.f. is usually in F-band (3–4 GHz).

5.1 Non-coherent Receiver

A typical non-coherent pulsed radar with range gating is shown in Fig. 5. The transmitter source can be a magnetron at frequencies up to 80 GHz, but, increasingly, impatt or Gunn devices are being employed. Between 140 GHz and 280 GHz, either a pulsed extended-interaction oscillator (EIO) or a carcinotron is used. A reflex klystron or solid-state source provides the local oscillator signal. Schottky barrier mixer diodes, which have been specifically developed by EMI Electronics, operate in radar systems up to 280 GHz.

In past years, 4 GHz travelling wave tubes provided i.f. amplification. Range gating was achieved by pulsing the first anode of one of the tubes. Currently a solid-state i.f. amplifier is used and range-gating is accomplished by means of a diode gate operating at i.f. In the non-coherent receivers, the range-gating is in the video circuitry. To ensure fidelity in all cases, the detector is operated at a substantially constant level by preceding it with a voltage controlled diode attenuator incorporated in an a.g.c. loop. This diode attenuator has a logarithmic law and its control voltage is used as the receiver output. Thus echoing area on a decibel scale can be measured over a range of about 40 dB.

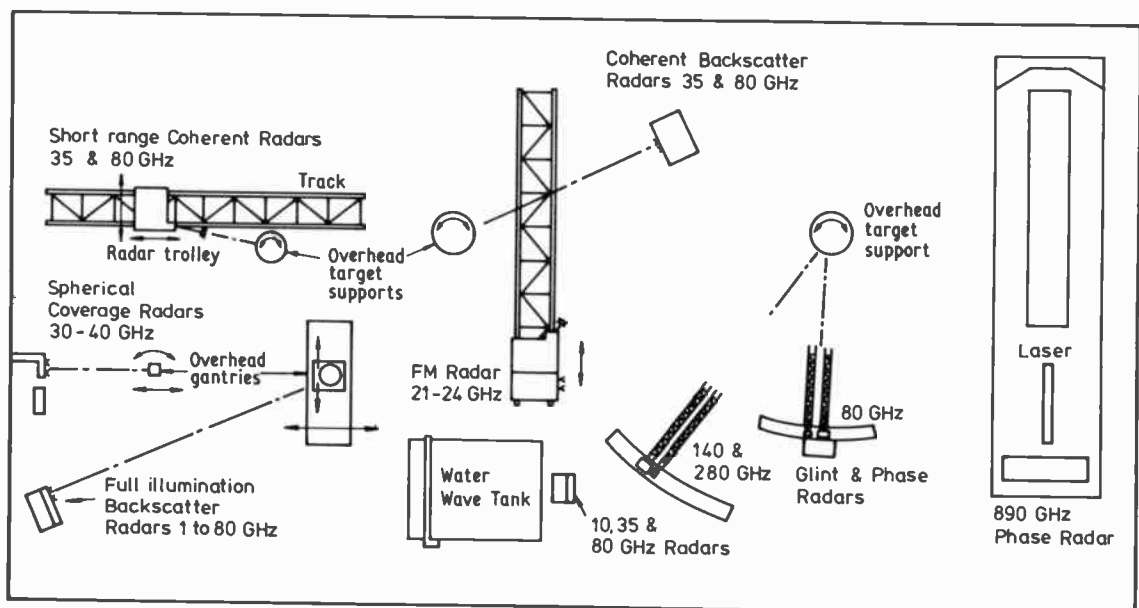


Fig. 3. Plan of radar modelling facilities.

5.2 Coherent Receiver

In a coherent radar (Fig. 6), to obtain a reference, a fraction of the transmitter power is delayed to coincide with the reception of the signal reflected by the target. The frequency of the reference signal is displaced by introducing a continuous change in its phase. Both the reference and the received target signals are mixed down to the first i.f. using separate mixers driven by the same local oscillator. The two mixer outputs, both in F-band (3-4 GHz), are separately amplified before being mixed together in a balanced detector. Due to the modified frequency of the reference signal all the Doppler components generated by the target appear as positive frequencies at the detector output. Values of instantaneous amplitude, a , and phase, ϕ , can be derived by processing the Doppler information in an on-line computer.

In an alternative coherent arrangement, a $\frac{1}{2}\pi$ phase shift can be injected into the reference channel periodically so that the in-phase and quadrature components can be determined in time multiplex. Such a radar will faithfully reproduce Doppler signals caused by target motion relative to the radar.

5.3 Direction Finding Receiver

Interference between radar waves reflected from different parts of a target can lead to perturbation of the associated phase fronts. This can result in angular glint errors in the directional indication given by the radar. An early form of a model radar operating at 80 GHz had a two-port aerial system in which the apertures were very tiny and were positioned side by side. A servo arrangement was used to align and maintain the aerial system normal to the phase front as the target aspect was changed. Currently a radar, such as that described in Section 5.2 is used to measure phase and amplitude.

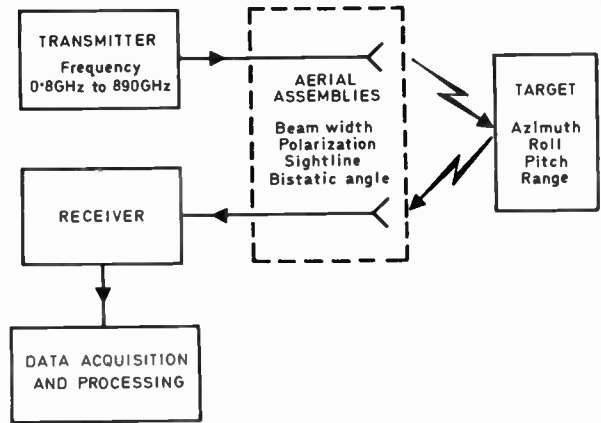


Fig. 4. Radar modelling measurement system.

Angular glint is then derived from the rate of change of phase with target aspect, using an on-line computer. Pulsed radars designed in this way are available up to and including 280 GHz.

Beyond 280 GHz optical technology becomes applicable and a laser source has been developed for use at sub-mm wavelengths.

5.4 Sub-millimetre Modelling

A homodyne coherent c.w. radar, operating at 890 GHz, has been in continuous use over the past five years. It is based on an HCN laser which is excited by gas discharge. This laser has been developed into a reliable, stable 30 mW source for radar modelling. The system can be used with models of large targets to determine angular glint or to identify echo sources within a target by using angular spectral analysis as discussed below. The radar system is shown in diagrammatic form in Fig. 7. Power is extracted from both ends of the laser, using coupling holes in the confocal mirrors which form the laser optical cavity. Most of the power is radiated

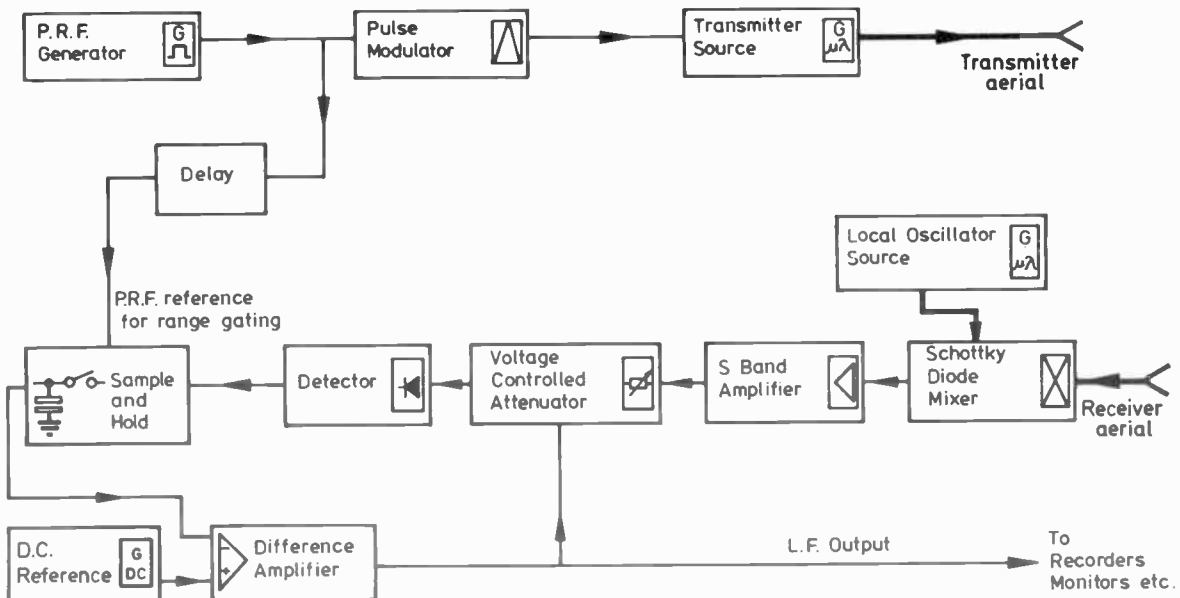


Fig. 5. Measurement radar with non-coherent receiver.

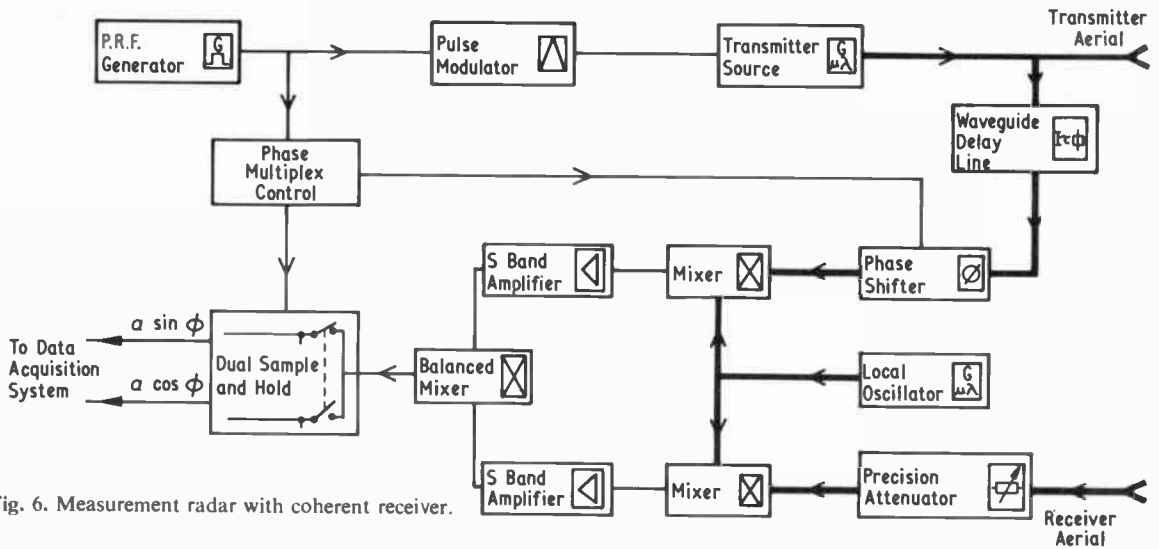


Fig. 6. Measurement radar with coherent receiver.

from the end pointing at the target and this is phase modulated ($0/\pi$) at 500 Hz, using a toothed dielectric wheel. The unmodulated signal from the back end of the laser provides the reference signal in the radar receiver. The balanced mixer uses indium antimonide photoconductors which require to be cooled in liquid helium to a temperature of 4.2 K. In the helium Dewar, the photoconductors are placed back to back and each is illuminated by the reference signal through its respective window. Diffraction gratings and mirrors are used to divide and direct the reference signal along the two separate paths. The received backscatter signal from the target is directed onto one mixer only, using a lens receiver aerial. The difference between the mixer output voltages is coupled out using a transformer and, in order to minimize its noise contribution, the transformer also

is included in the Dewar. The selected signal component at 500 Hz is amplified and then translated to base-band using a phase-detector and a 500 Hz reference derived from the $0/\pi$ phase-modulator drive. Quadrature detection of the coherent return is achieved with a $0/\frac{1}{2}\pi$ phase-modulator in the receiver path immediately before the mixer. Time multiplexed, in-phase and quadrature components are therefore provided by the receiver. An output bandwidth of 1 Hz is used in each channel and a signal-to-noise ratio of 30 dB is obtained from a target having a 10^{-4} m^2 echoing area when aerials of 3 deg beamwidth are used. (See Fig. 8.)

6 Organization and Validation of Data

Digital computer processing is essential to handle the outputs from the seven independent measurement

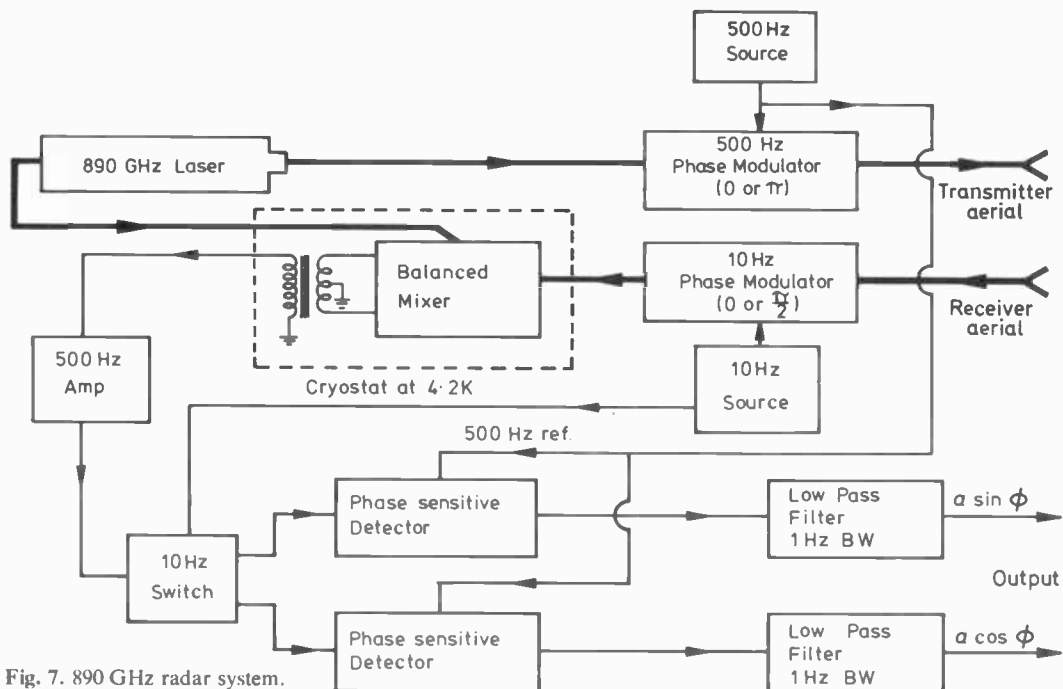


Fig. 7. 890 GHz radar system.

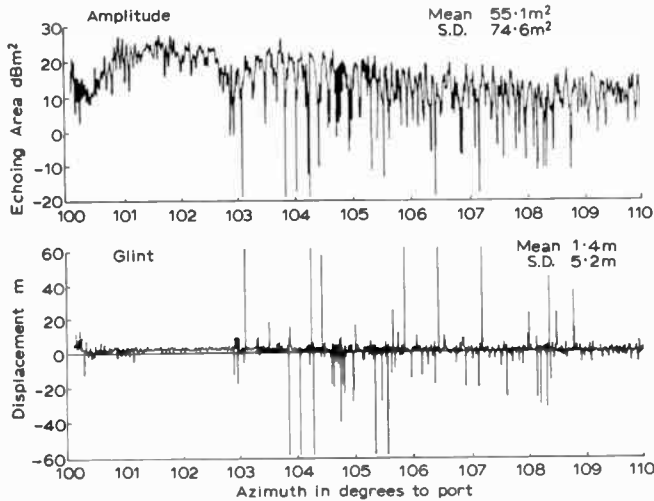


Fig. 8. Amplitude and glint plots from radar modelling.

radars. A mini-computer is provided at each site and Fig. 9 indicates how it is used to provide suitable monitor displays so that the experiment operator can confirm the validity of the experiment and of its data. The computer is also used to monitor target and radar settings and to add measurement conditions in the form of a header block, thus facilitating subsequent additional processing of the data in an off-line g.p. computer.

6.1 Processing and Use of Data

For some purposes, it is necessary for all of the data collected to be used in an analysis of the performance of an operational radar system. However, for many

assessments, the quantity of raw data is embarrassingly great and suitable summaries have to be devised and computed. Sometimes these summaries consist merely of mean, median and standard deviation values of, say, the echoing area or the angular glint error within a given aspect angle region around the target. Often a much fuller summary is needed.

For many years, angular spectral analysis techniques have been used at EMI Electronics for interpreting backscatter data.⁴ Information from an azimuthal scan around a target with a coherent radar is processed, using the appropriate weighting and 'window aperture', to obtain an angular spectrum. An angular spectrum gives the cross-range location and intensity of the elementary reflectors within a target. Further, by moving the window through the data recorded as a function of target aspect, the polar diagram of these sources can be determined. Figure 10 shows an angular spectrum for an aircraft viewed near 10 deg from head-on. A very succinct digital representation of a complex target can be derived from such information. It is often more efficient to store such a 'multi-source' representation of a target and compute the signal amplitude and glint at any aspect, than it is to store the initial data. The effectiveness of this method is illustrated by Fig. 11 which shows how well glint data calculated from a multi-source model compares with the measured data. It is possible, using the mathematical model, to compute the radar signal characteristics for ranges between target and radar other than that which was modelled. Thus, time-varying backscatter signals for an approaching target can be predicted by computation. To study the performance of

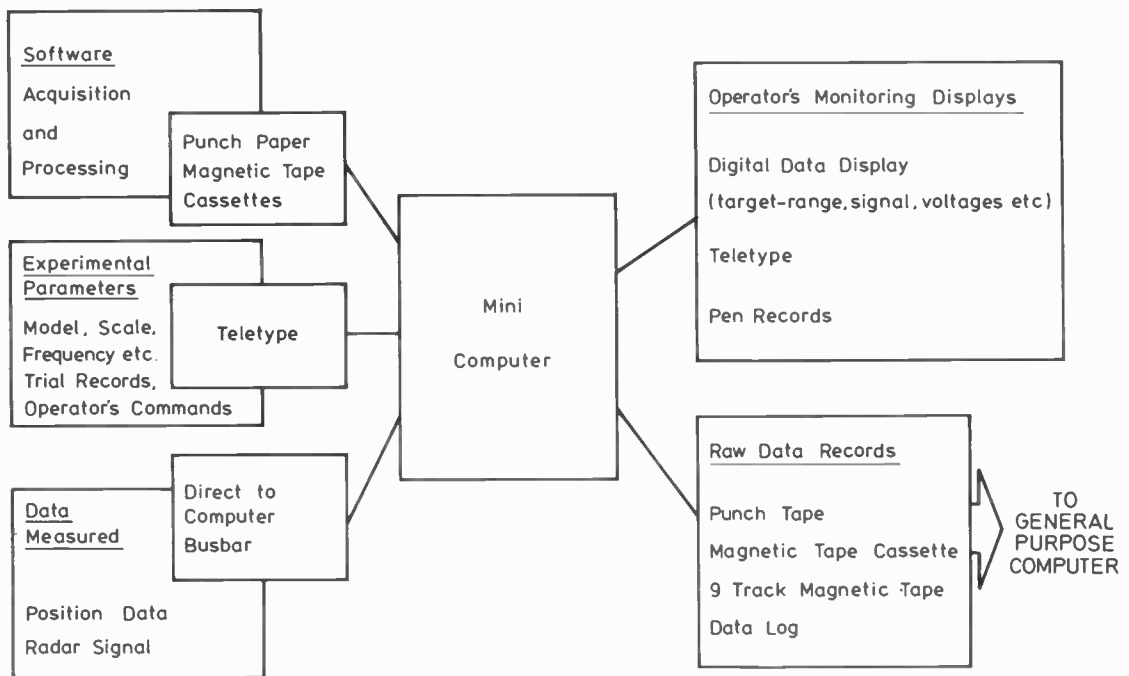


Fig. 9. Data collection and validation.

coherent radars with a computer, a multi-source model of the 'skin' Doppler backscatter would be derived as above and then a mathematical representation of Doppler components from turbines, compressors and propellers would be added.

7 The Nurturing of Near-millimetre Wave Technology

Greater exploitation of the band between 0.2 THz and 2 THz for radar modelling is anticipated and, as a consequence, new and improved sources and detectors are still being developed. EMI Electronics are presently using photons from CO₂ lasers to excite other gas molecules which provide stimulated emissions at any one of many frequencies in this band; methanol is a particularly fruitful molecule.⁵ Suitable outputs have now been achieved at 30 different frequencies. Several transitions have a sufficient bandwidth to promise pulsed sources suitable for 50 ns range gating.

8 Conclusions

The UK National Radar Modelling Facility has for 20 years served a dual purpose. It has improved the understanding of radar scattering phenomena and provided much essential data for the design and proving of British and of American radars. It has also encouraged the progress and consolidation of technology in the frequency band from 30 GHz to 1 THz. In both of these respects its service to engineering, to design and to science is expected to continue.

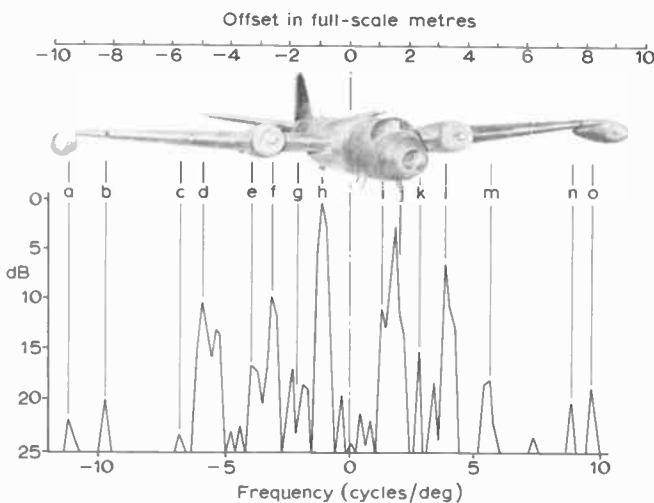


Fig. 10. Identification of sources by angular spectrum analysis.

- | | |
|------------------------------|-----------------------------|
| a Starboard wing tank | i Cockpit |
| b Starboard wing aerial | j Nose |
| c Starboard inner aerial | k Corner reflector— |
| d Starboard outer wing edge | Port engine + |
| e Starboard engine outer lip | Inner wing |
| f Starboard engine | l Port engine |
| g Tail | m Port wing control surface |
| h Corner reflector— | n Port outer aerial |
| Starboard inner wing + | o Port wing tank |
| Fuselage | |

Radar wavelength, 3 cm equivalent; azimuth window, between 7 deg and 17 deg to starboard.

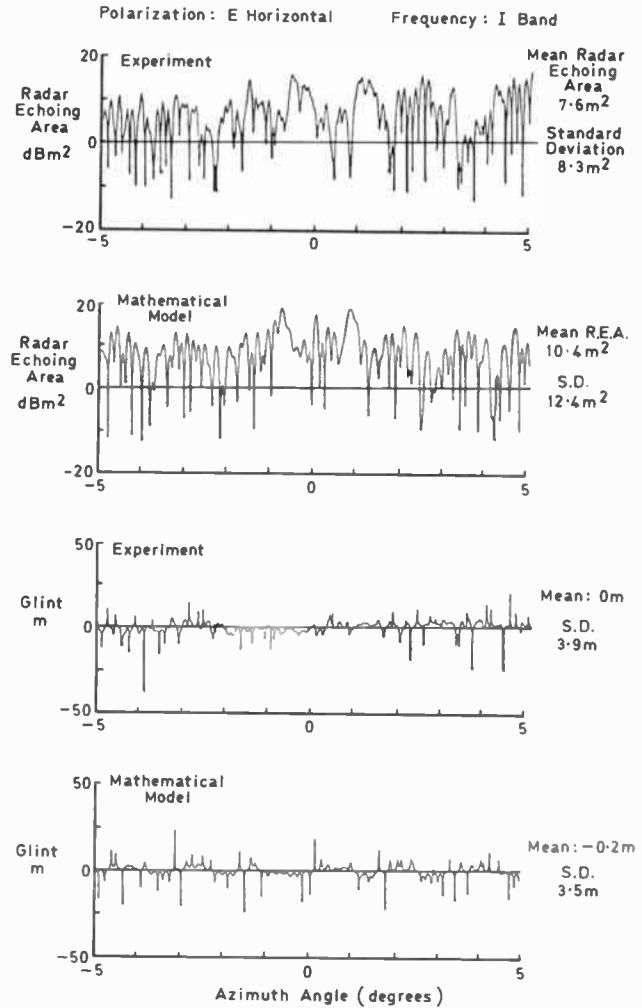


Fig. 11. Comparison of mathematical model predictions with experimental results.

9 Acknowledgments

The continued support of the MOD (PE) and of the RSRE in this work is gratefully acknowledged.

10 References

- 1 Cram, L. A., Woolcock, S. C. and Johnson, R. H., 'Radio scale modelling in support of radar system design and assessment of performance', 'Radar—Present and Future', IEE Conference Publication 105, pp. 422-30 (IEE, London, 1973).
- 2 Cram, L. A. and Staveley, J. R., 'Recent developments in scale modelling of radar reflections by radar and sonar methods', 'Radar 77', IEE Conference Publication 155, pp. 473-7 (IEE, London, 1977).
- 3 Cram, L. A., 'Determination and use of radar scattering characteristics', AGARD Lecture Series No. 59 (AGARD, Neuilly-sur-Seine, France, 1973).
- 4 Woolcock, S. C., 'Use of Radio Modelling', Lecture 3(b), AGARD Lecture Series No. 59 (AGARD, Neuilly-sur-Seine, France, 1973).
- 5 Bedwell, D. J., Duxbury, G., Herman, H. and Oregno, C. A., 'Laser, Stark and optical-optical double resonance studies of some molecules used in optically pumped sub-millimetre lasers', *Infrared Phys.*, 18, no. 5/6, pp. 453-60, December 1978.

Manuscript received by the Institution on 2nd April 1979
(Paper No. 1891/AMMS 97)

Waveguides for the 100–1000 GHz frequency range

Professor D. J. HARRIS,

O.B.E., B.Sc.(Eng.), Ph.D., C.Eng., F.I.E.E.,
F.I.E.R.E.*

SUMMARY

Waveguides used, or under consideration, for application at frequencies greater than 100 GHz include dominant-mode and overmoded rectangular guides, circular low-loss mode guide, microstrip, H and groove guides, various dielectric guide configurations, suspended strip and fin lines, and quasi-optic guides. Most existing systems, such as receivers, operating in the 100–300 GHz range have utilized rectangular TE_{10} guide, or some form of strip line operating in a rectangular guide system. Losses are high, and dimensions are very small, but the system length is short. Neither guide type has the potential for extension into the frequency range much above 300 GHz. A number of other guide types have some encouraging features, such as reasonably low loss, ease of construction or potential for component construction, but none is yet sufficiently advanced to demonstrate practicability to allow systems to give full exploitation to this part of the frequency spectrum.

* Department of Physics, Electronics and Electrical Engineering, University of Wales Institute of Science and Technology, King Edward VII Avenue, Cardiff CF1 3NU.

1 Introduction

Waveguide systems for frequencies below 50 GHz are well established and present no major problems for the system designer. Virtually all applications can be covered by the appropriate use of rectangular dominant mode waveguide, microstrip, coaxial line and circular TE_{01} waveguide. The difficulties increase significantly as the frequency becomes greater than 50 GHz however, because of increased losses and small dimensions for the first three guide types, whilst circular guide can be used only for signal transmission since few components can be made in that configuration. In spite of the difficulties, rectangular waveguide has been used, together with a range of components in the guide, at frequencies in the 100–300 GHz range. Microstrip has also been used at frequencies of about 100 GHz, but the problems are then formidable. The loss characteristics of rectangular guide and microstrip are progressively more prohibitive as the frequency is increased above 100 GHz, and alternative guide types must be sought.¹ A number of possibilities have been put forward.

The following guide types are considered in this paper:

Established techniques—

- (i) Dominant mode and overmoded rectangular guide
- (ii) Circular TE_{01} mode guide
- (iii) Microstrip guide

New approaches—

- (iv) H and groove guide
- (v) Dielectric guides
- (vi) Suspended strip line and fin line
- (vii) Quasi-optic guides

2 Dominant Mode and Overmoded Rectangular Waveguide

The use of dominant mode rectangular waveguide is the conventional approach, with dimensions and component structures scaled down in proportion to the wavelength. Since the broad dimension of the guide must be less than the wavelength, the hollow rectangular tube becomes exceedingly small in dimension for frequencies greater than 100 GHz (3 mm wavelength), with consequent difficulty and high expense of construction. The construction problem is even greater when components are considered. In addition to the dimensional problem there is the difficulty of increase of attenuation with increase in frequency. For a constant ratio of operating to cut-off wavelength, the theoretical attenuation per unit length increases as f^3 and the attenuation per wavelength increases as f^4 . In addition, it is found that the ratio of experimental to theoretical attenuation increases with frequency. A typical ratio² at 70 GHz is 1.5, but the ratio can be much greater at higher frequencies as shown in Fig. 1, in which the theoretical attenuation and some experimental values are shown for

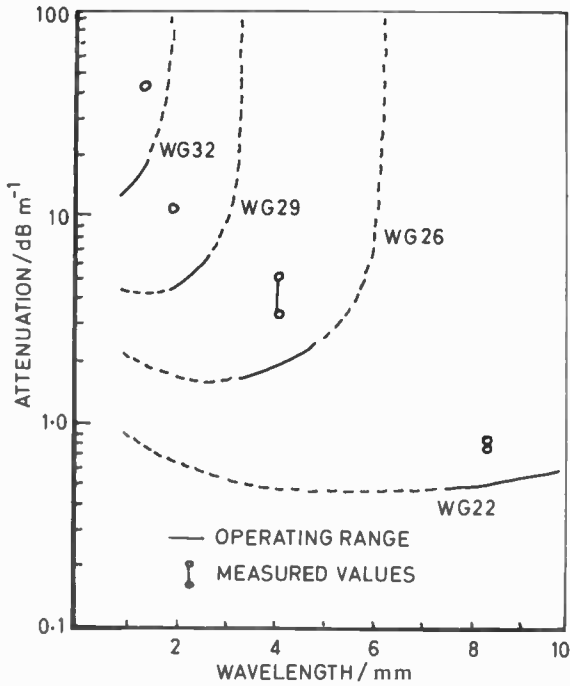


Fig. 1. Attenuation of TE₁₀ rectangular waveguide mode.

particular waveguide dimensions. The solid line shows the normal operating frequency region for each guide.

There is no satisfactory explanation at present for the extent of the increase in ratio of experimental to theoretical loss as the frequency is increased. The increasing importance of surface state as the skin depth decreases suggests that the extension of path length due to surface irregularities becomes significant, but the consequent effect on attenuation is not sufficient to explain the discrepancy.

In spite of the difficulties wide ranges of components have been constructed^{3, 4} in dominant mode guide up to about 300 GHz. At frequencies above 100 GHz, however, all the significant dimensions must be held within 0.025 mm (0.001 in) or less, and the constructional problems are severe with subsequent very high cost. The paper by B. J. Clifton⁵ in this issue, for example, includes discussion of detectors and receivers for these very high frequencies in dominant mode guide. One problem of dominant mode guide that cannot be overcome by constructional accuracy is that of power handling. The high losses result in dissipation problems as well as gas breakdown if high power levels are to be transmitted. This was no problem until recently since all power sources at these frequencies were at sub-watt levels. Recent developments of relativistic electron beam oscillators⁶ giving mean powers of about 1 kW at 1 mm wavelength have completely changed the situation however.

It is clear from Fig. 1 that one approach to reducing attenuation, and also increasing the power handling capability, is to use oversize guide. The problems and

capabilities of oversize guide have been considered,^{7, 8} including the construction of components. One approach is to use 'tall guide', in which rectangular guide for a lower frequency is used, but with the electric field parallel to the broad face of the guide. Oversized guide suffers from the generation and transmission of higher order modes produced at discontinuities, corners, etc. Trapped mode resonances can occur at specific frequencies for oversize guide with taper transitions to dominant mode guide at each end. Some control over these modes can be introduced by the use of mode filters, e.g. resistive film attenuation placed perpendicular to the broad faces of the guide, but higher-order mode generation may still cause problems and energy losses.

3 Circular TE₀₁ Mode Guide

A great deal of development was carried out on the low-loss mode in circular waveguide, with the aim of its use as a main trunk communication channel using the 30–100 GHz frequency range, and complete practical systems have been developed and subjected to operational working conditions. The Proceedings of the London conference⁹ in 1976 gives a full picture of the state of the art, although it is not likely now that such systems will achieve widespread use because of the slower-than-anticipated growth in communication traffic and the rapid improvement in fibre optic systems over the past few years.

The TE₀₁ circular guide mode, with the electric field in closed cylindrical loops and only circumferential currents in the guide wall, has the characteristic of a loss that decreases as the frequency increases. If the tube diameter is many wavelengths in dimension, the loss can be less than 1 dB per km,¹⁰ as shown in Fig. 2 which gives the loss of a practical dielectric-lined guide 6 cm in diameter. The TE₀₁ mode is not, however, the dominant mode, and many other modes may exist in the guide at the normal operating frequency. Mode filters can be included, e.g. the guide may be of tightly-wound helical

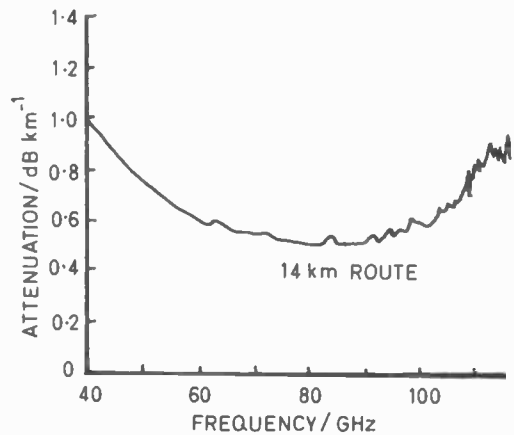


Fig. 2. Measured loss of 6 cm dia. TE₀₁ waveguide.¹⁰

wire construction to allow only the circumferential currents required for the TE_{01} mode to exist, whilst still retaining the low loss characteristic.

The main disadvantage of the TE_{01} circular guide is that whilst a transition from this mode to the rectangular TE_{10} rectangular guide mode can be constructed, the circular guide and mode form do not permit the design of components for signal manipulation in the guide itself. The low-loss mode is ideal for the transmission of signals over reasonable distances, but not for any other purpose. It is interesting to note that the output power from a gyrotron has a mode form that allows direct transfer by the low-loss circular guide mode, but this guide form is unlikely to find more widespread application.

4 Microstrip Guide

The use of microstrip, including microwave integrated circuits, is now standard¹¹ for many microwave applications where power levels are low and transmission lengths are short, for microwave wavelengths down to the longer millimetric region. The configuration normally used consists of a flat low-loss substrate with a conducting ground plane on one face and strip conductors deposited on the other, transmission being between the conducting plane and strip. A lesser-used system consists of a pair of parallel strips with narrow spacing, the transmission then being between the pair of strips. The strip configuration for the higher frequencies is usually produced by thin-film and photo-etching techniques. For frequencies above 50 GHz very thin (e.g. 125 μm) quartz is used as the substrate, in contrast to alumina and fused silica which are adequate for lower

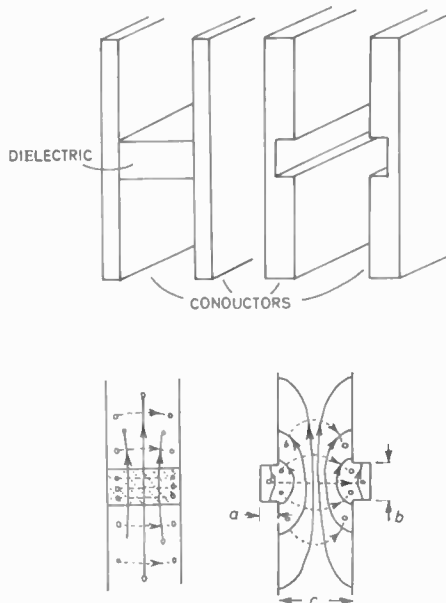


Fig. 3. Form and field distribution of H-guide and groove-guide
 —, E; ---, H.

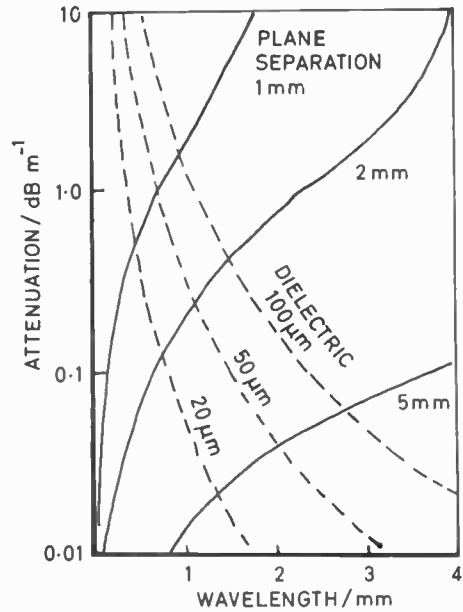


Fig. 4. H-guide attenuation ($\tan \delta = 10^{-3}$)
 —, conductor loss; ---, dielectric loss.

frequencies. Sapphire can be used for high quality small dimension circuits, and very thin GaAs has also been used as substrate. The thin-film circuit is usually of gold.

The companion paper by Clifton⁵ also discusses the use of microstrip for very short wavelength mixers and receivers. A major problem is one of loss. Measurements at 60 GHz gave a loss figure of about 0.1 dB per wavelength. It is thus clear that for short-millimetric wavelengths the loss will be prohibitive except for very short (e.g. less than 1 cm or so) transmission distances. The development of beam lead diodes for the short millimetric region, which fit well with the microstrip configuration, make this arrangement a good one for receivers. A number of components¹² such as couplers, isolators and filters have been constructed for the mid-millimetric region, but are likely to pose formidable difficulties at shorter wavelengths.

5 H and Groove Guides

The basic forms of these two guide types is shown in Fig. 3, with their field distributions. The H guide supports a hybrid mode with both E and H having a component in the direction of propagation, whilst groove guide supports a transverse electric mode. In both cases the fields are concentrated in the central region where the dielectric or groove exist. The loss characteristics of these guides are shown in Fig. 4 and Fig. 5, from which it can be seen that the theoretical loss can be less than 1 dBm^{-1} at a wavelength of 1 mm provided that the H-guide dielectric is very thin (e.g. < 50 μm), and that the conducting plane separation is large compared with the wavelength.

It has been shown,¹³ that in spite of the guide

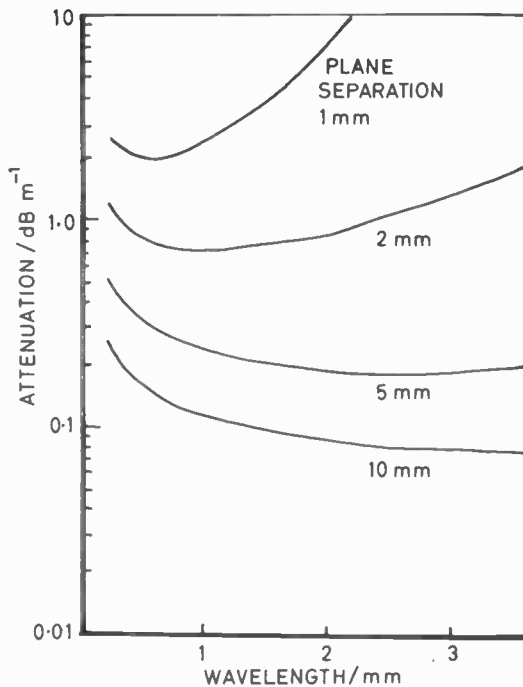


Fig. 5. Groove-guide attenuation
Groove width = $\frac{1}{2}$ plane separation
Groove depth = $\frac{1}{4}$ plane separation

dimensions being large relative to the wavelength, both guides can be made to transmit only the first order mode. In the case of groove guide it is a basic property¹⁴ of the guide that higher order modes are able to leak transversely from the central region, and can be removed by suitably placed absorbent material. The groove dimensions should have a simple and approximate relationship to the plane separation ($a \sim \frac{1}{4}c$, $b \sim \frac{1}{2}c$) and no dimension is critical to a fraction of a wavelength. For removal of higher order modes from H-guides the dielectric web must project into the conducting planes by a distance which is critical to a small fraction of a wavelength. Groove guide is thus much easier to construct than H-guide. The transverse extremities of the guide cross-section are shown open. Guide can be constructed in this manner, with spacers for rigidity, or closed at the top and bottom provided that attenuation is also added there to absorb unwanted higher order modes. The transverse dimensions must be sufficient to ensure that the required mode magnitude has decayed to a negligible value at the extremities.

Recent measurements¹⁵ at 3 mm and $\frac{1}{3}$ mm wavelengths on groove guide with plane separations of 10 mm and 4 mm respectively gave corresponding losses of 0.7 and 14 dBm⁻¹.

Both H and groove guides have the attractive features of large dimensions relative to the wavelength, single mode transmission, low dispersion, and a loss which is very low compared with rectangular guide. Groove

guide especially is simple to construct, and double groove guide suggests the basis for a coupler.¹⁶ The field configurations are somewhat similar to the rectangular guide situation, and it should be possible to construct components directly in the guide. Bends may well present problems with both guide types, however, and no work seems to have been done on this to date. Transitions have been made^{14, 17} between groove guide and rectangular guide, but ideally a system would be developed in which generation, transmission, signal manipulation and detection were all carried out in the same guide configuration.

6 Dielectric Guides

There are a number of configurations in which the microwave energy is guided essentially along a dielectric rod in the direction of required propagation. Of these the most widely considered are the dielectric cylindrical rod guide, image line, and inverted dielectric guide.

At optical frequencies very low attenuations, e.g. 3 dB per km, can be achieved with low-loss glass fibres. Unfortunately, no suitable dielectric materials are known having such low losses at millimetric or submillimetric wavelengths. Any dielectric guide with low attenuation must therefore operate with only a small fraction of the energy propagating in the dielectric material of the guide, i.e. the wave must be loosely bound to the guide. A dielectric rod with diameter small compared with the wavelength will satisfy this requirement, but is difficult to support, will radiate if allowed to sag or bend, and suffers from the possibility of rotation of the plane of polarization. Such a rod might be supported in dielectric foam if the cell size is approximately uniform. A rather more rigid guide with the same attenuation can be achieved by using a hollow dielectric tube.

Encouraging results have been claimed by Russian workers for pressurized dielectric tube.¹⁸ Little information is available, but a loss of 0.2 dBm⁻¹ at $\lambda = 0.8$ mm and 0.025 dBm⁻¹ at $\lambda = 2$ mm is claimed for a tube of polythene of diameter 12 mm and wall thickness 0.2 mm.

Some of the disadvantages of the dielectric rod can be overcome by supporting a rod of semicircular or rectangular cross-section on a conducting plane¹⁹⁻²¹—the image line—but at the cost of increased attenuation. In this case the plane of polarization will be set with the electric field perpendicular to the plane. The characteristics of these guides have been determined for both the half cylinder case and that of a thin dielectric tape such as PTFE (e.g. 0.05 mm \times 0.5 mm) on the conducting plane. Attenuations at 150 GHz are of the order of 3 dBm⁻¹. A practical problem exists with the bonding of the dielectric to the conducting plane. For longer-millimetre wavelengths, dielectrics of higher permittivity such as alumina ($\epsilon_r = 9$) have been used for image line.

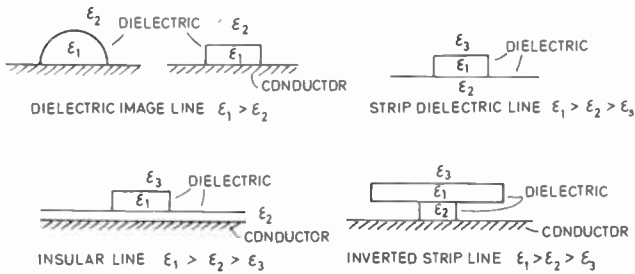


Fig. 6. Some forms of dielectric surface-wave guide cross-section.

A number of components such as filters, couplers and mixers have been constructed in image line²² and a complete millimetric receiver has been reported.²³ The losses of image line become very high for short millimetric wavelengths however.

A number of configurations combining dielectric strips and planes, with perhaps a conducting plane, are possible,²⁴ and some are shown in Fig. 6. The inverted strip dielectric guide²⁵ is perhaps of particular interest. The main dielectric strip in which the wave propagates is separated from the supporting conducting plane by a second narrow dielectric strip of lower permittivity than the main guide region. The object is to reduce conduction losses by removing the main region of high field from the supporting plane, and also eliminating many of the unwanted effects of the variable bonding between the main dielectric and the conductor. Recent work^{26,27} has resulted in some initial components in this guide.

7 Suspended Strip and Fin Line

Configurations which combine rectangular guide and strip line are shown in Fig. 7. Suspended strip line introduces a dielectric support parallel to the broad face of the guide, with a conducting strip on one face but no conducting surface on the other. Quartz has been used as the dielectric for very high frequencies, with a resultant loss of 15 dBm^{-1} at 94 GHz. Coupling into the strip from rectangular guide presents no great problem, the impedance can be varied by control of the strip width, and millimetre wave mixers^{28,29} have been made with good performance, e.g. at 94 GHz by combining this technique with beam-lead diodes. In the case of fin guide,^{30,31} a thin dielectric sheet is introduced parallel to the narrow face of the rectangular guide, and slot line is introduced on the dielectric by metallization of the dielectric. The metal fins can be connected to the metal waveguide, or insulated so that a d.c. bias can be applied to connected active devices. The metal surface of the slot line can be tapered in to give a good match with the rest of the rectangular guide. The loss of this guide is of the order of 0.1 dB per wavelength up to 40 GHz, increasing

for higher frequencies, but like suspended strip line it is envisaged for limited lengths of guide only. It has the advantage that active devices can be incorporated readily, and a number of components have been constructed. Fin line has been used for the production of a number of components, including mixers and receivers, and can be low cost whilst retaining good performance. E-plane circuits³² similar to fin line can be constructed in which the dielectric is allowed to bridge the common broad face of two adjacent rectangular guides giving controlled coupling between the guides.

8 Quasi-optic Guides

A wide-ranging programme has been carried out combining oversize guide and quasi-optic techniques, in which a large number of components were developed, mainly for the longer millimetric region. A comprehensive review of this work is available.³³ Interest in a simplified form of this approach has been renewed for use at frequencies of 300 GHz or more, particularly in connection with detection.³⁴ For more general application, however, the approach suffers from the basic problems of oversize guide.

A quasi-optic beam guide technique has also been investigated theoretically and experimentally in this frequency range, in which periodic modification of the phase front by lens or iris systems¹ is used to maintain the beam size. Russian workers³⁵ in particular have investigated these guides and made measurements at a wavelength of 0.9 mm. Losses for such guide of about 2 dBm^{-1} have been measured. Beam shaping by periodic reflection from appropriately shaped reflectors has also been investigated³⁶ and a loss equivalent to less than 0.1 dBm^{-1} measured at 4 mm wavelength. These systems suffer from large transverse dimensions, however, and require maintenance of high precision in the positioning of the periodic elements. They are not, therefore, attractive means of transmission.

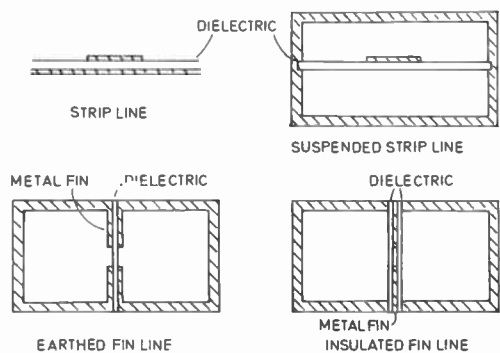


Fig. 7. Suspended strip-line and fin-line cross-sections.

9 Conclusions

A number of techniques have been used in practical systems, especially for mixers and receivers, at frequencies up to 300 GHz. Path lengths for these systems are very short so that high losses can be tolerated. Modified conventional guides can be used, although the small dimensions make construction difficult and tolerances very tight, with consequent very high costs.

For higher frequencies, or if a longer path length is required, high powers are to be transmitted, or costs are to be lower, none of the established techniques suffice. A number of alternative approaches are under investigation, but none is without problems yet to be overcome. It is not possible at present to forecast whether any of these alternatives will provide the sort of low-cost, low-loss system that is required if this part of the frequency spectrum is to be exploited more fully, and good use is to be made of the sources and detectors now available.

10 References

- Kroon, D. J. and van Nieuwland, J. M., 'Techniques of propagation at millimetre and submillimetre wavelengths', chap. 7, 'Spectroscopic Techniques for Far Infra-red, Submillimetre and Millimetre Waves', Martin, D. H. (Ed.) (North Holland Pub., 1967).
- Benson, F. A., 'Attenuation of rectangular waveguides', chap. 14, M & SW.†
- van Es, C. W., Gevers, M. and de Ronde, F. C., 'Waveguide equipment for 2 mm microwaves', *Philips Tech. Rev.*, **22**, pp. 131–5 and 181–9, 1960.
- Meredith, R. and Preece, G. H., 'Millimetre waveguide components', chap. 20, M & SW.†
- Clifton, B. J., 'Schottky diode receivers for operation in the 100–1000 GHz range', *The Radio and Electronic Engineer*, **49**, pp. 333–346, July/August, 1979.
- Andronov, A. A. *et al.*, 'The gyrotron: high power source of millimetre and submillimetre waves', *Infrared Phys.*, **18**, pp. 385, 93, 1978.
- Butterworth, H. J. and de Ronde, F. C., 'Oversized rectangular waveguide components for millimetre waves', *Philips Tech. Rev.*, **29**, pp. 86–101, 1967.
- Robson, P. N., 'Overmoded rectangular waveguides', chap. 15, M & SW.†
- 'Millimetric Waveguide Systems', IEE Conf. publication 146, November 1976.
- Warters, W. D., 'The WT4 waveguide transmission system', IEE Conf. Pub. 146, pp. 18–21, 1976.
- Oxley, T. H., 'Review of some microwave integrated circuit components utilizing microstrip techniques', *The Radio and Electronic Engineer*, **48**, pp. 3–22, 1978.
- Chrepta, M. M. and Jacobs, H., 'Millimetre wave integrated circuits', *Microwave J.*, **17**, pp. 45–8, 1974.
- Harris, D. J., Lee, K. W. and Reeves, J. M., 'Groove and H-waveguide design and characteristics at short millimetric wavelengths', *IEEE Trans. on Microwave Theory and Techniques*, MTT-26, pp. 998–1001, 1978.
- Nakahara, J. and Kurauchi, N., 'Transmission modes in the grooved guide', *Sumitomo Elect. Tech. Rev.*, **5**, pp. 65–71, 1965.
- Harris, D. J., Lee, K. W. and Batt, R. J., 'Low loss single mode waveguide for submillimetre and millimetre wavelengths', *Infrared Phys.*, **18**, pp. 741–7, 1978.
- Harris, D. J. and Lee, K. W., 'Characteristics of double groove guide at 3 mm wavelengths', *Electronics Letters*, **14**, pp. 726–7, 1978.
- Griemsmann, J. W. E., 'Groove Guide', Proc. Symp. Quasi-Optics, Inst. of Brooklyn, N.Y., 1964.
- Kazantsev, Y. N. and Udalov, V. V., 'Measurement of attenuation in gas-dielectric waveguides in the millimetre and decimillimetre wavelength regions', *Radio Eng. Electron. Phys. (USSR)*, **15**, pp. 544–6, 1970.
- Cohn, M., 'Surface wave transmission lines', chap. 17, M & SW.†
- Schlesinger, S. P. and King, D. D., 'Dielectric image lines', *Trans. IRE on Microwave Theory and Techniques*, MTT-6, pp. 261–99, 1958.
- Sobel, F., Wentworth, F. L. and Wiltse, J. C., 'Quasi-optical surface waveguide and other components for the 100–300 Gc region', *Trans. I.R.E.*, MTT-9, pp. 512–18, 1961.
- Knox, R. M. and Toullos, P. P., 'Integrated circuits for the millimeter through optical frequency range', Proc. Symp. on Submillimetre Waves, Polytechnic Inst. of Brooklyn, N.Y., 1970.
- Knox, R. M. and Toullos, P. P., 'A V-band receiver using image line integrated circuits', *Proc. Nat. Electronics Conf.*, **27**, pp. 489–92, 1974.
- Knox, R. M., 'Dielectric waveguide microwave integrated circuits—an overview', *IEEE Trans.*, MTT-24, pp. 806–14, 1976.
- Itoh, T., 'Inverted strip dielectric waveguide for millimetre wave integrated circuits', *IEEE Trans.*, MTT-24, pp. 1134–7, 1976.
- Rudokas, R. and Itoh, T., 'Passive millimetre-wave ic components made of inverted strip dielectric waveguides', *IEEE Trans.*, MTT-24, pp. 978–81, 1976.
- Itoh, T. and Herbert, A. S., 'Simulation studies of electronically scannable antennas and tunable filters integrated in a quasi-planar dielectric waveguide', *IEEE Trans.*, MTT-26, pp. 987–91, 1978.
- Wrixon, G. T., 'Low noise diodes and mixers for the 1–2 mm wavelength region', *IEEE Trans.*, MTT-22, pp. 1159–65, 1974.
- Cardiasmenos, A. G., Cotton, J. M. and Delconte, J. R., 'Low-noise thin-film downconverters for millimetre systems applications', *IEEE Conf. Pub. 78 CH 1355–7* MTT, pp. 399–401, 1978.
- Meier, P. J., 'Integrated fin-line millimetre components', *IEEE Trans.*, MTT-22, pp. 1209–16, 1974.
- Meier, P. J., 'Low cost high performance millimeter integrated circuits constructed by fin-line techniques', *Microwave J.*, **17**, pp. 53–8, 1974.
- Cohen, L. D. and Meier, P. J., 'E plane mm wave circuits', *Microwave J.*, **21**, pp. 63–6, 1978.
- Garnham, R. H., 'Quasi-optical components', chap. 21, M & SW.†
- Fettermann, H. R. *et al.*, 'Far-ir heterodyne radiometric measurements with quasi-optical Schottky diode mixers', *Appl. Phys. Letters*, **33**, pp. 151–4, 1978.
- Vershinina, L. N. and Shevchenko, V. V., 'Quasi-optical channels at submillimetre wavelengths', *Instr. Exp. Tech. (USSR)*, **14**, pp. 1120–2, 1971.
- Degenford, J. E., Sirkis, M. A. and Steier, W. H., 'The reflecting beam waveguide', *IEEE Trans.*, MTT-12, pp. 445–53, 1964.

Manuscript received by the Institution on 4th May 1979
(Paper No. 1892/CC 307)

† M & SW: Benson, F. A. (Ed.) 'Millimetre and Submillimetre Waves' (Iliffe, London, 1969).

Space applications and technology in the 100–1000 GHz frequency range

P. F. CLANCY, Ph.D., M.I.E.E.E.*

SUMMARY

This paper reviews the key applications areas for space-borne systems operating in the 100–1000 GHz spectral range. The strong interaction between the atmosphere and e.m. radiation at these frequencies is discussed and its consequences in terms of applications stated. For radio astronomy the heavy absorption by the atmosphere forces space-borne telescopes to be employed and the primary radio astronomy objectives in this frequency range are reviewed. The presence of atmospheric molecular transitions at these wavelengths allows extensive atmospheric studies to be conducted especially by the limb-sounding of important trace gases in the upper atmosphere. The possible application of this frequency range to inter-satellite communication links is also described. A detailed account of the present development status of receiver hardware technology is given with special reference to the importance of heterodyne techniques for tuneable, high resolution high sensitivity receivers.

* European Space Agency, European Space Research and Technology Centre (ESTEC), Zwarteweg 62, 2200 AG Noordwijk, Netherlands.

1 Introduction

In the millimetre and submillimetre frequency ranges, and particularly in the range 100–1000 GHz, the attenuation of electromagnetic power by the atmosphere is considerable. This attenuation occurs as a result of both absorption and scattering mechanisms.¹ Most of the absorption results either from water vapour, where the electric dipole moment of the H₂O molecule is involved, or from oxygen where the magnetic moment of the paramagnetic O₂ molecule interacts with the electromagnetic field. The scattering is caused both by irregularities associated with atmospheric turbulence and by rain water droplets and ice particles. The latter scattering is also usually associated with some absorption by the liquid or solid droplets.

In Fig. 1 is shown the total atmospheric absorption for a vertical path in clear air from a comparatively dry, sea level ($h = 47$ m) site having a water volume density at sea level of 5.55 g m^{-3} . In computing the absorption, the US Standard Atmosphere (1962) for the temperature and pressure variation with altitude, has been used.² The broad absorption features due to O₂ and H₂O result in attenuation increases of from tens of dB to many hundreds of dB. This attenuation can be expected to be enhanced by rain attenuation ranging from about 30 dB/km for a 5 mm/h rainfall rate to about 300 dB/km for a 100 mm/h rainfall rate roughly constant over the whole of the 100–1000 GHz range.¹

As a result of these extremely high levels of attenuation, the pursuit of radio astronomy becomes

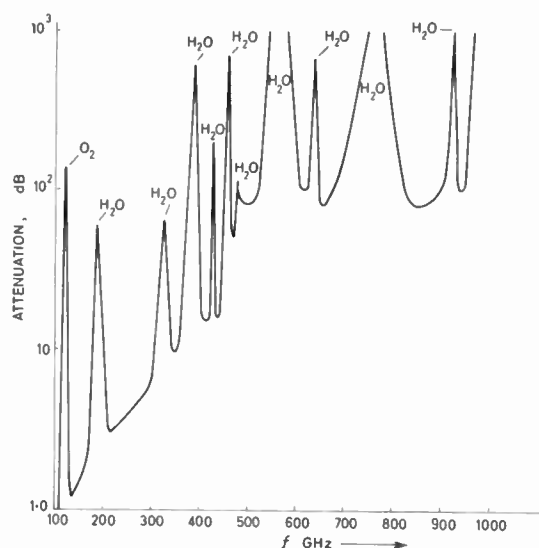


Fig. 1. Clear air attenuation of atmosphere for vertical path from sea level.

difficult, especially if very sensitive broadband spectroscopy (as, for example, the study of galactic molecular clouds) is required. To some extent the atmospheric attenuation can be reduced by using balloon or aeroplane flights or by siting the receiver/telescope at a high altitude site. As an example, taking the 326 GHz absorption peak from Fig. 1, the 65 dB attenuation from sea-level could be reduced to typically 8 dB by going to a 4 km altitude site and to about 1 dB by flying at 12 km altitude. However, since many of these solutions are costly and time limited, great interest centres on developing space-borne detectors at these frequencies.

As a further result of the high attenuation in the lower atmosphere, the space-borne spectral study of molecular species in the upper atmosphere promises a better global understanding since much of the energy balance at the Earth's surface is mediated by upper atmospheric gases such as ozone and carbon dioxide.

Lastly, the use of these frequencies for intersatellite links is possible, thus allowing other bands not subject to these severe attenuation levels to be employed for terrestrial links. The alternatives to this are millimetre wave or laser communications links.

2 Receiver Performances and Technology

Before discussing the detailed aspects of different applications areas a review of the key hardware configurations and performances can be made. For some years the more conventional infra-red or far infra-red detectors have been used into the submillimetre region and beyond. Thus the bolometer detector, which is essentially a temperature dependent resistor, and the photoconductive detector have both been employed for detection at hundreds of gigahertz. With the bolometer the incident radiation causes a temperature rise which is measured by the resistance change. The photoconductor (e.g. InSb) is a semiconductor detector which detects the incident radiation by the change in resistance caused by the raising of electrons from one energy level to another.

In more recent years the extension of classical radio and microwave techniques to higher frequencies has resulted in the extrapolation of heterodyne techniques into the submillimetre region. This approach operates on the principle of mixing the signal with a locally produced signal in a nonlinear mixer causing down conversion to an intermediate frequency (i.f.) in the radio or microwave region ready for demodulation/processing. The heterodyne detection is inherently sensitive, tuneable and broadband and retains all the signal information (including phase) at the i.f.

In common with receiver systems at lower frequencies, detectors operating in the 100–1000 GHz range are limited in their sensitivity by the noise performance of the front end. For the case of heterodyne detection, the

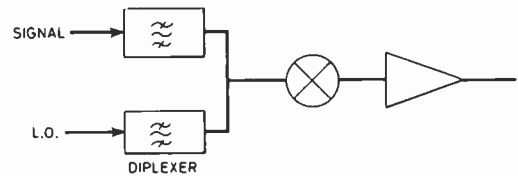


Fig. 2. Heterodyne front end configuration

basic electrical configuration of which is shown in Fig. 2, the layout of the front end implies that the noise performances of the signal and local oscillator diplexing arrangement, the nonlinear mixer, the local oscillator and the intermediate frequency amplifier first stage are critical parameters.

For this case the equation

$$T_S = T_M + L_M T_{IF}$$

serves to describe the total system noise temperature T_S in terms of the contribution both from the mixer itself and from the noise temperature of the i.f. amplifier input stage (L_M is the mixer conversion loss). In practice other factors have to be accounted for in estimating the total noise temperature and hence sensitivity of the front end. These include:

- Noise contribution of the local oscillator taking account of the rejection of the diplexer at the signal frequency.
- Losses in signal arm of the diplexer.
- Coupling efficiency and mismatches between the mixer and the i.f. amplifier.
- Miscellaneous noise sources such as radiation falling on the mixer from outside the field of view.

Table 1 shows the state of the art performances as of writing. These performances all relate to laboratory results but can be regarded as performances likely to be achieved within the next ten years with hardware specifically designed for space applications and capable of yielding these performances on a routine basis. The table is arranged in order of ascending frequency and also indicates the type of mixer employed in each case. It can be seen that three main mixer configurations are employed, these being:

- (i) GaAs Schottky barrier diode mixer operated at room temperature (i.e. ~ 290 K).
- (ii) GaAs Schottky mixer operated at cryogenic temperature (i.e. < 20 K).
- (iii) Josephson junction mixer operated at cryogenic temperature (i.e. ≤ 6 K).

From the space applications point of view the room temperature mixers are, of course, much more attractive since the problems associated with the provision of

Table 1 'State of the art' front-end performances

Frequency (GHz)	Mixer	Ref.	T_M (K)	L (dB)	T_S (K)	Remarks	
115	Josephson junction	at 6 K	3	120	0	120	Thermally recyclable Nb point contact
115	Schottky diode	at 16 K	4	265			Low l.o. power requirement ($\sim 100 \mu\text{W}$)
115	Mott diode	at 20 K	7	200			Low l.o. power requirement ($\sim 150 \mu\text{W}$)
170	Schottky diode	at 290 K	4	1200	7.5		Low l.o. power requirement ($\sim 125 \mu\text{W}$)
318	Schottky diode	at 290 K	6	3100	9.3	4000	Quasi-optical diplexer
380	Schottky diode	at 290 K	9	12900	16.0	19700	350-400 GHz system quasi-optical diplexer
455	Josephson junction	at 4.2 K	8	1120	5.8	4200	Non-thermally recyclable Nb point contact
670	Schottky diode	at 290 K	5	11800	11.6	19400	Quasi-optical mounting and diplexer
760	Schottky diode	at 290 K	5	15200	12.3	29000	Quasi-optical mounting and diplexer
891	Josephson junction	at 4.2 K	8	1200	10.0		Non-thermally recyclable Nb point contact

cryogenic cooling on a spacecraft are not inconsiderable. On the other hand results achieved with Josephson junctions in terms of low mixer noise temperatures and potentially zero conversion loss (or even gain) have kept interest focused on these devices. The recently reported³ fabrication of recyclable Josephson junctions implies steady progress towards a ruggedized device suitable for high reliability space application.

For the room temperature devices, the Schottky mixers offer the best noise temperature, conversion loss, bandwidth, tuneability and reliability. Although waveguide techniques may be used up into the submillimetric (> 300 GHz) region the dimensions become so small and difficult to manufacture with good tolerancing that so-called quasi-optical mounting and transmission techniques are quickly being developed. Here the use of teflon lenses, mirrors, mylar beam splitters, corner reflectors and other quasi-optical components allows the fabrication of Michelson and Fabry-Perot interferometric systems for signal and local oscillator diplexing, beam focusing onto the mixer and the other functions performed by waveguide transmission systems. Examples of the continuing development of these techniques include the introduction of the corner cube,²⁶ the biconical,²⁷ and double slot¹⁰ mixer mounts. Combined with a possible integration of the f.e.t. i.f. amplifier this approach could lead to a very attractive configuration as regards space qualification, since many of the mechanical (vibration) problems would be reduced. The suitability of this system to high frequency, high sensitivity detection has yet to be demonstrated.

The provision of local oscillator power for the operation of heterodyne receivers is something of a problem at frequencies in the high millimetre and submillimetre region. For the Josephson junction type of mixer, power levels of the order of tens of nanowatts are adequate and this can in principle be provided by multiplication techniques. However, for the GaAs Schottky mixers (at least for their operation at ~ 290 K) several tens of milliwatts are required. In order to meet these requirements ESA has supported the development of backward wave oscillator (b.w.o.) technology into the submillimetre region. In particular, tubes capable of a

substantial tuning range ($\sim 20\%$) have been developed by Thomson-CSF (F) for this purpose. Figure 3 shows such a tube with the output waveguide visible at the top of the housing. This unit employs a SmCo permanent magnet which has allowed a mass reduction of from about 35 kg to 16 kg over an earlier model employing a more conventional magnet. The performances of this tube can be summarized as follows:

tuning range	326-393 GHz
output power > 10 mW	335-393 GHz
> 40 mW	353-393 GHz
> 100 mW at	363 GHz
d.c. power consumption (max.)	120 W
total mass (incl. housing, etc.)	16 kg.

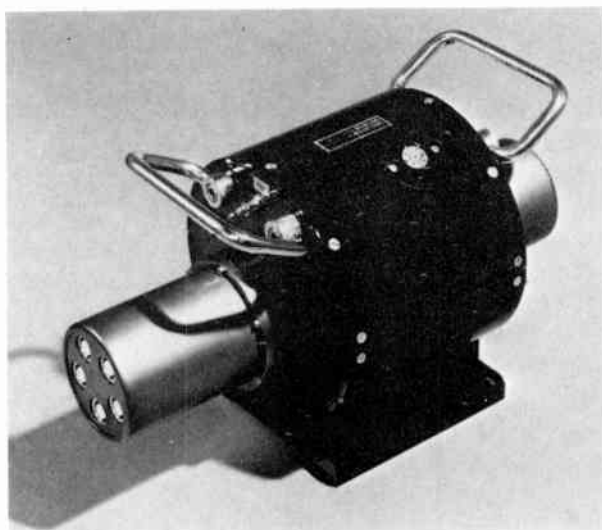


Fig. 3. Backward wave oscillator (330-400 GHz).

3 Antenna/Mirror Technology

This frequency range allows techniques both from classical microwave and classical optical approaches to be employed. The use of waveguide and quasi-optical techniques demonstrate this and a similar

situation obtains for the receiving/transmitting element. Thus one can conceive of extending conventional microwave antenna techniques from the millimetric into the submillimetric region with all the attendant requirements on reduced surface roughness and enhanced shape retention. On the other hand the extension of conventional mirror technology from the far infra-red could be envisaged but in this case mass reductions by the implementation of lightweight fabrication technologies must be contemplated. A study conducted by MATRA for ESA examined a number of lightweight technology options for mirrors up to 2.5 m diameter. These include classical glass ceramics using thin mirror approach, composite (carbon fibre or kevlar) with glass faceplate, multielement systems, and highly polished carbon fibre antenna structures. For mirrors up to 1 m diameter the composite + glass faceplate approach seems feasible assuming the thermal matching (between composite and glass) can be achieved. For a 1 m mirror the mass would be of the order of 20 kg.

4 Astronomy

Free of the severe obscuration of these frequencies by the atmosphere, the pursuit of astronomical research systematically covering the range from 100 GHz–1000 GHz can be expected to yield a rich harvest. Already, the results obtained using balloon and high altitude observatories are sufficient to indicate that short wave millimetre and submillimetre astronomy promises to answer fundamental questions on such diverse matters as:

- the fine scale structure of the cosmic (2.7 K) background radiation,
- the evolution of gas clouds in nearby galaxies and their links with the spiral structure of galaxies,
- the nature of dust grains in clouds and the mechanism of thermal radiation from these grains,
- the molecular chemistry and dynamics at the site of star formation and hence the processes involved in stellar evolution,
- the atmospheric composition and dynamics of comets and the giant planets,
- the nature of natural masers occurring in the envelopes of red giant stars,
- the links between the optical and radio emissions of quasars, radio galaxies and other cosmologically interesting objects.

In Fig. 4 is shown the spectral distribution of astronomically interesting sources both discrete and continuous. The continuous sources are chiefly:^{13,14}

- (i) the cosmic background radiation which is isotropically distributed blackbody radiation at 2.7 K believed to be the diluted and red-shifted remnant of the so-called ‘Big Bang’ radiation,

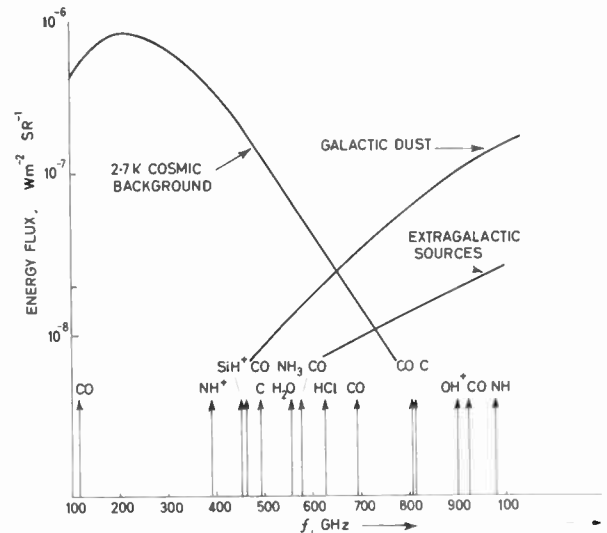


Fig. 4. Discrete and continuous astronomical sources in the 100–1000 GHz range.

- (ii) the thermal radiation from galactic dust grains at a few tens of kelvins, and
- (iii) the continuous radiation from other galaxies due to thermal emission from dust grains or other mechanisms such as synchrotron emission.

Interest in studying the cosmic background radiation centres on measuring small scale anisotropies (1 in 10^3 in temperature) in the otherwise isotropic radiation. Presently available results indicate that anisotropies of this order do exist. Studies to be carried out from spaceborne platforms will allow anisotropy effects due (i) to solar movement against the galactic rest frame (large angular scale) or (ii) to fluctuations in the primeval hot Big Bang plasma (small angular scale), to be investigated.

The emission of continuous radiation from dust grains extends into the submillimetre. Studies at these wavelengths can be expected to enhance understanding of these dust clouds.

The emission of synchrotron radiation by energetic extragalactic quasars, radio and Seyfert galaxies is known, but is not fully understood. In addition many galaxies such as M82, NGC 1068 and NGC 253 have their peak emissions in the far infra-red due, it is believed, to reradiation by optically thin dust.

As a consequence studies in the submillimetre region with a space telescope will yield a deeper understanding of the mechanisms leading to synchrotron emission, dust aggregation and dust heating.

The discrete frequency sources in this range (shown at the bottom of Fig. 4) are due to rotational (usually) transitions in the molecular species populating galactic clouds. Many of these species have been discovered by

their transitions at longer millimetre wavelengths. Investigation in the 100–1000 GHz range will certainly lead to the discovery of new species as well as shedding more light on the chemical and dynamical properties of already detected molecular clouds. Thus the transitions due to the hydrides including H₂O and OH and in particular the lines of NH⁺ (391 GHz), SiH⁺ (453 GHz), HCl (626 GHz) and NH (975 GHz) are expected to be detected. Molecular transitions in the submillimetre are sensitive probes of the conditions prevailing in different cloud regimes. Thus the line intensities of transitions due to molecules such as CO, H₂CO are determined by cloud temperatures. These clouds are often the sites of star formation in which the chemical evolution of these clouds plays a crucial role. In this context the transitions of neutral carbon at 491 GHz and 812 GHz and those of CO at 461, 576, 691, 807 and 922 GHz are important.

The high resolution ($R > 1$ in 10^6) of molecular lines allows the shape of spectral lines to be studied and hence the Doppler shifting caused by turbulence. Hence the internal energy balance (dependent on star formation or cloud collisions) can be deduced. The population inversion sometimes occurring in the complex spectrum of the water molecule can lead to the formation of natural masers some of which have already been detected at 22 GHz. This mechanism may occur for other species involving transitions in the 100–1000 GHz region.

Lastly, the contributions to our knowledge on the composition of the comets—thought to be samples of

In Table 2 are listed some spacecraft/platforms either proposed or fully adopted as missions to be carried out in the 1980s and which include instrumentation intended for astronomical observations falling in the 100 GHz to 1000 GHz range.

5 Atmospheric Studies

The potential application of millimetre and submillimetre frequencies to the study of the Earth's atmosphere should be apparent from the remarks made at the beginning of this paper. That is to say, most molecular atmospheric gases have rotational molecular transitions somewhere in this region, thus causing the absorption and emission of radiation at the transition frequencies. As a consequence, investigations of the spectral line characteristics of the different gases leads to enhanced understanding of the chemistry, temperature profile, pressure distributions, winds and concentration gradients in the Earth's upper atmosphere.

Figure 5 shows the concentration profiles (in volume mixing ratios) for some of the key atmospheric gases as a function of altitude. Gases of particular interest are (i) ozone (O₃) which is responsible for the absorption of the Sun's ultraviolet radiation (and hence protection of the Earth's surface), (ii) the oxides of nitrogen (NO_x) and (iii) ClO which is a very useful diagnostic species involved in the depletion of ozone by aerosols containing chlorine.

Table 2 Some proposed missions employing 100–1000 GHz range for astronomy in 1980s

Name	Sponsor	Mission and launch date	100 1000 GHz instrumentation
COBE Cosmic background explorer	NASA	Cosmic background; 1983/84	Far infra-red spectrometer 30–3000 GHz. Polarizing Michelson interferometer
LIRTS Large infra-red telescope on <i>Spacelab</i> ($D = 2.8$ m)	ESA	Photometry and spectroscopy; after 1985	Polarizing Michelson interferometer 600 3000 GHz. Heterodyne detector 300–800 GHz. Spectral resolution 10^7
SIRTF Shuttle infra-red telescope facility ($D = 1.2$ m)	NASA	Photometry and spectrometry; 1984	Cooled Fourier spectrometer 300–900 GHz. ³ He bolometer detector in 300–2500 GHz range
CIRBS/CRYOSTAT Cosmic i.r. background spectrometer	ESA/UK	Test of liquid He cryostat on <i>Spacelab</i> using cosmic background detectors; 1983	Polarizing interferometer using bolometer detectors

primordial material from the solar nebula—and the giant planets, can be greatly facilitated by the study of the atmospheric molecular gases. Molecules such as NH₃, PH₃, H₂O, H₂S and HCN all have transitions in the short millimetre and submillimetre region.

Questions related to the origin of the solar system and the outer planets can be expected to be clarified by deeper knowledge of the composition and dynamics of these bodies.

All the curves shown are measured results and the references are indicated on the Figure.

In recent years much concern has centred around the question whether man's technological activities are likely to affect the concentration of ozone in the stratosphere. In this respect three mechanisms have been identified as potential threats and these are: aircraft exhaust gases, chlorofluoromethane releases from aerosol propellants, and space shuttle exhausts.

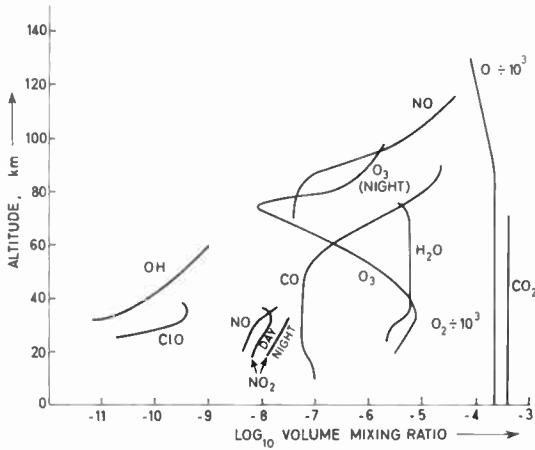


Fig. 5. Some important atmospheric gases

Species	O ₂	O ₃	NO	NO ₂	H ₂ O	OH	CO	CO ₂	ClO
Ref. no.	25	16	25	25	17	25	15	25	20

The ozone is produced in the stratosphere by the reaction of atomic and molecular oxygen in the presence of a third molecule. The atomic oxygen is produced at higher altitudes (> 90 km) by the photo-dissociation of O₂ under the influence of the Sun's ultraviolet radiation.

The chlorofluoromethane (CF_xCl_y with x+y = 4) gases are thought to diffuse up through the ozone layer and become photodissociated under the influence of solar ultraviolet which results in the liberation of atomic chlorine. This in turn depletes the ozone with the formation of ClO. Estimates¹⁹ of the depletion caused by emission rates of the early 1970s vary up to 8%. Again, great uncertainty in reaction, diffusion and transport rates results in uncertainty in these estimates.

The Space Shuttle employs solid motors which produce HCl as one of the effluents. HCl is the end-product in the removal of Cl from the atmosphere and therefore affects its equilibrium concentration. Estimates of the effects of 1 shuttle launch/week indicate approximately 0.2% reduction but again this has a large uncertainty due to the unknowns referred to.

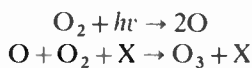
The use of a space-borne platform for the remote sensing and analysis of the atmosphere using high frequency millimetre and submillimetre passive receivers is expected to resolve many of these uncertainties. In principle two forms of observation are possible: limb sounding and down-looking methods. These are simply illustrated in Fig. 6.

The down-looking mode is typical of that used by conventional meteorological satellites and by surface

Table 3 Link parameters for different systems

Parameter	Nd-YAG laser	Millimetre system	Submillimetre system
<i>f</i>	564 THz (5320 Å)	25 GHz	400 GHz
<i>P</i> trans	~ -10 dBW	~ 10 dBW	~ -10 dBW
Telescope/antenna dia. (<i>d</i>)	~ 0.24 m	~ 1 m	~ 1 m
<i>G</i> trans	~ 123 dB	~ 48 dB	~ 72 dB
Losses	~ 3 dB	~ 3 dB	~ 3 dB
E.i.r.p.	~ 110 dBW	~ 55 dBW	~ 59 dBW
Range	~ 4 × 10 ⁷ m	~ 4 × 10 ⁶ m	~ 4 × 10 ⁶ m
Space loss	~ 300 dB	~ 192 dB	~ 217 dB
<i>G</i> rec	~ 123 dB	~ 48 dB	~ 72 dB
Losses	~ 3 dB	~ 3 dB	~ 3 dB
Rx noise	~ -175 dBW/Hz	~ -197 dBW/Hz	~ -193 dBW/Hz
Bit rate (<i>B</i>)	10 ⁹ bits s ⁻¹	10 ⁹ bits s ⁻¹	~ 10 ⁹ bits s ⁻¹
<i>E</i> / <i>N</i> ₀ (<i>N</i> _c /bit)	~ 10 dB	~ 10 dB	10 dB
Margin	~ 5 dB	~ 5 dB	~ 4 dB

This atomic oxygen diffuses downwards to the regions where ozone is formed, the peak concentration occurring at about 30 km. Thus:



In the case of aircraft exhausts it is believed that the main reactants affecting the ozone are the NO_x gases in the exhausts. Many estimates of the effects of these emissions have been made, some predicting depletion and some enhancement of the ozone depending on assumptions made and reaction rates used. A recent work¹⁸ covers the main aspects.

imaging as well as temperature and pressure sounding systems. For upper atmospheric studies limb sounding at these frequencies allows a reasonable (~ 10⁻³ rad) angular resolution to be obtained with a reasonable antenna size (~ 1 m dia.). For a spacecraft at 200 km altitude and operating at 300 GHz the spatial resolution at the limb (horizon) distance of 1600 km is therefore 1.6 km. Other advantages of this mode include:

- No background illumination is used so continuous measurements are possible.
- Pure emission measurements are possible due to cold background.
- Long atmospheric path length gives strongest signals.

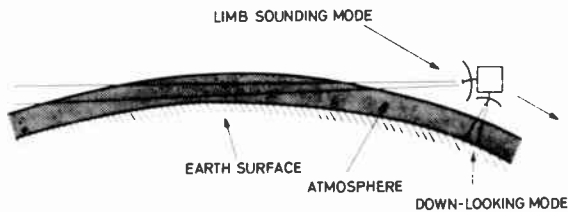


Fig. 6. Modes of atmospheric observation.

6 Communications

Considering the increases in antenna gain achieved by going to higher frequencies, the extension of communications techniques into the 100–1000 GHz region would seem to offer some advantages in terms of power requirements. For space applications the chief use would be for intersatellite links. At the present time the two chief candidates for this application are the millimetre (up to about 100 GHz) system and the laser optical/near infra-red system. The millimetre system offers the advantage of employing a not too great extrapolation of existing mature microwave technology coupled with the enhanced antenna gains and wide bandwidth (≥ 1 GHz) capabilities of millimetre wave systems. At the present time many studies are in progress for the use of 20/30 GHz bands for satellite communications. (See, e.g. Ref. 22.) The laser system offers even higher antenna gains even with small size (< 50 cm) mirrors (antennas) as well as theoretically high bandwidth. Utilization, however, of the highest antenna gains implies sophisticated acquisition and tracking requirements due to narrow beamwidth. Again, a number of studies of laser links have been made.^{23, 24} Typical is the example of a CO₂ system using heterodyne detection and operating at 10 μm .²³

The space testing of a Nd:YAG laser system is planned by the USAF²⁴ in the early 1980s. This system delivers a 1000 Mbit s⁻¹ data rate and features a solar- as well as lamp-pumped laser.

In order to demonstrate the main features of the three (millimetre, laser, submillimetre) possible intersatellite links, Table 3 shows typical values of link budget parameters such as output power, antenna gains, etc. The Table is not intended to represent a critical comparison of three different contenders, rather to highlight the unique features of each system. In every communications system the power and antenna gains must be large enough such that the system and space losses still leave a signal to noise ratio sufficient to ensure an adequately low bit error rate (b.e.r.). Assuming a b.e.r. of 10^{-6} a laser system using ideal pulse quaternary modulation requires a signal to noise ratio of 10 dB (measured in photoelectrons/bit).²⁴ Similarly in an r.f. system using ideal binary phase shift keying (p.s.k.) modulation a signal to noise ratio of about 10 dB is required for a b.e.r. of 10^{-6} . The signal to noise ratio is

measured as E/N_0 with E the energy/bit and N_0 the noise energy.

Some considerations made in deriving the figures are as follows:

The antenna gains are determined from the relation

$$G = \frac{\pi^2 d^2}{\lambda^2}.$$

The 3 dB losses at transmit and receive include output/input circuit losses due to antenna efficiencies less than unity.

The range for the laser link is assumed to be low Earth orbit to geostationary orbit such as might be used in transferring data from an Earth observation satellite (low Earth orbit) to a data relay satellite (geostationary orbit) for further onward transmission to a ground station.

For the millimetre and submillimetre links a range equal to that of two geostationary communications satellites separated by about 6° is used. This separation is about that required to ensure adequate separation of transmit beams from a ground station and hence allows frequency re-use.

The space loss is determined from the relation:

$$\frac{I}{L} = \left[\frac{\lambda}{4\pi R} \right]^2.$$

The receiver noise for the laser link is dominated by the quantum noise given by $h\nu/\eta$ with η the quantum efficiency. An extra 2 dB is assumed from miscellaneous sources.

For the millimetre system a 7 dB noise figure is assumed (i.e. $T \sim 1500$ K) and for the submillimetre system $T \sim 4000$ K is assumed.

The signal/noise ratio is derived from the equation

$$\frac{E}{N_0} = \frac{\text{e.i.r.p.} \times G_{\text{rec.}}}{\text{rec. noise} \times L \times B}$$

where e.i.r.p. = effective isotropically radiated power.

Some advantages and disadvantages as well as the unique features of each system can be stated. In the case of the laser system very large antenna gains are possible due to the short wavelength of operation. This is balanced somewhat by the higher space losses. The laser system also tends to have higher receiver noise since at these frequencies the quantum limit of $h\nu/\eta$ is applicable. The excess is about 20 dB over the thermal one (kT) applying to the millimetre and submillimetre cases. At the submillimetre wavelengths the scarcity of transmit power (currently ~ 100 mW available from backward wave oscillators) is offset by higher antenna gain. For the millimetre link the highest efficiencies are achieved with perhaps 20% d.c. to r.f. efficiency for the output tube

(travelling-wave tube amplifier) as against the rather low efficiencies of the laser ($\sim 0.1\%$) and the submillimetre ($\sim 0.1\%$) tube. An aspect of the laser system requiring attention is the extremely narrow beam and hence the need to provide adequate acquisition and tracking facilities. In this respect it is worth noting that a typical spacecraft pointing accuracy is of the order of $0.2^\circ\text{--}0.5^\circ$ whereas the Gaussian beamwidth (to the i/e^2 points) of a laser communications beam would be of the order of $5\ \mu\text{rad}$ (~ 1 arcsec). Thus the laser link hardware must include a system for acquiring and tracking the incoming beam. This assumes, of course, that the full antenna gain is being employed. Methods of defocusing and beam spreading can be used at the expense of antenna gain in order to simplify acquisition and tracking requirements.

7 Conclusions

The substantial attenuation of frequencies in the 100–1000 GHz range by the atmosphere ensures a considerable future use of these frequencies for space applications including radio astronomy, atmospheric sounding and possibly communications. The extension of heterodyne techniques into this region is a continuing process which is now resulting in the use of sensitive, low noise, high bandwidth, tuneable detectors such as Schottky barrier diode, and Josephson junction, mixers.

In combination with extensions of backward wave local oscillator technology into the submillimetre, the heterodyne detection applied to space-borne instrumentation is likely to lead to an enhanced understanding of, in particular, the cosmic background radiation, galactic molecular clouds involved in star formation, cosmological objects such as quasars, the composition of the Earth's upper atmosphere and the role played by ozone and the trace gases in determining the Earth's radiation budget. In addition, this frequency range has potential application to intersatellite communications links especially in view of the high antenna gains possible.

8 Acknowledgments

The author would like to express his gratitude to Th. De Graauw of the Space Science Department, ESTEC, for many useful comments on the astronomy and atmospheric physics sections, and to H. Lutz of the Instrument Technology Division, ESTEC, for advice on the laser communications aspects.

9 References

- Lane, J. A., 'Scatter and absorption in the troposphere', *Telecommunication J.*, **43**, no. 7, p. 475, 1976.
- 'Submillimetre wavelength astronomy for space', Report of submillimetre space telescope working group, Jet Propulsion Laboratory, A-1, February 1978.
- Taur, Y. and Kerr, A. R., 'Low noise Josephson mixers at 115 GHz using recyclable point contacts', *Appl. Physics Letters*, **32**, no. 11, p. 775, 1st June 1978.
- Vizard, D. R., Keen, N. J., Kelly, W. M. and Wrixon, G. T., 'New Schottky barrier diodes at 111 and 170 GHz with low local oscillator power requirements', *Electronics Letters* (to be published).
- Fetterman, H. R., Tannenwald, P. E., Clifton, B. J., Parker, C. D., Fitzgerald, W. D. and Erickson, N. R., 'Far-IR heterodyne radiometric measurements with quasi-optical Schottky diode mixers', *Appl. Physics Letters*, **33**, no. 2, p. 151, 15th July 1978.
- Erickson, N. R., 'A 0.9 mm heterodyne receiver for astronomical observations', 1978 IEEE MTT-S International Microwave Symposium Digest, p. 438, June 1978, Ottawa, Canada.
- Keen, N. J., Haas, R. and Perchtold, E., 'Very low noise mixer at 115 GHz using a Mott diode cooled to 20 K', *Electronics Letters*, **14**, no. 25, p. 825, 7th December 1978.
- 'A theoretical and experimental study of Josephson frequency mixers for heterodyne reception in the submillimetre wavelength region', Final Report ESTEC Contract 2337/74 (Submillimetre Josephson mixers) by National Physical Laboratory (U.K.).
- 'Evaluation of the Schottky barrier diode heterodyne receiver in the far infra-red', Final Report ESTEC Contract 3221/75 (Schottky diodes in the far infra-red) by Farran Research Associates (IRL).
- Kerr, A. R., Siegel, P. H. and Mattauch, R. J., 'A simple quasi-optical mixer for 100–120 GHz', IEEE-MTT International Microwave Symposium Digest 1977, p. 96.
- Murphy, R. A., Alley, G. D., Bozler, C. O., Fetterman, H. R., Tannenwald, P. E. and Clifton, B. J., 'Submillimetre wavelength surface-oriented diode mixers', IEEE-MTT International Microwave Symposium Digest 1978, p. 430.
- Fetterman, H. R., 'Advanced Schottky diode concepts', *Proc. Soc. Phot. Opt. Instrum. Engrs*, **105**, p. 35, 1977.
- Mather, J. C., 'Infrared and millimetre wave techniques for the cosmic background explorer satellite', *Proc. Soc. Phot. Opt. Instrum. Engrs*, **105**, p. 44, 1977.
- Mather, J. C., 'COBE—explorer of the primeval explosion', *Astronautics and Aeronautics*, October 1978, p. 61.
- Waters, J. W., Wilson, W. J. and Shimabukuro, F. I., 'Microwave measurement of mesospheric carbon monoxide', *Science*, **191**, p. 1174, 1976.
- Shimabukuro, F. I., Smith, P. L. and Wilson, W. J., 'Estimation of the daytime and nighttime distribution of atmospheric ozone from ground based mm-wavelength measurements', *J. Appl. Meteorology*, **16**, p. 929, 1977.
- Waters, J. W., Gustincic, J. J., Kakar, R. K., Kerr, A. R. and Roscoe, H. K., 'Interhemispheric survey of minor upper atmospheric constituents during October–November 1976', NASA TM X-73630 Lewis Research Centre 1977.
- Hidalgo, H. and Crutzen, P. J., 'The tropospheric and stratospheric composition perturbed by NO_2 emissions of high altitude aircraft', *J. Geophys. Res.*, **82**, p. 5833, 1977.
- 'Chlorofluoromethanes and the stratosphere', NASA Reference Publication 1010, 1977.
- Anderson, J. G., 'A simultaneous measurement of Cl and ClO in the earth's stratosphere', Int. Conf. on Stratosphere and Related Problems, Utah State Univ., 1976.
- Final Report on 'Study on Lightweight Mirrors for Space Optical Instruments', Matra, ESTEC Contract 3344/77, 1977.
- Proceedings of Symposium on Advanced Satellite Communication Systems using 20/30 GHz Bands, Genoa, 14th–16th December 1977, ESA-SP 138.
- McElroy, J. H. *et al.*, 'CO₂ laser communications systems for near-earth space applications', *Proc. IEEE*, **65**, no. 2, p. 221, February 1977.
- Barry, J. D., 'Space communications: practical applications of a visible Nd:YAG laser', *Optics and Laser Technology*, pp. 207–16, October 1977.
- Waters, J. W. and Wofsey, S. C., 'Applications of high resolution passive microwave satellite systems to the stratosphere, mesosphere and lower thermosphere', prepared for NASA Committee on High Resolution Passive Microwave Satellite Systems, January 1978.
- Krautle, H., Sauter, E. and Schultz, G. V., 'Antenna characteristics of whisker diodes used as submillimetre receivers', *Infrared Physics*, **17**, p. 477, 1977.
- Gustincic, J. J., 'Receiver design principles', *Proc. Soc. Phot. Opt. Instrum. Engrs*, **105**, p. 40, 1977.

Manuscript received by the Institution on 6th April 1979
(Paper No. 1893/AMMS 98)

Physical measurement in the 100–1000 GHz frequency range

M. J. BANGHAM, B.Sc., M.Inst.P.

J. R. BIRCH, B. Tech., Ph.D., M.Inst.P.

T. G. BLANEY, B.Sc., Ph.D., M.Inst.P.

A. E. COSTLEY, B.Tech., Ph.D.

J. E. HARRIES, B.Sc., Ph.D.

R. G. JONES, B.Sc., M.Sc., Ph.D., C.Eng.,
M.I.E.E.

and

N. W. B. STONE, M.Sc., Ph.D., M.Inst.P.*

SUMMARY

The exploration and exploitation of the submillimetre and millimetre wave regions of the electromagnetic spectrum have progressed steadily over the last twenty years. Sophisticated Fourier spectroradiometric instrumentation, matching in performance that of the conventional instruments developed for the infra-red and visible regions over the last century, has become commercially available. Frequency can now be determined in this region directly against the caesium frequency standard to about 1 part in 10^{10} , and the problem of reliable power measurement is being slowly resolved. The electrical properties of many materials have now been measured in this ultra-high frequency region, and the techniques are being successfully exploited in measurements of atmospheric composition and applied to the important area of plasma diagnostics.

1 Introduction

The decade of electromagnetic frequencies lying between 100 and 1000 GHz is in many ways a transitional region. It is, for instance, the region where our water-laden atmosphere changes from transparency to near-opacity, and where many common materials show sharp changes in their transmission properties. It is also the region in which a basic change in applied techniques occurs—from microwave cavities, horns and waveguides to such components as polished mirrors and lenses commonly associated with the optical region. Many important physical properties are characterized here. The pure rotation spectra of most light molecules fall partially within this band, together with lattice absorptions in solids and broad Poley-type absorption-bands in liquids. The wings of these condensed state absorption bands generally extend far into the microwave region, often dominating the losses at these longer wavelengths. Magnetically-contained plasmas of interest for thermonuclear power generation exhibit the phenomenon of electron cyclotron emission in this region, and at the ultra-high temperatures involved, this could constitute a significant energy loss mechanism in fusion reactors.

Millimetre and submillimetre waves have not so far been much exploited for dimensional measurement, though the possibilities were explored some years ago.^{1,2} The wavelengths are such that ordinary machined surfaces give rise to specular reflection, and interferometric techniques can be readily employed for detecting surface position. There may well be situations, therefore, where submillimetre waves could be profitably deployed for non-contact measurement, especially as the range of available coherent sources widens. But at present the main areas in which millimetre and submillimetre waves are being applied are atmospheric monitoring, plasma diagnostics and in the study of the 'optical'† constants of solids and liquids. It is these topics which are to be discussed here.

2 The Measurement of Frequency

At present, accurate frequency measurements are required in the 100–1000 GHz range for two main reasons:

- molecular spectroscopy, such as laser magnetic resonance,³ and
- as part of frequency measurement chains which link the standard frequency from the caesium clock near 9 GHz to laser frequencies in the near-infrared and probably soon in the visible region.^{4,5}

† The 'optical' constants of a material are the real and imaginary parts of the complex refractive index, related to the real and imaginary parts of the complex relative permittivity by the expression

$$\hat{\epsilon} = \hat{n}^2.$$

* National Physical Laboratory, Teddington, Middlesex, TW11 0LW.

Frequency measurements on monochromatic sources can be realized throughout the range by wavelength interferometry, although as the precision required exceeds 0.1% or so, the experimental complexity and inconvenience become such that direct (i.e. time-domain) measurements become much more attractive. Time-domain measurements are essential to achieve uncertainties better than 1 in 10^6 .

Up to frequencies of a few tens of gigahertz, counters are available commercially and are used to compare the 'unknown' frequency with that of a known harmonic of a standard frequency source, usually a quartz-crystal oscillator. At higher frequencies, a frequency is usually compared with a 'countable' frequency by harmonic mixing. A suitable non-linear device generates a known harmonic (the N th) of the countable frequency f_c and mixes it with the frequency to be measured f_m , to give a 'beat' Δf . Thus $f_m = Nf_c \pm \Delta f$. If the signal-to-noise ratio at Δf is sufficiently large, there is the possibility that the source of f_m can be phase-locked to the countable source, or vice versa if a continuous frequency check on f_m is required.⁶

Various harmonic-mixing devices are used in the 100–1000 GHz range and beyond. Point-contact diodes, either metal–metal⁷ or metal–semiconductor⁸ have been used, although evaporated-film Schottky diodes are becoming more common (see for example Refs. 9, 10). Usually, these devices do not usefully generate harmonics to $N > 20$, although $N = 82$ has been reported in a Schottky diode.¹¹ Superconductor–superconductor point contacts (Josephson junctions) have also been employed, their advantages being the high values of N which can be obtained (up to $N = 825$ has been reported by Blaney and Knight¹²) and their low input power requirements. This makes possible the frequency monitoring of a source by the phase-locking technique when only a few tens of microwatts of source power are available (see Ref. 13 and Fig. 1), and also the

direct comparison of a source with the harmonic of a quartz crystal oscillator.¹⁴

The mixer device can be in a waveguide mount, but for frequencies above a few hundred gigahertz, open-structure mounts are more usual. In the latter, radiation from the high-frequency source is focused down with a lens or mirror, and coupled to the mixer device via the antenna formed by the connecting wires.¹⁵

State-of-the-art frequency-measurement systems have intrinsic uncertainties of 1 part in 10^{10} or better for measurements up to 1000 GHz and for measurement times of around one second. In most cases, this potential accuracy exceeds the stability and reproducibility of the sources under test. For example, free-running molecular lasers have a tuning range of a few parts in 10^6 , and even if 'locked' to the centre of the gain curve, stability to better than a few parts in 10^7 is seldom achieved. Some improvement is possible if the laser can be locked to a molecular absorption feature or Lamb dip.¹⁶ Atomic beams of magnesium have been suggested as the basis of a high-quality frequency standard near 600 GHz.¹⁷ Information on laser frequencies which have been measured is included in a report by Knight.¹⁸

Thus the means for good frequency measurements exist, but considerable improvements in convenience are desirable to make them accessible to more potential users.

3 The Measurement of Power

Absolute power measurements are required in the spectral range mainly for the comparison and specification of sources, detectors, and other components. Unfortunately, there are presently no formalized standards for the measurement of power in the two decades of frequency above about 100 GHz, and various *ad hoc* techniques are used.

Power-measuring techniques are usually somewhat different for systems operating in (a) single-mode (or slightly overmoded) waveguides, which are used up to about 300 GHz; and (b) free space, with single-mode laser beams or highly overmoded incoherent radiation, which are used above 300 GHz.

In waveguide systems below 100 GHz, power standards are realized by the use of electrically-calibrated dry-load calorimeters.¹⁹ Radiation power is absorbed in a matched termination and the temperature rise, which is detected by a suitable sensor (e.g. thermopile or resistance thermometer), is compared with that produced by a known amount of d.c. electrical power dissipated in the same structure. Calibration corrections must be made, for example, for attenuation and heat generated in the input waveguide section, mismatch errors, and different thermal distributions created by the two types of heating. Some work has extended these techniques to higher frequencies. Keen²⁰ has described a

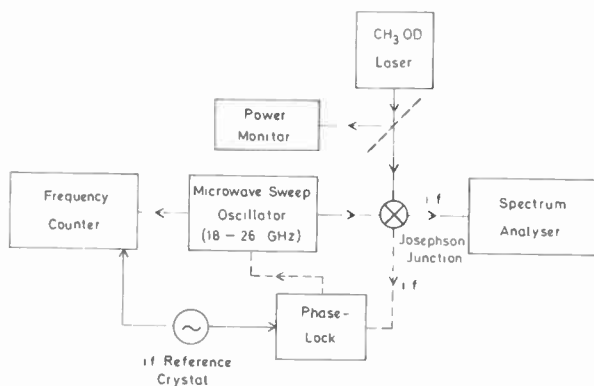


Fig. 1. A system for measuring the frequency of lasers to beyond 2000 GHz. A 'countable' oscillator is harmonically mixed (and possibly phase-locked) to a laser (in this case a CH_3OD gas laser) via a point-contact Josephson junction. (From Ref. 13.)

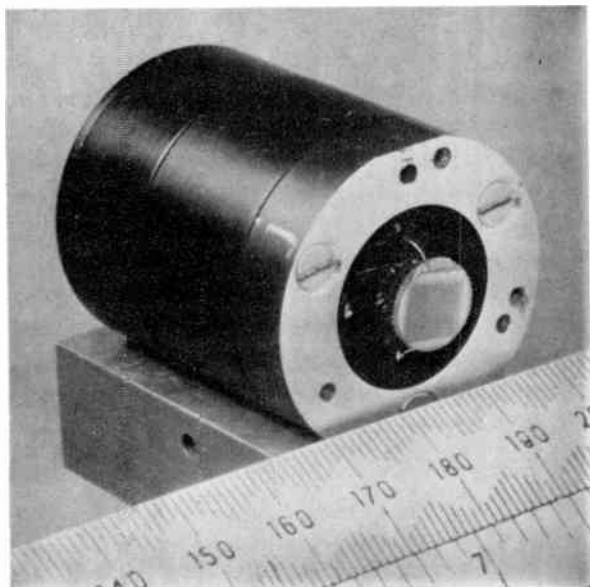


Fig. 2. A prototype-standard disk thermopile for laser power measurement at 891 GHz. The thin copper disk (supported by the thermopile wires) carries a thin glass disk on which is evaporated an inscribed square of nichrome which serves to absorb radiation and act as a resistance for d.c. electrical calibration. In use, a windowed cowl protects the disk from draughts. (From Ref. 24.)

fundamental-mode-waveguide calorimeter for 90–140 GHz with an estimated uncertainty of about 4% at the 10 mW level, and with a settling time of about 25 s. Stevens²¹ has described calorimeters of a generally similar principle which operate up to 325 GHz, where the estimated uncertainty is about $\pm 10\%$ at 10 mW. Yet another of similar design has been operated with overmoded waveguide up to 300 GHz with approximately similar estimated precision.²² Commercial calorimeters with useful performance above 100 GHz are available from Anritsu, Japan (up to 140 GHz) and C & K Engineering, West Germany (up to about 300 GHz). Water-flow calorimeters have been used for several years by one manufacturer of backward-wave-oscillators to measure power outputs (usually ≥ 10 mW) at frequencies up to nearly 1000 GHz.²³

Less work has been carried out in providing working standards for free-space measurements. One approach is to use a detector (e.g. a Golay cell, pyroelectric or bolometer) which has been calibrated in another spectral range (e.g. the infra-red). This is often unreliable, as detector characteristics, such as étendue and radiation absorption properties, are often strongly wavelength-dependent. A prototype standard detector based on a thermopile with a thin metal film absorber (which also serves as an electrical resistance for d.c. calibration) has been described²⁴ for use at 891 GHz (see Fig. 2). With laser power of about 1 mW, a preliminary uncertainty of about $\pm 15\%$ is estimated (D. W. E. Fuller, private communication). With further work, reduction of the

uncertainty, and extension to longer wavelengths, appears possible. Other electrically-calibrated detectors have been noted by Blaney.²⁵

For more convenience, disk thermopiles with specially-thickened black-paint absorbers may well provide power measurements at the 1 mW level and at frequencies down to about 300 GHz with an uncertainty of better than about 20% (D. W. E. Fuller, private communication).

Another aspect of calibrations is the use of standard sources. These often take the form of noise sources (more usually called black or grey bodies in multimode systems) with known effective temperatures. Although some commercial noise tubes with effective temperatures of the order of 10^4 K for use in single-mode waveguides have been offered for frequencies in excess of 100 GHz, 300 K and 77 K (liquid N₂) loads are often used for calibrations where the signal level from these is sufficient. For multimode free-space systems, iron-loaded epoxy foams are often employed as black bodies, although no detailed accounts of the emissive characteristics of these materials at these high frequencies appear to have been published. Some attempts have been made to build and assess black bodies of higher temperature, such as those by Lichtenberg and Sesnic,²⁶ who described a source of about 500 K for 2 mm and shorter wavelengths.

A significant problem in the development of standard sources is the determination of emissivity. Llewellyn-Jones and Gebbie²⁷ have described a method using a heavily-overmoded cavity which allows the emissivity of a thermal source to be determined, and its radiation compared with that of the source to be calibrated. The system appears particularly suitable for calibrations in the 100–1000 GHz range.

Thus while power measurements in this range are not presently satisfactory, refinement of existing techniques will probably solve many of the problems.

4 The Determination of Optical Constants by Dispersive Fourier Transform Spectrometry

In broad band spectrometry at millimetre and submillimetre wavelengths the optical constants of a medium have traditionally been determined from the measured power transmission or reflection spectrum of a specimen by the use of any of a variety of approximate methods.²⁸ This is an adequate approach for many purposes, provided that the limitations of the particular method are fully understood, including the nature of the systematic errors introduced by the use of the approximations. The recent development of dispersive Fourier transform spectrometry (DFTS), in which the amplitude attenuation and phase shift caused by a specimen are directly measured, has introduced an alternative and more precise method for determining the optical constants. In this Section we shall outline the

development of DFTS and discuss present-day measurement capabilities.

Dispersive Fourier transform spectrometry differs from conventional Fourier transform spectrometry in the positioning of the specimen. In the latter method the specimen is placed between the interferometer and the detector. The symmetry of the measurement ensures that the phase shift caused by the specimen is not determined and, as only one quantity, the amplitude, has been measured, it is not possible to calculate both optical constants exactly. In the dispersive method the specimen is placed in one arm of the interferometer and the ratio of the complex spectra obtained from the transformations of interferograms recorded with and without the specimen present gives both the amplitude attenuation and phase shift caused by the specimen. Thus, a single measurement has determined the two quantities that are most directly related to the optical constants, enabling them to be calculated exactly. Detailed descriptions of the theory of DFTS are available.²⁹⁻³³

In principle, such measurements are very simple, but the accurate determination of the phase spectrum imposes stringent stability requirements on an interferometer. The basic interferometer configurations used in DFTS are shown in Fig. 3. For transmitting specimens the instrument shown in Fig. 3(a) would be used with the specimen in the fixed mirror arm of the interferometer and the radiation passing through it twice, although variations on this, in which the optics have been arranged so that the radiation only passes through the specimen once, have been used to study more absorbing solids. For very highly absorbing and opaque specimens the reflection instrument shown in Fig. 3(b) would be used, with the specimen replacing the fixed mirror of the interferometer. The configurations of Fig. 3 are typical of those used for solid specimens. The study of fluids requires the use of windowed cells to contain the specimen, but, although this complicates the interferometer design, the basic transmission and reflection configurations for the study of any phase of matter remain those of Fig. 3.

The containment of gaseous and liquid specimens not only complicates the interferometer design, but also the experimental procedure, as it becomes necessary to allow

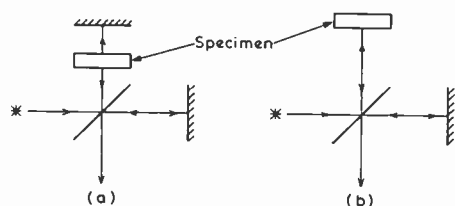


Fig. 3. The basic interferometer configurations used for the study of specimens by DFTS, (a) in transmission, (b) in reflection.

for the cell window phase and attenuation effects as these can change significantly when the specimen is introduced. However, the low complex refractive indices of gases and vapours under typical experimental conditions means that these effects can generally be completely ignored³³ and these materials are, in fact, the most convenient to study by DFTS methods. Their low absorption indices mean that long gas cells may be used without excessive loss of signal so that large phase shifts can be produced, leading to the attainment of high measurement precision. The first DFTS measurements on gases were by Chamberlain and Gebbie on hydrogen halides³⁴ in the spectral region below 60 cm^{-1} (1.8 THz). With various co-workers they subsequently determined the refraction spectra of gaseous ammonia³⁵ and GeCl_4 ,³⁶ while developing a near infra-red interferometer used to study part of the fundamental vibration band of HCl at about 3000 cm^{-1} .³⁷ The far infra-red measurements of these authors were made at modest spectral resolutions of about 1 cm^{-1} (30 GHz). During the same period Sanderson³⁸ used an interferometer developed for DFTS measurements on solids³⁹ to study the pure rotation spectrum of HCl at the same resolution and then developed an instrument specifically designed for high resolution dispersive and non-dispersive studies of gases and vapours.⁴⁰ It could attain a maximum resolution of 0.05 cm^{-1} , but only appears to have been used to 0.4 cm^{-1} in the dispersive mode. The cell windows of these two interferometers were flexible polymer sheets. This leads to difficulty in the determination of the cell length and, hence, introduces a systematic error in the overall level of the measured refraction spectrum. Birch⁴¹ has recently described a high resolution interferometer with rigid windows that overcomes this problem and enables accurate refraction measurements to be made. It can be used to a resolution of about 0.14 cm^{-1} and its performance illustrates current dispersive measurement capabilities for gases. In the long wavelength region below 50 cm^{-1} (1.5 THz), the level of systematic error in refractive index determinations was estimated to be less than 3.6×10^{-7} , while the level of random error was found to be about 2×10^{-7} , at the highest resolutions. Thus, it is possible to determine the refractive indices of gases in the long submillimetre wavelength region with an uncertainty of about 5×10^{-7} . Figure 4 shows the refraction spectrum of water vapour measured with this instrument between 10 and 50 cm^{-1} .⁴² The experimental points are shown as crosses, while the continuous curve represents a theoretical calculation. There is a small difference of about 5×10^{-6} between the two, which could be due to a small error in the pressure measurement.

Three types of interferometer configuration have been used to contain liquids for DFTS studies. The liquid can form a free, gravity-held layer over the fixed mirror of the

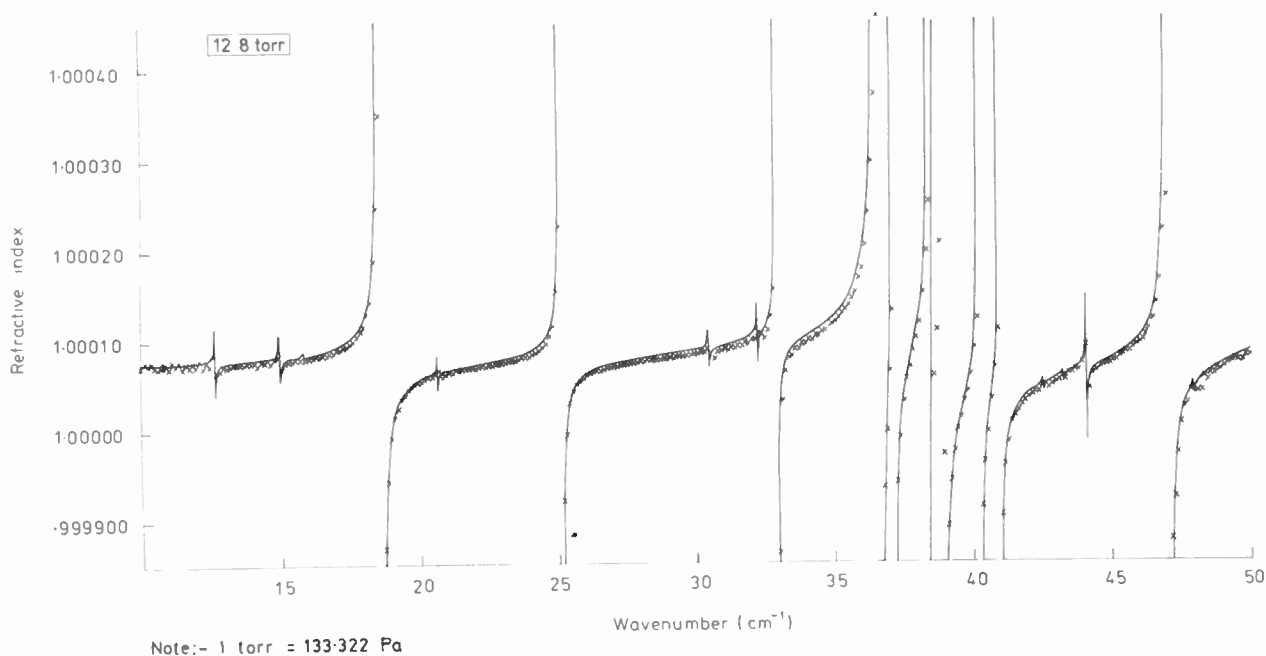


Fig. 4. The refractive index of water vapour at 12.8 torr pressure and 293 K temperature measured by transmission DFTS. (From Ref. 42.)
 × experimental data, — theoretical model.

interferometer and be measured in transmission. This is the free liquid layer method.^{29,44-46} For highly absorbing and opaque liquids the reflection method is used^{46,47} in which the liquid is poured over a transparent window in the fixed mirror arm of the interferometer and the complex reflectivity of the window-liquid interface measured. Alternatively, these two methods can be combined into one by the use of variable thickness liquid-cell methods.⁴⁸⁻⁵² In these the liquid is contained between a fixed transparent window and a movable mirror, so that either variable thickness specimens can be studied in transmission or the thickness can be made sufficiently large that only the window-liquid interface reflection is seen. Liquids have much higher refractive indices than gases, so the reflections that occur at the liquid-cell interfaces play a significant role in determining the measured insertion loss and, therefore, must be explicitly allowed for in the calculation of the optical constants.⁴³ The ease with which this may be done is simplified by the fact that the thickness of a liquid specimen may be easily varied and in the free layer method it is usual to use one of the experimental methods developed by Chamberlain and co-workers for this purpose. Thus, in order of application to decreasing layer thickness one would use the editing,⁴⁵ subtraction,⁵³⁻⁵⁵ two-thickness,^{46,56} or double subtraction⁴⁶ methods. Similar allowances have to be made in the transmission liquid-cell methods and analogous procedures to those described above have been used.

The accuracy that can be achieved from measurements made on free liquid layers depends on two factors. First, the level of absorption in the liquid. If this is low, thick layers can be used to give high accuracy in the measured refraction spectra. Secondly, if the liquid has a high saturated vapour pressure the presence of its vapour over the liquid surface will cause errors in the calculated optical constants, especially if the vapour possesses a strong line spectrum in the region of interest. Measurements on solutions of *p*-difluorobenzene in cyclohexane,⁵⁷ a relatively transparent system, gave a reproducibility in the measured refractive index of ± 0.0003 . Recent measurements on the more absorbing liquid chlorobenzene⁵⁸ led, however, to the conclusion that the free layer method resulted in an uncertainty of $\pm 2\%$ in absorption coefficient, and in a refraction spectrum having random errors not exceeding 0.2% and systematic errors not exceeding 0.6%. With even more absorbing liquids, for which the absorption coefficient approaches 50 neper. cm^{-1} , the error in the determination of the absorption coefficient by this method can exceed 20%.⁵⁹

Reflection DFTS intrinsically provides poorer measurement precision than does transmission DFTS as the former must measure phase angles that might only be tens of milliradians, while the latter usually has to deal with tens of radians, or more. It is, however, the only viable method for the study of very highly absorbing liquids and, as such, is an extremely valuable measuring tool. Measurements made on water^{60,61} with this

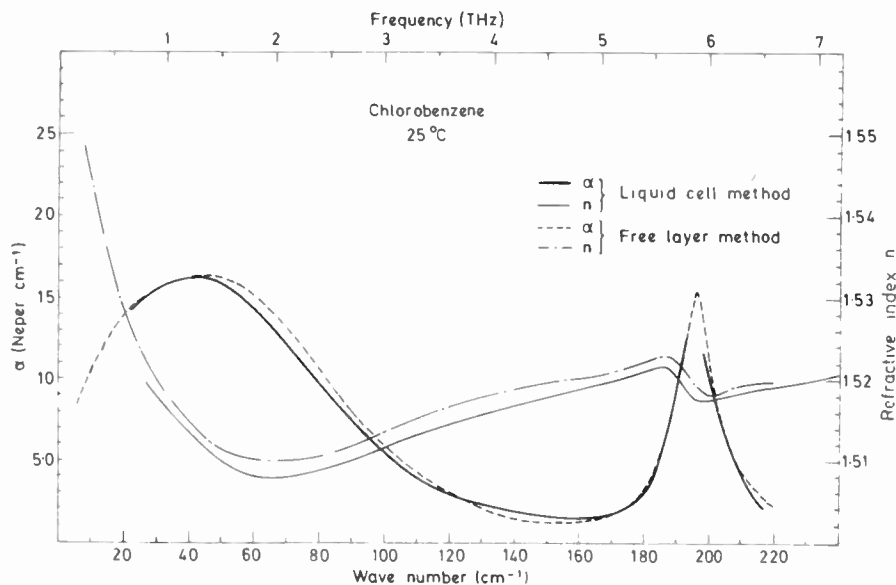


Fig. 5. The refractive index, n , and power absorption coefficient, α , of chlorobenzene at 25°C determined by both free liquid layer and liquid cell methods. (From Ref. 52.)

technique using a silicon window have enabled absorption coefficients in excess of 2000 Np. cm^{-1} to be determined to within $\pm 5\%$ with a corresponding error in the refractive index of ± 0.005 .

The variable thickness liquid-cell methods are not necessarily more accurate than the free layer and reflection methods. Their main advantages stem from the absence of any vapour in the optical path, the ease of controlling the temperature of the specimen, the ability to maintain very thin layers ($\sim 10 \mu\text{m}$) (not possible with free liquid layers due to surface tension effects), and the convenience of having both transmission and reflection measurement capabilities present in a single interferometer. Passchier *et al.*^{51,62} have considered the error sources present in all of these methods and conclude that for well-designed experiments free layer and liquid-cell methods should give comparable results for transmission studies on transparent liquids and for reflection studies on highly absorbing liquids. This is illustrated for the transmission case by the results shown in Fig. 5 which show free layer and liquid-cell determinations of the optical constants of chlorobenzene below 220 cm^{-1} at 25°C. The refractive indices agree to within 0.2% and the absorption indices generally to within 1 or 2%.

In common with liquids the study of solids by DFTS is supported by three basic interferometer configurations. Transparent specimens would be studied in a double pass system similar to that of Fig. 3(a). More heavily absorbing, but not opaque, specimens would use a single pass method, while very heavily absorbing solids would be studied in the reflection configuration of Fig. 3(b). Initial developments in these areas were carried out by the NPL group concentrating mainly on transmission studies of polymers^{36,63-65} and by the Ohio State University group who developed an instrument suitable

for both single pass transmission measurements and reflection measurements on solids.^{39,66-69} At the present time several groups are active in the DFTS of solids, and all three measurement methods are being improved and developed.

The measurement precision that can be achieved in double pass studies on fairly transparent solids may be illustrated by recent measurements on silicon between 5 and 120 cm^{-1} at 290 K.⁷⁰ The uncertainty in the measured refractive index was estimated to be between 0.0001 and 0.0002 and that in the absorption coefficient to be about 0.05 Np. cm^{-1} . Similar measurements on fused quartz⁷¹ gave somewhat larger uncertainties, but the specimen used was more absorbing and had a smaller aperture than that used in the former measurements. Single pass measurements have been made on quite transparent solids,^{68,69} but one of the main uses of this particular method is the study of heavily absorbing solids not accessible to double pass measurement. Thus, recent single pass measurements⁷² on KBr in the wings of its *reststrahlen* band at 90 and 300 K have resulted in values of the optical constants having uncertainties of a few percent in regions of the spectrum where the absorption coefficient is $\sim 400 \text{ Np. cm}^{-1}$. Additionally, the 300 K measurements were in good agreement with those of an earlier study.⁷³

Dispersive reflection measurements on absorbing solids can be performed in one of two ways. The replacement method can be used, in which the specimen physically replaces the fixed mirror of the interferometer, and specimen and reference interferograms are recorded sequentially. This was the basis of the original instrument of Russell and Bell,³⁹ and also of subsequent instruments used by other groups.⁷⁴⁻⁷⁶ Using this technique at room temperature with fairly large

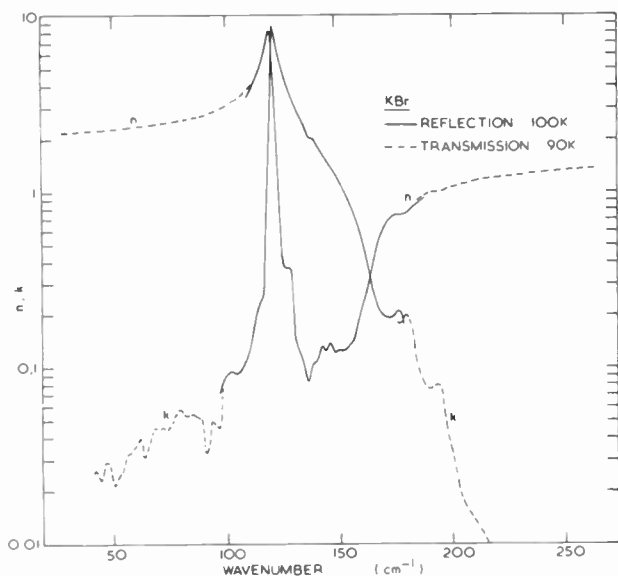


Fig. 6. The refractive index, n , and the absorption index, k , of KBr determined by dispersive reflection methods at 100 K and by dispersive transmission spectroscopy at 90 K. (From Ref. 72.)

specimens (~ 40 mm diameter) has allowed the optical constants of highly absorbing solids to be determined to better than 0.1 at wavenumbers below 400 cm^{-1} ,⁷⁶ and similar precision has recently been obtained at temperatures down to 6 K.⁷⁷ In the second method of measurement the specimen is fixed in position and its surface partially aluminized. A system of screens is used to expose either the aluminized or the non-aluminized sectors to the incident radiation and specimen and reference interferograms are again recorded sequentially. This is the method of the division of the field of view,^{78,79} and in measurements on alkali halides⁸⁰ and ferroelectrics⁸¹ the uncertainty in the measured values of the optical constants at 300 K was found to vary between about 0.01 and 3.0, typically corresponding to an uncertainty of a few per cent. A recent extension of the method down to temperatures of 7 K has given similar results.⁸² A typical result obtained with this method is shown in Fig. 6. The continuous curves represent the optical constants of KBr determined by the reflection method in the region of the *reststrahlen* band. The dashed curves represent the optical constants determined by single pass transmission measurements in the wings of the band, and the excellent agreement between the two in the region of overlap is a further indication of the precision obtainable with dispersive methods. Staal and Eldridge⁸³ have described an extension of the division of field of view method, in which the pattern of the aluminized surface makes better use of the symmetry of the incident radiation beam. It can be used in a mode of operation that eliminates the effects of backlash in the drive system by recording specimen and reference interferograms in one scan of the interferometer, rather

than sequentially, by repetitive switching of the position of the screen system.

5 Open Resonator Measurements in the Millimetre Wave Region

Open resonators as used in the microwave and submillimetre region are usually composed of two metal reflectors placed so as to form a resonant structure similar to that of a Fabry–Perot *étalon*. Resonators have been constructed for frequencies between 10 GHz⁸⁴ and 890 GHz.⁸⁵ The two basic types are shown in Fig. 7. Figure 7(a) shows a ‘confocal’ resonator which has two concave mirrors and Fig. 7(b) shows a ‘hemispherical’ resonator with one concave and one plane mirror. The positions of the samples under test in the two cases are indicated by AA in the diagrams. In the case of a gas the sample would of course fill the resonator. At frequencies up to about 300 GHz the energy can be coupled in and out of the resonator by waveguides as indicated by C and D. These waveguides are generally soldered into the back of the mirror in such a way that the end of the waveguide is closed by a thin metal wall with a coupling hole in it. Coupling at the centre reduces the number of possible modes of oscillation of the cavity⁸⁶ and this is important because of the possibility of mode degeneracy which would reduce the accuracy of measurement. At frequencies above about 300 GHz the energy can be focused by a lens through a small hole in a mirror.⁸⁵ Beam splitter coupling has also been used.⁸⁷

The theory of a confocal resonator containing a solid sample at the centre, Fig. 7(a), has been developed by Cullen and Yu⁸⁴ using a Gaussian beam formulation. This is an improvement on earlier methods using a plane wave formulation. Jones⁸⁶ has adapted this for use with a hemispherical resonator where the sample is placed on

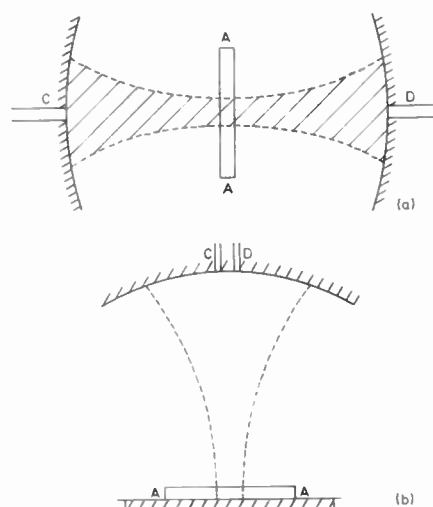


Fig. 7. Open resonators, (a) confocal, (b) hemispherical; AA indicate sample position; CD indicate input and output waveguides. The shaded areas show the extent of the microwave beam in the resonator.

Table 1
Dielectric properties of cyclohexane at 25°C⁸⁸

Frequency GHz	ϵ'	δ μ rad
35-56	2.014 \pm 0.003	79 \pm 4
72	2.018 \pm 0.002	154 \pm 8
144	2.016 \pm 0.004	294 \pm 8

the plane mirror (Fig. 7(b)). The hemispherical resonator has certain advantages in that the sample is located and aligned automatically whereas in the confocal resonator the sample must be located at the centre and carefully aligned to be perpendicular to the axis. The hemispherical resonator is also much more convenient for measurements on liquids. Open resonators in general have an advantage over closed cavity methods where the sample must fit the waveguide. In the open resonator the sample can be any shape provided it exceeds a certain minimum size determined by the diameter of the microwave beam in the cavity. Cullen and Yu⁸⁴ and Jones^{86,88} have made measurements on solids and liquids at frequencies between 10 GHz and 150 GHz. Accuracies of $\pm 0.2\%$ for ϵ' and 2% to 5% for ϵ'' have been obtained. Table 1 lists some data obtained on cyclohexane at 25°C. The high Q values obtained with open resonators mean that the lowest loss materials available can be measured. The Q of a resonator 130 mm long operating at 144 GHz is 260 000.

Open resonators can also be used to measure the dielectric properties of thin plastic films⁸⁹ and because of the polarized nature of the microwaves in the resonator anisotropic materials can be investigated.^{89,90}

Measurements have been made on gases by French and Arnold⁸⁷ who have measured nitric oxide at 150 GHz, and Valkenberg and Derr⁹¹ have measured water vapour at frequencies between 100 GHz and 300 GHz. Batt and Harris⁸⁵ have used a folded version of the confocal resonator by introducing a third plane mirror in an intermediate position between the two concave mirrors. This system has been used for measurements on atmospheric gases at 890 GHz using an HCN laser as a source.

6 Measurements of the Atmospheric Emission Spectrum between 100 and 1000 GHz

The pure rotation spectra of all light molecular gases fall in the short millimetre and submillimetre wavelength regions of the electromagnetic spectrum. Moreover, the energy levels from which they are derived are well populated thermally at normal atmospheric temperatures. Those gases which possess finite dipole moments may therefore emit or absorb strongly in this region. Since most of the gases present in the atmosphere, both naturally occurring and due to atmospheric pollution,

are relatively small and light, it is not surprising that the millimetre, submillimetre and middle infra-red regions are widely used to characterize the atmosphere, particularly the high atmosphere, in terms of its composition. The measurement of trace gases in the stratosphere has become a matter of some importance in recent years, owing to concern about the effect of pollutants upon the photochemistry of the stratosphere in the vicinity of the critical ozone layer. Ozone is of course the Earth's principal shield from the Sun's ultraviolet radiation in the 200–300 nm range, and any cause for disturbance of the equilibrium is of immediate environmental interest.

The vast majority of gases in the atmosphere are in fact dipolar; even the homonuclear oxygen possesses a significant magnetic dipole moment giving rise to a weak far infra-red spectrum. Nitrogen is the main exception, having no allowed rotational transitions, but because of its abundance, coupled with a strong electric quadrupole, it is the main foreign gas line broadening agent to be contended with.

Water vapour absorption dominates the atmospheric submillimetre wave spectrum down to wavelengths of 20 μ m or less. However, on the long wavelength side of this intense band, beyond 250 μ m (40 cm^{-1}), the absorptions become fewer and weaker, and between 100 and 1000 GHz (3 cm^{-1} to 30 cm^{-1}) many absorptions between the lines of the water spectrum can be identified. This is particularly so in the stratosphere, where the mixing ratio of water vapour falls to a few parts per million. In applying millimetre and submillimetre wave techniques to the problem of detailed stratospheric analysis therefore, we must scan this huge range of frequencies at a resolution and with a signal-to-noise ratio adequate to detect extremely small traces of gas, often as low as a few parts in 10⁹. Fourier spectrometry still provides the most powerful method of doing this, largely because of its high 'étendue' or radiation grasp and the wide spectral coverage of a single observation.

In general, variants of the Michelson interferometer^{92,93} have been used for this purpose. The polarizing interferometer of Martin and Puplett⁹⁴ in which the dielectric film beam divider of earlier instruments is replaced by an accurately wound fine tungsten-wire grid is shown in one of its forms in Fig. 8. In the long-wave region $\lambda > 50$ μ m, this instrument possesses two considerable advantages. In the first place, the instrumental transmission is not modified by interference between the two surfaces of the film, as in the case of dielectric film beam dividers, and so a flat spectral response can be achieved from millimetric wavelengths down to 100 μ m or lower. And secondly, beam division very close to 50% may be realized. It is necessary, of course, to polarize the incoming signal at a cost of 50% reduction of incident power, but using an appropriate component layout, the instrument can be simultaneously

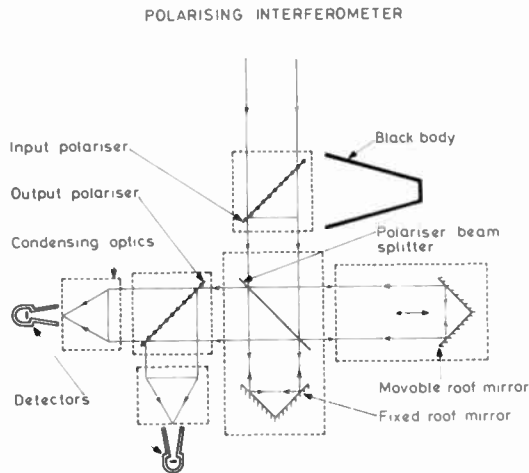


Fig. 8. Configuration of polarising interferometer as used in submillimetre wave aircraft observations.

calibrated with a black-body source using the perpendicular component of the incoming radiation. This is illustrated in Fig. 8.

A number of measurements^{95–99} of the stratospheric emission spectrum have now been made from high-flying aircraft and using balloon-borne instrumentation. Figure 9 shows a section of a high resolution spectrum¹⁰⁰ of the upper troposphere and stratosphere computed from an interferogram recorded from an aircraft flying at 10.8 km altitude and viewing the atmosphere at a zenith angle of 80°. The instrument was a polarising interferometer and the resolution realized was 0.03 cm⁻¹. The upper curve shows the experimental spectrum, and the lower a calculated spectrum including the main emitting features of water vapour, ozone and oxygen, and also nitrous oxide. The arrows indicate the small features assigned to N₂O.

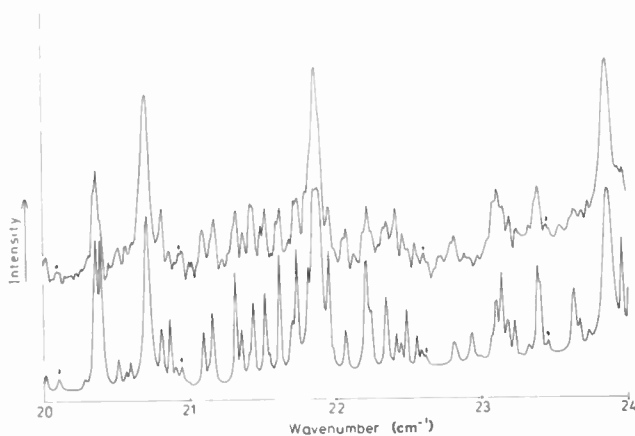


Fig. 9. Section of submillimetre wave emission spectrum measured from an aircraft flying at 10.5 km. Positions of N₂O lines arrowed. Upper curve, observed; lower curve, calculated.

The calculated spectrum is obtained using the known spectroscopic parameters of the constituent gases in a layered model of the atmosphere at and above flight level. The line shapes used in the calculations were Lorentzian. Although the point-by-point correlation between the curves is not perfect, it is seen that we can now achieve a very satisfactory simulation of the atmosphere which enables us to identify many trace species in the narrow windows between the major emission lines, and most of the small features present in the observed spectrum can in fact be reliably assigned. It is not always possible to make accurate estimates of trace gas concentrations directly by measuring the intensities of emission lines, particularly if they are small shoulders on the edge of much stronger lines. In practice, a preliminary estimate of concentration is made from the observed spectrum, and this estimate is then used in calculating the compound theoretical spectrum. A comparison of the two then leads to improved values for the concentrations.

7 Physical Measurements on Plasmas Using the 100–1000 GHz Range

Physical measurements on plasmas at high frequencies are aimed at determining the magnitude of the main plasma parameters like the electron density n_e and the electron temperature T_e and at improving our understanding of the plasma state. They can be conveniently divided into two types, *active* and *passive*. In the former a beam of radiation is launched at the plasma and the effects of interactions between the beam and the plasma are monitored: examples of this type are refraction and absorption measurements. In the latter, radiation emitted by the plasma through thermal and non-thermal processes is recorded. In both cases the disturbance of the plasma is minimal and this is the main advantage of these particular methods.

Refraction and scattering are the most commonly employed active interactions. The refractive index of a plasma is simply related to the electron density and so it is in principle possible to determine the latter by measuring the refractive index with an interferometer. In practice, however, the plasmas are rarely homogeneous with the result that only the integral of the density $\int n_e(l) dl$ along the line of sight can be determined with a single probing beam. Moreover, other effects like beam-bending, diffraction and mechanical vibrations have to be taken into account. Usually the optimum frequency is a compromise between beam-bending at low frequencies and sufficient phase shift for accurate measurements at high frequencies. For plasmas of interest in current thermonuclear fusion research, e.g. the tokamak (toroidal) type, the frequencies lie in the 100–1000 GHz range. For these plasmas the electron density is in the range $10^{18} < n_e < 10^{22} \text{ m}^{-3}$, the electron temperature is

typically 10^7 K and the physical size of the plasma typically 0.50 m (minor diameter).

At frequencies below about 200 GHz microwave instrumentation and techniques are usually employed. A typical system consists of a klystron, a power divider, a phase-shifter, appropriate lengths of waveguide, transmitting and receiving horn antennae and a crystal video detector arranged in a Mach-Zehnder type arrangement.^{101,102} Several probing beams are usually employed so that, assuming cylindrical symmetry, the full spatial dependence of the density can be obtained by a process known as Abel inversion. An example of a density profile obtained in this way is shown in Fig. 10. The sensitivity of the system is typically 10^{17} m^{-3} (minimum detectable density variation) and the maximum density that can be measured is $\sim 10^{20} \text{ m}^{-3}$. Systems of this type are now used routinely in fusion research.

At higher frequencies, necessary at high densities, submillimetre-wave techniques are employed. In one well-developed system the source is an HCN laser oscillating at 890 GHz, while the reflectors, beam-splitters and detectors are aluminium-coated glass, crystal quartz plates and pyroelectric detectors respectively.¹⁰³ Systems of this type can be used up to densities $\sim 10^{22} \text{ m}^{-3}$ and since high densities are beginning to be achieved in fusion experiments, these systems are receiving wider application.

Radiation at frequencies in the 100–1000 GHz range is scattered from laboratory plasmas by fluctuations in the plasma electron density. This is called 'collective' or 'co-operative' scattering. In a plasma free from impurities the density fluctuations follow the ion thermal motions and so the scattered radiation is broadened simply by the Doppler effect. The spectral width Δf_i of the scattered radiation is therefore directly related to the ion temperature T_i through

$$\Delta f_i = f_0(2kT_i/m_i c^2)^{1/2}$$

from which we see that it is possible in principle to determine T_i by measuring Δf_i . Here f_0 is the frequency of the incident radiation, k is Boltzmann's constant, m_i is the ion mass and c the speed of light.¹⁰⁴ Unfortunately, however, the scattered spectrum is extremely sensitive to the presence of small populations of impurities, and typically a 1% contamination of fully-stripped oxygen in a hydrogen plasma would be sufficient to prohibit the measurement of T_i .¹⁰⁵ In this situation, however, it should still be possible to determine the effective ionic charge defined as

$$Z_{\text{eff}} = \sum_i n_i Z_i^2 / n_e$$

which is a useful measure of the impurity level. Here n_i and Z_i are the density and ionic charge of the i th species. Since alternative methods of measuring the ion

temperature are subject to certain limitations and, in particular, may not be feasible for the next generation of large-scale tokamaks, e.g. the Joint European Torus (JET), considerable effort is being devoted to developing this diagnostic technique.

The main practical limitation arises from the fact that the ratio of the scattered to incident power is very small, typically 10^{-12} , and so high-power lasers and sensitive (heterodyne) detectors are required. However, the ratio of laser power to detector sensitivity is now just sufficient to make an experiment feasible and several groups are preparing to make the attempt.

If the plasma is turbulent then the scattered power can be enhanced by several orders of magnitude. By measuring the spectrum of the scattered power as a function of scattering angle it is possible to determine the level and spectrum of the density fluctuations. The scattering wave vector and frequency shift must be in the range of the expected microinstability and for those of particular interest in current fusion research, e.g. drift-waves, this means that frequencies in the range 100 to 300 GHz and scattering angles in the range 3° – 30° are required. Using microwave instrumentation several successful experiments have been performed.^{106,107}

Three other active methods should be mentioned: microwave reflectometry, harmonic generation and measurements of polarization changes on transmission (Faraday rotation type). In the first case a microwave beam is launched at the plasma and the phase of the reflected beam is compared with the phase of the incident beam at a reference point. In this way it is possible to determine movements of the plasma on a fast time-scale and fluctuations in the local electron density.^{101,108} In the second, a relatively powerful beam of radiation at frequency f is launched at the plasma and harmonic radiation at frequency $2f$ is generated through a non-linear wave plasma interaction. The angle of polarization of the generated radiation is measured.¹⁰⁹ From the measurements it is possible to determine the magnitude

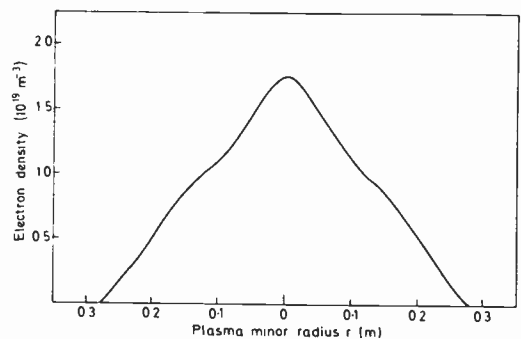


Fig. 10. Spatial profile of the electron density of a plasma produced by the DITE tokamak at the Culham Laboratory, UKAEA. Measurements made with a multichannel microwave interferometer operating at 136 GHz. (DITE tokamak group, unpublished work.)

and direction of the magnetic field inside the plasma, an important parameter in fusion research. The same parameter can also be determined by measuring the changes that occur in the state of polarization of a relatively high-frequency beam on transmission through the plasma.^{110–112} Thus far only preliminary results have been obtained, but these are very encouraging.¹¹³ With further development this latter relatively simple technique could receive widespread application.

We turn now to the passive methods. At high frequencies radiation is emitted by plasmas as the result of two elementary processes: collisions between the free electrons and relatively stationary positive ions (*bremsstrahlung* emission), and gyrations of the free electrons around the lines of the penetrating magnetic field (electron cyclotron emission). In some circumstances it can also be the result of collective non-thermal phenomena like plasma oscillations.¹¹⁴

Bremsstrahlung emission is essentially independent of frequency over the wide range $f_{pe} < f < kT_e/h$, where f_{pe} is the electron plasma frequency, typically 100 GHz and kT_e/h lies in the ultraviolet region. Here h is Planck's constant. In principle it is possible to determine the electron density and temperature by measuring the *bremsstrahlung* emission, but in practice only spatially averaged values can usually be obtained. On the other hand, measurements of electron cyclotron emission, particularly from toroidal plasmas, can provide spatially resolved information. Electron cyclotron emission occurs at the electron cyclotron frequency

$$f_{ce} = \frac{eB}{2\pi m_e}$$

and at its low harmonics, and for current plasmas the emission lines are broadened mainly by the inhomogeneity in the magnetic field. Here e and m_e are the electron charge and mass respectively and B is the magnetic field strength. Since the spatial dependence of the magnetic field is known, the point of origin of radiation at a particular frequency can be determined, i.e. there is a one-to-one correspondence between frequency and space. Therefore from a measurement of the emission in an optically thick line (emission at local black-body level), it is possible to obtain the spatial dependence of the electron temperature $T_e(r)$. Similarly from a measurement of the emission in an optically thin line it should be possible to determine the spatial dependence of the electron density $n_e(r)$.¹¹⁵ For present-day plasmas the magnetic fields employed are in the range $2T < B < 8T$ and so the emission occurs in the range $60 < f < 600$ GHz.

Several attempts to realize this diagnostic potential have been made.^{116–118} Since the plasmas are pulsed (typical duration 300 ms), special measurement techniques have had to be devised. Broad band filters, diffraction gratings, Fabry–Perot interferometers and

microwave heterodyne receivers have been employed, but probably the most successful technique is based on Fourier transform spectroscopy: this gives the complete spectrum of the emission with a resolving power of typically 30 and a time resolution ~ 10 ms.¹¹⁹ Electron temperature profiles determined by this method are similar to those obtained using the established technique of ruby laser scattering (for example, see Fig. 11). However, observations are more easily made using this technique which is now being widely applied.

In summary, measurements on plasmas at high frequencies can provide the magnitudes of several of the main plasma parameters, particularly n_e and T_e , can potentially give T_i , Z_{eff} and the internal magnetic field, and can provide qualitative information on turbulence. Often they provide this information more accurately and conveniently than by other methods and so increased application of these techniques is likely.

8 Physical Measurements Using Narrowband Sources

Physical measurements of the dielectric properties of materials depend critically on the availability of appropriate sources and detectors. The detection situation has improved significantly over the last decade, and video detectors of n.e.p. $\gtrsim 10^{-12}$ WHz⁻¹ are now readily available in the 100–1000 GHz region while

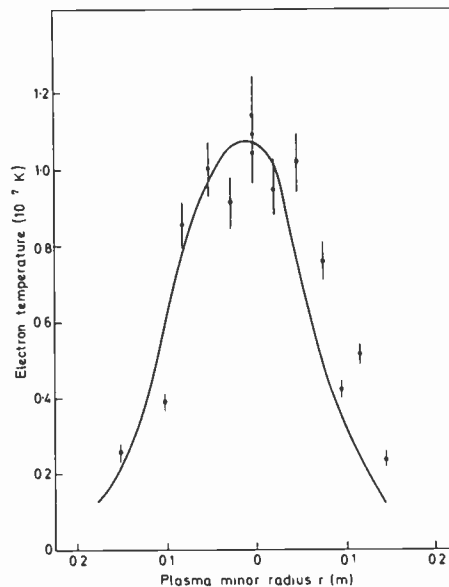


Fig. 11. Spatial profile of the electron temperature of a DITE plasma obtained from measurements of the electron cyclotron emission (—) compared with the profile measured by the established technique of ruby laser scattering (◊). The cyclotron emission measurements were made on a single plasma pulse while the laser scattering measurements were made on many pulses. The cyclotron profile has been set equal to the scattering profile at $r = 0$ to facilitate comparison of shape. (A. E. Costley and DITE tokamak group, unpublished work.)

heterodyne receivers of good sensitivity are being developed.

The source situation has been less favourable, however. Thermal sources are relatively weak, particularly at the lower frequencies of the range, and the capabilities of Fourier spectrometry are often very restricted near 100 GHz because of this. Narrowband fixed and tunable sources of various kinds have been developed although considerable further progress is required before the situation can be considered satisfactory. However, these latter types of source have introduced new factors into physical measurement in the 100–1000 GHz range. Firstly, these sources provide a means of confirming, at discrete frequencies, measurements of absorption and refraction made using broadband methods. And secondly, if tunable, they can be used for very high resolution spectrometry, to measure the fine structure in molecular spectra or the precise form of collision or Doppler broadened line shapes.

Some of the earliest tunable-source measurements were made with power produced by harmonic generation from the microwave region,¹²⁴ and this method continues to be used. Discrete-frequency lasers are also used. The discharge-pumped HCN laser has been used for many years, giving particularly strong lines at 311 and 337 μm wavelength. Optically-pumped lasers offer many more lines¹²¹ and have been used increasingly in recent years. Apart from the usual fixed-frequency measurements, these lasers can be used for Stark,¹²⁰ Zeeman³ and cyclotron-resonance spectroscopy¹²⁵ when the electric or magnetic fields available allow the resonance to be tuned to the laser frequency.

In the USSR the problems of spectroscopy at the long-wave end of the range have been attacked vigorously using beam waveguide techniques. The Lebedev Institute, and the Institute of Radioengineering & Electronics (IRE), Moscow, for instance, are actively engaged in permittivity measurements on all phases of matter using a range of tunable backward-wave oscillators. Vinogradov and Mandelstam (Lebedev) have worked extensively on ferro-electrics and semi-conductors in the wavelength range 0.3 to 3.0 mm with resolving power of 10^5 using these techniques, while Meriakri and his colleagues at IRE have made many measurements of absorption and refraction on polymers and ceramics.

A large number of high-quality measurements of atmospheric transmission have also been made in the Soviet Union and an introduction to Soviet work in these areas can be found in the proceedings of two recent conferences.^{122, 123} A wealth of information regarding the whole field of submillimetre physics worldwide is in fact available in the second of these.

9 Conclusions

This somewhat selective review shows that physical measurements in this spectral region have an impact in a variety of applications. While several of these applications are of technological importance, the techniques themselves are largely the prerogative of the specialist researcher, rather than being available to the non-specialist in terms of commercially-engineered equipment. Most of the measurement techniques are spectroscopic in nature or related to spectroscopy. However, as larger-scale applications are developed the measurement needs and capabilities will change.

As the field matures, much more attention is being paid to assessing and improving the precision of measurements. Calibration procedures and standards of measurement are sometimes inadequate even for present needs. In the future, there is bound to be a trend towards the further use of coherent systems based on tunable sources and heterodyne systems. This will widen the range of both the measurements which can be made and the requirements for standards.

10 References

- Gebbie, H. A., Osborne, C. F. and Stone, N. W. B., 'Radar for engineers', *New Scientist*, 17 October 1968, p. 29.
- Stone, N. W. B., 'Submillimetre waves in measurement techniques', *Optics Technology*, 2, no. 1, p. 8, 1970.
- Davies, P. B. and Evenson, K. M., 'Laser magnetic resonance spectroscopy of free radicals', Lecture Notes in Physics, vol. 43, 'Laser Spectroscopy'. Proceedings of the Second International Conference, Megève, June 23rd–27th, 1975, pp. 132–43 (Springer, Berlin, 1975).
- Blaney, T. G., Bradley, C. C., Edwards, G. J., Jolliffe, B. W., Knight, D. J. E., Rowley, W. R. C., Shotton, K. C. and Woods, P. T., 'Measurement of the speed of light, I. Introduction and frequency measurement of a carbon dioxide laser'. *Proc. R. Soc.*, A355, pp. 61–88, 1977.
- Evenson, K. M., Jennings, D. A., Petersen, F. R. and Wells, J. S., 'Laser frequency measurements: A review, limitations, extension to 197 THz (1.5 μm)', in 'Laser Spectroscopy III', Ed. J. L. Hall and J. L. Carsten, pp. 56–68 (Springer, Berlin, 1977).
- Blaney, T. G. and Knight, D. J. E., 'Experiments using a superconducting point-contact harmonic mixer near 1 THz', *J. Phys. D. (Appl. Phys.)*, 6, pp. 936–52, 1973.
- Kramer, G. and Weiss, C. O., 'Frequencies of some optically-pumped submillimetre laser lines', *Appl. Phys.*, 10, pp. 187–8, 1976.
- Dangoisse, D., Deldalle, A., Spingard, J.-P., and Bellet, J., 'Mesure précise des émissions continues du laser submillimétrique à acide formique', *C.R. Acad. Sci. Paris*, 283, pp. B115–18, 1976.
- Radford, H. E., Petersen, F. R., Jennings, D. A. and Mucha, A., 'Heterodyne measurements of submillimetre laser spectrometer frequencies', *IEEE J. Quantum Electronics*, QE-13, pp. 92–4, 1977.
- Godone, A., Weiss, C. O. and Kramer, G., 'F.m. noise measurements on an optically-pumped FIR laser', *IEEE J. Quantum Electronics*, QE-14, pp. 339–42, 1978.
- Fetterman, H. R., Tannenwald, P. E., Clifton, P. J., Murphy, R. A. and Parker, C. D., 'Advances in Schottky diode receivers and planar GaAs diode detectors', Digest of the 3rd International Conference on Submillimetre Waves and their Applications, University of Surrey, 1978, pp. 241–2 (Institute of Physics).

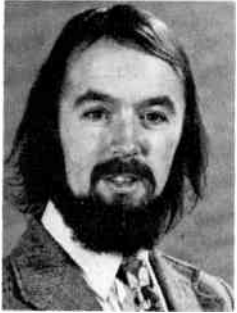
- 12 Blaney, T. G. and Knight, D. J. E. 'Direct 825th harmonic mixing of a 1 GHz source with an HCN laser in a Josephson junction', *J. Phys. D. (Appl. Phys.)*, **7**, pp. 1882–6, 1974.
- 13 Blaney, T. G., Knight, D. J. E. and Murray Lloyd, E. K., 'Frequency measurements of some optically-pumped laser lines in CH₃OD', *Opt. Commun.*, **25**, no. 2, pp. 176–8, May 1978.
- 14 Blaney, T. G., Cross, N. R. and Knight, D. J. E., 'Harmonic mixing and frequency measurements at 2.5 THz using Josephson junctions', *J. Phys. D. (Appl. Phys.)*, **9**, pp. 2175–80, 1976.
- 15 Krautle, H., Sauter, E. and Schultz, G. V., 'Properties of a submillimetre mixer in an open structure configuration', *Infrared Phys.*, **18**, pp. 705–12, 1978.
- 16 Bradley, C. C., Edwards, G. J. and Knight, D. J. E., 'Absolute measurements of submillimetre and far-infrared laser frequencies', *The Radio and Electronic Engineer*, **42**, pp. 321–7, 1972.
- 17 Strumia, F. 'A proposal for a new absolute frequency standard, using a Mg or Ca atomic beam', *Metrologia*, **8**, pp. 85–90, July 1972.
- 18 Knight, D. J. E., 'Ordered list of optically-pumped laser lines', NPL Report No. Qu45, 1978.
- 19 Fantom, A. E., 'Standards for power measurement in the millimetre wave region'. Digest of IEE Colloquium on the Measurement of Power at Higher Microwave Frequencies, Digest No. 1979/2, January 1979, pp. 3.1–3.4.
- 20 Keen, N. J., 'Milliwatt calorimeter for the 90–140 GHz band', *Electronics Letters*, **10**, pp. 384–5, 1974.
- 21 Stevens, E. (EMI Electronics), private communication, 1979.
- 22 Keen, N. J., 'Broad-band multimode millimetre-wave calorimeters'. Private communication, and to be published in *Microwaves*.
- 23 Schoer, A., 'Millimetre BWO's', *Microwave J.*, April 1970, pp. 69–72.
- 24 Stone, N. W. B., Harries, J. E., Fuller, D. W. E., Edwards, J. G., Costley, A. E., Chamberlain, J., Blaney, T. G., Birch, J. R. and Bailey, A. E., 'Submillimetre-wave measurements and standards', *Proc. Instn Elect. Engrs*, **122**, No. 10R, October 1975 (IEE Reviews).
- 25 Blaney, T. G., 'Radiation detection at submillimetre wavelengths', *J. Phys. E. (Sci. Instrum.)*, **11**, pp. 856–81, September 1978.
- 26 Lichtenberg, A. J. and Sesnic, S., 'Absolute radiation standard in the far-infrared', *J. Opt. Soc. Am.*, **56**, pp. 75–9, 1966.
- 27 Llewellyn-Jones, D. T. and Gebbie, H. A., 'A new technique for power measurement in the near millimetre wave region using the untuned cavity', Colloquium on the Measurement of Power at the Higher Microwave Frequencies, IEE, January 1979, Digest No. 1979/2, p. 8.1.
- 28 Bell, E. E., 'Optical constants and their measurement', *Handbuch der Physik*, **25**, pp. 1–58, 1967.
- 29 Chamberlain, J. E., Gibbs, J. E. and Gebbie, H. A., 'The determination of refractive index spectra by Fourier spectroscopy', *Infrared Phys.*, **9**, pp. 185–209, 1969.
- 30 Chantry, G. W., 'Submillimetre Spectroscopy' (Academic Press, London, 1971).
- 31 Bell, R. J., 'Introductory Fourier Transform Spectroscopy' (Academic Press, New York, 1972).
- 32 Chamberlain, J. E., 'The Principles of Interferometric Spectroscopy', Ed. G. W. Chantry and N. W. B. Stone (Wiley, London, 1979) (in press).
- 33 Birch, J. R. and Parker, T. J., 'Dispersive Fourier transform spectroscopy', in 'Infrared and millimetre waves', vol. 2, Ed. K. J. Button (Academic Press, London, 1979) (in press).
- 34 Chamberlain, J. E. and Gebbie, H. A., 'Submillimetre dispersion and rotational line strengths of the hydrogen halides', *Nature*, **208**, pp. 480–1, 1965.
- 35 Chamberlain, J., Costley, A. E. and Gebbie, H. A., 'The submillimetre dispersion, rotational line strengths and dipole moment of gaseous ammonia', *Spectrochimica Acta*, **25A**, pp. 9–18, 1969.
- 36 Chantry, G. W., Evans, H. M., Chamberlain, J. and Gebbie, H. A., 'Absorption and dispersion studies in the range 10–1000 cm⁻¹ using a modular Michelson interferometer', *Infrared Phys.*, **9**, pp. 85–93, 1969.
- 37 Chamberlain, J. E., Findlay, F. D. and Gebbie, H. A., 'The measurement of the refractive index spectrum of HCl gas in the near infrared using a Michelson interferometer', *Appl. Optics*, **4**, pp. 1382–5, 1965.
- 38 Sanderson, R. B., 'Measurement of rotational line strengths in HCl by asymmetric Fourier transform techniques', *Appl. Optics*, **6**, pp. 1527–30, 1967.
- 39 Russell, E. E. and Bell, E. E., 'Measurement of the far infrared optical properties of solids with a Michelson interferometer used in the asymmetric mode: Part II, The vacuum interferometer', *Infrared Phys.*, **6**, pp. 75–84, 1966.
- 40 Sanderson, R. B. and Scott, H. E., 'High resolution far infrared interferometer', *Appl. Optics*, **10**, pp. 1097–1102, 1971.
- 41 Birch, J. R., 'A modular interferometer for the dispersive Fourier transform spectrometry of gases and vapours', *Infrared Phys.*, **18**, pp. 275–82, 1978.
- 42 Kemp, A. J., Birch, J. R. and Afsar, M. N., 'The refractive index of water vapour: A comparison of measurement and theory', *Infrared Phys.*, **18**, pp. 827–33, 1978.
- 43 Chamberlain, J., 'Interface effects in Fourier transform spectrometry', *Infrared Phys.*, **12**, pp. 145–64, 1972.
- 44 Chamberlain, J. E., Costley, A. E. and Gebbie, H. A., 'Submillimetre dispersion of liquid tetrabromoethane', *Spectrochimica Acta*, **23A**, pp. 2255–60, 1967.
- 45 Davies, M., Pardoe, G. W. F., Chamberlain, J. and Gebbie, H. A., 'Submillimetre- and millimetre-wave absorptions of some polar and non-polar liquids measured by Fourier transform spectroscopy', *Trans. Faraday Soc.*, **66**, pp. 273–92, 1970.
- 46 Afsar, M. N., Hasted, J. B. and Chamberlain, J., 'New techniques for dispersive Fourier transform spectrometry of liquids', *Infrared Phys.*, **16**, pp. 301–10, 1976.
- 47 Chamberlain, J., Zafar, M. S. and Hasted, J. B., 'Direct measurement of the refraction spectrum of liquid water at submillimetre wavelengths', *Nature (Physical Science)*, **243**, pp. 116–7, 1973.
- 48 Passchier, W. F., Honijk, D. D. and Mandel, M., 'The determination of complex refractive indices with Fourier transform interferometry—III. Computation of the refractive index spectrum', *Infrared Phys.*, **15**, pp. 95–109, 1975.
- 49 Honijk, D. D., Passchier, W. F., Mandel, M. and Afsar, M. N., 'The determination of complex refractive index spectra of liquids in the far infrared spectral region 5–500 cm⁻¹ with dispersive Fourier transform spectrometry', *Infrared Phys.*, **16**, pp. 257–62, 1976.
- 50 Honijk, D. D., Passchier, W. F., Mandel, M. and Afsar, M. N., 'The determination of complex refractive indices with Fourier transform interferometry—V. Methods for the determination of complex refractive index spectra of liquids in the far infrared spectral region (5–500 cm⁻¹) using a variable pathlength, variable temperature cell', *Infrared Phys.*, **17**, pp. 9–24, 1977.
- 51 Passchier, W. F., Honijk, D. D., Mandel, M. and Afsar, M. N., 'The determination of complex refractive indices with Fourier transform interferometry—VI. Error analysis of liquid cell experiments', *Infrared Phys.*, **17**, pp. 381–91, 1977.
- 52 Afsar, M. N., Honijk, D. D., Passchier, W. F. and Goulon, J., 'Dispersive Fourier transform spectrometry with variable-thickness, variable temperature liquid cells', *IEEE Trans. on Microwave Theory and Techniques*, **MTT-25**, pp. 505–8, 1977.
- 53 Chamberlain, J., Afsar, M. N. and Hasted, J. B., 'Direct measurement of the refraction spectrum of ethanol at submillimetre wavelengths', *Nature (Physical Science)*, **245**, pp. 28–30, 1973.
- 54 Chamberlain, J., Afsar, M. N., Murray, D. K., Price, G. D. and Zafar, M. S., 'Submillimetre wave dielectric measurements on absorbing materials', *IEEE Trans. Instrumentation and Measurement*, **IM-23**, pp. 483–8, 1974.
- 55 Afsar, M. N., Chamberlain, J. and Hasted, J. B., 'The measurement of the refraction spectrum of a lossy liquid in the far infrared region', *Infrared Phys.*, **16**, pp. 587–99, 1976.
- 56 Afsar, M. N., 'The measurement of the power absorption coefficients of liquids and solids by transmission dispersive Fourier transform spectrometry', NPL Report DES42, June 1977.
- 57 Davies, G. J. and Chamberlain, J., 'High accuracy submillimetre-wave solution measurements', *J. Phys. A*, **5**, pp. 767–72, 1972.
- 58 Afsar, M. N., Chamberlain, J., Chantry, G. W., Finsy, R. and Van Loon, R., 'Assessment of random and systematic errors in

- microwave and submillimetre dielectric measurement', *Proc. Instn Elect. Engrs.*, **124**, pp. 575–7, 1977.
- 59 Afsar, M. N., Hasted, J. B., Zafar, M. S. and Chamberlain, J., 'Absorption bands in liquid chloroform and bromoform', *Chem. Phys. Letters*, **36**, pp. 69–72, 1975.
- 60 Afsar, M. N. and Hasted, J. B., 'Measurements of the optical constants of liquid H₂O and D₂O between 6 and 450 cm⁻¹', *J. Opt. Soc. Am.*, **67**, 902–4, 1977.
- 61 Afsar, M. N. and Hasted, J. B., 'Submillimetre wave measurements of optical constants of water at various temperatures', *Infrared Phys.*, **18**, 835–41, 1978.
- 62 Passchier, W. F., Honijk, D. D. and Mandel, M., 'The determination of complex refractive indices with Fourier transform interferometry—IV. Error analysis of free layer experiments', *Infrared Phys.*, **16**, pp. 389–401, 1976.
- 63 Chamberlain, J. E., Gibbs, J. E. and Gebbie, H. A., 'Refractometry in the far infrared using a two beam interferometer', *Nature*, **198**, pp. 874–5, 1963.
- 64 Chamberlain, J. E. and Gebbie, H. A., 'Dispersion measurements on polytetrafluorethylene in the far infrared', *Appl. Optics*, **5**, pp. 393–6, 1966.
- 65 Chamberlain, J. and Gebbie, H. A. 'Phase modulation in far infrared (submillimetre wave) interferometers II—Fourier spectrometry and terametrology', *Infrared Phys.*, **11**, pp. 57–73, 1971.
- 66 Bell, E. E., 'Measurement of spectral transmittance and reflectance with a far infrared Michelson interferometer', *Jap. J. Appl. Phys.*, **4** (Suppl. 1), 412–6, 1965.
- 67 Bell, E. E., 'Measurement of the far infrared optical properties of solids with a Michelson interferometer used in the asymmetric mode: Part I. Mathematical formulation', *Infrared Phys.*, **6**, pp. 57–74, 1966.
- 68 Russell, E. E. and Bell, E. E., 'Measurements of the optical constants of crystal quartz in the far infrared with the asymmetric Fourier transform method', *Opt. Soc. Am.*, **57**, pp. 341–8, 1967.
- 69 Russell, E. E. and Bell, E. E., 'Optical constants of sapphire in the far infrared', *J. Opt. Soc. Am.*, **57**, pp. 543–4, 1967.
- 70 Birch, J. R., 'The absolute determination of complex reflectivity', *Infrared Phys.*, **18**, 613–20, 1978.
- 71 Parker, T. J., Ford, J. E. and Chambers, W. G., 'The optical constants of pure fused quartz in the far infrared', *Infrared Phys.*, **18**, 215–9, 1978.
- 72 Parker, T. J., Chambers, W. G., Ford, J. E. and Mok, C. L., 'A Fourier spectrometer for determining the optical constants of transparent solids in the far infrared from 77 to 300 K', *Infrared Phys.*, **18**, pp. 571–6, 1978.
- 73 Johnson, K. W. and Bell, E. E., 'Far infrared optical properties of KCl and KBr', *Phys. Rev.*, **187**, pp. 1044–52, 1969.
- 74 Gast, J. and Genzel, L., 'An amplitude Fourier spectrometer for infrared solid state spectroscopy', *Optics Comm.*, **8**, pp. 26–30, 1973.
- 75 Gast, J., Genzel, L. and Zwick, U., 'The performance of an amplitude Fourier spectrometer for far infrared solid state spectroscopy', *IEEE Trans. on Microwave Theory and Techniques*, **MTT-22**, pp. 1026–7, 1974.
- 76 Birch, J. R. and Murray, D. K., 'A modular interferometer for dispersive reflectivity measurements on highly absorbing solids', *Infrared Phys.*, **18**, pp. 283–91, 1978.
- 77 Mead, D. G. and Genzel, L., 'Interferometry in the asymmetric mode', *Infrared Phys.*, **18**, 555–64, 1978.
- 78 Parker, T. J. and Chambers, W. G., 'A new technique for dispersive reflection spectroscopy in the far infrared', *IEEE Trans. on Microwave Theory and Techniques*, **MTT-22**, pp. 1032–6, 1974.
- 79 Parker, T. J., Chambers, W. G. and Angress, J. F., 'Dispersive reflection spectroscopy in the far infrared by division of the field of view in a Michelson interferometer', *Infrared Phys.*, **14**, pp. 207–15, 1974.
- 80 Pai, K. F., Parker, T. J., Tornberg, N. E., Lowndes, R. P. and Chambers, W. G., 'Determination of the complex refractive indices of solids in the far infrared by dispersive Fourier transform spectroscopy—I. Alkali halides', *Infrared Phys.*, **18**, pp. 199–214, 1978.
- 81 Pai, K. F., Parker, T. J., Tornberg, N. E., Lowndes, R. P. and Chambers, W. G., 'Determination of the complex refractive indices of solids in the far infrared by dispersive Fourier transform spectroscopy—II. Pseudo-displacive ferroelectrics', *Infrared Phys.*, **18**, pp. 327–36, 1978.
- 82 Parker, T. J., Lowndes, R. P. and Mok, C. L., 'A Fourier spectrometer for dispersive reflection measurements on highly absorbing solids in the far infrared at temperatures down to 4.2 K', *Infrared Phys.*, **18**, pp. 565–70, 1978.
- 83 Staal, P. R. and Eldridge, J. E., 'Improvements in dispersive reflection spectroscopy using a commercial Michelson interferometer', *Infrared Phys.*, **17**, pp. 299–303, 1977.
- 84 Cullen, A. L. and Yu, P. K., 'The accurate measurement of permittivity by means of an open resonator', *Proc. R. Soc., A*, **325**, p. 493, 1971.
- 85 Batt, R. J. and Harris, D. J., 'An open resonator technique for the measurement of atmospheric propagation characteristics at submillimetre wavelengths', *Infrared Phys.*, **16**, p. 325, 1976.
- 86 Jones, R. G., 'Precise dielectric measurements at 35 GHz using an open microwave resonator', *Proc. Instn Elect. Engrs*, **123**, p. 285, 1976.
- 87 French, I. P. and Arnold, T. E., 'High Q Fabry–Perot resonator for nitric oxide absorption measurements at 150 GHz', *Rev. Sci. Instrum.*, **38**, p. 1604, 1967.
- 88 Jones, R. G., 'Microwave dielectric measurements on low loss liquids', IEE Conference Publication 152, Euromas 77, p. 25.
- 89 Schlegel, D. and Stockhausen, M., 'Measurements of dielectric anisotropy of films in the microwave region by resonator perturbation method', *J. Phys. E*, **5**, p. 1045, 1972.
- 90 Jones, R. G., 'The measurement of dielectric anisotropy using a microwave open resonator', *J. Phys. D*, **9**, p. 819, 1976.
- 91 Valkenberg, E. P. and Derr, V. E., 'A high Q Fabry–Perot interferometer for water vapour absorption measurements in the 100 GHz to 300 GHz frequency range', *Proc. IEEE*, **54**, p. 493, 1966.
- 92 Bader, M., Cameron, R. M., Burroughs, W. J. and Gebbie, H. A., 'Submillimetre wave observations at an altitude of 40,000 ft.', *Nature*, **214**, no. 5086, p. 37, 22 April 1967.
- 93 Harries, J. E. and Burroughs, W. J., 'Measurements of submillimetre wavelength radiation emitted by the stratosphere', *Quart. J. R. Met. Soc.*, **97**, no. 414, pp. 519–36, October 1971.
- 94 Martin, D. H. and Pulett, E., 'Polarised interferometric spectrometry for the millimetre and submillimetre spectrum', *Infrared Phys.*, **10**, pp. 105–9, 1969.
- 95 Harries, J. E., Swann, N. R. W., Carruthers, G. P. and Robinson, G. A., 'Measurement of the submillimetre stratospheric emission spectrum from a balloon platform', *Infrared Phys.*, **13**, pp. 149–55, 1973.
- 96 Harries, J. E., 'Measurements of some hydrogen–oxygen–nitrogen compounds in the stratosphere from Concorde 002', *Nature*, **241**, no. 5392, pp. 515–9, 1973.
- 97 Mankin, W. G., 'Comparison of calculated and observed atmospheric transmittances in the far infrared', *Proc. Soc. Photo. Instrum. Engrs*, **67**, pp. 69–75, 1975.
- 98 Harries, J. E., Moss, D. G., Swann, N. R. W., Neill, G. F. and Gildwarg, P., 'Simultaneous measurements of H₂O, NO₂ and HNO₃ in the daytime stratosphere from 15 to 35 km', *Nature*, **259**, no. 5541, pp. 300–302, 29 January 1976.
- 99 Clark, T. A. and Kendall, D. J. W., 'Far infrared emission spectra of the stratosphere from balloon altitudes', *Nature*, **260**, pp. 31–2, 1976.
- 100 Carli, B., Martin, D. H., Pulett, E. F. and Harries, J. E., 'Very-high-resolution far infrared measurements of atmospheric emission from aircraft', *J. Opt. Soc. Am.*, **67**, pp. 917–21, 1977.
- 101 Heald, M. A. and Wharton, C. B., 'Plasma Diagnostics with Microwaves', chap. 6 (Wiley, New York, 1965).
- 102 Gorbunov, E. P., Dnestrovskii, Yu. N., Kostomarov, D. P. and Mulchenko, B. F. In 'Recent Advances in Plasma Diagnostics' (Ed. V. T. Tolok), vol. 2, p. 1 (Consultants Bureau, New York, 1971).
- 103 Veron, D., 'High sensitivity HCN laser interferometer for plasma electron density measurements', *Opt. Commun.*, **10**, pp. 95–8, 1974.
- 104 Evans, D. E. and Katzenstein, J., 'Laser light scattering in laboratory plasmas', *Rep. Prog. Phys.*, **32**, pp. 207–71, 1969.

- 105 Evans, D. E., 'The effect of impurities on the spectrum of laser light scattered by a plasma', *Plasma Phys.*, **12**, pp. 573–84, 1970.
- 106 Mazzucato, E., 'Small-scale density fluctuations in the adiabatic toroidal compressor', *Phys. Rev. Letters*, **36**, pp. 792–4, 1976.
- 107 Koechlin, F., Glaude, V. and How, J. A., 'Instability measurements in a dense hot plasma by millimetre wave scattering', *Revue Phys. Appliquée*, **12**, pp. 1797–1804, 1977.
- 108 Anisimov, A. I., Vinogradov, N. I., Golant, U. E. and Konstantinov, B. P., 'Method of investigating electron spatial distribution in a plasma', *Sov. Phys-Tech. Phys.*, **5**, pp. 939–48, 1961.
- 109 Cano, R., Etievant, C. and Hosea, J. C., 'Second harmonic generation at the upper hybrid layer in the ST Tokamak', *Phys. Rev. Letters*, **29**, 1302–5, 1972.
- 110 De Marco, F. and Segre, S. E., 'The polarization of an EM wave propagating in a plasma with magnetic shear', *Plasma Phys.*, **14**, 245–52, 1972.
- 111 Craig, A. D., 'The measurement of electron density and poloidal magnetic field in a Tokamak by polarization changes in an EM wave', *Plasma Phys.*, **18**, pp. 777–89, 1976.
- 112 Segre, S. E., 'The measurement of poloidal magnetic field in a Tokamak by the change of polarization of an electromagnetic wave', *Plasma Phys.*, **20**, 295–307, 1978.
- 113 Kunz, W., 'First measurement of poloidal-field-induced Faraday rotation in a Tokamak plasma', *Nuclear Fusion*, **18**, pp. 1729–32, 1978.
- 114 Bekefi, G., 'Radiation Processes in Plasmas', chap. 5 (Wiley, New York, 1966).
- 115 Engelmann, F. and Curatolo, M., 'Cyclotron radiation from a rarefied inhomogeneous magnetoplasma', *Nuclear Fusion*, **13**, pp. 497–507, 1973.
- 116 Brossier, P., Costley, A. E., Komm, D. S., Ramponi, G. and Tamor, S., 'Electron cyclotron emission from Tokamak plasmas: Experiment and computation', in 'Plasma Physics and Controlled Nuclear Fusion Research', Proc. 6th Intern. Conf., Berchtesgaden, 1976, vol. 1, pp. 409–14 (IAEA, Vienna, 1977).
- 117 Hosea, J., Arunasalam, V. and Cano, R., 'Electron cyclotron emission from the PLT Tokamak', *Phys. Rev. Letters*, **39**, 408–11, 1977.
- 118 Stauffer, F. J. and Boyd, D. A., 'Fourier transform spectral analysis of the cyclotron radiation from the PLT Tokamak', *Infrared Phys.*, **18**, pp. 755–62, 1978.
- 119 Costley, A. E., Hastie, R. J., Paul, J. W. M. and Chamberlain, J., 'Electron cyclotron emission from a Tokamak plasma: experiment and theory', *Phys. Rev. Letters*, **33**, pp. 758–61, 1974.
- 120 Duxbury, G. and Jones, R. G., 'High resolution Stark spectroscopy using an HCN maser', *Molecular Phys.*, **20**, pp. 721–34, 1971.
- 121 Hodges, D. T., 'A review of advances in optically pumped far-infrared lasers', *Infrared Phys.*, **18**, pp. 375–84, 1978.
- 122 Seminar on Atmospheric Propagation at Millimetre and Submillimetre Wavelengths, Institute of Radioengineering and Electronics, Moscow, December 1977.
- 123 'Submillimetre Waves and their Applications', Proceedings of the Third International Conference, *Infrared Phys.*, **18**, nos. 5/6, December 1978.
- 124 Jones, G. and Gordy, W., 'Extension of submillimeter wave spectroscopy below a half-millimeter wavelength', *Phys. Rev.*, **135**, pp. A295–6, 1964.
- 125 Landwehr, G., 'Semiconductor cyclotron resonance: transport and surface phenomena', *J. Opt. Soc. Am.*, **67**, pp. 922–8, 1977.

Manuscript received by the Institution on 2nd April 1979
(Paper No. 1894/MI11)

The Authors

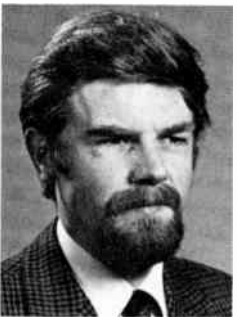


Michael Bangham graduated from St Andrew's University in 1961. He joined the National Physical Laboratory in the same year where he built the first atomic hydrogen maser in Britain. In 1972, he moved to the Environmental Standards section, where he has worked mainly on theoretical and computational aspects of atmospheric infra-red spectrometry.



James Birch graduated from Brunel University in 1968 and immediately joined NPL. His research interests have been in the field of Fourier spectrometric techniques and their application to measurements on the atmosphere, semiconductors and other dielectric materials in the submillimetre-wavelength region. In particular, he has developed various techniques of dispersive Fourier spectrometry. He was awarded a Ph.D.

degree by London University in 1979.



Tom Blaney graduated at Durham University in 1963, and was awarded a Ph.D. degree by the University of Cambridge in 1967 for work on the low temperature properties of metals. After two years of low-temperature research in the USA, he joined NPL in 1969. He has since worked on various topics related to the technology of the submillimetre-wavelength region particularly Josephson devices, heterodyne metrology and measurement

receivers, laser-frequency standards.



Alan Costley graduated from Brunel University and has since worked at NPL. In recent years, his research has led him into the field of plasma diagnostics. He has developed techniques for the measurement of the millimetre/submillimetre wave emission from magnetically-contained fusion-type plasmas using in particular the methods of time-resolved Fourier spectroradiometry. He was awarded a Ph.D. degree by London University in 1976.



John Harries graduated at Birmingham University in 1967 and moved directly to NPL where he has worked continuously in the field of atmospheric physics. In particular, he is an authority on submillimetre-wave and infra-red spectrometric measurements of stratospheric trace gases.



Gareth Jones graduated from Manchester University in 1963, and was awarded the degrees of M.Sc.Tech. and Ph.D. for work done at the Institute of Science and Technology at that University. Since joining NPL in 1966, he has worked in submillimetre-wavelength physics, particularly on lasers, modulation devices and laser spectroscopy of gases. In recent years he has investigated techniques for the

precise measurement of dielectric properties at millimetre wavelengths, particularly using open resonators.



Walford Stone graduated from London University in 1945, and has worked at NPL in the areas of precision metrology and submillimetre-wave research for the whole of his career except for a year's appointment as visiting associate professor at Kansas State University from 1964 to 1965.